A

General questions

Thèmes d'ordre général

Allgemeine Fragen

I

Bases of calculations; safety

Bases de dimensionnement et sécurité

Bemessungsgrundlagen und Sicherheit

General Reporter—Rapporteur général—Generalberichterstatter

PROF. DR. h.c. E. TORROJA
Madrid

1

Loading of bridges and structures (influence of wind, earthquakes, etc.)

Les surcharges des ponts et charpentes (effet du vent, tremblement de terre, etc.)

Belastung von Brücken und Hochbauten (Windwirkung, Erdbeben, usw.)

2

Dynamic problems

Problèmes dynamiques

Dynamische Probleme

3

Consideration of the actual conditions for deformation (plasticity, creep, etc.)

Prise en compt des lois réelles de déformation (plasticité, fluage, etc.)

Berücksichtingung der tatsächlichen Formänderungsverhältnisse (Plastizität, Kriechen, usw.)

4

General conclusions regarding safety of structures

Conclusions générales relatives à la sécurité des ouvrages

Allegemeine Schlussfolgerungen über die Sicherheit der Bauwerke

A

General questions

Thèmes d'ordre général

Allgemeine Fragen

I

Bases of calculations; safety

Bases de dimensionnement et sécurité

Bemessungsgrundlagen und Sicherheit

General report — Rapport général — Generalbericht

PROF. DR. h.c. E. TORROJA
Madrid

The various subjects in the theme AI, although apparently quite independent, are none the less related by a common interest. This common link is the philosophical idea of safety, and it is interesting to notice how at present there is a growing tendency to focus these problems in a manner entirely disparate from that which served initially to establish the nominal concept of safety factor.

Whilst, according to classical theory, structures are designed so that extreme working stresses fall within the limiting permissible stresses, the modern tendency is to refer most definitely to the final breaking loads, or to loading conditions immediately prior to failure.

The idea of permissible stress derives from the supposition that, under a certain system of loading, the members behave in a certain way. Modern criteria on limiting conditions of loading are based on the system of externally applied forces that will cause the collapse of the structure.

According to the first of these two methods, the factor of safety is a number which divides certain yield or breaking stresses.

In the second method the external applied forces, or the set of forces acting on a section, are multiplied by the factor of safety, and the structure is then designed so that it will just fail at the resulting values.

Each procedure has its pros and cons. The first of these methods is widely accepted, and there are few codes that do not specify it in a more or less direct manner. The second method has the advantage of expressing the conditions of failure more rigorously. The first one is more easy to apply in most cases. The latter provides a more generalised description of the concept of safety. It can be applied both to problems of buckling and to modern prestressed structures.

If building materials exactly satisfied Hooke's Law, it would be satisfactory to apply either of the two methods. The exact linear correspondence between stress and strain implied by this law means a close proportionality between stresses and applied loads, and so both methods will be identical. Conversely, if this proportionality cannot be extended up to the point of failure, there is no longer a linear correlation between cause and effect, and the two concepts of safety mentioned will differ.

In strict rigour, the real solution has something of both criteria. To allow for the natural uncertainty in the mechanical properties of the material and inevitable defects in the process of manufacture, it is wise to rely on a yield or breaking stress that is lower than the estimated value. This will provide some margin of safety to cover the possibility of these aforementioned defects. Thus the limiting stress should be lowered, and it seems logical to divide this stress R by a partial safety factor C_r, so that the probability that the estimated design stress R' will not surpass the value R/C_r is sufficiently small.

Furthermore, any unforeseen increase in the overload, any error in the layout of the structures or in the sizes of the structural parts when actually made, any calculation mistakes, either in the arithmetical work or in the initial hypotheses, may result in actual or virtual increase of the estimated applied forces acting on a given section. This uncertainty necessitates that a factor of safety be accepted which, on multiplying the design forces by it, will give the structure the required measure of safety. By this means the chance that a set of sufficiently unfavourable circumstances shall coincide will be rendered small enough to meet the particular requirements of the case.

Often this distinction between factors of safety which multiply loads and those which divide top stresses is unnecessary, and it suffices to design the structure for a product of both factors. But in other cases it is necessary to make this distinction to reduce the cost without sacrificing safety.

Lack of sufficient experimental work has made it impossible to calculate the distribution of these two factors in metal structures. Tests on the change in strength of concrete if there is an excess of water or deficient proportioning of cement have made it possible to obtain a statistical law relating the magnitude of the defects and their probable incidence. In constructional work there will be several sources of error: variations in the quality of materials, mistakes in the actual construction, errors in dimensioning, arithmetical mistakes and faulty hypotheses, fluctuations in the overload, etc. These various sources of error have been expressed in the form of probability laws.

By means of successive compositions and eliminations of these laws, it was possible to obtain the relationship between the safety factor C_e by which loads should be multiplied and the total factor C.*

* This relation is, with fair approximation, equal to one plus the third of the total factor of safety, namely: $C_e=1+C/3$, and $C_r=C/C_e$ is the partial factor of safety by which maximum stresses should be divided.

These two partial factors of safety C_e and C_r provide a more precise description of the problem. The former describes the possibility that external loads should increase unforeseeably. The second describes the measure of confidence that can be placed on the materials selected for the work.

The paper submitted by B. G. Neal and P. S. Symonds on "The calculation of plastic collapse loads for plane frames" is a magnificent example of the diversity of these concepts. The authors advocate the adoption of a factor of safety of 1·75 as the factor by which dead-weight and foreseeable loads are to be multiplied; design calculations being based on the effect of such a system of externally applied loads. Having obtained their final results, they adopt the same procedure for external forces and wind load. For this set of forces they take a factor of safety of 1·4, as an indication of the lesser likelihood that the most adverse loading conditions shall operate simultaneously.

This manner of estimating maximum loads enables one to calculate stresses in hyperstatic structures, based on the elasto-plastic behaviour of the metal. Only under loadings that are 75% or 40%—according to the case—greater than those estimated will the structure begin to yield slowly. Such collapse occurs when a sufficient number of plastic hinges have formed to transform the statically indeterminate structure into a mechanism.

Thus the final condition of failure is clearly indicated by the previous "yielding" phase of the material. Apart from involving more laborious calculations, the method of permissible stresses enables one to describe only the distribution of stresses within the structure. It cannot correctly describe its safety against the danger of collapse with the vigour, clarity and simplicity of the theories initiated and developed under the direction of Prof. J. F. Baker.

This subject, novel and capable of rational analysis, involves the arduous, complex problem of the safety of hyperstatic structures. Both in the previously mentioned paper and also in the paper submitted by J. Heyman, "Plastic analysis and design of steel-framed structures," it is remarked how the initial measure of redundancy of the structure tends to impede the general movement of the system.

If these ideas are applied to the simple case of a pitched-roof portal frame, it will be noticed that the structure would collapse if the steel were to reach the point of yield prematurely. A defect in rolling, an internal air bubble or a defective weld would suffice for a given section to fail to withstand the forces for which it is designed. The section becomes plastic and a plastic hinge appears at a given point.

If the structure is statically determinate, failure will occur more or less suddenly. Conversely, if the system is highly redundant, the conditions of safety vary. Before a highly redundant multi-bay portal frame can collapse laterally, under the action of a horizontal force, all the vertical members have to become plastically hinged and rotate. A local defect in one of them implies a point of weakness, but the danger of collapse becomes notably reduced by the supporting strength of the other vertical members. Only at the final moment, when the externally applied forces are very severe, does the whole structure fail. Each member, fully strained under excessive loading, cannot render further assistance to its neighbours, and these, unable to withstand the load, subdivide and collapse.

In this sense, pin joints and other flexible joints seem to limit the capacity of the system to resist. They are veritable boundaries, or barriers, forcing adjacent members to depend only slightly on other members. This isolation and great autonomy are sometimes prejudicial, sometimes advantageous. Flexibility is an inestimable advantage in all those instances where it is to be anticipated that foundations will subside.

The fact that a structure may have to withstand a given set of loads effectively, as well as the strains arising from subsidences, makes it difficult to establish general conditions of safety for this dual form of loading.

Perhaps one of the most important points arising from the work inspired by Prof. J. F. Baker relates to the new concept of safety. The whole structure fails although at the instant when it begins to collapse the most loaded fibres have not reached their ultimate failing stress.

This new idea, this mutation of the concept of ultimate strength in order to substitute it for the critical instant at which the steel begins to yield, sets new problems. The nature of failure is shown, not as a sudden phenomenon but as a steady state of transition towards instability. In this situation the rheological behaviour of the material acquires a predominant importance. If failure requires that loads shall be kept applied for a certain time, i.e. if the collapse is not sudden, then damage due to accident will be less severe than in the case of a brittle collapse. If damage is less, the required factor of safety will diminish. The structure can be designed with a smaller margin of safety than if a sudden collapse is anticipated.

This effect of the time-variable leads to a new aspect of the behaviour of the material during the critical phase in which the creep phenomenon appears. In tests in which the load has been rapidly applied, it has been found that the moment at which plasticity begins may differ, according to the definition of J. F. Baker, from the critical moment at which, if the load is applied during a certain interval, the member yields. All will depend on the position within the stress–strain diagram of the theoretical or conventional creep limit.

Tests by Prof. Campus in which steel has been subjected to tensile stresses at ordinary temperatures have revealed the different behaviour of various kinds of steel and the influence of rolling or strain on the point of the limit of creep. This position does not seem to be directly related to the real, or conventional, yield point, nor to the arbitrary proportional limit.

This behaviour of the material under sustained loading sets two problems that so far have not been satisfactorily overcome, and which can be enunciated briefly as follows:

What is the bending moment which, if applied indefinitely, leads to considerably larger strains than those due to a slightly smaller moment? In tests in which loads are maintained over a long period, is there any indication of discontinuity, or is there a point at which steel suddenly begins to strain rapidly? In these circumstances has the previous history of cyclic loading any influence?

It cannot be overlooked that, rheologically, short-time tests only illustrate one facet, a partial aspect, of the strain problem. The loading processes which the structure will have to withstand involve conditions entirely different from those under which tests are often conducted. These begin with a rapidly increasing loading, until failure occurs. But the collapse of a structure is usually preceded by a long, uncertain history during which there may have been many unforeseeable loading cycles. Sometimes the collapse is due to the violent action of an external system of forces; these, acting statically or dynamically, sometimes after repeated cycles, are capable of causing failure either suddenly, or slowly or by successive steps. On other occasions some important defect in one or several sections of the structure imposes severe working conditions. The member, being stressed nearly to its ultimate capacity under normal loading, is strained to a point close to its creep or yield limit. Strains grow continuously under design loads, and failure may even occur for smaller strains than the maximum strains attained during a short-time test. The material, prematurely aged,

is not able to resist any further. It withstood the initial loading, but time was the direct cause of its final failure.

In a sense, the effect of permanently applied loads is akin to the phenomenon of alternating or cyclic loading. A single cycle of loading and unloading does not suffice to break a structural member, but continuous repetition of loading cycles may lead to fatigue failure. The endurance limit seems to have some relationship with the critical load the material can withstand indefinitely. This critical load, according to tests on concretes by J. R. Shank, is 86% of the instantaneous ultimate strength.

For the present very little can be said about a possible correlation between fatigue and ageing phenomena due to loads permanently applied. The urgent problem faced by high-pressure-steam plant makers regarding the rheological behaviour of steel at high temperatures has been only partly classified, in spite of great efforts and advances made in this field. Nor is the similarity of the strain–time diagrams for constant stress, at various temperatures to the strain–time diagrams for various stresses at constant temperature of much help in formulating a satisfactory relationship between these two types of phenomena. There is a remote possibility that a relationship may exist between the behaviour of steel under sustained loading over a long period at a given temperature and a similar behaviour at a different temperature, by making some corresponding, but so far obscure, compensation in the time factor. But such a suggestion, for all its interest, cannot be formulated with any pretence to scientific rigour.

Only experimental research can clear up the complex strength behaviour of materials under permanently applied loads. New results on the behaviour of material under repeated loading can only be obtained by a systematic programme of tests.

All estimates about the future are tinged with uncertainty. As a first approximation the designer may guess intuitively, or may estimate the limiting value of certain loads to be statically applied. If he wants to get nearer the truth, he may take account of their effect on the structure when applied over a certain time span. Dead weights and permanent overloads constitute a system of forces which never cease to operate.

But additional to these, and concomitantly with accidental overloads which may operate over long periods, phenomena of the opposite type may supervene. Two examples of intermittent loading are the wind, with its gusts of capricious intensity, and the regular cadence of a train crossing a bridge. Its action endures hours or minutes, but in contrast to permanent loading which remains uniform, the magnitude of loading is modulated, varying according to arbitrary laws, and is always dependent on many variables which are difficult to estimate.

At times such intermittent loading may induce oscillations, which, if the structure is very flexible, will merely cause discomfort to users. A typical example of this is the Whitestone Suspension Bridge, near New York. The structure was capable of withstanding hurricanes and gusty winds, but when these attained a given intensity, the amplitude of oscillations at the centre of the main span was sufficiently large to cause justifiable qualms among those travelling over it. The magnitude of these displacements did not imply the slightest risk to the stability of the structure, but the heavy traffic and the adverse psychological condition induced in those who normally used it became an adequate motive for widening the deck as well as correcting its exaggerated flexibility, by increasing the depth of the stiffening beams. This is a complex matter, difficult to accommodate within normal safety criteria, though undoubtedly it requires attention for the sake of the peace of mind of those who use such a structure.

In this connection the paper submitted by Prof. Dr. E. Friedrich is very interesting.

The considerable oscillations caused by all types of traffic over the bridge at Villach necessitated the restriction of speed of wheeled traffic. The consequence of this, which from a functional aspect was logical, was an interference with the movement of traffic so that at certain times of day the difficulty became acute.

Starting from this particular case of statically determinate beams Prof. Friedrich has investigated the resonance of a simply supported beam, and has inferred that the best way to eliminate an unfavourable combination of oscillations is to suspend a longitudinal mass, like a beam, from the main stringers by means of springs and dash-pots. This will avoid resonance. The additional mass will only account for 10% of the total weight of the bridge, and the calculations for the design of this device are easy, using the formulae worked out by him.

In order to simplify calculations and arrive at practical results, Prof. E. Friedrich has substituted a somewhat equivalent mechanism for the actual system. Even in its most simple case, the investigation of the effects on a simply-supported girder over which a single load moves smoothly at a constant speed involves enormous difficulties of calculation. These difficulties have been pointed out by Dr. A. Hillerborg. The contribution he has submitted is a summary account of the results announced in the publication *Dynamic Influences of Smoothly Running Loads on Simply Supported Girders*. This work has been published by the Royal Institute of Technology of Stockholm, under the direction of Prof. Wästlund.

The theoretical merit of the work done by Dr. Hillerborg is evident. The mathematical work is developed with much ability and scientific rigour, but the practical consequences are disappointing due to the vast amount of work necessary to ascertain the dynamic factors applicable to even the most simple and elementary case.

The difficulties met in analysing a particular case are technically almost insurmountable. Actual conditions are such that for the time being they seem to defy direct calculation. The applied loads move with variable speeds. The hypothesis is made that effects are to be superimposed. The structure will consist of one or several spans, straight, or curved, independent, or not. The cross-section of the members changes frequently in accordance with functional requirements. The damping of the oscillations is closely linked with the rheological mechanism of the material.

But in spite of all this the engineer has to keep on constructing. It is not right to avoid the use of a particular type of structure, which intuition informs us to be adequate, simply because its dynamic behaviour is unknown. Theoretical research must continue, but until the desired aim is attained new resources have to be devised that will reveal the stability of the structure. It is not prudent to ignore the evidence of phenomena, even if they cannot be fully grasped by our reason.

In the present state of technology, it appears that only experimental work can lead to cogent results. Scale-model tests make it possible to study the most complex cases. By such means the influence of given phenomena can be measured, and the structure can be subjected to systems of forces very similar to the actual anticipated overloads.

The experimental work by C. Scruton at the National Physical Laboratory, on behalf of the British Ministry of Transport, is an example of this kind of attempt to study the behaviour of a structure subjected to the dynamic action of wind operating continuously or in gusts. The model was placed in a wind tunnel suitable for this type of test. By turning it conveniently around, it was possible to observe the effects: first on the structure as a whole, then separately on the deck.

As it was practically impossible to reproduce the structure so that similarity would be maintained in density, elasticity modulus, damping and speed and viscosity of the wind, this last factor was ignored because of its negligible influence. The test on the

full model served to compare results with tests on sectional models, suitably mounted. These latter tests also served to measure in a simple manner different types of decks, so that by a process of trial and error, the most satisfactory deck was evolved, careful account having been taken of the results obtained with some of these decks in relation to the full model.

As so often happens the experiment by-passes the obstacles of calculation and solves problems that lie beyond the reach of theory. Sometimes it serves to determine the effect of imposed loads. At other times it reveals the behaviour of the material employed and corrects or checks the truth of the hypotheses, which often are too idealised to be correct.

Model research and work on test-pieces performs two distinct functions, both most valuable. The former overcomes problems beyond the scope of mathematical computation, and the latter reveals properties and defines qualities that broaden or limit the strength and mechanical possibilities of a given material.

Both are most valuable aids to technical research. Methods of calculation based on the plastic behaviour of materials, when applied to the dimensioning of reinforced-concrete sections, and by Prof. F. Baker to metal structures, are the result of good observation of the mechanical properties of steel.

The advantages of this procedure are not only that it provides a method more simple to apply, but also that it corresponds more closely to the actual behaviour of the material.

But to solve the stress–strain laws, as well as their evolution in the course of time under different kinds of loading, it is necessary to return to the basic material and to observe all its changes, its elongations and contractions.

With this end in view, Prof. J. F. Baker has undertaken a series of tests. These have been done in the Engineering Laboratory of Cambridge University by M. R. Horne.

Simultaneously, A. Lazard has arranged another set of tests, also on mild steel full-web double-T girders, and has compiled valuable data from other experimental centres.

As A. Lazard points out, the interest of the subject is such that there appears to be justification for a vast systematic research programme, not only into the behaviour of beams under an increasing bending moment, but also on structural pieces subjected to cyclic loadings, either in the form of repeated loadings, or of alternating or oscillating forces.

Other interesting aspects of this subject are buckling phenomena of the compression flange, the influence of shear stresses, rivet holes, and internal stresses due to rolling or welding. Further, this investigation should include tests on simply-supported beams, fixed-ended girders, continuous beams over several supports, portal frames, etc., and it should include rolled and built-up sections. It will be realised how vast is the field that awaits systematic exploration. The synoptic table prepared by A. Lazard gives a clear idea of the magnitude of the problem, to which it would probably be necessary to add the series of tests on strains and failures due to the action of permanently applied loads.

The task is enormous, but the consequences and the advantages that would result in reduced cost would far outweigh the effort made. Firstly, sizes could be cut down, since the behaviour of the material would be better known. In the investigation presented by M. R. Horne on the most efficient shape of fixed-ended beams it is shown that a saving of 16% can be achieved. A study into the optimum values that should be given to the safety factors which multiply loads and divide limiting stresses could lead to an additional saving of between 10% and 20%.

If to these percentages is added the reduction in the value of the safety factor due to the extensive research into the behaviour of structural members under long-acting dynamic loads, and due to the better estimation and precise functional operation of the structure, it can be well understood that those figures can be increased even more. So the safety factor might be lowered even further, all this as a result of a better knowledge of the materials and more accurate design hypotheses.

For these reasons, based on the highly promising results implied by Prof. J. F. Baker's theory, as expounded by B. F. Neal, P. S. Symonds, J. Heyman and M. R Horne in its various aspects, the general reporter seconds the proposal of A. Lazard, and takes great pleasure in communicating this most interesting proposal to the Congress—a proposal that is full of difficulties, and that will involve many hours of hard work, but which leads him to hope for a technological evolution from which all engineers will benefit.

Summary

In the general report concerning the contributions to theme AI, the different criteria are first explained on which the conception of the safety of structures is based. For this purpose it is suggested that the factor of safety C should be split into two partial factors C_e and C_r whose product is C. With one partial factor, the calculated shearing forces are to be multiplied; with the other, the strengths or limiting stresses are to be divided. The relation between these two partial coefficients results also from mathematical-statistical considerations.

The general reporter describes the special points of the various papers submitted. According to the above considerations, these are divided into two groups. To the first belong the papers on the deduction of the shearing forces from the dynamic or static loadings. In the second group are summarised the papers for extending the knowledge of materials with the help of experimental research on the behaviour of materials under the influence of static and dynamic loads.

Finally, the economic advantages which would result from these studies are explained. The materials would be better utilised when one or other of the partial factors of safety is reduced, so that the fundamental assumptions underlying the calculations are improved and a more accurate knowledge is obtained of the mechanical properties of the materials that are used.

Résumé

Dans ce rapport général, qui sert d'introduction à la discussion des travaux présentés à la Section AI, le rapporteur général expose les différents critères sur lesquels est basé le concept de la sécurité des structures. A cet effet, il suggère la décomposition de la valeur numérique C du coefficient de sécurité, en deux coefficients partiaux C_e et C_r, dont le produit est égal à C. L'un d'eux est destiné à multiplier les moments fléchissants, les efforts tranchants et les efforts normaux prévus; et l'autre, à diviser les résistances ou contraintes limites. La relation entre ces deux coefficients partiaux est basée sur des considérations de mathématique statistique.

Ensuite, le rapporteur expose sommairement les particularités qu'offrent les différents travaux présentés. Conformément aux idées antérieures, il les classe en deux groupes. Le premier groupe est formé par les thèmes qui traitent de la déduction des efforts produits par les surcharges, soit dynamiques, soit de type statique. Dans le deuxième groupe, il inclut toutes les contributions destinées à compléter la connaissance des matériaux au moyen de l'étude expérimentale de leur comportement sous l'action de charges statiques, dynamiques et permanentes.

Enfin, le rapporteur indique les avantages économiques qui résultent de ces travaux et portent sur une meilleure mise en valeur des matériaux et sur la réduction de l'un et l'autre des coefficients de sécurité partiaux, par l'amélioration des hypothèses de base de calcul et par la connaissance plus exacte des caractéristiques mécaniques des matériaux employés.

Zusammenfassung

Im Generalbericht über die eingereichten Arbeiten der Abteilung AI werden zunächst die verschiedenen Kriterien dargelegt, auf die sich der Begriff der Sicherheit der Baukonstruktionen gründet. Zu diesem Zweck wird die Aufteilung des Sicherheitsfaktors C in zwei Teilfaktoren C_e und C_r, deren Produkt C ist, nahegelegt. Mit dem einen sind die berechneten Schnittkräfte zu multiplizieren, durch den andern die Festigkeiten oder Grenzspannungen zu dividieren. Die Beziehung zwischen diesen beiden Teil-Beiwerten ergibt sich aus mathematischstatistischen Betrachtungen.

Sodann beschreibt der Generalberichterstatter zusammenfassend die Besonderheiten der verschiedenen eingereichten Arbeiten. Gemäss den vorstehenden Ueberlegungen werden diese in zwei Gruppen eingeteilt. Zur ersten gehören die Beiträge über die Ableitung der Schnittkräfte aus den dynamischen oder statischen Belastungen. In der zweiten Gruppe sind die Beiträge zur Vervollkommnung der Materialkenntnisse mit Hilfe der Versuchsforschung über das Materialverhalten unter dem Einfluss statischer und dynamischer Lasten zusammengefasst.

Schliesslich werden die wirtschaftlichen Vorteile dargelegt, die sich aus diesen Arbeiten ergeben, welche erlauben, die Materialien um soviel besser auszunützen, als es gelingt, den einen oder den andern der Teilsicherheitsfaktoren zu verkleinern, indem die grundlegenden Rechnungsannahmen verbessert werden und eine genauere Kenntnis der mechanischen Eigenschaften der verwendeten Baustoffe erreicht wird.

Leere Seite
Blank page
Page vide

AI 1

An investigation of the oscillations of suspension bridges in wind

Etude sur les oscillations de ponts suspendus sous l'effet du vent

Eine Untersuchung über die Schwingungen von Hängebrücken infolge Winddruck

C. SCRUTON, B.Sc., A.F.R.Ae.S.
National Physical Laboratory, Teddington, England

1. Introductory

The paper gives a brief review of experiments on the aerodynamic stability of suspension bridges which have been carried out by the National Physical Laboratory on behalf of the Ministry of Transport. The specific purpose of the investigation was to give guidance on the aerodynamic design aspects of a proposed bridge over the River Severn with a centre span of 3,240 ft. (987 m.) The experiments were commenced in 1946 and were concluded early in 1951 by tests which provided a final confirmation of the stability of the preferred design for the bridge.

Although in the time available no fundamental research could be undertaken to elucidate the root causes of the aerodynamic oscillations, much information of a general nature was gained which should be helpful in the design of future suspension bridges. A previous paper* submitted by the author to the 3rd Congress summarised the preliminary stages of the work.

The wind-excited oscillations which have occurred on long-span suspension bridges (notably the original Tacoma Narrows Bridge) have been basically either vertical bending or torsional motions. In vertical oscillations the suspended platform moves up and down and the two cables displace equally and in step. In torsional oscillations the platform twists about a spanwise axis and the cables displace equally but in opposite directions. Both types of motion can occur at various frequencies and in a variety of modes. The instantaneous shape of a spanwise reference line during an oscillation is termed the *wave form* of the oscillation and is either

* C. Scruton, "An Experimental Investigation of the Aerodynamic Stability of Suspension Bridges," *Preliminary Publication for the 3rd Congress I.A.B.S.E.*

"symmetric" or "antisymmetric" with respect to the centre of the bridge according as the displacements of the two half-spans are in the same phase or in anti-phase.

In the investigation to be described the oscillatory behaviour of bridges was studied experimentally by tests of models in wind-tunnels. The two types of model used were similar to those used by Farquharson, Vincent and others* at the University of Washington (U.S.A.) in the extensive investigations which followed the collapse of the Tacoma Bridge in 1940. These were:

(a) *Sectional models*

A sectional model is a short rigid model of a sample length of the suspended structure and is mounted across the wind-tunnel (with its span horizontal and normal to the wind-stream) with freedom to oscillate against spring constraints. In the present investigation the model mountings permitted vertical translatory motions and pitching motions.† These motions, which were the two-dimensional equivalents of the vertical bending and torsional motions of the complete bridge, could take place at the same time for coupled motion tests, or could be isolated for tests with a single freedom.

In general the wind tests of these models involved no more than the observation and measurement of the critical wind speeds and frequencies bounding the ranges over which oscillations were maintained by the wind. Occasionally the damping rates of oscillations in the wind-stream were measured. The tests were made in transverse winds with inclinations varying between ∓ 15 degrees. It was not considered practicable to test sectional models in horizontally inclined winds.

(b) *Full models*

A full model is a replica of a complete bridge so constructed that its behaviour in a wind-stream is similar to the full-scale bridge. The full model used in this investigation was installed in a large wind-tunnel‡ specially built by the Ministry of Transport for the investigation. The direction of the tunnel wind-stream could not be varied but the effect of inclined winds, both horizontally and vertically, was simulated by inclining the model. Critical wind speeds, frequencies and oscillation modes were recorded.

In the early stages of the investigation it was uncertain whether the stability of a complete bridge could be predicted satisfactorily from experiments on a sectional model alone, since with this method of test the influence of several factors cannot be represented directly. Such factors include, for example, the tower stiffnesses and inertias, the longitudinal camber, the oscillation wave form and the horizontal inclination of the wind. However, it was also clear that full models were unsuitable for routine comparisons between different forms of suspended platform, owing to the length of time required for construction and the high cost. To provide a practical programme it was therefore decided to depend on tests of sectional models for an indication of the most promising structural forms. Whilst the tests were in progress, the design and construction of a full model was also put in hand, with a view to tests of the correlation between the two different experimental methods. This full model was necessarily based on a very early design for the bridge, and it became available for wind-tunnel tests in 1948. The results obtained with these two types of models

* "The Aerodynamic Stability of Suspension Bridges with special reference to the Tacoma Narrows Bridge," *Bulletin No.* 116 *of the University of Washington Engineering Experiment Station.*

† A few tests were also made with lateral motion (i.e. translation normal to the span and in the plane of the decks).

‡ The wind-tunnel is briefly described in Appendix II.

led to the conclusion that sectional model tests were sufficient for reliable full-scale prediction, and accordingly the construction of a further full model based on the design finally preferred for the bridge was considered to be unnecessary. A final verification of the stability of this design was, however, provided by tests of a large-scale sectional model. An increase of the linear scale from 1/100 to 1/32 was considered advisable, because previous tests had shown that the stability was sensitively influenced by details of the structural form which could not be copied with sufficient accuracy on a small-scale model.

2. Notation

ρ air density
ν kinematic viscosity of air
B width of bridge between stiffening trusses
g acceleration due to gravity
σ typical material density
E typical elastic modulus
θ angular torsional displacement of suspended platform at any instant of oscillation (radians)
z linear vertical displacement of structure at any instant of oscillation
I_θ torsional moment of inertia per unit spanwise length
I_z mass per unit spanwise length
N_θ and N_z natural frequencies of oscillation in torsional and vertical bending modes respectively
e_θ and e_z elastic stiffnesses corresponding respectively to I_θ, N_θ and I_z, N_z.
δ natural logarithm of the amplitude of successive cycles of oscillation (logarithmic decrement)
δ_θ and δ_z logarithmic decrements for torsional and vertical oscillations in still air respectively
$\delta_{\theta A}$ and δ_{zA} logarithmic decrements due to still air damping
$\delta_{\theta s}$ and δ_{zs} logarithmic decrements due to structural damping
$\delta_{\theta w}$ logarithmic decrement of torsional oscillations due to the wind-stream
V and V_c wind speed and critical wind speed respectively
N and N_c frequencies of oscillation corresponding to V and V_c respectively
$V_r = V/NB$ reduced velocity
$V_s = V/N_\theta B$
α angular inclination of wind to the bridge platform in a vertical plane —upwinds positive (degrees)
β angular inclination of the wind to the bridge in a horizontal plane ($\beta=0$ and 90 degrees for transverse and longitudinal winds)

3. Model and full-scale similarity

(i) *Full models*

The motions of similar-shaped suspension bridges in wind may be influenced by the bridge size (B), by the density, damping and elasticity of the bridge structure (σ, δ_s, E) and by the viscosity, density and velocity of the air (ν, ρ, V).

By the usual principles of dimensional analysis these parameters can be grouped in the following independent non-dimensional combinations:

$$\left.\begin{array}{ll} \text{(a)} & \sigma/\rho \quad \text{(density)} \\ \text{(b)} & E/\rho V^2 \quad \text{(elasticity)} \\ \text{(c)} & \delta_s \quad \text{(structural damping*)} \\ \text{(d)} & gB/V^2 \quad \text{(gravitational)} \\ \text{(e)} & VB/\nu \quad \text{(viscosity)} \end{array}\right\} \quad \ldots\ldots\ldots \quad (1)$$

Full dynamic similarity between model and full-scale is achieved if the model is geometrically similar to full-scale and the above numbers are equal for both systems.

For tests in atmospheric wind tunnels of practicable dimensions and wind speeds the full-scale value of (e) cannot be achieved. The velocity scale would moreover be incompatible with that required by (d). However, there is evidence that the aerodynamic forces acting on bluff bodies such as bridge structures depend mainly on pressure action and only indirectly on viscous action and hence the validity of full-scale prediction by model testing is not seriously impaired by incorrect scaling of the viscous forces.

The design and construction of a model to accord with the similarity numbers (a) to (d) presents considerable difficulties. It will be found generally that materials of construction do not exist which possess the requisite combinations of density and elastic moduli, and that even were such materials available, the exact small-scale reproduction of details might be impracticable. However, it is sufficient if the correct overall inertias and elastic stiffnesses are reproduced in the model. Equivalent similarity numbers to those given in (1) but using inertia and elastic stiffness terms are:

$$\left.\begin{array}{ll} \text{(a)} & I_\theta/\rho B^4, \quad I_z/\rho B^2, \text{ etc.} \\ \text{(b)} & e_\theta/\rho V^2 B^2, \quad e_z/\rho V^2, \text{ etc.} \\ \text{(c)} & \delta_{\theta s}, \quad \delta_{zs}, \text{ etc.} \\ \text{(d)} & gB/V^2 \end{array}\right\} \quad \ldots\ldots\ldots \quad (2)$$

With a linear scale of $1/n$ the foregoing numbers yield a velocity and a frequency scale of $1/\sqrt{n}$ and $\sqrt{n}$ respectively. The values of V_r and V_s are therefore the same for the full-scale bridge as for the model.

(*ii*) *Sectional models*

With strict inertial scaling

True similarity conditions are obviously not observed in the sectional model method of test. The use of the method for full-scale prediction assumes that oscillations of a complete bridge arise from the aerodynamic action on the suspended structure alone and that the other components (e.g. cables) contribute to the dynamic properties only. It also implies that critical values of V_r are not influenced by oscillation wave form.

The inertial coefficients of sectional models represent the total contribution of suspended structure and cables. The model stiffnesses are merely those which provide the required oscillation frequencies and need not, as in the case of full models, be derived from correctly proportioned gravitational and elastic forces. When (d) is

* It is shown in Appendix I that when the influence of viscosity is negligible values of $\delta_{\theta A}$ are the same for model as for full-scale provided strict inertial scaling is observed. Hence, for the full model tests and for the sectional model tests with strict inertial scaling δ_θ may be used in place of $\delta_{\theta s}$.

omitted and expressions for natural frequencies are substituted in (b), the similarity numbers for sectional models become:

$$\left.\begin{array}{ll}(a)\ I_\theta/\rho B^4, & I_z/\rho B^2 \\ (b)\ V/N_\theta B, & V/N_z B \\ (c)\ \delta_{\theta s}, & \delta_{zs}\end{array}\right\} \quad \ldots\ldots\ldots \quad (3)$$

where I_θ, I_z now represent overall values.

Thus the actual velocity and frequency scale for sectional models are interdependent but one or other may be chosen at convenience.

Inertial scaling not attempted

In the writer's previous paper* tests of sectional models involving isolated motions only were considered. The requirements for similarity were then approached through the solutions of the equations of motion. Similarity conditions equivalent to those given in (3) were, of course, obtained; but in addition, it was shown that when $N_\theta = N_c$ approximately, strict inertial scaling is not essential and the critical values of V_r depend only on the geometric shape of the structure and on the product of (a) and (c) i.e. on $I_\theta \,.\, \delta_{\theta s}/\rho B^4$ and $I_z \,.\, \delta_{zs}/\rho B^2$ for angular and linear motions respectively.

Procedure for prototype prediction from sectional model test data

Some remarks may be useful on the procedure in the two cases where strict inertial scaling of the model is observed, or is not attempted and $N_c = N_\theta$ approximately.† The critical values of V_r obtained from the models by both these methods are applicable to the prototype, provided the values of $\delta_{\theta s}$ satisfy the stated conditions.‡ Strict inertial scaling is essential for values of V_s (and N_c) to be applicable: critical speeds are then determined from critical values of V_s or V_r by either of the relations $V_c = N_\theta B V_s$ or $V_c = N_c B V_r$. The value of N_c required by the latter relation is not given by the other method, and it is therefore necessary to use the approximation $V_c = N_\theta B V_r$. Experience with various types of bridge sections indicates that this approximation introduces no serious discrepancies within the range of normal winds.

4. The full model experiments

Model construction

A photograph of the 1/100-scale full model is reproduced in fig. 1. The model was designed to give wide scope for modifications both to the elastic properties and to the form of the suspended structure. It represented a truss-stiffened bridge of width 107 ft. (32·6 m.) and of total span 5,040 ft. (1,535 m.); the centre span of length 3,000 ft. (914 m.) had a sag ratio of 1/10. The two roadways of width 39 ft. (11·9 m.) were separated by an 8·3 ft. (2·53 m.) wide reservation.

The required stiffness and inertial properties of the suspended structure were obtained by the use of light rigid components with steel interconnecting springs. These rigid components were mainly of aluminium-balsawood sandwich construction and each component spanned one bay of 60 ft. (18·3 m.). The use of spring interconnections enabled the stiffnesses to be altered and also had the advantage that the structural damping was kept to a sufficiently low value, since the deformations occurred mainly

* *Loc. cit.*

† For convenience, pitching oscillations only are discussed here. The procedure applies equally well to other motions.

‡ See note at foot of page 40.

through flexing of the springs. Both the elastic and inertial properties of the towers were variable, but it was not considered necessary to reproduce the correct external shape of either the towers or the anchorages. The model cable consisted of piano wire of diameter 0·024 in. (0·61 mm.), which provided the equivalent of a full-scale cross-sectional area of about 450 in.^{2} (2,900 cm.^{2}) with a 1/100 reduction of Young's

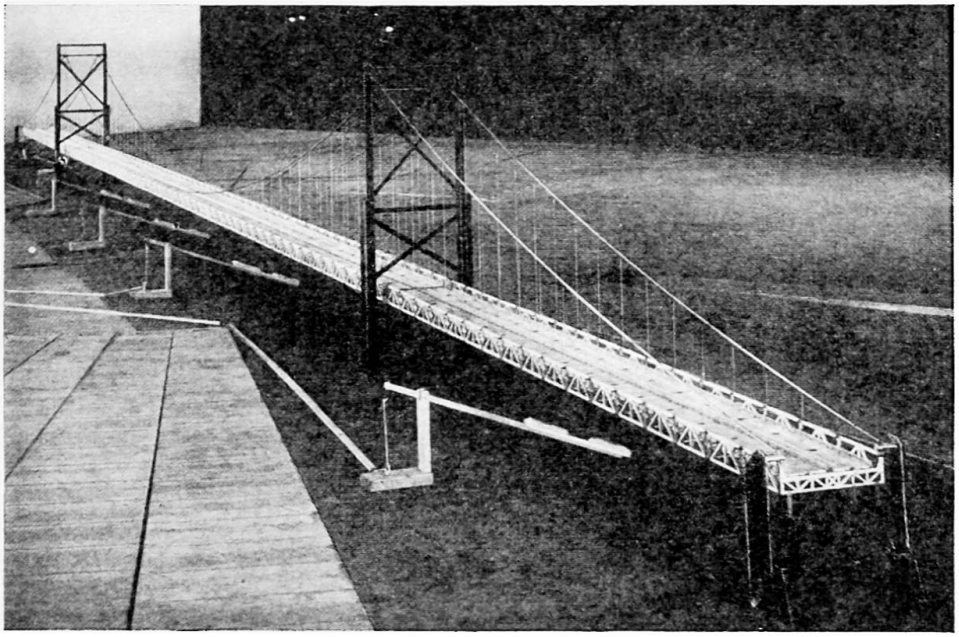

Fig. 1. The 1/100-scale full model mounted in the wind-tunnel

modulus. To obtain the correct mass and external shape, hollow brass cylinders were spaced along the wire and fixed to it by a single grub screw. The model suspenders were made of fishing line which had been prestretched and treated with a beeswax coating to reduce the effect of humidity changes on its length.

The model was mounted on the horizontal turntable which fitted flush with the floor of the wind-tunnel test chamber (see Appendix II and fig. 7). Changes of the horizontal wind direction were reproduced by rotation of the turntable and the effect of vertically inclined winds was simulated by tilting the whole model about a spanwise axis near the wind-tunnel floor.* In the second case, the correct representation of the gravitational forces was then restored by attaching suitably angled and spring tensioned cords at several points along the span. The additional elastic stiffnesses contributed by this arrangement were rendered small by the use of long cords and very weak springs.

Test procedure

In still air tests resonance modes and frequencies were observed by exciting the model through weak springs driven by a reciprocating motion. The logarithmic decrements of the artificially excited oscillations were measured in the usual way from photographic records.

In wind tests the tunnel speed was gradually increased from zero to a maximum corresponding on full-scale to a little over 200 ft./sec. (61 m./sec.). The critical wind

* The provision made for tilting the model is not shown on fig. 1.

speeds and frequencies for maintained oscillations in the various modes were noted. In general the modes were observed visually, but cinematograph records were taken of certain typical oscillations.*

Results and conclusions

Tests on the full model were carried out for various vertical wind inclinations α and horizontal wind inclinations β. The effective angle α produced by a given tilting inclination α' of the model depended on the value of β and was given to a close approximation by $\alpha=\alpha' \cos \beta$. Except for longitudinal or near longitudinal winds, the values of vertical inclination attained ranged between ± 15 degrees.

Tests were made on the influence of several design variations such as grade-line camber, tower stiffness and cable loading; and also on the effects of modifications to the external shape of the suspended structure. By covering the stiffening truss panels with paper it was possible to simulate the aerodynamic effect of a plate-girder-stiffened bridge. In this condition the model reproduced many of the modes of oscillation which occurred on the original Tacoma Bridge.

The more important results and conclusions are given below.

(a) *Coupling between vertical bending and torsional motions*

Each wind-induced oscillation observed corresponded in mode and in frequency to a natural oscillation induced by resonance tests in still air. From this experimental evidence, and from independent visual observations, it was concluded that coupling effects between the vertical bending and torsional motions had little influence on the oscillations. However, it should be noted that the natural frequency ratio N_θ/N_z for corresponding wave forms was approximately 2 and was therefore more appropriate to a bridge with a double rather than a single plane of lateral bracing. There was no means on the full model of substantially reducing this ratio. The effect of a close approach to equality of the natural frequencies in sectional model tests is described later.

(b) *Influence of oscillation form*

With a given wind inclination and model condition all the different types of torsional oscillation appeared for approximately the same constant value of V_r. A similar conclusion applied for vertical bending oscillations. This indicates that the influence of oscillation wave form is unimportant.

(c) *Influence of shape of suspended structure*

The stability depended on the shape and arrangement of the components of the suspended structure. The model with plate-girder stiffening exhibited a high degree of instability in both vertical bending and torsional oscillations. No instability in vertical bending motion was found in any test with a truss-stiffened model. Torsional oscillations occurred for certain arrangements of the truss-stiffened model.

The influence of shape is discussed in more detail in the description of the sectional model tests.

* Some of these records have been incorporated in a short silent film entitled "Oscillations of a Model Suspension Bridge in Wind."

(d) *Influence of elastic stiffnesses and natural frequencies*

Critical values of V_r were not appreciably influenced by variation of the stiffnesses and natural frequencies due to structural modifications which did not involve change of shape of the suspended structure. Such modifications included variation of the tower stiffnesses, unloading the sidespan cables, and fitting a centre tie between truss and cable.

(e) *Influence of wind inclination*

The highest degree of instability was found in transverse winds ($\beta=0$) and the stability characteristics improved progressively with increase of β. Vertical bending oscillations of the plate-girder-stiffened model persisted, but with decreasing amplitude, up to a value of β between 30 and 45 degrees, while weak torsional oscillations were still present at $\beta=60$ degrees. No instability of any type was found in steady longitudinal winds.

The stability was sensitive to the vertical inclination of the wind. The highest degree of instability of the plate-girder-stiffened bridge occurred with slight negative vertical inclination, and that for the truss-stiffened bridges with slight positive inclination.

(f) *Effect of grade-line camber*

The stability was not greatly influenced by variations of the grade-line camber. The indications were that a cambered grade-line yielded very slightly better stability characteristics than a level grade-line.

(g) *Effect of gusty winds*

Some tests were attempted with several types of disturbed airflow, none of which, however, was necessarily representative of natural gusty winds. In longitudinal, as well as in transverse winds, irregular vertical oscillations were set up by the buffeting action of large-scale eddies shed from the gust-making device, but no tendency to torsional motion was observed.

(h) *Correlation between sectional and full model tests*

The full model tests showed that critical values of V_r for specific values of the structural damping were determined by the shape of the suspended platform and were not substantially affected by other structural properties or by the wave form of the oscillation. Also in these tests the highest degree of instability was produced in transverse winds. It was concluded that sectional model tests would be adequate for stability prediction provided they yielded the same critical values of V_r as those given by the corresponding full model.

Table 1 sets out a comparison of the results obtained with the full model and with its sectional model copy. The alignment of the vertical motion in the sectional model tests were not strictly correct except at zero incidence, since the direction of model motion was not altered to correspond to the incidence change. The error in alignment increased with incidence and hence may account for the lack of correlation between the results at $\alpha=\pm 10$ degrees for vertical oscillations of the plate-girder-stiffened section. With this exception all the results showed very good agreement between the two methods of test and support the conclusion that reliable predictions of the stability of proposed suspension bridges may be based on sectional model tests only.

TABLE I

Comparative results from sectional and full model tests

The models represented a mid-deck bridge of section A, fig. 3. In its *standard* condition (fig. 1) the model decks were separated by an open reservation and were fitted with paling-type handrailing and truss-type roadway stringers. The values for the structural damping were:

Full Model: $\delta_{zs}=0{\cdot}035$, $\delta_{\theta s}=0{\cdot}05$
Sectional Model: $\delta_{zs}=0{\cdot}06$, $\delta_{\theta s}=0{\cdot}05$

The full model was tested up to speeds corresponding to values of V_r of 15 and 8 for vertical and torsional oscillations respectively. Higher values were reached in the sectional model tests, but for the purpose of this comparison the above values are taken as the limits for both types of test and a result is given as STABLE when no oscillations occurred up to these limits. Only the lowest critical values are quoted here, since on the full model the critical speeds for the upper limit of the instability range were usually masked by the onset of a further mode of oscillation.

Model Configuration	α degrees	Lowest critical values of V_r			
		Vertical Oscillations		Torsional Oscillations	
		Sectional Model	Full Model	Sectional Model	Full Model
Standard	−15, −10, −5, 0, 5, 10, 15			STABLE	STABLE
Standard but with all handrailing removed	10			7·0	6·8
	−15, −10, −5, 0, 5, 15			STABLE	STABLE
Standard but with solid plate handrailing	0			3·4	3·8
	−15, −10, −5, 5, 10, 15	STABLE	STABLE	STABLE	STABLE
Standard but with castellated handrailing	−15, −10, −5, 0, 5, 10, 15			STABLE	STABLE
Standard but with the handrailing on the inner edges of the carriageways removed and a solid cover fitted over of the central reservation	15			5·0	4·5
	10			5·4	4·8
	5			7·2	6·9
	0, −5, −10, −15			STABLE	STABLE
Standard but with the stiffening trusses covered to represent the aerodynamic effect of solid plate-girder stiffening	15	STABLE	STABLE	5·5	STABLE
	10	STABLE	1·8	2·6	2·5
	5	1·7	1·7	2·4	2·7
	0	1·8	1·6	2·4	2·6
	−5	1·8	1·7	2·4	2·5
	−10	STABLE	1·7	2·8	2·4
	−15	STABLE	STABLE	5·8	4·2

5. Experiments with 1/100-scale sectional models

A typical 1/100-scale sectional model is shown by fig. 2. The models were of rigid wooden construction and represented a 340-ft. (103·5 m.) length of the bridge-suspended structure. They were tested in a wind-tunnel with a working section measuring 4 ft. by 3·40 ft. (1·22 m. × 1·035 m.). Two types of mounting, here referred to as the "original" and the "improved," were used.

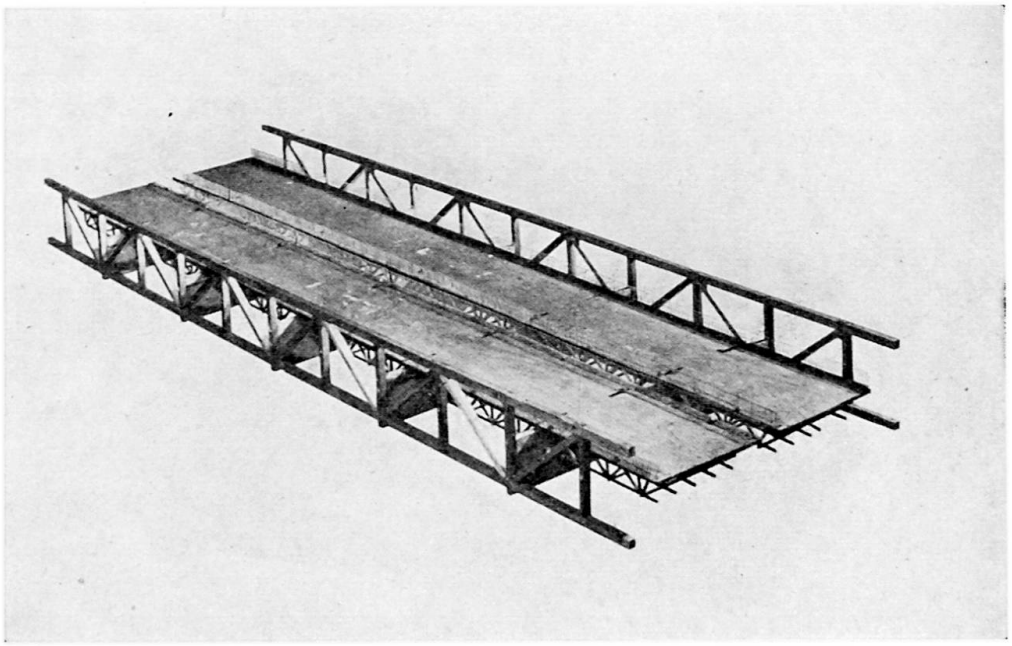

Fig. 2. Typical 1/100-scale sectional model.

The original mounting

This permitted both vertical bending and pitching motions, either singly or together. The apparatus damping was not directly variable, and the inertias of the model on this mounting were very much greater than those required by correct scaling of the prototype values. However, since in the tests $N_c = N_\theta$, the similarity conditions given in paragraph 3 were applicable.

The model was attached at both ends to circular plates which were supported on ball bearings so that pitching motion could take place against the elastic constraint provided by helical springs. Each bearing and spring assembly was carried on a framework which was constrained to move vertically by a steel-strip device; helical springs again providing stiffness. The circular end-plates fitted flush with the walls of the wind-tunnel.

The improved mounting

This was used for pitching motion tests with correct inertial scaling and with the apparatus damping variable from a low initial value. As in the case of the original mounting the model was carried between discs. Each disc was supported on a steel-strip suspension which maintained a fixed axis of oscillation and also provided the required elastic stiffness. The damping due to this suspension was very small. Additional damping was supplied by the action of a thin segment of copper which oscillated with the model and passed between the pole-pieces of an electromagnet.

The damping moment produced by the eddy currents set up in the copper was proportional to the velocity of the motion and could be readily varied by adjusting the current through the coils of the electromagnet.

Discussion of results

The main types of bridge section tested are shown in fig. 3. They were all stiffened by trusses of the single Warren type, but could be readily converted to represent plate-girder-stiffened sections by the attachment of solid covers to the trusses. The models were usually tested with a pitching axis placed approximately centrally with respect to the four stiffening-truss-chords members, but some tests were made with

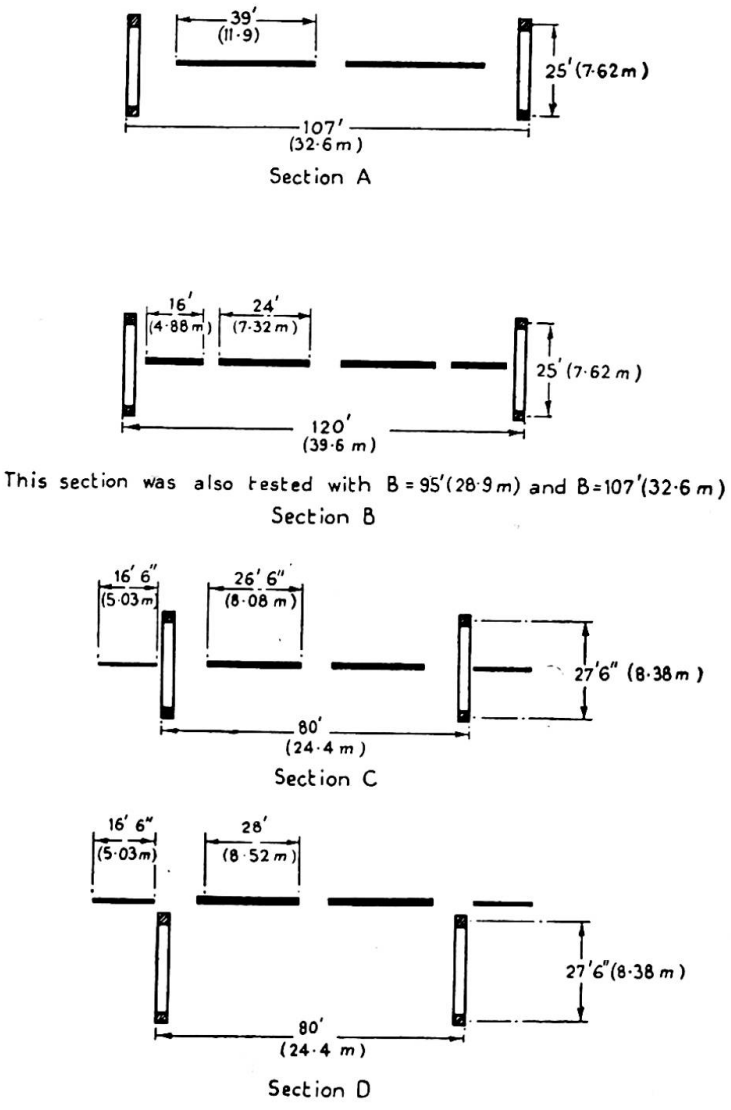

Fig. 3. Main types of bridge sections tested

other axis positions. The maximum of V_r or V_s obtainable in the tests depended on the test conditions, but in all cases corresponded to full-scale wind speeds of well over 100 miles/hr. (161 km./hr.).

Some of the models were tested on both the original and improved mountings.

The good agreement obtained between corresponding sets of results provided experimental verification for the similarity conditions stated in paragraph 3 for the case where strict inertial scaling is not attempted.

The main conclusions derived from the results of the sectional model test are summarised below.

(a) *Influence of structural damping*

A typical diagram showing the influence of structural damping on the stability of a plate-girder-stiffened section is reproduced in fig. 4. Similar tendencies were exhibited by truss-stiffened sections.

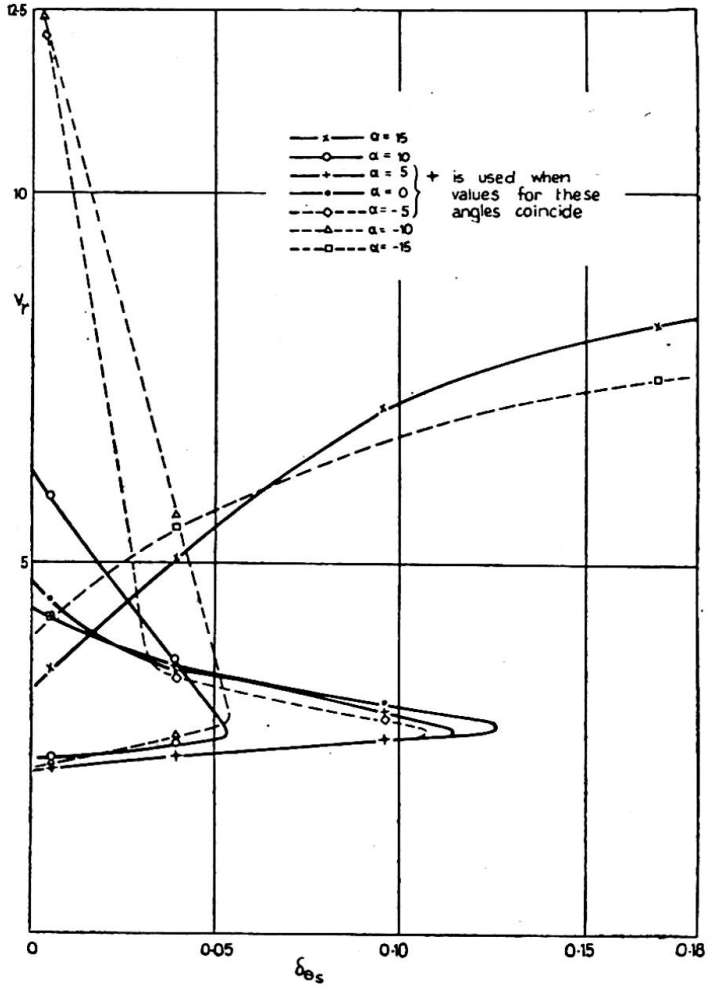

Fig. 4. Influence of damping on the pitching oscillations of the plate girder stiffened section A

Increase of $\delta_{\theta s}$ narrowed the instability range by increasing the critical speeds for the lower boundary and decreasing those for the upper boundary. The magnitude of $\delta_{\theta s}$ necessary to prevent oscillations for all wind speeds provided a qualitative indication of the relative strengths of the instabilities.

(b) *Influence of location of pitching axis*

The vertical position of the pitching axis was varied in tests of the mid-deck section (B, fig. 3) and of the top-deck section (D, fig. 3). For axes lying midway between the stiffening trusses the stability of both these sections was least when the axis was located near the level of the deck.

(c) *Coupling between vertical bending and pitching oscillations*

In sectional model tests with coupled motions particular attention was given to ratios of the natural frequencies near unity, since it was expected that the influence of coupling would then be most marked. Except when the frequency ratio N_θ/N_z closely approached unity, one of the motions was always found to predominate, and the critical frequency and reduced velocity were in fair agreement with those obtained in the corresponding isolated motion test. When $N_\theta/N_z=1$ both motions were present in substantial proportions. In one instance coupled oscillations occurred when $N_\theta/N_z=1$ which were absent when $N_\theta/N_z>1$ or when the motions were isolated. Hence it was concluded that sectional models can be tested satisfactorily with the vertical and pitching freedoms isolated, unless the frequencies for corresponding modes are approximately equal.

(d) *Influence of structural form of suspended platform*

Plate-girder-stiffened sections. These sections were considerably more unstable than truss-stiffened ones. The majority of them were obtained by covering the stiffening trusses of the sections shown in fig. 3 and thus the plate girders represented were rather deeper than is usual in practice. All the plate-girder sections showed instability in both vertical and pitching motions, generally at low wind speeds. For example, the critical values of V_r for the section derived by covering the trusses of A (fig. 3) were about 1·7 and 2·5 for vertical and pitching oscillations respectively (see Table I).

Truss-stiffened sections. No vertical oscillations were excited with any of the truss-stiffened sections. The pitching oscillations were influenced by the form and arrangement of the structural components of the bridge, and were especially sensitive to those of the roadway deck fittings. The results have been discussed in greater detail in the writer's previous paper.* Only those factors which were found to have a corrective influence on aerodynamic instability in pitching oscillations will be listed here:

Stiffening truss chords of high width/depth ratio;
Separation of traffic lanes by open slots or gratings;
Truss-type deck stringers in preference to the plate-type;
Castellated handrailing, or other types of handrailing designed to break up the continuity of the airflow pattern;
Sidetracks (e.g. footpaths, cycle-tracks, etc.) mounted outboard of the stiffening truss.

By the inclusion of a number of these stabilising features in the design, a satisfactory degree of stability was achieved for each of the types of section shown in fig. 3. However, the stability still proved to be sensitive to other factors such as the relative levels of the various roadways and the positioning of the roadway stringers. These effects were only noted and not investigated systematically. In view of the many design features which may possibly influence the stability it is considered that model tests provide the only satisfactory basis for stability prediction.

The sections A to D shown in fig. 3 are lettered in the chronological order of the tests and illustrate successive steps in the evolution of a design with very good stability characteristics. Section A represented a mid-deck design with two roadways separated by an open central reservation. The presence of the gap between the

* *Loc. cit.*

roadways greatly improved the stability. Further improvement was obtained on dividing the two roadways into four, provided adjacent roadways were separated by an open reservation (section B). The two outer roadways, termed "sidetracks," each represented the combination of cycle-track and footpath; the inner ones represented carriage-ways. For economy in the construction of the piers and towers the width between trusses was reduced to 80 ft. (24·4 m.) in section C and the sidetracks were supported outside the trusses. This change also improved the stability. The top-deck section D was the last of this series of 1/100-scale models and it allowed horizontal cross bracing to be incorporated in two widely separated planes. Its stability characteristics were superior to those of the sections tested previously, and this fact, in conjunction with the considerable increase in torsional frequency due to the two planes of bracing, increased the estimated critical speed for torsional oscillations of the full-scale bridge to over 250 miles/hr. (400 km./hr.). Two models of section D were used, the second of which approximately represented the design finally adopted for the Severn Bridge.

6. Confirmatory tests of the stability of the proposed Severn Bridge

Since earlier tests had already shown sectional models to be adequate for the prediction of the stability of a complete bridge, the construction of a full model representing the preferred design for the Severn Bridge was considered to be unneces-

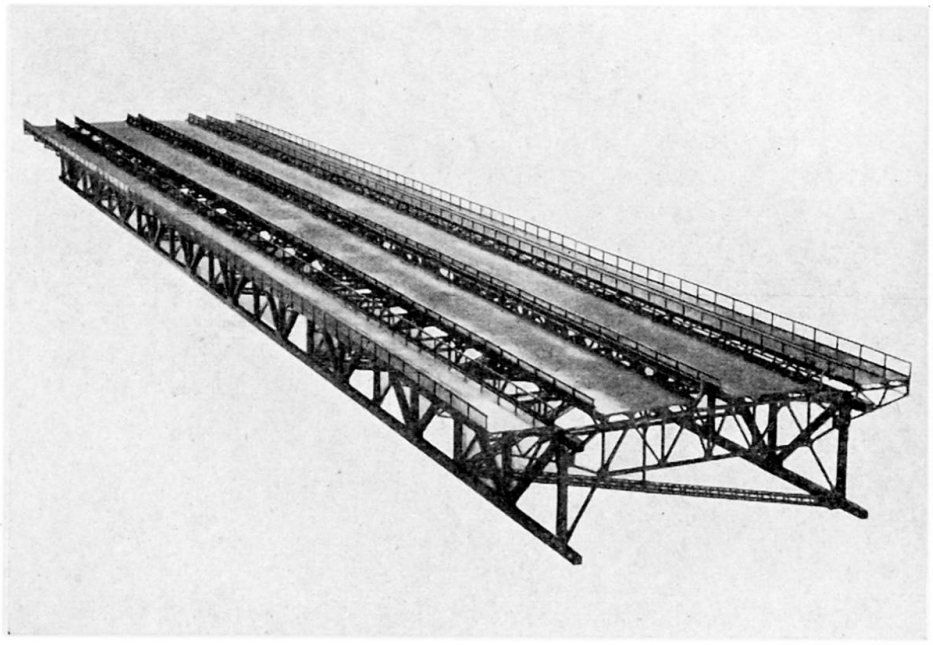

Fig. 5. Sectional model of design proposed for the Severn Bridge (1/32-scale)

sary. However, to provide a final confirmation of the stability, tests were carried out in the large wind-tunnel on a 1/32-scale sectional model. This increase of the linear scale* allowed a more accurate reproduction of fine structural detail.

The model (see fig. 5) represented 600 ft. (183 m.) of the suspended structure and considerable care was taken in its construction to reproduce all the important features

* Preliminary experiments had indicated that the oscillations of a still larger model might be affected by the proximity of the tunnel roof and floor.

of the full-scale design. It was mounted on steel-spring suspensions carried by frames which tilted to give the desired vertical incidence to the wind. The suspension arrangements permitted pitching combined with either vertical translation or lateral translation motions, as well as tests with each of these motions isolated. Tests with the lateral freedom included were necessary, since with the top-deck structure the

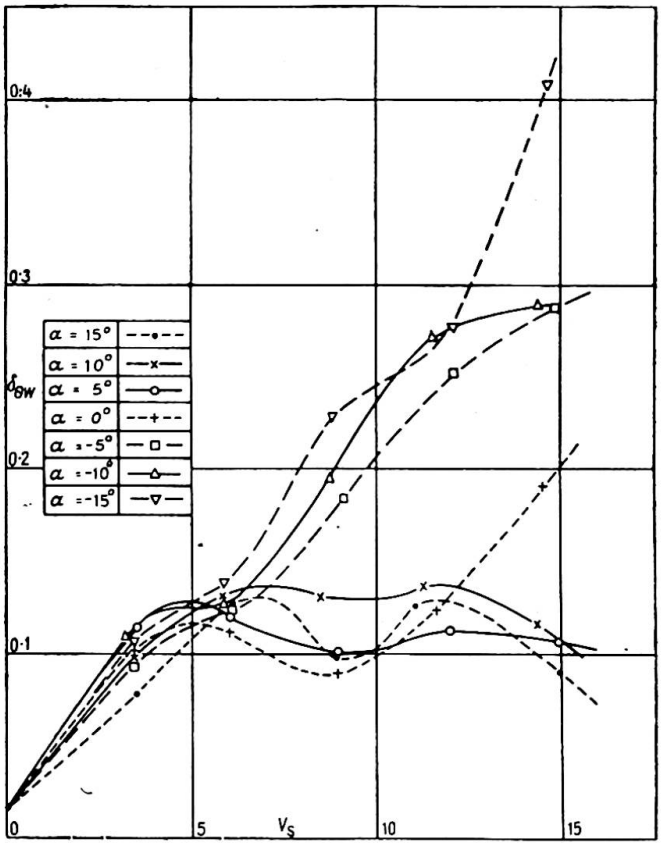

Fig. 6. Damping rates of pitching oscillations due to wind (1/32-scale model of proposed Severn Bridge)

lateral and pitching motions were inertially coupled due to the offset of the centre of mass above the elastic axis of the structure. In all three motions viscous oil dampers were provided to enable the amount of structural damping represented to be varied.

The inertias of the model conformed with the requirements for strict inertial scaling. Initially the frequencies were adjusted to values 3·2 times greater than those calculated for full-scale. This yielded a speed-scale of 1/10 and enabled the tests to be carried out up to wind speeds corresponding to approximately 140 miles/hr. (225 km./hr.). The minimum values of $\delta_{\theta s}$ and δ_{zs} were 0·01 and 0·06 respectively. No instability of any type occurred in these tests.

No further tests involving the lateral and vertical motions were made. With the more important pitching motion* N_θ was reduced to allow tests to be carried out up to wind speeds equivalent on full-scale to about 250 miles/hr. (400 km./hr.). The value of $\delta_{\theta s}$ for these tests was 0·02. No instability was observed for these conditions, but to provide further information the variation of the damping rate due to wind only ($\delta_{\theta w}$) with wind speed was measured. The curves of $\delta_{\theta w}$ against V_s for several wind incidences are reproduced in fig. 6. These show that for negative wind incidences

* On models and on actual bridges with truss stiffening, instability has been recorded only in torsional (pitching) motions.

the damping rate became increasingly positive. For positive incidences the damping rate increased with the initial increases of V_s and thereafter maintained a substantial positive value for the whole speed range tested. These results verified that the design of suspended structure proposed for the Severn Bridge was satisfactory from the standpoint of aerodynamic stability.

In addition, the model was used to confirm some of the results found on the 1/100-scale models and also to obtain some information on the effect of the width/length ratio of sectional models. Some unstable configurations of the model (e.g. that obtained by covering the central reservation) were tested with model lengths representing 600 ft. (183 m.) and 300 ft. (91·5 m.). The results obtained with these two model lengths showed only small differences.

ACKNOWLEDGEMENTS

The work described above was carried out in the Aerodynamics Division of the National Physical Laboratory on behalf of the Ministry of Transport. This paper is published by permission of the Director of the Laboratory and with the approval of the Ministry of Transport. Throughout the investigation close collaboration has been maintained with the staff of the Joint Engineers for the Severn Bridge.*

The author wishes to acknowledge the collaboration of his senior colleague, Dr. R. A. Frazer, F.R.S., and also the assistance rendered by other colleagues in the construction of models and apparatus and in the observational work.

APPENDIX I

NOTE ON THE DAMPING PROPERTIES OF BRIDGES

The total damping rate (δ) of a structure in still air is made up of the contributions due to the structure only (δ_s) and that due to the surrounding air (δ_A). The application of model test results to prototype prediction requires a knowledge of the values of δ_s for both model and prototype. There is as yet no reliable method for calculating these values for a proposed bridge, and measurements of δ on actual bridges, which might be used for statistical estimates, have only been made on bridges of short span.† The values of δ found for short-span bridges varied from 0·05 to over 0·2. Model test values are, of course, readily obtained by decaying oscillation experiments.

The aerodynamic damping arises from the effects of viscosity and pressure. For oscillations of bridge sections, dimensional analysis yields:

$$\delta_{\theta A}=\frac{\rho B^4}{2I_\theta} f\left[\frac{\nu}{B^2 N_\theta}, \theta_0\right] \quad . \quad . \quad . \quad . \quad . \quad . \quad . \quad (1)$$

where θ_0 is the amplitude and $\delta_{\theta A}$ denotes the values of δ_A for pitching oscillations.

The scanty experimental evidence available supports the assumption that the influence of the viscosity parameter is very small and that equation (1) can be written:

$$\delta_{\theta A}=\frac{\rho B^4}{2I_\theta}[a_0+a_1\theta_0+a_2\theta_0^2+ \ . \ . \ .] \quad . \quad . \quad . \quad . \quad . \quad . \quad (2)$$

where the coefficients a_o, a_1, etc., are approximately constant.

The equivalent expression for linear motions is:

$$\delta_{zA}=\frac{\rho B^2}{2I_z}\left[b_0+b_1\left(\frac{z_0}{B}\right)+b_2\left(\frac{z_0}{B}\right)^2+ \ . \ . \ .\right] \quad . \quad . \quad . \quad . \quad . \quad (3)$$

* Messrs. Mott, Hay and Anderson and Messrs. Freeman, Fox and Partners.

† Arne Selberg, "Dampening Effect in Suspension Bridges," *I.A.B.S.E. Publications*, Tenth Volume.

Thus with the same inertial scaling as that required for the wind tests, the values of δ_A are the same for model as for full-scale.

Values of δ_A for complete bridges or their models will be influenced by the oscillation wave form and may be calculated if the sectional values and the wave form are known.

Some values of $\delta_{\theta A}$ were measured during the course of the Severn Bridge investigation. The results obtained for sections A and D shown in fig. 3 gave respectively the relations:

$$\delta_\theta = \rho B^4/2I_\theta \ (0{\cdot}01+0{\cdot}29\ \theta_0)$$

and

$$\delta_{\theta A} = \rho B^4/2I_\theta \ (0{\cdot}05+3{\cdot}40\ \theta_0)$$

APPENDIX II

The Large Wind-Tunnel

Design and construction

The wind-tunnel (see fig. 7) was not required as a permanent structure and hence the main considerations governing the design were that of low cost of construction rather than that of high aerodynamic efficiency. For this reason the tunnel was of the non-return flow type and used only one fan. It was erected in a disused aircraft

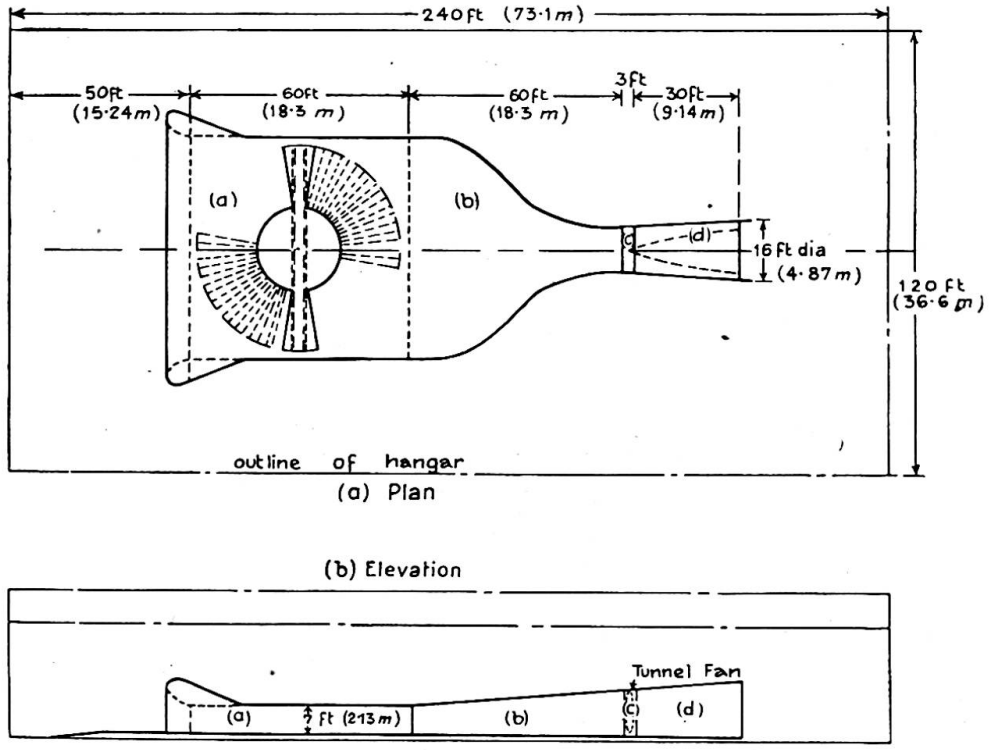

Fig. 7. The wind-tunnel

hangar and was raised from the hangar floor only by the few feet necessary to accommodate a well for the turntable. The fabric of the tunnel consisted mainly of a timber framework lined with wallboard, and the roof was suspended from Bailey bridge girders supported at their ends by vertical concrete pillars. The four main components of the tunnel were:

(*i*) *The test chamber, (a) fig. 7*

This had a floor area of 60 ft. by 60 ft. (18·3 m.) and was 7 ft. (2·13 m.) high. The air entered the test chamber through a conventional bell-mouth fairing and a wire-mesh screen for smoothing the airflow. In the centre of the chamber was a 55-ft. (16·75 m.) long turntable contained within a shallow quadrantal pit which allowed a rotation of 90 degrees. The flooring over the central part of the turntable was carried by the turntable itself and the outer annular area was filled in by wedges of 5-degree angles constructed of boarded trestles, which were lifted successively when the model had to be rotated relative to the wind direction.

(*ii*) *The contraction chamber, (b) fig. 7*

The contraction chamber was 60 ft. long (18·3 m.) and in this distance the cross-section developed smoothly from a 60-ft. rectangle to the 12-ft. (3·65 m.) diameter circle of the adjoining fan annulus. A wire-mesh screen at the front of the contraction chamber helped to ensure even airflow in the test chamber.

(*iii*) *The fan and fan annulus, (c) fig. 7*

The fan annulus, 12 ft. (3·65 m.) in diameter and 3 ft. (0·91 m.) in length, was of all-timber construction and stiffened to ensure that the small clearance between it and the two-bladed fan was maintained. The fan was driven by a concentric 130-h.p. motor with fine speed control.

(*iv*) *The diffuser, (d) fig. 7*

This was of circular section, 30 ft. (9·14 m.) in length, and expanded from the fan annulus to a diameter of 16 ft. (4·87 m.) at the discharge.

Performance

Tests of the aerodynamic characteristics were made initially on a 1/12-scale model of the tunnel and hangar.

In the actual wind-tunnel extensive measurements of the distribution of airflow within the test chamber showed that at all speeds up to the maximum of 22 ft./sec. (6·7 m./sec.) the velocity variations both along the length of the chamber and vertically were less than 3%. In the horizontal direction across the test chamber the variation of wind speed of nearly 10% was recorded at a distance of 5 ft. (1·52 m.) from the sides. A variation of this order was predicted by the model tunnel tests and was not considered important in view of the clearance of nearly 5 ft. between the full-model anchorages and the sides of the chamber.

Summary

The paper presents a general review of the experiments carried out in an investigation of the aerodynamic stability of suspension bridges undertaken by the National Physical Laboratory of the Department of Scientific and Industrial Research on behalf of the Ministry of Transport. The specific purpose of the investigation was to assist the designers of the proposed Severn Bridge, but much of the information gained is applicable to suspension bridges generally.

Wind-tunnel tests using both sectional and full models are described and the limitations of these two experimental techniques are discussed. The reliability of the use of data obtained from sectional model tests alone for the prediction of the

behaviour of full-scale bridges is verified by comparisons of the results obtained by both methods. A comparison is made of the stability of various bridge sections and the design features favourable to the promotion of stability are indicated. The sectional models used for these tests illustrate the evolution of the design of the suspended platform for the proposed Severn Bridge and the results show that a satisfactory degree of stability can be attained by attention to the structural shape and arrangement of the details of the suspended platform.

Résumé

Cette communication constitue un bref exposé de recherches relatives à la stabilité aérodynamique des ponts suspendus. Ces recherches ont été entreprises par le National Physical Laboratory du Department of Scientific and Industrial Research, à l'instigation du Ministère des Transports. Le but spécifique était de fournir des informations aux dessinateurs chargés de l'établissement du projet de pont sur la Severn. Toutefois, un grand nombre de renseignements ainsi obtenus s'appliquent également aux ponts suspendus en général.

L'auteur expose également les essais qui ont été effectués en soufflerie, tant sur modèles complets que sur modèles partiels; il étudie les avantages et les inconvénients de chacune des deux méthodes. La valeur des résultats obtenus exclusivement sur modèles partiels, du point de vue de la prévision du comportement des ponts réels, a été confirmée par la comparaison entre les deux méthodes.

Différents profils de ponts font l'objet de comparaisons du point de vue de la stabilité et l'auteur indique les dispositions qui permettent d'accroître la stabilité.

Les modèles partiels qui ont été utilisés pour ces essais mettent en évidence le développement de la conception du tablier; les résultats montrent que l'étude minutieuse de la forme et des caractéristiques de détail du tablier permet d'obtenir une stabilité suffisante.

Zusammenfassung

Die vorstehende Arbeit gibt einen kurzen Ueberblick über Versuche, die für das Ministry of Transport im National Physical Laboratory des Department of Scientific and Industrial Research im Zusammenhang mit einer Untersuchung der aerodynamischen Stabilität von Hängebrücken ausgeführt wurden.

Die Untersuchung wurde ursprünglich für den Konstrukteur der geplanten Severn-Brücke ausgeführt, aber die Ergebnisse erscheinen von allgemeinem Interesse für die Konstruktion von Hängebrücken.

Windkanalversuche an Teilmodellen sowohl als vollständigen Modellen werden beschrieben, und die Vor- und Nachteile der beiden Methoden besprochen. Die Zuverlässigkeit von ausschliesslich an Teilmodellen erhaltenen Ergebnissen für die Voraussage des Verhaltens von Brücken in natürlicher Grösse wurde bestätigt durch den Vergleich von mit den beiden Methoden erhaltenen Ergebnissen.

Die Stabilität verschiedener Brückenprofile wird verglichen, und Konstruktionen werden vorgeschlagen, die die Stabilität erhöhen.

Die in den Versuchen benutzten Teilmodelle zeigen die Entwicklung der Konstruktion der Fahrbahnplatte der geplanten Brücke; und die Ergebnisse zeigen, dass durch geeignete Form und sorgfältig ausgearbeitete Einzelheiten der Fahrbahnplatte ausreichende Stabilität erzielt werden kann.

Leere Seite
Blank page
Page vide

AI 2

Die Dämpfung von Brückenschwingungen

The damping of oscillations in bridges

L'amortissement des oscillations des ponts

PROF. DR. TECHN. DIPL. ING. ERICH FRIEDRICH
Vorstand der Lehrkanzel für Betonbau an der Universität für Technische Wissenschaften in Graz, Österreich.

EINLEITUNG

Durch das Bestreben immer leichter und kühner zu bauen, wird es auch im Betonbau erforderlich, das Bauwerk unter den Verkehrsbelastungen nicht mehr als statisch ruhend zu betrachten, sondern den Einfluss der bewegten Belastung zu berücksichtigen. Der alte Grundsatz, dass, je schwerer gebaut wird, um so sicherer das Bauwerk ist, gilt nicht mehr. Wir kommen dazu, auch im Betonbau unliebsame dynamische Einflüsse zu ergründen und, wenn erforderlich, ihnen durch bauliche Massnahmen entgegenzutreten. Die gesamte Frage der Sicherheit von Bauwerken, die Frage der Einführung eines *n*-freien Bemessungsverfahrens und die Frage, wie man zweckmässig bestehende Bauten auf ihre Tragfähigkeit untersucht, kann durch die Betrachtung des Bauwerkes als dynamisches Gebilde in viel umfassenderer Weise beantwortet werden. Der Bauingenieur wird hier vielfach die bereits im Maschinenbau gewonnenen Erfahrungen und Erkenntnisse für seine Bedürfnisse umformen und anwenden können.* Im nachfolgenden wird auf eine dieser Fragen eingegangen, wobei die bei dynamischen Untersuchungen bereits bekannten Verfahren auf das Gebiet des Brückenbaues übertragen und dem Bauingenieur erschlossen werden sollen. Bei einem Maschinenfundament hat man es in der Regel mit einer gleichbleibenden Schwingungszahl zu tun. Im Brückenbau hingegen wird das Bauwerk von Fahrzeugen mit verschiedener Belastung und verschiedenen Schwingungszahlen befahren, so dass man darauf Rücksicht nehmen und die Untersuchungen auf veränderliche Schwingungszahlen ausdehnen muss.

Bei einer bestehenden Brücke in Villach traten unter der Verkehrsbelastung erhebliche Schwingungen auf. Man hatte daraufhin die Verkehrsbelastung beschränkt und die Geschwindigkeit, mit der die Brücke befahren wird, herabgesetzt. Beide Massnahmen störten empfindlich den gesamten Verkehr und wirkten sich

* I. P. Den Hartog, *Mechanische Schwingungen.* Deutsche Bearbeitung von Dr. Gustav Mesmer Julius Springer, Berlin, 1936.

vielfach nachteilig aus. So hatte die Beschränkung der Geschwindigkeit zur Folge, dass die Brücke ständig mit der vollen Verkehrslast belastet war, weil sich die Kraftwagen auf der Brücke zusammendrängten. Auch die Beschränkung der Höchstbelastung wirkte sich nachteilig auf den gesamten Verkehr aus. Ausserdem ist es praktisch unmöglich, bei dem stets zunehmenden Verkehr diese Beschränkung aufrechtzuerhalten.

Zunächst ist die Frage interessant, welche Schwingungen von den Kraftwagentypen auf die Brücke ausgeübt werden. Bei der Brücke in Villach handelt es sich um ein Bauwerk, das wohl statisch einwandfrei ist, aber mit der Eigenschwingungszahl gerade in dem Bereich der von den Fahrzeugen ausgeübten Schwingungen liegt, sodass die Brücke stets Resonanzschwingungen ausführt.

Vom Institut für Kraftfahrzeugbau an der Technischen Hochschule in Graz wurden für einige Fahrzeugtypen folgende Schwingungszahlen angegeben. Im Mittel schwanken die Schwingungen von Fahrzeugfedern zwischen 0,9 und 2,30 Hertz.

TAFEL I

Ausgeübte Schwingungen in Hertz

Fahrzeugtype	Belastung	Vorderfeder	Hinterfeder
Steyr 220	ohne Nutzlast	1,85	2,30
Steyr 220	100 kg. (1 Person)	—	2,03
Steyr 220	400 kg. (4 Personen)	—	1,62
Fiat Topolino	ohne Nutzlast	1,77	2,23
Fiat Topolino	3 Personen	2,70	1,67
Fiat 1100	ohne Nutzlast	1,40	1,42
Fiat 1100	6 Personen	1,27	1,29

Durch den Marschtritt werden etwa 2,2 Hertz ausgeübt. Der Einfluss der Unebenheiten der Fahrbahn verursacht beim Befahren ebenfalls Schwingungen. Um auch hier Anhaltspunkte zu gewinnen, sei folgendes mitgeteilt: Bei Fahrbahnen mit Kopfsteinpflaster ist der mittlere Abstand der Höcker $a=10\div15$ cm., bei Fahrbahnen mit Schlaglöchern beträgt der Abstand der Schlaglöcher rd. $50\div100$ cm. Bei Landstrassen ist der Abstand der Höcker rd. $20\div400$ cm. Man kann auch hieraus auf die Stösse schliessen, die ein Fahrzeug auf die Fahrbahn ausübt.

$$f\,(\text{Hertz})=\frac{V\,(\text{km./h.})}{3{,}6a\,(\text{m.})}$$

Bei einer Geschwindigkeit z.B. von $V=16$ km./h. ergibt sich hieraus bei einer Höckerentfernung von rd. 1 m. eine Schwingungszahl von rund 5 Hertz. Die Frage, die gestellt wird, ist die, ob es möglich ist, durch einen Einbau die Schwingungen für die Brücke unschädlich zu machen, und weiter, wie dieser Schwingungsdämpfer aussehen muss.

DIE EIGENSCHWINGUNG VON BRÜCKEN

Für einen frei aufliegenden Träger mit der Elastizitätszahl E, dem Trägheitsmoment J und der Stützweite l ergibt sich bei konstanter Masse μ je Längeneinheit die Eigenschwingungszahl (Abb. 1).

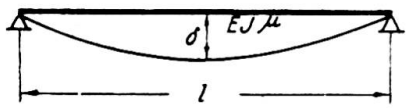

Abb. 1

$$\omega=\frac{\pi^2}{l^2}\cdot\sqrt{\frac{EJ}{\mu}} \quad \ldots\ldots \quad (1)$$

Die Schwingungsdauer T, das ist die Zeit, die der Träger braucht um von einer Lage ausgehend wieder in die gleiche Lage zurückzukehren, ist mit ω durch folgende Gleichung gegeben.

$$T \cdot \omega = 2\pi \quad . \quad . \quad . \quad . \quad . \quad . \quad . \quad . \quad . \quad . \quad . \quad (2)$$

Die Zahl der Schwingungen in einer Sekunde (Hertz genannt) beträgt:

$$f = \frac{1}{T} = \frac{\omega}{2\pi} \quad . \quad . \quad . \quad . \quad . \quad . \quad . \quad . \quad . \quad . \quad . \quad . \quad (3)$$

Um die Rechnung zu vereinfachen, genügt es, an Stelle des wirklichen Systems einen einfachen Schwinger zu betrachten (Abb. 2). Ein einfacher Schwinger besteht aus einer Feder mit der Federkonstanten c und einer darunter angehängten Masse m. Die Federkonstante c ist jene Kraft, die erforderlich ist, um die Feder um 1 cm. zu verlängern. Wird die Masse aus der Ruhelage gebracht, indem an der Masse m nach abwärts gezogen wird, und wird die Feder losgelassen, so schwingt das System mit der Eigenschwingungszahl

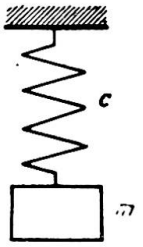

Abb. 2

$$\omega = \sqrt{\frac{c}{m}} \quad . \quad . \quad . \quad . \quad . \quad . \quad . \quad . \quad . \quad (4)$$

Bei einem Träger ist die statische Durchbiegung δ in Feldmitte bei gleichmässiger Lastverteilung $G=mg$ ($g=981$ cm./sec.^{2}=Erdbeschleunigung) gegeben. Die Federkonstante ist daher

$$c = \frac{mg}{\delta} \quad . \quad . \quad . \quad . \quad . \quad . \quad . \quad . \quad . \quad . \quad . \quad . \quad . \quad (5)$$

oder

$$\omega = \sqrt{\frac{c}{m}} = \frac{\sqrt{g}}{\sqrt{\delta}} \doteq \frac{10 \cdot \pi}{\sqrt{\delta}} \quad . \quad . \quad . \quad . \quad . \quad . \quad . \quad . \quad . \quad (6)$$

$$f = \frac{\omega}{2\pi} = \frac{5}{\sqrt{\delta}} \quad . \quad . \quad . \quad . \quad . \quad . \quad . \quad . \quad . \quad . \quad . \quad . \quad (7)$$

Die statische Durchbiegung des Trägers unter der gegebenen Massenverteilung ist daher ein Mass für die Eigenschwingungszahl des Trägers.

Man sollte in Hinkunft in die Brückenbestimmungen eine Vorschrift aufnehmen, die die Eigenschwingungszahl beschränkt. Damit würde allerdings die Durchbiegung unabhängig von der Stützweite beschränkt werden. Wenn nun eine Brücke mit der Eigenschwingungszahl in der Nähe der durch den Verkehr auftretenden Schwingungen liegt, so können die durch die Resonanz bedingten grossen Verformungen die Tragfähigkeit der Brücke wesentlich herabsetzen. Die statische Durchbiegung δ_{st} ist mit einem Vergrösserungsfaktor

$$\mathfrak{B} = \frac{1}{1 - \left(\frac{\Omega}{\omega}\right)^2} \quad . \quad . \quad . \quad . \quad . \quad . \quad . \quad . \quad . \quad . \quad (8)$$

zu multiplizieren, um die unter der Verkehrslast auftretenden Verformungen zu erhalten. In dieser Gleichung ist Ω die durch den Verkehr hervorgerufene Schwingungszahl und ω die Eigenschwingungszahl. Wird $\Omega/\omega=1$ so wird $\mathfrak{B}=\infty$. Eine Abminderung dieses Faktors bekommt man durch die Dämpfung D.

Setzt man die Dämpfung proportional der Geschwindigkeit, so lautet für das Ersatzsystem (Abb. 2) die Differentialgleichung

$$m\ddot{x} + k\dot{x} + cx = 0 \quad . \quad . \quad . \quad . \quad . \quad . \quad . \quad . \quad . \quad (9)$$

Als Dämpfung bezeichnet man

$$D=\frac{k}{2\sqrt{cm}} \quad \ldots\ldots\ldots\ldots \quad (10)$$

Bei einer Dämpfung ist die Vergrösserungsfunktion für die Durchbiegung

$$\mathfrak{V}=\frac{1}{\sqrt{\left(1-\left(\frac{\Omega}{\omega}\right)^2\right)^2+4D^2\frac{\Omega^2}{\omega^2}}} \quad \ldots\ldots\ldots \quad (11)$$

An Hand von ausgeführten Versuchen, über die Oberregierungsbaurat Arthur Lämmlein berichtet,* kann man sich ein Bild über den Dämpfungsfaktor machen. In der nachfolgenden Tafel II ist für den Resonanzfall die Vergrösserungsfunktion ermittelt.

TAFEL II

Nr.	Name	Bauweise	Dämpfung	Vergrösserungs-faktor	Eigen-schwingungs-zahl in Hz.
1	Bleibachbrücke	Spannbeton	0,014	35,7	4,25
2	Brücke bei Emmendingen	Spannbeton	0,008	125	3,14
3	Brücke Oberhausen	Verbund	0,0065	154	6,88
4	Hügelsheim	Stahlbeton-platte	0,1213	8,2	10,60

Man erkennt aus diesen Zahlen, dass bei Resonanz Werte auftreten können, die für die Brücke ausserordentlich bedenklich sind. Auch bei der Brücke in Villach ist die Dämpfung der Brücke selbst gering. Der Wert D liegt bei 0,010, sodass der Vergrösserungsfaktor rd. 100 ist. Um diese Brücke zu beruhigen, wird ein Dämpfungsträger vorgeschlagen, der nun berechnet und beschrieben wird.

DIE DÄMPFUNG EINER BRÜCKE

Beschreibung der Konstruktion

Zunächst soll an Hand der Systemskizze Abb. 3 der Gedanke der Dämpfung erläutert werden. Unter dem Brückentragwerk I befindet sich ein Träger II, der

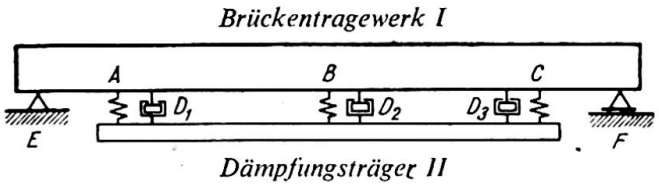

Abb. 3

Dämpfungsträger genannt wird. Dieser Dämpfungsträger II ist an drei Federn A, B, C mit dem Hauptträger verbunden. Zwischen den beiden Trägern sind ausserdem Flüssigkeitsdämpfer D eingebaut. Natürlich befindet sich der Dämpfungsträger II mit den Einbauten bei dem tatsächlichen Bauwerk nicht unterhalb des Hauptträgers, sondern zwischen den Hauptträgern und ist nicht sichtbar. Der Dämpfungsträger hat $\frac{1}{10}$ der Masse des Hauptträgers.

* Arthur Lämmlein, "Schwingungsmessungen an Strassenbrücken verschiedener Bauarten," *Beton und Stahlbeton*, Heft 5, 1951.

Die Wirkungsweise des Einbaues des Dämpfungsträgers zeigt Abb. 4. Als Ordinate ist die Vergrösserungsfunktion $\mathfrak{V}$ und als Abszisse das Verhältnis der aufgezwungenen Schwingung zur Eigenschwingung aufgetragen. Die Vergrösserungsfunktion nimmt höchstens den Wert 4,6 an. Bis zu einer Vergrösserungsfunktion

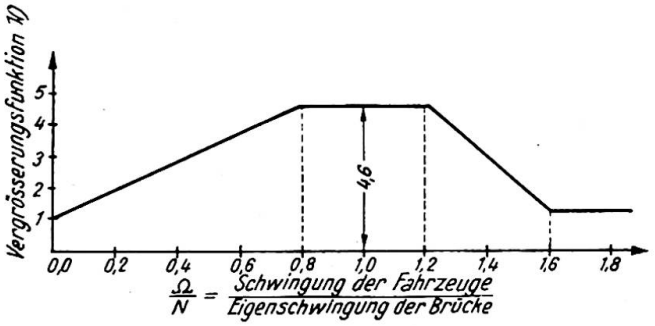

Abb. 4

von 5 kann man im allgemeinen damit rechnen, dass die dadurch hervorgerufenen Spannungen innerhalb der zulässigen Grenzen bleiben. Die Flüssigkeitsdämpfer D_1, D_2, D_3 und die Federn sind leicht konstruierbar. Die nun beschriebene Wirkungsweise und der Zusammenhang zwischen den einzelnen Grössen soll nun erörtert werden.

*Ableitung der Gleichung**

Die Ableitung der Differentialgleichung ist in mehreren Schritten möglich. An Stelle des wirklichen Systems wird das Ersatzschwingsystem untersucht.

Abb. 5

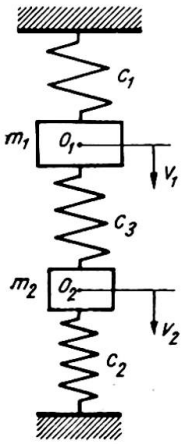

1. *Schritt.* Zwei Massen m_1 und m_2 sind mit zwei Federn c_1 und c_2 mit der Decke und Fussboden verbunden (Abb. 5). Zwischen den beiden Massen m_1 und m_2 befindet sich eine Feder c_3. Die Ruhelage sei durch die beiden Punkte O_1 und O_2 gekennzeichnet. Die Bewegungsgleichung ist aufzustellen. Wenn die Masse m_1 sich nach unten bewegt, zieht die Kraft $c_1 v_1$ die Masse zurück. Die Zusammendrückung der mittleren Feder ist $v_1 - v_2$. Die Kraft, die dadurch ausgeübt wird, ist $c_3(v_1 - v_2)$. Die Bewegungsgleichung lautet (Abb. 6)

$$m\ddot{v}_1 = -c_1 v_1 - c_3(v_1 - v_2) \quad . \quad . \quad . \quad . \quad . \quad (12)$$

Ebenso kann man eine entsprechende Gleichung für die Masse m_2 aufstellen. Die Bewegungsgleichungen lauten:

$$\left.\begin{aligned} m_1\ddot{v}_1 + (c_1 + c_3)v_1 - c_3 v_2 = 0 \\ m_2\ddot{v}_2 + (c_2 + c_3)v_2 - c_3 v_1 = 0 \end{aligned}\right\} \quad . \quad . \quad . \quad . \quad (13)$$

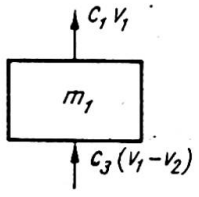

Abb. 6

Wir stellen uns nun folgende Frage: Gibt es eine harmonische Bewegung dieses Systems und wie gross sind die Ausschläge a_1 und a_2 der Massen m_1 bzw. m_2? Welche Schwingungszahl liefert eine harmonische Bewegung?

Wir machen also für die Bewegung die Ansätze:

$$\left.\begin{aligned} v_1 = a_1 \sin \omega t \\ v_2 = a_2 \sin \omega t \end{aligned}\right\} \quad . \quad . \quad . \quad . \quad . \quad . \quad (14)$$

* Den Hartog, Seite 77.

und bestimmen die Ableitungen nach der Zeit. Setzt man diese Werte in die Bewegungsgleichung (13) ein, so ergibt sich:

$$\left.\begin{aligned} a_1(-m_1\omega^2+c_1+c_3)-a_2c_3=0 \\ -a_1c_3+a_2(-m_2\omega^2+c_2+c_3)=0 \end{aligned}\right\} \quad \ldots\ldots \quad (15)$$

Aus der ersten Gleichung von (15) kann man den Wert a_1/a_2 und aus der zweiten Gleichung kann man ebenfalls das Verhältnis ausrechnen. Wenn es eine Lösung gibt, müssen beide Werte einander gleich sein. Man erhält auf diese Weise eine Gleichung für die Eigenschwingungszahl ω, die lautet:

$$\omega^4-\omega^2\left[\frac{c_1+c_3}{m_1}+\frac{c_2+c_3}{m_2}\right]+\frac{c_1c_2+c_2c_3+c_1c_3}{m_1m_2}=0 \quad \ldots\ldots \quad (16)$$

Es gibt zwei Lösungen ω_1^2 und ω_2^2 für die eine harmonische Bewegung möglich ist.

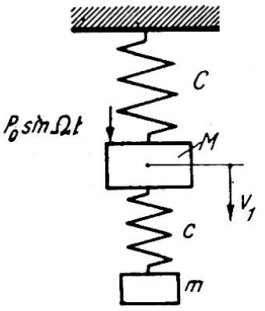

Abb. 7

2. *Schritt.* Nun soll die Aufgabestellung etwas abgeändert werden. Auf die Brücke mit der Masse M (Abb. 7) soll durch die Verkehrsbelastung eine harmonische Kraft $P=P_0 \sin \Omega t$ aufgebracht werden. An der Brücke sei ein zweiter Träger mit der Masse m und der Federkonstante c befestigt. Die Frage lautet: welche Schwingung führt dieses System aus? Man bekommt die Bewegungsgleichungen, indem man in den Gleichungen (13) den Wert $c_2=0$ setzt und in der ersten Gleichung die aufgezwungene Schwingung berücksichtigt.

$$\left.\begin{aligned} M\ddot{v}_1+(C+c)v_1-cv_2=P_0 \sin \Omega t \\ m\ddot{v}_2+c(v_2-v_1)=0 \end{aligned}\right\} \quad \ldots \quad (17)$$

Setzen wir $v_1=a_1 \sin \Omega t$ und $v_2=a_2 \sin \Omega t$ ein, so erhält man für jene aufgezwungene Schwingungszahl Ω eine harmonische Schwingung, für die folgende Gleichungen erfüllt sind:

$$\left.\begin{aligned} a_1(-M\Omega^2+C+c)-ca_2=P_0 \\ -a_1c+a_2(-m\Omega^2+c)=0 \end{aligned}\right\} \quad \ldots\ldots\ldots \quad (18)$$

Man setzt in dieser Gleichungsgruppe die Eigenschwingungszahl der Brücke $N=\sqrt{C/M}$, die Eigenschwingungszahl des Dämpfers $\nu=\sqrt{c/m}$ und das Verhältnis der Masse des Dämpfers zu der der Brücke, $\mu=m/M$, ein. Die Durchbiegung der Brücke unter der Last P_0 sei $\delta_{st}=P_0/C$.

Man erhält aus der Gleichungsgruppe (18)

$$\left.\begin{aligned} a_1\left(1+\frac{c}{C}-\frac{\Omega^2}{N^2}\right)-\frac{c}{C}a_2=\delta_{st} \\ a_1=a_2\left(1-\frac{\Omega^2}{\nu^2}\right) \end{aligned}\right\} \quad \ldots\ldots\ldots \quad (19)$$

Aus dieser Gleichung erhält man

$$\left.\begin{aligned} \frac{a_1}{\delta_{st}}&=\frac{1-\frac{\Omega^2}{\nu^2}}{\left(1-\frac{\Omega^2}{\nu^2}\right)\left(1+\frac{c}{C}-\frac{\Omega^2}{N^2}\right)-\frac{c}{C}} \\ \frac{a_2}{\delta_{st}}&=\frac{1}{\left(1-\frac{\Omega^2}{\nu^2}\right)\left(1+\frac{c}{C}-\frac{\Omega^2}{N^2}\right)-\frac{c}{C}} \end{aligned}\right\} \quad \ldots\ldots\ldots \quad (20)$$

Aus der ersten Gleichung bekommt man $a_1=0$, wenn $\Omega=\nu$ wird. Die Brücke bleibt dann in Ruhe, wenn die Eigenschwingungszahl des Dämpfungsträgers gleich der aufgezwungenen Schwingung Ω wird. Die Schwingung des Dämpfungsträgers wird

$$a_2=-\delta_{st}\frac{C}{c}=-\frac{P_0}{C}\cdot\frac{C}{c}=-\frac{P_0}{c}$$

Setzt man noch $\nu=N$, d.h. die Eigenschwingungszahl der Brücke gleich der Eigenschwingungszahl des Dämpfungsträgers, so wird

$$\frac{c}{m}=\frac{C}{M} \text{ oder } \frac{c}{C}=\frac{m}{M}=\mu$$

$$\left.\begin{aligned} v_1&=\delta_{st}\cdot\sin(\Omega t)\frac{1-\frac{\Omega^2}{\nu^2}}{\left(1-\frac{\Omega^2}{\nu^2}\right)\left(1+\mu-\frac{\Omega^2}{\nu^2}\right)-\mu}\\ v_2&=\delta_{st}\cdot\sin(\Omega t)\frac{1}{\left(1-\frac{\Omega^2}{\nu^2}\right)\left(1+\mu-\frac{\Omega^2}{\nu^2}\right)-\mu}\end{aligned}\right\} \quad \ldots\ldots \quad (21)$$

Fragen wir noch, ob es eine Resonanzschwingung gibt. Resonanz ist dann vorhanden, wenn die beiden Werte v_1 und v_2 für eine bestimmte aufgezwungene Schwingung unendlich werden. Dies ist der Fall, wenn der Nenner in den beiden Gleichungen (21) null wird.

$$\left(1-\frac{\Omega^2}{\nu^2}\right)\left(1+\mu-\frac{\Omega^2}{\nu^2}\right)-\mu=0 \quad \ldots\ldots\ldots \quad (22)$$

Setzt man $\frac{\Omega^2}{\nu^2}=\Phi$, so wird: $\Phi^2-2\Phi\left(1+\frac{\mu}{2}\right)+1=0$

Woraus folgt:

$$\left.\begin{aligned}\Phi_1&=1+\frac{\mu}{2}+\sqrt{\mu+\frac{\mu^2}{4}}\\ \Phi_2&=1+\frac{\mu}{2}-\sqrt{\mu+\frac{\mu^2}{4}}\end{aligned}\right\} \quad \ldots\ldots\ldots \quad (23)$$

Wenn $\mu=0{,}10$ angenommen wird, so erhält man folgendes Ergebnis:

$$\Phi_1=1{,}38, \qquad \Phi_2=0{,}73$$

Durch den Dämpfungsträger wurde also folgendes erreicht:

(*a*) Bei einer aufgezwungenen Schwingung, die der Eigenschwingung der Brücke gleich ist, bleibt die Brücke in Ruhe. Für diesen Fall hat der Dämpfungsträger eine Bedeutung.

(*b*) Dafür ist aber bei einer Schwingung, die 27% unter und 38% über der Eigenschwingungszahl des Hauptträgers liegt, eine Resonanz vorhanden.

Hätte man nur eine einzige Schwingungszahl, so könnte man in einfacher Weise durch den Dämpfungsträger erreichen, dass der Brückenträger in Ruhe bleibt. Da aber die Schwingungszahl der aufgebrachten Schwingung sehr veränderlich ist, muss noch eine Dämpfung eingebaut werden, wodurch die in Abb. 4 dargestellte Wirkung erreicht wird.

3. *Schritt.* Wenn nun zwischen Brückentragwerk und Dämpfungsträger ein Flüssigkeitsdämpfer eingeschaltet wird, lauten die Bewegungsgleichungen

$$\left.\begin{aligned} M\,.\,\ddot{v}_1+Cv_1+c(v_1-v_2)+k(\dot{v}_1-\dot{v}_2)&=P_0\,.\,\sin\Omega t\\ m\ddot{v}_2+c(v_2-v_1)+k(\dot{v}_2-\dot{v}_1)&=0\end{aligned}\right\} \quad (24)$$

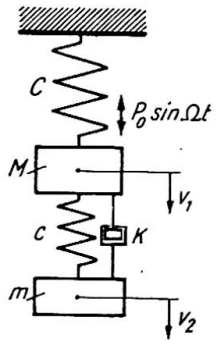

Abb. 8

Versucht man nun die Lösung mit dem Ansatz:

$$v_1=a_1\,.\,e^{i\Omega t} \qquad v_2=a_2\,.\,e^{i\Omega t}$$

so erhält man:

$$\dot{v}_1=a_1\,.\,i\Omega\,.\,e^{i\Omega t} \qquad \ddot{v}_1=-a_1\,.\,\Omega^2\,.\,e^{i\Omega t}$$

$$\dot{v}_2=a_2\,.\,i\Omega\,.\,e^{i\Omega t} \qquad \ddot{v}_2=-a_2\,.\,\Omega^2\,.\,e^{i\Omega t}$$

Diese Werte in die Gleichung (24) eingesetzt ergeben

$$\left.\begin{aligned} -Ma_1\Omega^2+Ca_1+c(a_1-a_2)+ik\Omega(a_1-a_2)&=P_0\\ -m\Omega^2a_2+c(a_2-a_1)+ik\Omega(a_2-a_1)&=0\end{aligned}\right\} \quad . \; . \; . \quad (25)$$

In den Gleichungen (25) sind a_1 und a_2 unbekannt. Rechnet man sich den Wert a_1 aus, so erhält man:

$$a_1=P_0\frac{(c-m\Omega^2)+i\Omega k}{[(-M\Omega^2+C)(-m\Omega^2+c)-m\Omega^2c]+i\Omega k[-M\Omega^2+C-m\Omega^2]} \quad . \; . \quad (26)$$

Nun kann man hier die komplexen Grössen durch die reellen Werte ausrechnen:

$$a_1{}^2=P_0{}^2\frac{(c-m\Omega^2)^2+\Omega^2k^2}{[(-M\Omega^2+C)(-m\Omega^2+c)-m\Omega^2c]^2+\Omega^2k^2[-M\Omega^2+C-m\Omega^2]^2} \quad . \quad (27)$$

Setzt man noch die Eigenschwingungszahl der Brücke $N^2=C/M$, die Eigenschwingungszahl des Dämpfungsträgers $\nu^2=c/m$, die Durchbiegung der Brücke unter der Last P_0 gleich δ_{st}, sodass $\delta_{st}=P_0/C$ wird, ferner das Verhältnis der Eigenfrequenz des Dämpfungsträgers zu dem der Brücke $\psi=\nu/N$ und die Dämpfungszahl $D=k/2mN$, das Verhältnis der Masse des Dämpfungsträgers zu der der Brücke $\mu=m/M$ und das Verhältnis der Schwingungszahl der aufgezwungenen Schwingung zur Eigenschwingungszahl der Brücke $\zeta=\Omega/N$, so wird:

$$a_1=\delta_{st}\,.\,\sqrt{\frac{(2D\zeta)^2+(\zeta^2-\psi^2)^2}{(2D\zeta)^2(\zeta^2-1+\mu\zeta^2)^2+[\mu\psi^2\zeta^2-(\zeta^2-1)(\zeta^2-\psi^2)]^2}} \quad . \; . \quad (28)$$

Dies ist die Gleichung, die die Vergrösserungsfunktion für die statische Auslenkung angibt:

$$\mathfrak{V}=\pm\sqrt{\frac{(2D\zeta)^2+(\zeta^2-\psi^2)^2}{(2D\zeta)^2(\zeta^2-1+\mu\zeta^2)^2+[\mu\psi^2\zeta^2-(\zeta^2-1)(\zeta^2-\psi^2)]^2}} \quad . \; . \; . \quad (29)$$

In der beifolgenden Tafel III sind die Zahlenwerte für verschiedene Dämpfungen D angegeben. Die Abb. 9 zeigt das Ergebnis. Setzt man die Dämpfung $D=0$, so erhält man

$$\mathfrak{V}=\pm\frac{\zeta^2-\psi^2}{\mu\psi^2\zeta^2-(\zeta^2-1)(\zeta^2-\psi^2)} \quad . \; . \; . \; . \; . \; . \; . \quad (30)$$

TAFEL III

Vergrösserungsfaktor $\mathfrak{V}$

ζ	$D=0$	$D=0{,}10$	$D=0{,}16$	$D=0{,}20$	$D=\infty$
0,50	1,40	1,40	1,40	1,39	1,38
0,60	1,73	1,73	1,72	1,72	1,65
0,70	2,56	2,50	2,42	2,38	2,17
0,80	13,10	4,97	4,10	3,87	3,38
0,82	30,20	5,23	4,44	4,24	3,84
0,84	6,00	4,92	4,70	4,62	4,47
0,86	2,25	3,84	4,50	4,75	5,37
0,88	0,99	3,15	4,29	4,82	6,75
0,90	0,25	2,71	4,06	4,82	9,17
0,92	0,27	2,49	3,90	4,77	14,48
0,94	0,71	2,46	3,82	4,73	35,70
0,96	1,13	2,56	3,84	4,72	72,75
0,98	1,58	2,78	3,97	4,73	17,70
1,00	2,10	3,18	4,10	4,75	10,00
1,02	2,76	3,57	4,32	4,75	6,92
1,04	3,72	4,16	4,50	4,66	5,27
1,06	5,29	4,85	4,62	4,51	4,23
1,08	8,55	5,52	4,60	4,27	3,53
1,10	19,72	5,87	4,40	3,97	3,02
1,16	7,61	4,35	3,34	2,99	2,08
1,20	4,06	3,20	2,68	2,45	1,63
1,30	1,89	1,77	1,65	1,58	1,15

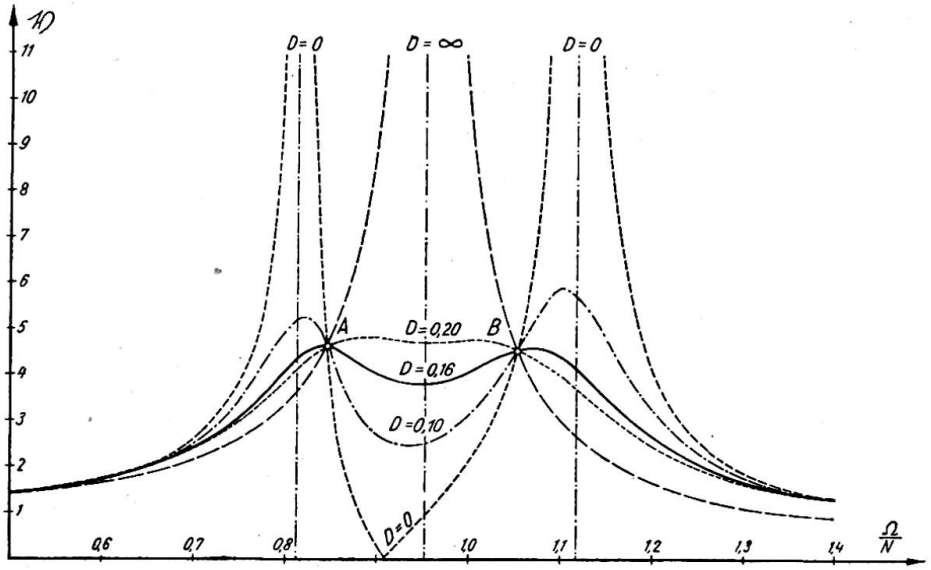

Abb. 9

Dieser Wert stimmt mit (20) inhaltlich überein. Für $D=\infty$ erhält man volle Verbindung der beiden Träger, also praktisch nur einen Träger mit der Masse $(M+m)$. In diesem Fall ist die Vergrösserungsfunktion

$$\mathfrak{V}=\frac{1}{1-(1+\mu)\zeta^2} \quad . \quad . \quad . \quad . \quad . \quad . \quad . \quad . \quad (31)$$

Der Wert stimmt mit der Gleichung (8) überein.

Man kann nun die Gleichung (29) noch weiter untersuchen und die Frage stellen, ob es ζ-Werte gibt, die von der Dämpfung D unabhängig sind. Von der Dämpfung unabhängig wird der Ausdruck $\mathfrak{V}$ dann, wenn die Dämpfungszahl im Zähler und Nenner von (29) gekürzt werden kann. Dies ist dann der Fall, wenn

$$\left(\frac{1}{\zeta^2-1+\mu\zeta^2}\right)^2=\left(\frac{\zeta^2-\psi^2}{\mu\zeta^2\psi^2-(\zeta^2-1)(\zeta^2-\psi^2)}\right)^2 \quad . \quad . \quad . \quad . \quad (32)$$

Man erhält eine quadratische Gleichung

$$\zeta^4-2\zeta^2\frac{\mu\psi^2+1+\psi^2}{2+\mu}+\frac{2\psi^2}{2+\mu}=0 \quad . \quad . \quad . \quad . \quad . \quad . \quad (33)$$

Es gibt also zwei Werte ζ_1 und ζ_2, für die die Lösung von der Dämpfung unabhängig ist. Dies sind die Punkte A und B in Abb. 9. Die Werte für A und B kann man aus der viel einfacheren Gleichung (31) berechnen. Man kann nun noch—und das ist das Ziel der Untersuchung—fragen, wie man die Eigenschwingungszahlen ν und N aufeinander abstimmen muss, um die Vergrösserungsfunktion $\mathfrak{V}$ in den beiden Punkten A und B gleich gross zu erhalten. Ist dies der Fall, so muss

$$\frac{1}{1-\zeta_1^2(1+\mu)}=-\frac{1}{1-\zeta_2^2(1+\mu)} \quad . \quad . \quad . \quad . \quad . \quad . \quad . \quad (34)$$

Das Minuszeichen kommt daher, dass zu einem positiven Wert von A der Punkt B′ mit negativem Vorzeichen gehört. Aus der Gleichung (34) folgt

$$\zeta_1^2+\zeta_2^2=\frac{2}{1+\mu} \quad . \quad . \quad . \quad . \quad . \quad . \quad . \quad . \quad . \quad (35)$$

Andererseits muss die Gleichung (33) erfüllt sein. Da die Summe der Lösungen $\zeta_1^2+\zeta_2^2$ in jeder quadratischen Gleichung gleich dem negativen mittleren Glied ist, wird

$$\frac{2}{1+\mu}=\frac{2(\mu\psi^2+1+\psi^2)}{2+\mu} \quad . \quad . \quad . \quad . \quad . \quad . \quad . \quad . \quad (36)$$

Daraus ergibt sich

$$\psi=\frac{1}{1+\mu} \quad . \quad . \quad . \quad . \quad . \quad . \quad . \quad . \quad . \quad . \quad (37)$$

Wenn man $\mu=0{,}1$ wählt, d.h. also die Masse des Dämpfungsträgers zu $\frac{1}{10}$ der Masse des Hauptträgers, wird

$$\psi=\frac{1}{1{,}1}=0{,}909091 \quad . \quad . \quad . \quad . \quad . \quad . \quad . \quad . \quad (38)$$

Dieser Wert ist in der Tafel III gewählt worden. Der Dämpfer muss eine Eigenschwingungszahl haben, die nur 0,91 der Eigenschwingungszahl des Hauptträgers ist.

Die Vergrösserungsfunktion $\mathfrak{V}$ wird in diesem Fall

$$\mathfrak{V}=\sqrt{1+\frac{2}{\mu}}=\sqrt{21}=4{,}58$$

Nun wurde für $D=0{,}10$, $D=0{,}20$ und $D=0{,}16$ der Verlauf der Vergrösserungsfunktion gerechnet. Als diejenige Linie, die über die Punkte A und B nicht hinausgeht, wurde die Linie mit $D=0{,}16$ ermittelt. Das Ergebnis ist somit:

(1) Der Dämpfungsträger muss eine Eigenschwingungszahl einschliesslich der Federn, mit denen er mit dem Hauptträger verbunden ist, haben, die das 0,91-fache der Eigenschwingungszahl des Hauptträgers beträgt.
(2) Die Masse des Trägers ist $\frac{1}{10}$ der Masse des Hauptträgers.
(3) Die Dämpfung muss $D=0{,}16$ sein.

Dadurch ist der Dämpfungsträger eindeutig festgelegt. Ein Beispiel soll die Konstruktion zeigen.

Beispiel

Der Dämpfungsträger einer vorgespannten Betonbrücke ist zu entwerfen. Die Abmessungen der Brücke sind in Abb. 10 angegeben.

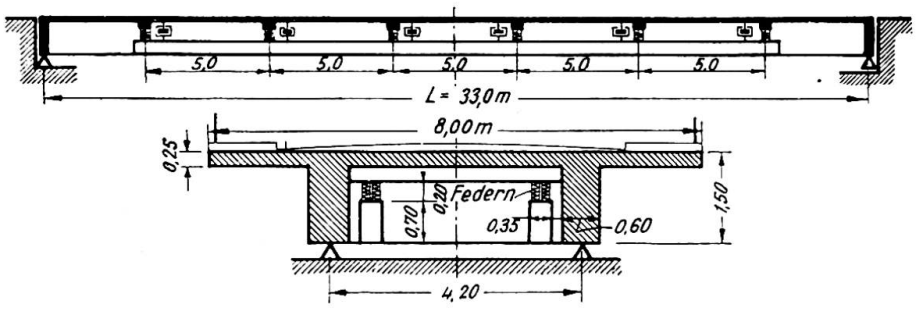

Abb. 10

Zahlenwerte:

Trägheitsmoment der Brücke: $J_I=688{,}10^5$ cm.^{4}
Masse der Brücke: $\mu_I=0{,}0956$ kg./cm.^{2} sec.^{2}
Elastizitätsmodul: $E=210\,000$ kg./cm.^{2}

Die Eigenschwingungszahl der Brücke ergibt sich aus (1) zu:

$$N=\frac{\pi}{2\,.\,3300^2}\sqrt{\frac{210\,000\,.\,688\,.\,10^5}{0{,}0965}}=1{,}76 \text{ Hertz}$$

Die erforderliche Masse des Dämpfungsträgers beträgt:

$$m=0{,}1\,.\,0{,}0956\,.\,33=0{,}316 \text{ kg./cm.}^2 \text{ sec.}^2$$

Gewählt werden zwei Dämpfungsträger mit den Abmessungen:

$$l=25 \text{ m.}, \quad b=35 \text{ cm.}, \quad d=70 \text{ cm.}$$

$$\mu_{II}=\frac{0{,}316}{25}=0{,}0126 \text{ kg./cm.}^2 \text{ sec.}^2$$

Die erforderliche Eigenschwingungszahl der Dämpfungsträger beträgt:

$$\nu=0{,}91\,.\,1{,}76=1{,}6 \text{ Hertz}$$

Bezeichnet man mit ν_1 die Eigenschwingungszahl der Dämpfungsträger mit starrer Befestigung, mit ν_2 die Eigenschwingungszahl der starr gedachten Dämpfungsträger mit elastischer Befestigung, mit J_{II} das Trägheitsmoment der Dämpfungsträger und

mit C_F das Gesamtfedermass aller Aufhängefedern, so gilt nach Dunkerley* angenähert:

$$\frac{1}{\nu^2}=\frac{1}{\nu_1{}^2}+\frac{1}{\nu_2{}^2} \quad \ldots\ldots\ldots \quad (39)$$

Mit: $\nu_1=\dfrac{\pi}{2\left(\frac{l}{5}\right)^2}\sqrt{\dfrac{EJ_{II}}{\mu_{II}}}$, $\nu_2=\dfrac{1}{2\pi}\sqrt{\dfrac{C_F}{\mu_{II}\,.\,l}}$, $J_{II}=\dfrac{70^4}{12}=20\,.\,10^5$ cm.^{4}, $\nu=1{,}6$ Hertz, $l=2500$ cm.

ergibt sich aus (39) das erforderliche Gesamtfedermass aller Aufhängefedern zu: $C_F=3200$ kg./cm.

Zusammenfassung

In Zukunft muss man den dynamischen Kräften auch im Stahlbetonbrückenbau entgegnen. An einem Beispiel wird gezeigt, wie man durch den Einbau eines Dämpfungsträgers den unliebsamen Schwingungen einer Brücke bei Resonanz begegnen kann.

Summary

In future, means must be adopted to counteract the effects of dynamic forces in reinforced-concrete bridges. From an example it is shown how, in a case of resonance, the undesirable oscillations of a bridge can be obviated by adding a damping girder.

Résumé

Il sera, à l'avenir, nécessaire de faire face aux efforts dynamiques, même dans la construction des ponts en béton armé. L'auteur montre, en s'appuyant sur un exemple, comment l'on peut s'opposer aux oscillations inopportunes qui peuvent se manifester par résonance, à l'aide d'une poutre d'amortissement.

* Dunkerley, *Philosophical Transactions*, 1894.

AI 2

Dynamic increments in an elementary case

Les influences dynamiques considérées dans un cas élémentaire

Dynamische Zuschläge in einem einfachen Fall

Dr. ARNE HILLERBORG
Stockholm

In the Preliminary Publication to the Congress in Liège in 1948, the author presented the first results of an investigation of dynamic influences of moving loads on girders. This work was carried out at the Institution of Structural Engineering and Bridge Building at the Royal Institute of Technology, Stockholm, Sweden, under the supervision of Professor G. Wästlund. The final results of the investigation were published in 1951 in a treatise,* which also describes the theoretical and experimental methods used. A summary of the practical results will be given here.

The case that has been studied is that of a single load moving smoothly at a constant speed along a simply supported girder. The girder has been supposed to be of uniform section and to be straight under dead load. The following factors have been taken into account:

the mass of the girder,
the mass of the load,
the velocity of the load,
spring-mounting of the load,
viscous damping of the girder (internal and external),
dry friction in the load-carrying spring.

These factors have been given a dimensionless form by introducing the notations:

$$\nu = \frac{\text{mass of load}}{\text{mass of girder}}$$

$$\alpha = \frac{\text{velocity of load}}{2 \times \text{length of girder} \times \text{frequency of girder}}$$

$$\mu = \frac{\text{frequency of load}}{\text{frequency of girder}}$$

$$\theta = \frac{\text{spring friction force}}{\text{weight of load}}$$

$e^{-\frac{2\pi\beta}{\sqrt{1-\beta^2}}}$ = ratio of two consecutive amplitudes in the same direction of the free vibration of the girder.

* *Dynamic Influences of Smoothly Running Loads on Simply Supported Girders.*

In the above notations, the frequency of the girder is the fundamental frequency of the undamped girder at no load.

Two different values are used for the constant β. One of them, denoted only by β, refers to an external damping force, while the other, denoted by β_1, refers to an internal damping force.

In the investigation, a distinction was made between two cases, viz. spring-borne and non-spring-borne loads, but, as the former is of much greater practical importance, only the results relating to spring-borne loads will be given here.

A dynamic increment in a quantity is defined by:

$$\epsilon = \frac{\text{dynamical value}}{\text{static value}} - 1$$

To make the definition strict, it is also necessary to know what kind of quantity is measured and what dynamical and static values are to be used. This is indicated

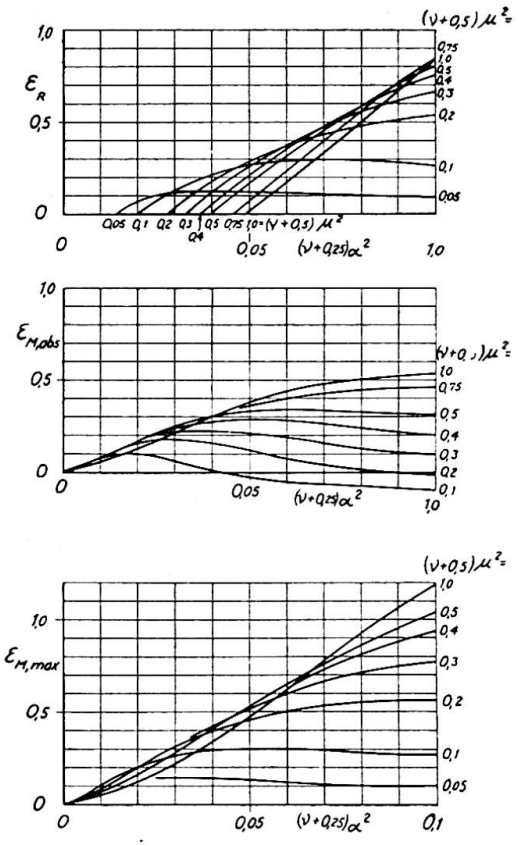

Fig. 1

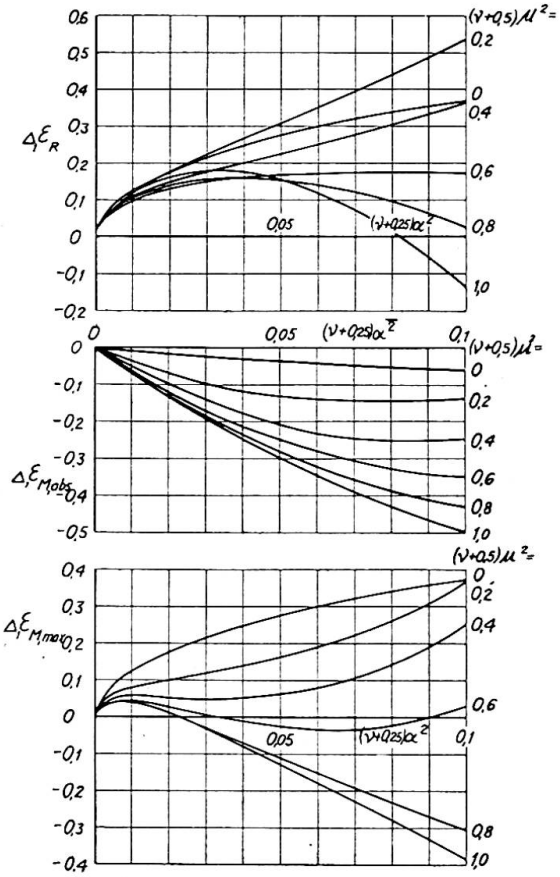

Fig. 2

by subscripts as follows: M for moments, Q for shearing forces, and R for reaction forces. The following definitions show what values are to be taken:

$$\epsilon_{abs} = \frac{\text{greatest dynamical value for the girder}}{\text{greatest static value for the girder}} - 1$$

$$\epsilon_{max} = \text{maximum of } \frac{\text{greatest dynamical value at any point}}{\text{greatest static value at the same point}} - 1$$

The value ϵ_{abs} (the absolute increment) expresses the greatest influence of a given kind (for instance, the greatest moment) on the girder, and is therefore the most interesting value in dealing with girders of uniform strength. The value ϵ_{max} gives the greatest dynamic increment at any section of the girder. This value is of great interest in studying girders of non-uniform strength (for instance, reinforced-concrete girders).

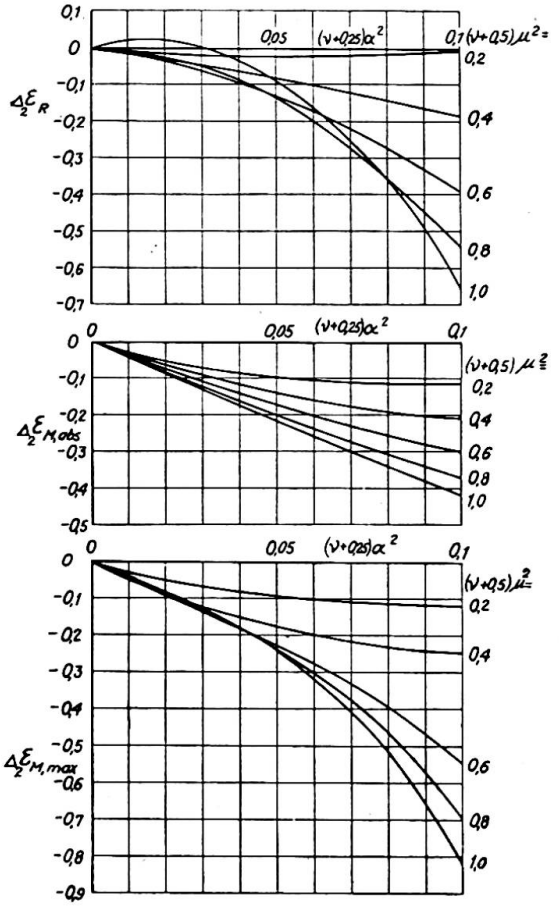

Fig. 3

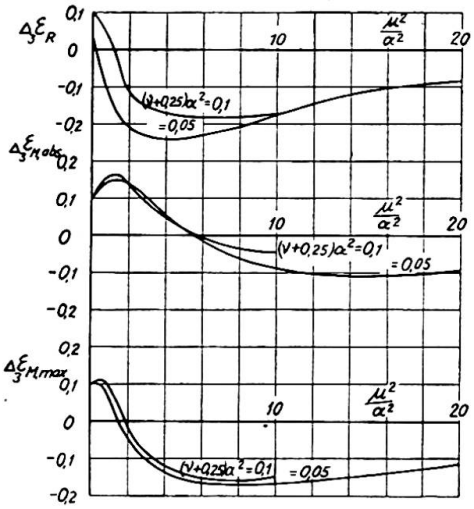

Fig. 4

The most interesting dynamic increments are $\epsilon_{M,\,max}$, $\epsilon_{M,\,abs}$, $\epsilon_{Q,\,max}$, $\epsilon_{Q,\,abs}$, and ϵ_R. The latter has only one subscript, as the gauge point must be at the support, and the definition of ϵ_R is:

$$\epsilon_R=\frac{\text{greatest dynamical reaction force}}{\text{greatest static reaction force}}-1$$

It can be shown that:

$$\epsilon_{Q,\,abs}=\epsilon_R$$

Further, it has been shown that $\epsilon_{Q,\,max}$ may with sufficient accuracy be put equal to $\epsilon_{M,\,max}$ in this case. It is therefore sufficient to plot diagrams for the dynamic increments $\epsilon_{M,\,max}$, $\epsilon_{M,\,abs}$, and ϵ_R. Such diagrams are shown in figs. 1 to 4, from which the dynamic increments for any arbitrary values of ν, α, μ, β, β_1, and θ (within practical limits) can be calculated by means of the formula:

$$\epsilon=\epsilon_o+\frac{\beta}{\sqrt{\nu+0\cdot5}}\cdot\Delta_1\epsilon+\frac{\beta_1}{\sqrt{\nu+0\cdot5}}\cdot\Delta_2\epsilon+\frac{\theta}{0\cdot1}\cdot\Delta_3\epsilon$$

In this formula ϵ is the value taken from fig. 1, and the three $\Delta\epsilon$-values are taken from figs. 2 to 4.

The values of ϵ which are given by this formula are approximate, as it has been constructed in the way that is described below, but it seems always to give sufficiently accurate values.

For studying the dynamic increments, use can be made of the theoretical methods described in the above-mentioned treatise. In the general case, however, the calculations are so intricate that it takes about two days to carry them out for a single case. If complete calculations including four values of each of the six variables were to be made, the number of calculations would be $4^6=4096$, and the time required would be about twenty-five years. This is obviously impracticable, and some other method must be found in order to limit the work, even if the results will be less accurate.

For plotting the diagrams in figs. 1 to 4 the following method has been used. To begin with, the case $\nu=\infty$ has been studied, that is, the case where the mass of the

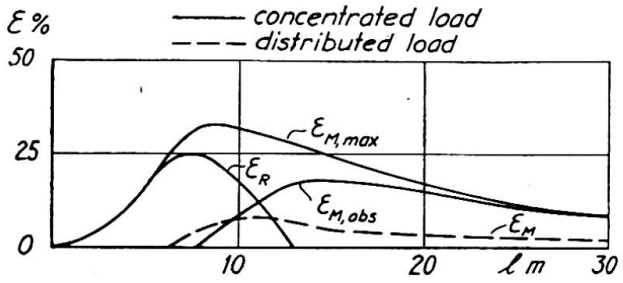

Fig. 5

girder is neglected in comparison with that of the load. In this case the calculations are so simple that they can be carried out almost completely. When studying the results of these calculations, trials have been made to find simple approximate relations between ϵ and the variables. It was then found that the above formula gave sufficiently accurate results in this case. This formula and the corresponding diagrams have thus first been made for the case $\nu=\infty$, in which the numbers 0·25 and 0·5 added to ν are without significance. It is to be noted that, in this case, the values of $\nu\alpha^2$, $\nu\mu^2$, and $\frac{\beta}{\sqrt{\nu}}$ are finite.

After the case $\nu=\infty$ had been studied theoretically, a very complete series of tests comprising ν-values between 0·75 and 5 was made. The test values were then compared with the theoretical values for $\nu=\infty$, and it was found that if ν was increased by the values given in the formula and the diagrams, the agreement was sufficiently close for all test values.

In order to give an idea of the order of magnitude of the dynamic increments caused by the influence studied in this investigation, the diagram in fig. 5 has been plotted on the following assumptions:

(1) The deflection under live load is 1/1250 of the span length.
(2) The velocity is 30 m./sec (=108 km./hour).
(3) The mass of the girder is neglected (this gives too small values of ϵ).
(4) The damping is neglected.
(5) The frequency of the load is 3 cycles per second.

For comparison, a curve for a distributed load is also shown in fig. 5. The

assumptions on which this curve is based are such that it gives only a lower limit for the increments.

The investigation has shown that dynamic influences of moving loads of nearly any kind on simply supported girders can be calculated theoretically, but in complicated cases the calculations are very laborious. This difficulty is still more pronounced when the girder is supported in a more intricate manner, for instance when it is continuous, although the calculations are possible in principle. On the other hand, the investigation has also shown that a comparatively simple test set-up can give reliable test values with a small amount of work. It therefore seems advisable that future investigations of this subject should mostly be based on model tests, especially in relatively complicated cases. Theoretical studies are of course of great value for the right understanding of the dynamical problems, but the number of numerical calculations should be limited.

In addition to such studies of elementary cases, it is of course also valuable to make tests on real bridges under real loads. However, these tests must be carried out and treated in a scientific and methodical way, and not at random. Thanks to the development of measurement engineering, we are today much better equipped for making such tests than we were only ten years ago. Resistant wire strain gauges and oscillographic recorders have made it possible to get accurate records of strains in any points of the load-carrying structures without much work and at small costs.

It seems to the author that the conditions are now favourable for acquiring a much better knowledge of the dynamical problems in bridge building if they are attacked methodically.

Summary

The practical results of an investigation of dynamic problems are summarised. A complete report on the investigation was published in 1951 in a book entitled *Dynamic Influences of Smoothly Running Loads on Simply Supported Girders.*

It is pointed out that the conditions are now favourable for acquiring a better knowledge of the dynamic problems if they are attacked methodically.

Résumé

L'auteur expose sommairement les résultats pratiques d'une étude relative aux problèmes dynamiques. Un rapport complet sur cette étude a été publié en 1951 dans un livre intitulé *Dynamic Influences of Smoothly Running Loads on Simply Supported Girders* (Influences dynamiques des charges roulantes à allure uniforme sur les poutres à appuis simples).

L'auteur fait remarquer que les conditions actuelles sont favorables à l'approfondissement de nos connaissances des problèmes dynamiques, si l'on aborde ces problèmes d'une manière méthodique.

Zusammenfassung

Der vorliegende Bericht enthält eine Zusammenfassung der praktischen Ergebnisse einer Untersuchung dynamischer Probleme. Ein vollständiger Bericht über diese Untersuchung wurde 1951 in einem Buch unter dem Titel *Dynamic Influences of Smoothly Running Loads on Simply Supported Girders* (Dynamische Einflüsse gleichmässig beweglicher Lasten auf einfach unterstützten Trägern) veröffentlicht.

Der Verfasser weist darauf hin, dass die gegenwärtigen Verhältnisse für eine Vertiefung unserer Kenntnisse der dynamischen Probleme günstig sind, wenn diese Probleme methodisch in Angriff genommen werden.

Leere Seite
Blank page
Page vide

AI 3

The calculation of plastic collapse loads for plane frames

Le calcul des charges plastiques de rupture des cadres plans

Die Berechnung der plastischen Brucklasten ebener Rahmentragwerke

B. G. NEAL and P. S. SYMONDS

Engineering Department, Cambridge University

Brown University, Providence, R.I., U.S.A.

INTRODUCTION

Plastic design methods have been developed with a view to providing a more rational and economical approach to the design of framed structures whose members possess a high degree of ductility.[1] The methods are applicable to cases in which the members of a frame possess a relation between bending moment and curvature of the form illustrated in fig. 1. The important features of this type of relation are:

(i) If the curvature increases indefinitely, the bending moment tends to a limiting value $\pm M_p$, termed the fully plastic moment, regardless of the previous history of loading.

(ii) An increase of curvature is always accompanied by an increase of bending moment of the same sign, unless the bending moment has attained its fully plastic value.

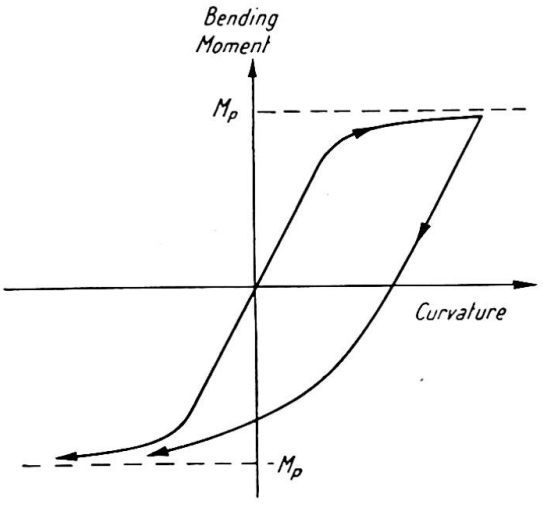

Fig. 1

The behaviour of mild steel beams conforms quite closely to these assumptions, and experimental investigations have confirmed the validity of applying plastic methods of design to framed structures of mild steel.[2] As yet, little consideration has been given to the possibility of applying the plastic methods

[1] For references see end of paper.

to framed structures of other ductile materials, such as certain of the light alloys.

When the fully plastic moment is attained at a particular cross-section of a member, the curvature at this cross-section is indefinitely large, so that a finite change of slope can occur over an indefinitely short length of the member at this cross-section. The member therefore behaves as though a hinge existed at this cross-section, rotation of the hinge being possible only when resisted by the fully plastic moment. This concept of a plastic hinge was first introduced by Maier-Leibnitz,[3] and it is of great value in considering the behaviour of framed structures under load.

For the sake of simplicity, consider first a framed structure subjected to several loads, each load maintaining the same proportion to each of the other loads. If the loads are steadily increased, the structure will first support the loads by wholly elastic action. Eventually a plastic hinge will form at the most highly stressed cross-section. If the loads are increased still further, this plastic hinge will rotate under a constant bending moment, its fully plastic moment, and further plastic hinges will form and rotate in other parts of the structure. Finally, a condition will be reached in which a sufficient number of plastic hinges have formed to transform the structure into a mechanism. The structure will then continue to deform to an indefinite extent while the loads remain constant, until the geometry of the structure is changed appreciably. Such changes may either check the growth of the deflections, or cause a catastrophic collapse by accentuating the effects of the loads. In practice, strain-hardening also checks the growth of deflections. The theoretical condition of indefinite growth of deflection under constant loads is termed plastic collapse.

The methods of plastic design are used in conjunction with a load factor. The structure is designed so that the most unfavourable combination of the working loads, when multiplied by the chosen load factor, would just cause a failure by plastic collapse. This procedure is justifiable even when the loads do not necessarily maintain the same proportions to one another, for it has been shown that plastic collapse of a structure will occur at the same set of loads regardless of the sequence in which the individual loads were brought up to their collapse values. It is clear that the load factor has a very precise meaning in plastic design, for it represents the margin of safety which is provided against an actual physical failure of the structure.

Several methods for computing plastic collapse loads have been suggested.[4, 5] These methods have been capable, in principle, of determining plastic collapse loads for framed structures of any degree of complexity. In practice, however, their application has been limited by the amount of time required for the necessary computations. In the present paper a method is presented which enables plastic collapse loads and their corresponding mechanisms to be determined very simply. The method consists essentially of building up the actual collapse mechanism from a certain number of independent components, which are termed the independent partial collapse mechanisms. Corresponding to any mechanism which is being investigated, a value can be found for the applied load by applying the Principle of Virtual Work.[6] It has been shown that the correct collapse mechanism is the one to which there corresponds the smallest possible value of the applied load. The method consists therefore of combining the independent partial collapse mechanisms in a systematic manner in order to reduce the corresponding value of the applied load to its least possible value. In order to explain and justify the method, a simple example will first be discussed. Detailed calculations will then be given for a single-bay pitched-roof portal frame, and the calculations for a three-bay pitched-roof portal frame will also be outlined. Calculations for a two-bay three-storey rectangular frame have been given elsewhere.[7]

SIMPLE ILLUSTRATIVE EXAMPLE

The rectangular portal frame shown in fig. 2 will be used as a basis for the discussion of the method. All the joints of this frame are assumed to be rigid, and the feet of the stanchions are rigidly built in. The dimensions of the frame are as shown, and horizontal and vertical loads W are applied at the positions indicated in the figure. The fully plastic moment of each member is M_p, and the problem is to find the value of W which causes failure by plastic collapse.

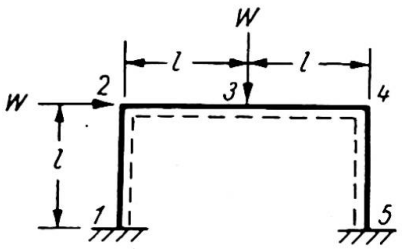

Fig. 2

For this particular type of structure it is known that there are only three possible collapse mechanisms, and these mechanisms are shown in figs. 3(*a*), 3 (*b*) and 3(*c*). In these figures the magnitudes of the plastic hinge rotations are all shown in terms of a single parameter θ. For reference, the signs of the plastic hinge rotations are also given, although in the technique to be described there is no need to take account of these signs. The sign convention adopted is that a hinge rotation is positive if the hinge is opening when viewed from inside the frame.

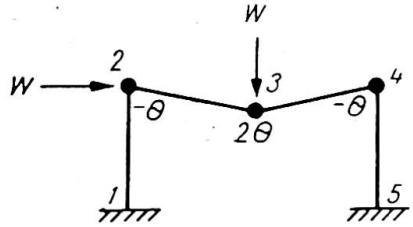

Fig. 3(*a*)

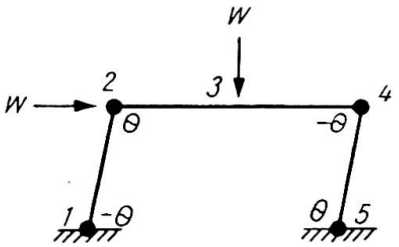

Fig. 3(*b*)

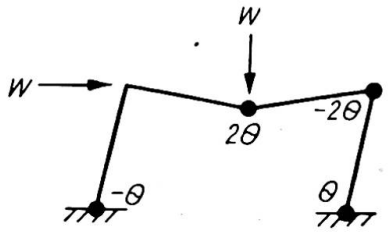

Fig. 3(*c*)

For each mechanism it is possible to calculate a corresponding value of W by applying the principle of virtual work in the special form that the virtual work done by the applied loads during a small displacement of the mechanism is equal to the virtual work absorbed in the plastic hinges. Considering the mechanism of fig. 3(*a*), for example, it is seen that during the small mechanism displacement shown, the horizontal load W does no work and the vertical load W, displaced through a distance $l\theta$, does virtual work $Wl\theta$. To calculate the virtual work absorbed in the plastic hinges, it is noted that the work absorbed in any individual hinge is always positive. Since the fully plastic moment is M_p everywhere in the frame, the virtual work absorbed in the plastic hinges is at once seen to be $4\theta M_p$, since the total rotation of all the plastic hinges is 4θ. Applying the principle of virtual work:

$$Wl\theta = 4\theta M_p, \text{ or } W = 4\frac{M_p}{l} \quad . \quad . \quad . \quad . \quad . \quad . \quad . \quad . \quad (1)$$

Similar calculations for the mechanisms of figs. 3(*b*) and 3(*c*) are readily made. The results of these calculations are:

fig. 3(*b*): $$Wl\theta=4\theta M_p, \text{ or } W=4\frac{M_p}{l} \quad . \ . \ . \ . \ . \ . \ . \ . \quad (2)$$

fig. 3(*c*): $$2Wl\theta=6\theta M_p, \text{ or } W=3\frac{M_p}{l} \quad . \ . \ . \ . \ . \ . \ . \ . \quad (3)$$

The correct collapse mechanism can now be distinguished by applying what has been termed the *kinematic principle* of plastic collapse.[6, 8] This principle states that: " For a given frame and loading, the correct collapse mechanism is the mechanism to which there corresponds the smallest possible value of the applied loads." For the particular problem of fig. 2, it follows that the actual collapse mechanism is the mechanism shown in fig. 3(*c*), which yields the lowest value of W, namely $3M_p/l$.

Examination of figs. 3(*a*), 3(*b*) and 3(*c*) reveals the fact that the mechanism of fig. 3(*c*) is a direct combination of the mechanisms of figs. 3(*a*) and 3(*b*), in the sense that the displacements and plastic hinge rotations of this mechanism are obtained by summing the corresponding quantities for the mechanisms of figs. 3(*a*) and 3(*b*). In fact, as will be seen later, these latter two mechanisms are the independent partial collapse mechanisms for this structure and loading. In general, all possible collapse mechanisms can be formed by combining the independent partial collapse mechanisms. In the simple problem under consideration there is, of course, only one possible combination to be investigated.

The particular feature of the combination of the independent mechanisms of figs. 3(*a*) and 3(*b*) which is of interest is that for both these mechanisms the corresponding value of W was $4M_p/l$, whereas for the mechanism of fig. 3(*c*) which resulted from their combination the value of W was only $3M_p/l$. This reduction of W is due to the cancellation of the plastic hinge at the cross-section 2 which occurs when the mechanisms are combined. When the two mechanisms are superposed, the virtual work done by the loads in each case may be added to obtain the virtual work done in the resulting mechanism. However, to obtain the virtual work absorbed in the plastic hinges in the resulting mechanism, work $2\theta M_p$ must be subtracted from the sum of the virtual work absorbed in the two independent mechanisms. This is to account for the term θM_p which was included in the virtual work absorbed in each of these mechanisms for the plastic hinge at the cross-section 2, which disappears as a result of the superposition. The virtual work equation for the resulting mechanism is thus obtained by adding equations (1) and (2), and subtracting $2\theta M_p$ from the resulting work absorbed in the plastic hinges, giving:

$$Wl\theta+Wl\theta=4\theta M_p+4\theta M_p-2\theta M_p$$

or $$2Wl\theta=6\theta M_p,$$

which was previously obtained as equation (3).

In general, the technique for combining the independent mechanisms thus consists in selecting pairs of independent mechanisms which themselves yield low values of W, and which can be combined so as to cancel a plastic hinge. Such a combination may, as has been seen, result in a value for W which is lower than the value corresponding to either of the mechanisms which were combined. Even in complicated problems, the combinations to be tried are usually small in number, so that a solution can be obtained with great rapidity.

It is, of course, essential to start an analysis with the correct number of independent mechanisms. In fact, the number of independent mechanisms is always equal to the

number of independent equations of equilibrium for the frame. To justify this statement, it is necessary to consider the statics of the illustrative example of fig. 2, although it should be stressed that in actual applications of the technique there is no need to write down the equations of equilibrium. However, it is recommended that solutions should always be checked by statics, making use of the *principle of uniqueness of solution*,[6, 8] which states that: "If a sufficient number of plastic hinges occur in a frame to transform the frame into a mechanism, and if a bending moment diagram can be constructed for the frame in which the fully plastic moment occurs at each plastic hinge position, then the corresponding load is the correct collapse load if the fully plastic moment is not exceeded anywhere in the frame."

Examples of this form of check are given later in the paper.

The equations of equilibrium

The equations of equilibrium for the frame illustrated in fig. 2 are written down most conveniently in terms of the bending moments at the five cross-sections numbered from 1 to 5 in fig. 2. It will be seen from this figure that when these five bending moments are known, the bending moment distribution for the entire frame is determined, for between any adjacent pair of these cross-sections the shear force is constant, so that the bending moment must vary linearly along the length of the member. These five bending moments are denoted by $M_1, M_2, \ldots M_5$, the suffix indicating the relevant cross-section. The sign convention adopted for these bending moments is that a positive bending moment causes tension in the fibres of a member adjacent to the dotted line in fig. 2.

This frame has three redundancies, for if a cut is imagined to be made at section 1, for example, and the values of the shear force, thrust and bending moment at this section are known, the entire frame becomes statically determinate. These three quantities can therefore be regarded as the redundancies of the frame. Since there are five unknown bending moments, it follows that there must be two independent equations of equilibrium.

The first of these equations of equilibrium expresses the fact that the vertical load W is carried by the shear forces in the horizontal member 234. Fig. 4 shows the

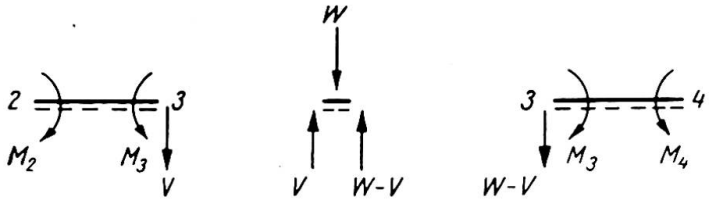

Fig. 4

relevant forces and bending moments, the load W being carried by a shear force V in the member 23 and a shear force $W-V$ in the member 34. Taking moments for the equilibrium of the members 23 and 34, it is found that

$$M_3-M_2=Vl$$

$$M_3-M_4=(W-V)l$$

On adding these equations to eliminate V, it is found that

$$2M_3-M_2-M_4=Wl \quad . \quad . \quad . \quad . \quad . \quad . \quad . \quad . \quad (4)$$

In a similar way, an equation expressing the fact that the horizontal load W is carried

by the shear forces in the vertical members 12 and 45 may be found. This equation is

$$M_2-M_1+M_5-M_4=Wl \quad . \quad . \quad . \quad . \quad . \quad . \quad . \quad . \quad (5)$$

Equations (4) and (5) constitute the two independent equations of equilibrium.

In the mechanism of fig. 3(*a*) plastic hinges have formed at the cross-sections 2, 3 and 4, so that the magnitude of the bending moment at each of these cross-sections is M_p. Having regard to the sign convention, these bending moments are

$$M_2=-M_p, \quad M_3=M_p, \quad M_4=-M_p$$

When these values are substituted in equation (4), a value for W is immediately found, this value being $W=4M_p/l$.

It will be seen that the mechanism of fig. 3(*a*) corresponds to equation (4) in the special sense that in this mechanism each of the bending moments appearing in equation (4) takes on its fully plastic value, and that the sign of each bending moment is such as to give rise to the largest possible value of W. In a similar way, the mechanism of fig. 3(b) may be said to correspond to equation (5). If each of the bending moments appearing in equation (5) is given its fully plastic value, and the sign of each bending moment is such that the largest value of W is obtained, the following values are found:

$$M_1=-M_p, \quad M_2=M_p, \quad M_4=-M_p, \quad M_5=M_p.$$

These are the fully plastic moments appearing in the mechanism of fig. 3(*b*).

To generalise, it may be said that any mechanism corresponds in this special sense to a particular equation of equilibrium. It follows that for any particular frame and loading the number of independent mechanisms will be equal to the number of independent equations of equilibrium. In the particular example under consideration there are only two independent equations of equilibrium, namely equations (4) and (5) and any other equation of equilibrium must be obtainable by combining these two equations. Correspondingly, it follows that any possible mechanism will be found to be a combination of the mechanisms of figs. 3(*a*) and 3(*b*). In this particular example, there is only one possible combination of these mechanisms, which is illustrated in fig. 3(*c*). The equation of equilibrium which corresponds to this mechanism is obtained by adding equations (4) and (5) so as to eliminate M_2, giving

$$2M_3-M_1-2M_4+M_5=2Wl \quad . \quad . \quad . \quad . \quad . \quad . \quad . \quad (6)$$

This addition corresponds to the superposition of the mechanisms of figs. 3(*a*) and 3(*b*). The bending moments at the plastic hinges may be seen from this equation, or from the mechanism of fig. 3(*c*), to be

$$M_1=-M_p, \quad M_3=M_p, \quad M_4=-M_p, \quad M_5=M_p,$$

and the corresponding value of W is $3M_p/l$.

For convenience of discussion, the loads have previously been referred to as the variables, whereas in an actual design the loads will be given quantities and the problem is to find the required fully plastic moments of the members. When viewed in this light, the problem just discussed amounts to determining the *greatest* value of M_p, rather than the least value of W, corresponding to any possible mechanism, for it is the quantity Wl/M_p which is determined for any particular mechanism by a virtual work analysis, and minimising W for given values of M_p and l amounts to maximising M_p for given values of W and l.

To summarise, then, the proposed method is as follows:

(1) Determine the correct number of independent mechanisms by calculating the number of independent equations of equilibrium.
(2) Calculate the required values of the fully plastic moments of the members by virtual work for these independent mechanisms.
(3) Investigate combinations of these mechanisms so as to maximise the required fully plastic moments.
(4) Check the solution by constructing a bending moment diagram.

An application of the method to a single-bay pitched-roof portal frame will now be given in detail, followed by a brief indication of the application of the method to a three-bay pitched-roof portal frame.

PITCHED-ROOF PORTAL DESIGN

As an illustration of the practical application of the proposed method of design, typical calculations for a pitched-roof portal frame will now be given. The dimensions of the frame are as indicated in fig. 5, the roof slope being $22\frac{1}{2}°$. The working loads on the frame are also shown in fig. 5. These working loads, which are given in tons, are assumed to be spread uniformly over the purlins and sheeting rails shown in the figure. Of these loads, the vertical loads of 2·61 tons, acting on each rafter, are due to dead and superimposed (snow) loads, and the remaining loads are wind pressures and suctions. The frame is to be designed to a load factor of 1·75 for the case in which only the dead and superimposed loads are acting, and to a load factor of 1·4 for the case in which the wind loads are also acting. Each member of the frame will be taken to have the same cross-section, with a fully plastic moment M_p.

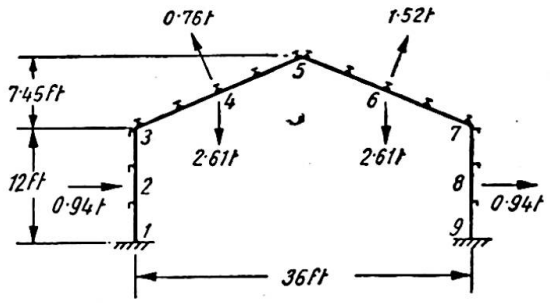

Fig. 5

Design for dead, superimposed and wind loads

The first design case which will be considered is the design to a load factor of 1·4 for the case in which the wind loads are acting in conjunction with the dead and superimposed loads. The first step is to decide how many independent partial collapse mechanisms must be considered. The number of such mechanisms for any given frame and loading has been shown to be equal to the number of independent equations of equilibrium. It is therefore necessary to calculate the number of independent equations of equilibrium, and this is done most conveniently by counting the number of bending moments which are needed to specify the bending moment distribution for the entire frame and subtracting the number of redundancies.

For each of the four members of the frame, the loads will be assumed to be uniformly distributed, so that the distribution of bending moment is parabolic. Each parabola will be completely specified if the values of the bending moment at three sections are known. These three sections are chosen most conveniently for the present purpose as the two end sections and the central section in each member. It follows that the bending moment distribution for the entire frame will be specified completely by the values of the bending moments at the nine cross-sections numbered

from 1 to 9 in fig. 5. This frame has three redundancies, and so there must be six independent equations of equilibrium.

It follows that there must be six independent partial collapse mechanisms. These mechanisms are illustrated in figs. 6–11, inclusive. It will be seen that the mechanisms of figs. 6, 7, 8 and 9 are merely simple beam failure mechanisms, and fig. 10 shows a simple sidesway mechanism. If it were not known that there must be six independent mechanisms, it might be concluded that these five mechanisms constituted the independent partial collapse mechanisms, and thus a calculation of the correct number of independent mechanisms is a vital preliminary operation in the analysis. However, a sixth independent mechanism must be selected, and the most convenient choice is the mechanism shown in fig. 11. In each figure the rotation of each plastic hinge is given in terms of a single variable θ. There is no need to consider the signs of the plastic hinge rotations, since the virtual work absorbed in a plastic hinge is always positive. However, for convenience in the later stages of the calculations when the solution is checked by statics, the signs of the plastic hinge rotations are also given, the sign convention being that a hinge rotation is positive if the joint is opening when viewed from within the portal.

In the simple beam failure mechanisms of figs. 6, 7, 8 and 9, the plastic hinges within the spans are all shown as occurring at mid-span. However, the loads on these spans are all assumed to be uniformly distributed in the first instance, so that these plastic hinges might occur anywhere within the spans. This is because a plastic hinge within a span must occur at a position of maximum bending moment, and the positions at which the maximum bending moments occur are not known until a later stage in the analysis. However, in the preliminary calculations it is convenient to take these plastic hinges as occurring in mid-span.

Now consider the mechanism of fig. 6. For the hinge rotations shown, the plastic hinge at mid-span moves through a distance 6θ ft. The average displacement of the uniformly distributed load of 0·94 tons is therefore 3θ ft., so that the virtual work done by this load, taking into account the load factor of 1·4, is $0{\cdot}94 \cdot 1{\cdot}4 \cdot 3\theta$ tons-ft. The total plastic hinge rotation involved in the mechanism is 4θ, so that the virtual work absorbed in the plastic hinges is $4\theta M_p$. Applying the principle of virtual work, it is found that

$$4\theta M_p = 0{\cdot}94 \cdot 1{\cdot}4 \cdot 3\theta = 3{\cdot}95\theta$$
$$M_p = 0{\cdot}99 \text{ tons-ft.} \quad \ldots\ldots\ldots\ldots \quad (7)$$

The virtual work equation for the mechanism of fig. 7 is precisely the same as

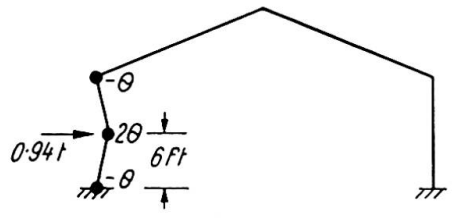

Fig. 6

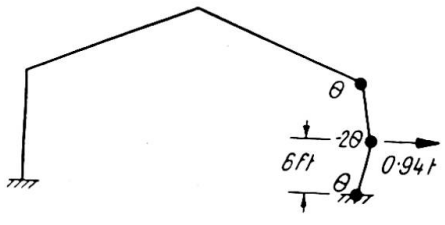

Fig. 7

equation (7). Corresponding virtual work equations may be written down at once for the mechanisms of figs. 8 and 9. These equations are:

fig. 8:
$$4\theta M_p = 1{\cdot}4[2{\cdot}61 \cdot 4{\cdot}5\theta - 0{\cdot}76 \cdot 4{\cdot}87\theta] = 11{\cdot}3\theta$$
$$M_p = 2{\cdot}83 \text{ tons-ft.} \quad \ldots\ldots\ldots\ldots \quad (8)$$

fig. 9:
$$4\theta M_p = 1{\cdot}4[2{\cdot}61 \cdot 4{\cdot}5\theta - 1{\cdot}52 \cdot 4{\cdot}87\theta] = 6{\cdot}08\theta$$
$$M_p = 1{\cdot}52 \text{ tons-ft.} \quad \ldots\ldots\ldots\ldots \quad (9)$$

The geometry of the sidesway mechanism of fig. 10 is also simple. Each side load of 0·94 tons moves through an average distance of 6θ ft., and the entire roof moves laterally through a distance 12θ ft. The virtual work equation is

$$4\theta M_p = 1{\cdot}4[2\,.\,0{\cdot}94\,.\,6\theta + 0{\cdot}76 \sin 22\tfrac{1}{2}^\circ\,.\,12\theta] = 20{\cdot}7\theta$$

$$M_p = 5{\cdot}18 \text{ tons-ft.} \quad . \quad . \quad . \quad . \quad . \quad . \quad . \quad . \quad . \quad . \quad . \quad . \quad (10)$$

The geometry of the mechanism of fig. 11 is a little more complicated. If the hinge at joint 3 rotated through an angle $-\theta$ while the joint 5 remained rigid, joint 7 would

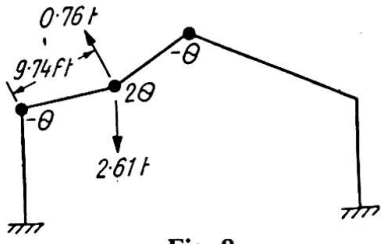

Fig. 8

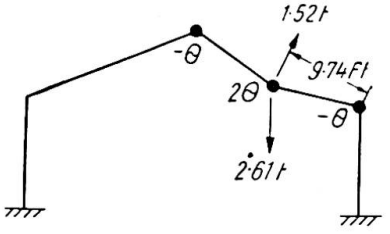

Fig. 9

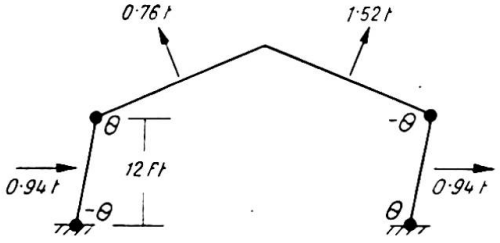

Fig. 10

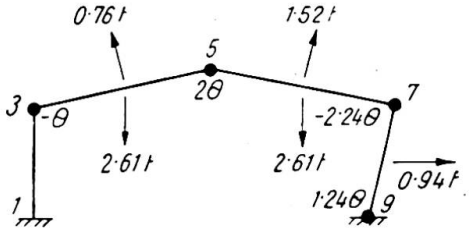

Fig. 11

move downwards through a distance 36θ ft. Since there can be no downwards motion of joint 7 for a small displacement of the mechanism, it follows that the hinge at joint 5 must rotate through an angle $36\theta/18 = 2\theta$ so as to reduce the vertical displacement of joint 7 to zero. This hinge rotation causes a horizontal displacement of joint 7 through a distance $2\theta\,.\,7{\cdot}45 = 14{\cdot}9\theta$ ft., so that the rotation of the hinge at joint 9 is $14{\cdot}9\theta/12 = 1{\cdot}24\theta$. The hinge rotation at joint 7 is then seen to be $-2{\cdot}24\theta$, and it is found that the centre of the member 57 moves $11{\cdot}2\theta$ ft. to the right and 9θ ft. downwards. The virtual work equation for this mechanism may now be written down as follows:

$$6{\cdot}48\theta M_p = 1{\cdot}4[2\,.\,2{\cdot}61\,.\,9\theta - 0{\cdot}76\,.\,9{\cdot}74\theta + 1{\cdot}52 \sin 22\tfrac{1}{2}^\circ\,.\,11{\cdot}2\theta$$
$$- 1{\cdot}52 \cos 22\tfrac{1}{2}^\circ\,.\,9\theta + 0{\cdot}94\,.\,7{\cdot}45\theta]$$
$$= 56{\cdot}6\theta$$
$$M_p = 8{\cdot}73 \text{ tons-ft.} \quad . \quad . \quad . \quad . \quad . \quad . \quad . \quad . \quad . \quad . \quad . \quad . \quad (11)$$

Among the six independent partial collapse mechanisms, the highest values of M_p are thus 5·18 tons-ft. and 8·73 tons-ft. for the mechanisms of figs. 10 and 11, respectively. The next step is thus to investigate the combination of these two mechanisms. It is seen that if the mechanism of fig. 10 is superposed on the mechanism of fig. 11, the rotation of the hinge at joint 3 is cancelled, so that the resulting mechanism is as shown in fig. 12. The virtual work equation for this mechanism is obtained by adding equations (10) and (11), and subtracting $2\theta M_p$ from the resulting virtual work

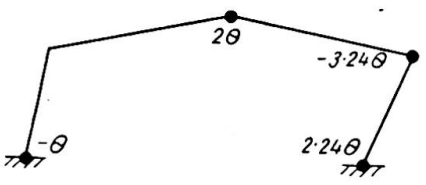

Fig. 12

absorbed in the plastic hinges, since a term θM_p was included in each of these equations for the plastic hinge at joint 3. The virtual work equation is thus:

$$(4+6\cdot48-2)\theta M_p=20\cdot7\theta+56\cdot6\theta$$

$$8\cdot48\theta M_p=77\cdot3\theta$$

$$M_p=9\cdot12 \text{ tons-ft.} \quad . \quad . \quad . \quad . \quad . \quad (12)$$

The highest value of M_p obtained from the other four independent mechanisms of figs. 6, 7, 8 and 9 was 2·83 tons-ft. for the mechanism of fig. 8, and it is readily seen that there is no possible combination of these mechanisms with the mechanism of fig. 12 which will result in a further increase in the value of M_p. It is therefore concluded that the mechanism of fig. 12 is the actual collapse mechanism, subject to the proviso that no consideration has yet been given to the possibility of the occurrence of plastic hinges at positions other than those numbered from 1 to 9 in fig. 5. When this solution is checked by statics it will, in fact, be found that the plastic hinge shown at the apex of the roof in fig. 12 should be located somewhat to the left of the apex.

Check by statics

The solution can be checked by constructing a bending moment diagram for the frame. If the fully plastic moment is not exceeded at any cross-section, the solution is correct. The actual bending moment at a cross-section may be regarded as the sum of the "free bending moment," produced in the frame by the applied loads when a cut has been made at some cross-section so as to render the frame statically determinate, and the "redundant bending moment" produced in the frame by the three redundancies. For convenience, the form of the redundant bending moment diagram will be considered first.

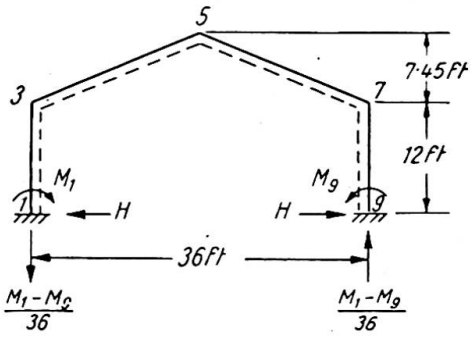

Fig. 13

The three redundancies may be taken as the bending moments, M_1 and M_9, at the feet of the vertical members, and the horizontal thrust H, as in fig. 13. With no external loads acting on the structure, the vertical reactions at the feet of the vertical members would be equal and opposite, and of magnitude $(M_1-M_9)/36$ as shown in the figure. In drawing the bending moment diagrams, the sign convention will be that a positive bending moment will cause a member to sag inwards, and thus to produce tension in the flange of the member which is adjacent to the dotted line in fig. 13. With the redundancies as shown in this figure, the redundant bending moment diagram is thus of the form indicated in fig. 14, in which the members of the frame have been redrawn to a horizontal base, and positive bending moments are plotted as ordinates below this base. In fig. 14 the dotted line

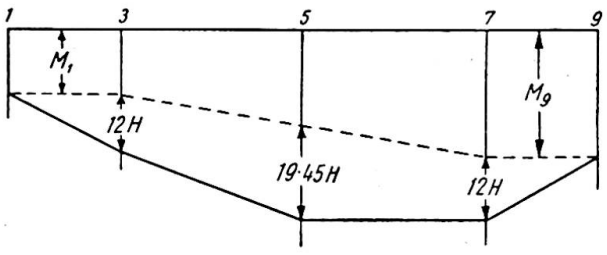

Fig. 14

indicates the form of the redundant bending moment diagram for the case in which H is zero, and the full line indicates the effect of superposing the bending moment diagram for the case in which H acts alone.

The free bending moment diagram refers to the bending moments produced in the frame by the applied loads when a cut is made at any arbitrary cross-section. The most convenient choice of cross-section for this purpose is the roof apex. Fig. 15 shows the free bending moment diagram, consisting of three parabolas, which is obtained in this way, the loads having been multiplied by the load factor of 1·4.

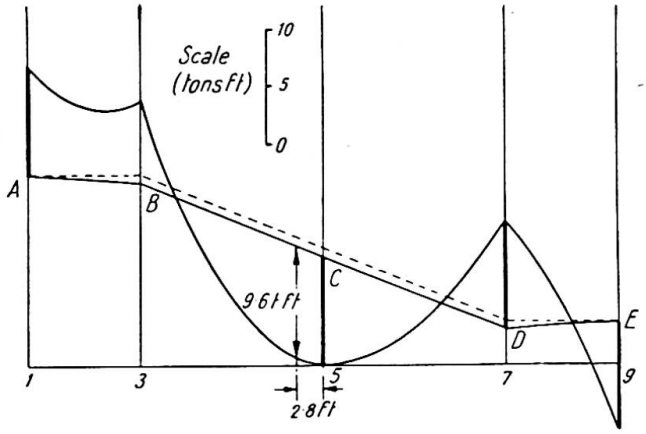

Fig. 15

The collapse mechanism of fig. 12 has four plastic hinges at the cross-sections 1, 5, 7 and 9, so that at these cross-sections the bending moment has its fully plastic value, which was found to be 9·1 tons-ft. To check the solution, it must be verified that a diagram of actual bending moments can be constructed in which the bending moment has the value 9·1 tons-ft. at these four cross-sections, and does not exceed this value at any other cross-section in the frame. Now the actual bending moment is equal to the sum of the free and redundant bending moments, so that if a redundant bending moment diagram is drawn in fig. 15 with the signs of the bending moments changed, the actual bending moment will be represented by the difference in ordinate between this diagram and the free bending moment diagram. The appropriate diagram is shown in fig. 15 as ABCDE.

The construction for this diagram is to lay off from the free bending moment diagram the calculated fully plastic moment of 9·1 tons-ft., with appropriate sign, at the four cross-sections 1, 5, 7 and 9. This gives the four points A, C, D and E on the redundant bending moment diagram. Referring to fig. 14, it is seen that the point B may then be plotted by making the slope of AB equal in magnitude to the slope of DE, but of opposite sign. A check can then be made by observing that the vertical intercept between C and the dotted line in fig. 15 is 19·45 H, whereas the corresponding intercept at D is 12 H. These intercepts both correspond to a value of H of 0·05 tons, thus checking the solution. However, it will be seen that although the bending moment at the cross-section 3 is less than the calculated fully plastic moment of 9·1 tons ft., a higher value of the bending moment occurs at a distance of 2·8 ft. along the left-hand rafter member from the apex joint, this value being 9·6 tons-ft. This does not imply an error in the virtual work calculations, for in those calculations the choice of plastic hinge positions was restricted to the ends and centres of the members. The calculation of the required fully plastic moment could be refined by carrying out

a fresh virtual work calculation in which the plastic hinge at the apex joint 5 was moved to the new position 2·8 ft. along the left-hand rafter member. However, it is unnecessary to perform this calculation, for it will be seen that the design is, in fact, not governed by this loading case but by the dead and superimposed loading case. It is therefore noted that a value of M_p between 9·1 and 9·6 tons-ft. would be adequate for dead, superimposed and wind loads in conjunction.

Design for dead and superimposed loads

The design for dead and superimposed loads to a load factor of 1·75 will now be considered. The relevant working loads are merely loads of 2·61 tons uniformly distributed over the two rafters, as shown in fig. 16. Since this loading is symmetrical, the bending moment distribution for the frame is also symmetrical, and so only four bending moments are needed to specify the bending moment distribution. These may be taken as the bending moments at the cross-sections 1, 3, 4 and 5 in fig. 16. Due to symmetry, the frame has only two redundancies, for the bending moments at the cross-sections 1 and 9 are equal. The bending moment at cross-section 1 and the horizontal thrust can thus be regarded as the two redundancies. It follows that there are only two equations of equilibrium, and therefore two independent mechanisms. Both of these mechanisms must be symmetrical.

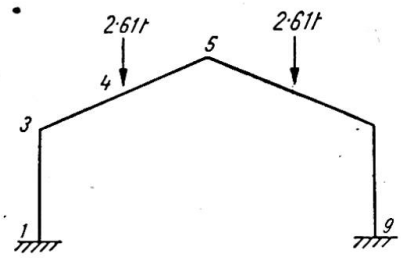

Fig. 16

The two independent mechanisms are illustrated in figs. 17 and 18. Fig. 17 merely represents failure of the two rafters as beamS, and the equation of virtual work is

$$8\theta M_p = 2 \,.\, 2{\cdot}61 \,.\, 1{\cdot}75 \,.\, 4{\cdot}5\theta = 41{\cdot}1\theta$$

$$M_p = 5{\cdot}14 \text{ tons-ft.} \quad . \quad . \quad . \quad . \quad . \quad . \quad . \quad . \quad . \quad . \quad . \quad (13)$$

In the mechanism of fig. 18, the hinge rotation θ at cross-section 1 would produce a horizontal movement of $19{\cdot}45\theta$ at the roof apex if there were no hinge rotation

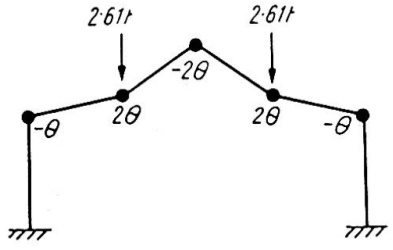

Fig. 17

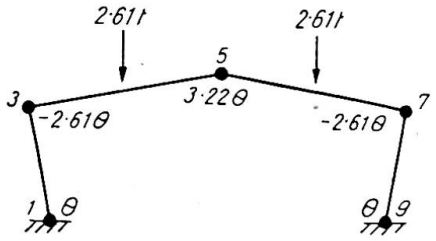

Fig. 18

at cross-section 3. The hinge rotation at cross-section 3 must therefore be $-19{\cdot}45\theta/7{\cdot}45 = -2{\cdot}61\theta$ in order that there should be no horizontal movement at the apex. The downwards vertical displacement at the apex is thus $18 \,.\, 1{\cdot}61\theta = 29{\cdot}0\theta$ ft. The virtual work equation is:

$$10{\cdot}44\theta M_p = 2 \,.\, 2{\cdot}61 \,.\, 1{\cdot}75 \,.\, 14{\cdot}5\theta = 132{\cdot}5\theta$$

$$M_p = 12{\cdot}7 \text{ tons-ft.} \quad . \quad . \quad . \quad . \quad . \quad . \quad . \quad . \quad . \quad . \quad . \quad (14)$$

It will be noted that this value of M_p exceeds the value found for the case in which the wind loads act in conjunction with the dead and superimposed loads. It follows

that the design must be governed by the present case in which only the dead and superimposed loads are acting.

Considering now the combination of the independent mechanisms, it will be seen that cancellation of the plastic hinge rotation at the roof apex can be achieved by superposing the mechanism of fig. 17, with all the hinge rotations and displacements increased by a factor of $3{\cdot}22/2=1{\cdot}61$, on the mechanism of fig. 18. The mechanism thus obtained is illustrated in fig. 19. The virtual work equation for this mechanism is obtained by adding equation (13), multiplied by 1·61, to equation (14), and subtracting $6{\cdot}44\theta M_p$ from the resulting virtual work absorbed in the plastic hinges, since a plastic hinge rotation of $3{\cdot}22\theta$ in each of the mechanisms at the roof apex has been cancelled. The resulting equation is:

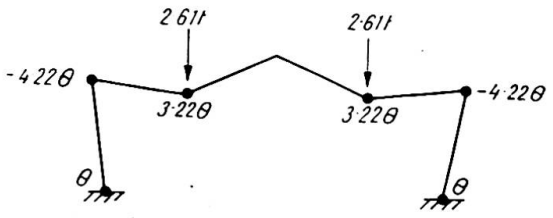

Fig. 19

$$(8\ .\ 1{\cdot}61+10{\cdot}44-6{\cdot}44)\ \theta M_p=41{\cdot}1\ .\ 1{\cdot}61\theta+132{\cdot}5\theta$$

$$16{\cdot}88\theta M_p=198{\cdot}7\theta$$

$$M_p=11{\cdot}8 \text{ tons-ft.} \quad . \quad . \quad . \quad . \quad . \quad . \quad (15)$$

The highest value of M_p obtained from these mechanisms is thus 12·7 tons-ft. for the mechanism of fig. 18. This is therefore the actual collapse mechanism, subject to possible alterations due to the occurrence of plastic hinges within the spans of the members rather than at the joints. A statical check will reveal, in fact, that the plastic hinge at the roof apex should be replaced by one plastic hinge in each rafter member.

Check by statics

The free bending moment diagram for the frame, cut at the roof apex, when subjected to the factored loads, is shown in fig. 20, together with the redundant bending moment diagram. This latter diagram is constructed by setting off the calculated fully plastic moment of 12·7 tons-ft. from the free bending moment diagram at the

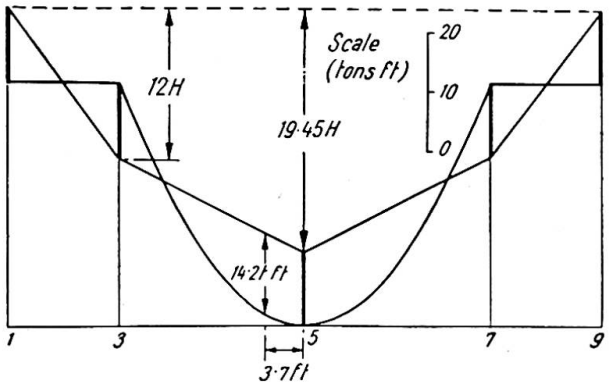

Fig. 20

cross-sections 1, 3, 5, 7 and 9. The value of the horizontal thrust can be calculated from the intercepts between the redundant bending moment line and the dotted line in fig. 20 at both the cross-sections 3 and 5. The value obtained in each case is 2·1 tons, thus checking the virtual work calculation. It will be seen that the greatest bending moment which occurs with this bending moment distribution is 14·2 tons-ft. at a distance of 3·7 ft. from the roof apex. Thus in the correct collapse mechanism

there should be plastic hinges in each rafter at a distance of about 3·7 ft. from the roof apex in place of the single plastic hinge shown at the apex in fig. 18. A fresh calculation for these new plastic hinge positions is readily made, either by virtual work or by adjusting the redundant bending moment line on the bending moment diagram, and the resulting value of M_p is found to be 13·2 tons-ft. A final refinement is to take account of the fact that the loads are not, in fact, uniformly distributed over the rafters, but are carried by five uniformly spaced purlins, as shown in fig. 5. The plastic hinges in the rafters will be located beneath the purlins which are adjacent to the roof apex, and the corresponding value of M_p is found to be 13·0 tons-ft. or 156 tons-in.

A choice of section can now be made. The fully plastic moment for a rolled steel joist is known to exceed the moment at which the yield stress is just reached in the outermost fibres by a factor termed the shape factor, which is about 1·15 for most sections.[4] Taking a yield stress of 15·25 tons/in.^{2}, the fully plastic moment M_p is thus:

$$M_p = 1{\cdot}15 \,.\, 15{\cdot}25 \,.\, Z = 17{\cdot}5\, Z \text{ tons-in.}$$

where Z in.^{3} is the section modulus. The required value of Z in the present case is:

$$Z = 156/17{\cdot}5 = 8{\cdot}91 \text{ in.}^3$$

The nearest available British Standard beam section is a 7×4×16 lb., with a section modulus of 11·29 in.^{3} This is therefore the required section. From the point of view of stability, the purlins and sheeting rails, together with some cross-bracing, would provide adequate stiffening for this section over the given spans.

THREE-BAY PITCHED-ROOF PORTAL FRAME

To illustrate the scope of the technique which has been described in detail, calculations for the three-bay frame whose dimensions and loads are as shown in fig. 21 will now be outlined briefly. As before, all the loads are assumed to be uniformly

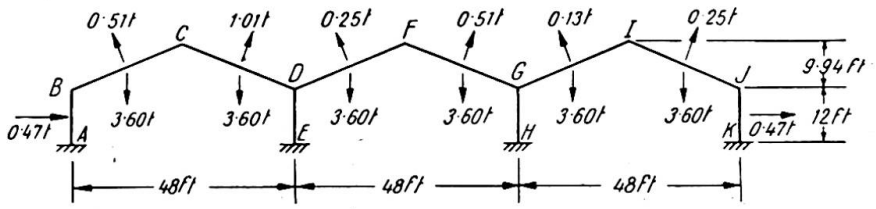

Fig. 21

distributed, and the vertical loads of 3·60 tons on each rafter member are due to dead and superimposed loads, the remaining loads being wind loads. In the first instance, it will be assumed that all the members of the frame are of the same cross-section, with a fully plastic moment M_p.

Design for dead, superimposed and wind loads

For this loading case, a load factor of 1·4 will be used. Examination of fig. 21 shows that twenty-three bending moments are needed to specify the bending moment distribution for the entire frame, which has nine redundancies. There must therefore be fourteen independent mechanisms. Eight of these mechanisms are accounted for by the simple beam type of failure mechanism (as in figs. 6, 7, 8 and 9, for example) occurring in the members AB, BC, CD, DF, FG, GI, IJ and JK. For these mechanisms, the highest value of M_p is obtained for the member GI, this value of M_p being

7·28 tons-ft. Two mechanisms must be counted for rotations of the joints D and G in fig. 21, for it will be realised that for each of these joints there will be an equation of rotational equilibrium between the three bending moments acting on the joint. There will also be one sidesway mechanism, with plastic hinges in the vertical members at A, B, D, E, G, H, J and K, for which the corresponding value of M_p is 1·69 tons-ft. The remaining three independent mechanisms may be chosen in a variety of ways, but the three mechanisms illustrated in figs. 22, 23 and 24 are probably the most convenient for the present purpose. It will be seen that each of these mechanisms is basically of the same type, with the rafters collapsing in one bay and thus causing sidesway of those parts of the frame lying to the right of the collapsing bay. For reference, the plastic hinge rotations are shown in these figures in magnitude only. It will be noted that the joints D and G remain unrotated in each of these mechanisms, since in each case any rotation of these joints would increase the work absorbed in the plastic hinges and so reduce the value of M_p.

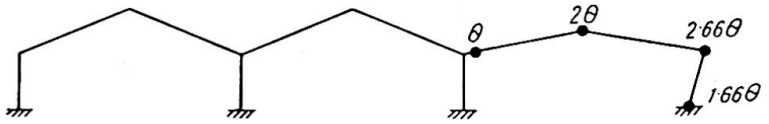

Fig. 22

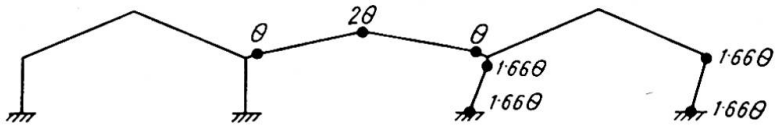

Fig. 23

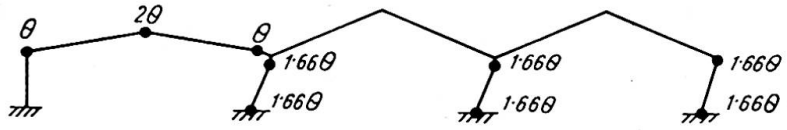

Fig. 24

The virtual work equations for these three mechanisms are found to be:

fig. 22: $7{\cdot}32\theta M_p = 123{\cdot}5\theta$, $M_p = 16{\cdot}9$ tons-ft. . . . . (16)

fig. 23: $10{\cdot}64\theta M_p = 120{\cdot}4\theta$, $M_p = 11{\cdot}3$ tons-ft. . . . . (17)

fig. 24: $13{\cdot}96\theta M_p = 115{\cdot}1\theta$, $M_p = 8{\cdot}25$ tons-ft. . . . . (18)

The highest value of M_p obtained from the independent mechanisms is thus 16·9 tons-ft. for the mechanism of fig. 22. It is easily seen that this value of M_p will not be increased by combination with any of the simple beam mechanisms, for which the highest value of M_p was found to be 7·28 tons-ft. It is also clear that the sidesway mechanism, for which M_p was found to be only 1·69 tons-ft., cannot be combined with advantage. It remains to investigate possible combinations of the three mechanisms of figs. 22, 23 and 24.

The mechanisms of figs. 22 and 23 can be combined if the hinge rotations and displacements in the mechanism of fig. 22 are all multiplied by a factor of 1·66, and

then superposed on the mechanism of fig. 23. This enables a clockwise rotation, of magnitude $1{\cdot}66\theta$, to be given to joint G, which cancels plastic hinge rotations of $1{\cdot}66\theta$ in the members GI and GH at this joint, while increasing the plastic hinge rotation in the member GF by $1{\cdot}66\theta$. This produces a net reduction in the virtual work absorbed of $1{\cdot}66\theta M_p$. The resulting virtual work equation for this combination is then seen from equations (16) and (17) to be:

$$1{\cdot}66 \,.\, 7{\cdot}32 \,.\, \theta M_p + 10{\cdot}64\theta M_p - 1{\cdot}66\theta M_p = 1{\cdot}66 \,.\, 123{\cdot}5\theta + 120{\cdot}4\theta$$

$$21{\cdot}1\theta M_p = 325\theta$$

$$M_p = 15{\cdot}4 \text{ tons-ft.} \quad . \quad . \quad . \quad . \quad (19)$$

This value of M_p is smaller than the value of 16·9 tons-ft. obtained for the mechanism of fig. 22, and it is clear that no other possible combination of the three mechanisms of figs. 22, 23 and 24 will yield a larger value of M_p. It is therefore concluded that the mechanism of fig. 22 is the actual collapse mechanism. This solution will not be adjusted to allow for the possible occurrence of plastic hinges at cross-sections other than the ends and centres of the members, for when the dead plus superimposed loading case is considered, it will be found that the wind loading case does not govern the design.

An interesting feature brought out by this analysis is that there are only four plastic hinges in the collapse mechanism, whereas the frame has nine redundancies. At collapse, therefore, only the right-hand bay of the frame is statically determinate, and in carrying out a statical check the bending moment diagram for the other two bays could not be constructed directly. Instead, it would be necessary to carry out a trial and error investigation to show that the six redundancies of these two bays could be chosen in at least one way so as to produce a resultant bending moment diagram in which the fully plastic moment was not exceeded anywhere in the frame. This would be a tedious process, and in view of the fact that this is not the loading case which governs the design, the check is probably not worth performing.

Design for dead and superimposed loads

A load factor of 1·75 will be used for this loading case. The loading, consisting merely of the vertical loads of 3·60 tons on each rafter, is symmetrical, so that the collapse mechanism and the bending moment distribution at collapse must also be symmetrical. It will be seen that the values of eleven bending moments will specify the bending moment distribution for the entire frame, and that owing to symmetry there are only five redundancies. There are thus six independent mechanisms, which must all be symmetrical. Three of these mechanisms are the simple beam type of failure mechanism in the *pairs* of rafters BC and IJ, CD and GI, and DF and FG. For each of these mechanisms, the corresponding value of M_p is 9·45 tons-ft. One mechanism must be counted for rotation of the joints D and G. The remaining two mechanisms are most conveniently chosen as the mechanisms shown in figs. 25 and 26.

The virtual work equations for these two mechanisms are:

fig. 25: $14{\cdot}64\theta M_p = 302{\cdot}4\theta, \quad M_p = 20{\cdot}6$ tons-ft. . . . . (20)

fig. 26: $10{\cdot}64\theta M_p = 151{\cdot}2\theta, \quad M_p = 14{\cdot}2$ tons-ft. . . . . (21)

The only possible combination of these mechanisms is obtained if the hinge rotations and displacements in the mechanism of fig. 25 are all multiplied by a factor of 0·83, and then superposed on the mechanism of fig. 26. This enables a counter-clockwise rotation of the joint D, of magnitude $0{\cdot}83\theta$, to be made, thus cancelling plastic rotations of $0{\cdot}83\theta$ in the members DC and DE at this joint, while increasing

the plastic hinge rotation in the member DF by $0{\cdot}83\theta$. This produces a net reduction in the virtual work absorbed of $0{\cdot}83\theta M_p$, and a similar reduction can be achieved by a clockwise rotation of the joint G. The resulting virtual work equation is then seen from equations (20) and (21) to be:

$$0{\cdot}83\,.\,14{\cdot}64\theta M_p+10{\cdot}64\theta M_p-1{\cdot}66\theta M_p=0{\cdot}83\,.\,302{\cdot}4\theta+151{\cdot}2\theta$$

$$21{\cdot}1\theta M_p=402\theta$$

$$M_p=19{\cdot}1 \text{ tons-ft.} \quad . \quad . \quad . \quad . \quad (22)$$

This value of M_p is less than the value of 20·6 tons ft. which was found to correspond to the mechanism of fig. 25. It may also be checked that the beam collapse mechanisms for the rafters cannot be combined with any of these mechanisms to produce a value

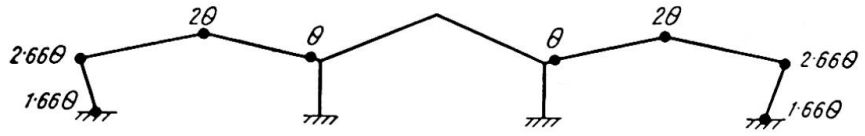

Fig. 25

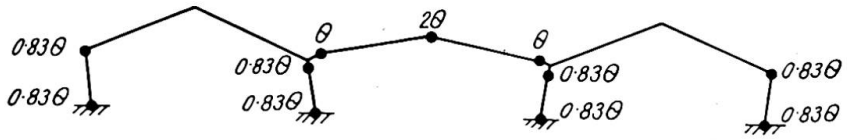

Fig. 26

of M_p greater than 20·6 tons-ft. The mechanism of fig. 25 is thus the actual collapse mechanism, subject to alterations due to the occurrence of plastic hinges at positions other than at the ends and centres of the members. A statical check will now be made which will also serve to indicate such alterations in the position of the plastic hinges.

Check by statics

Because of symmetry, the statical check need only be made for one half of the frame, say the left-hand half. For this portion of the frame, the free bending moment diagram is constructed by imagining cuts to be made at the apices C and F. The resulting diagram is given in fig. 27, for the case in which the loads have been multiplied by the load factor of 1·75. It will be seen that there is no free bending moment in the vertical member DE, and the diagram for this member has not been drawn.

For the members AB, BC and CD the redundant bending moment diagram may be constructed directly, since the bending moment has its fully plastic value at A, B, C and D. The horizontal thrust H in this bay can be calculated from the vertical intercept between the redundant bending moment diagram and the dotted line in fig. 27. In each case a value of 3·44 tons is obtained, thus checking the solution. Since the centre bay of the frame is not statically determinate at collapse, the redundant bending moment diagram for the member DF cannot be constructed directly. However, it is clear from the symmetry of the diagram about D that one possible redundant bending moment line for DF is the dotted line df shown in fig. 27, where fF represents the calculated fully plastic moment of 20·6 tons-ft. This line has a slope equal in magnitude to the line cd in fig. 27, and this corresponds to the same value of the

horizontal thrust of 3·44 tons which was found for the left-hand bay of the frame. If this were the actual redundant moment line for the member DF at collapse, it follows that there would be no resultant horizontal thrust on the vertical member DE, which would thus have zero bending moment throughout its length. It is therefore possible to construct a bending moment diagram for the entire frame in which the fully plastic moment is not exceeded at any cross-section, except within the spans of

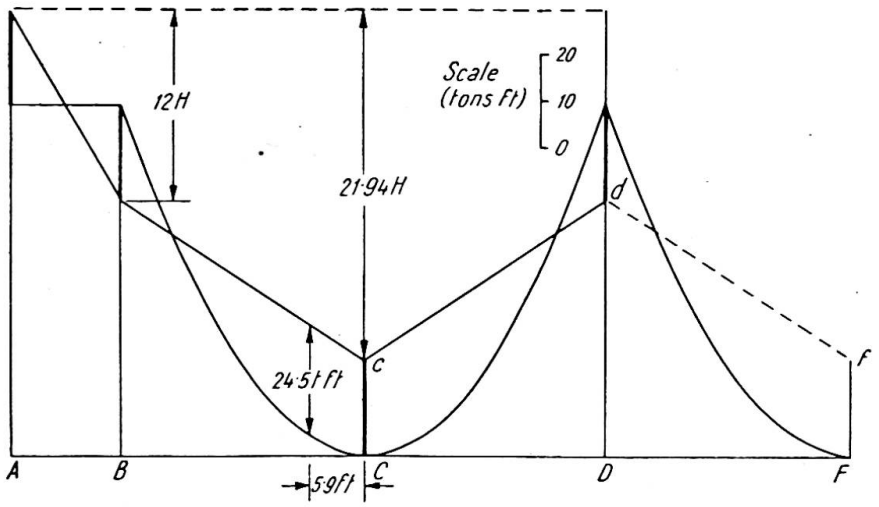

Fig. 27

the rafter members. This confirms that the correct solution was found by the virtual work analysis.

It will be seen from fig. 27 that plastic hinges will actually occur in the rafter members at distances of 5·9 ft. from the apices C and G, rather than at these apices. When this is taken into account, the value of M_p is found to be 21·9 tons-ft.

The statical check reveals the fact that the internal stanchions DE and GH need not be called upon to participate in the collapse mechanism, for it is possible to construct a resultant bending moment diagram in which these members are free from bending moment. These members, which were assumed in the first instance to possess a fully plastic moment M_p, thus function merely as props which hold up the rafter members. They could therefore be designed simply as compression members, and made of hollow tubing.

Conclusions

The merits of the method of design described in this paper can really be appreciated only by applying the method to practical examples. However, the foregoing examples serve to illustrate some of its advantages. The outstanding feature of the method is, of course, its rapidity. This is mainly due to the ease with which corresponding values of M_p can be obtained by the principle of virtual work, and this in turn is due largely to the fact that there is no need to establish sign conventions when applying this principle, since the virtual work absorbed in a plastic hinge must always be positive. A further important advantage of the method is that it enables solutions to be found without difficulty for those cases in which the entire frame is not statically determinate at collapse. Such cases have hitherto been somewhat intractable.

REFERENCES

(1) BAKER, J. F., "A Review of Recent Investigation into the Behaviour of Steel Frames in the Plastic Range," *J. Inst. Civ. Engrs.*, **31**, 188, 1949.
(2) BAKER, J. F., and HEYMAN, J, "Tests on Miniature Portal Frames," *The Structural Engineer*, **28**, 139, 1950.
(3) MAIER-LEIBNITZ, H. "Die Bedeutung der Zähigkeit des Stahles," *Prelim. Publ. 2nd Congress Intl. Assoc. Bridge and Structural Eng. Berlin*, 1936, p. 103.
(4) BAKER, J. F., "The Design of Steel Frames," *The Structural Engineer*, **27**, 397, 1949.
(5) NEAL, B. G., and SYMONDS, P. S., "The Calculation of Collapse Loads for Framed Structures," *J. Inst. Civ. Engrs.*, **35**, 20, 1950.
(6) GREENBERG, H. J., and PRAGER, W., "On Limit Design of Beams and Frames," *Proc. A.S.C.E.* **77**, *Separate* No. 59, 1951.
(7) NEAL, B. G., and SYMONDS, P. S., "The Rapid Calculation of the Plastic Collapse Load for a Framed Structure" (to be published in *Proc. Inst. Civ. Engrs. Part III*, **1**).
(8) HORNE, M. R., "Fundamental Propositions in the Plastic Theory of Structures," *J. Inst. Civ. Engrs.*, **34**, 174, 1950.

Summary

In suitable instances the application of plastic design methods to plane frames of ductile material, such as mild steel, leads to more rational and economical designs. These design methods are based on the calculation of the loads at which a structure collapses owing to excessive plastic deformation. Such collapses occur when a sufficient number of plastic hinges have formed to transform the structure into a mechanism, so that deflections can continue to grow, due to rotations of the plastic hinges, while the loads remain constant.

It is known that among all possible collapse mechanisms for a given frame and loading, the actual collapse mechanism is the one to which there corresponds the smallest possible value of the load. Recently, it has been pointed out that all the possible collapse mechanisms for a frame can be regarded as built up from a certain number of simple mechanisms. This has led to the development of a new technique for determining plastic collapse loads, in which these simple mechanisms are combined in a systematic manner so as to reduce the corresponding value of the load to its least possible value. For each mechanism which is investigated, the corresponding value of the load is determined very quickly by applying the Principle of Virtual Work.

In the present paper, the theoretical basis of this new technique is discussed, and typical calculations for a pitched-roof portal frame are given.

Résumé

Dans différents cas, l'application de la théorie de la plasticité au calcul des cadres plans en matériaux forgeables, comme l'acier fondu, conduit à des solutions rationnelles économiques. Cette méthode de calcul repose sur la détermination des charges sous lesquelles un ouvrage cède à la suite de déformations plastiques infiniment grandes. La rupture se produit à la suite de la formation d'articulations plastiques en nombre suffisant pour transformer l'élément porteur en un "mécanisme"; à la suite du processus de rotation des articulations plastiques, les déformations prennent des amplitudes de plus en plus grandes, tandis que la charge reste constante.

On sait que parmi tous les processus possibles de rupture d'un cadre donné sous l'action de conditions de mise en charge données, le processus décisif est celui qui correspond à la plus petite valeur possible de la charge. On a montré récemment que tous les processus possibles de rupture d'un cadre peuvent être considérés comme composés d'un certain nombre de processus habituels. Ceci a conduit à la mise au

point d'un nouveau procédé pour la détermination de la charge plastique de rupture, procédé dans lequel les processus simples sont combinés d'une manière systématique en vue de réduire la charge correspondante à sa plus petite valeur possible. Les valeurs de la charge peuvent être déterminées très rapidement pour chaque processus ainsi introduit, par l'application du principe des travaux virtuels.

Les auteurs discutent dans le présent rapport les bases théoriques du nouveau procédé et exposent les modes de calcul caractéristiques pour un cadre-portique avec toit incliné.

Zusammenfassung

In verschiedenen Fällen führt die Anwendung der Plastizitätstheorie bei der Berechnung ebener Rahmen aus schmiedbarem Material, wie z.B. Flusstahl, zu rationellen und wirtschaftlichen Lösungen. Diese Berechnungsmethode beruht auf der Bestimmung derjenigen Lasten, unter welchen ein Bauwerk infolge unendlich grossen plastischen Verformungen versagt. Das Versagen tritt ein, wenn sich plastische Gelenke in genügender Zahl ausgebildet haben, um das Tragwerk in einen Mechanismus umzuwandeln; als Folge der Drehungen der plastischen Gelenke vergrössern sich dann die Formänderungen weiter, während die Belastung konstant bleibt.

Es ist bekannt, dass unter allen möglichen Bruchmechanismen eines gegebenen Rahmens mit gegebener Belastungsanordnung derjenige massgebend ist, dem der kleinstmögliche Wert der Belastung entspricht. Unlängst wurde gezeigt, dass alle möglichen Bruchmechanismen eines Rahmens als aus einer gewissen Zahl von gewöhnlichen Mechanismen zusammengesetzt betrachtet werden können. Dies hat zur Entwicklung eines neuen Verfahrens zur Bestimmung der plastischen Bruchlast geführt, bei welchem die einfachen Mechanismen systematisch kombiniert werden, um so den entsprechenden Wert der Last zu seiner kleinstmöglichen Grösse zu reduzieren. Die Werte der Last können für jeden eingeführten Mechanismus sehr schnell durch Anwendung des Prinzips der virtuellen Arbeit bestimmt werden.

Im vorliegenden Aufsatz wird die theoretische Grundlage des neuen Verfahrens diskutiert, und es werden die typischen Berechnungen für einen Portalrahmen mit geneigtem Dach gegeben.

AI 3

Plastic analysis and design of steel-framed structures

Analyse plastique et calcul des ouvrages métalliques en cadres

Plastizitäts-Untersuchung und -Berechnung von Rahmenkonstruktionen aus Stahl

JACQUES HEYMAN, M.A., Ph.D.
Cambridge University

Introduction

The methods presented in this paper for the analysis and design of rigid structures are purely mathematical in character; that is, techniques are formulated on the basis of certain fundamental assumptions. These assumptions may or may not be true for any particular structure; for example, the instability of axially loaded stanchions is ignored, as is the lateral instability of beams subjected to terminal bending moments. While for some simple structures under particular conditions of loading these effects may be relatively unimportant, recent work by Neal (1950a) and Horne (1950) has shown that the problem may in fact be critical. In addition, it will be seen below that an "ideal" plastic material is assumed. Structural mild steel approximates to such an ideal material, but a highly redundant frame will experience strain-hardening which may invalidate the calculations. The techniques presented here, in short, in no sense form a practical design method; however, it is felt that they are of sufficient interest to warrant a description of some of the more important results.

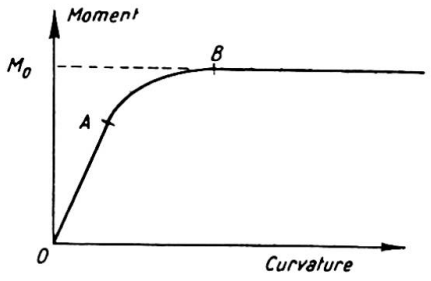

Fig. 1

The characteristic ideally plastic behaviour of a beam in pure bending is shown in fig. 1. From O to A increase of bending moment is accompanied by purely elastic (linear) increase of curvature. Between A and B, increase of bending moment is accompanied by a greater increase of curvature, until at the point B the full plastic moment M_0 is attained. At this moment the curvature can increase indefinitely, and "collapse" occurs.

In a general plane structural frame, a section at which the bending moment has the value M_0 is called a plastic hinge, and has the property that rotation at the hinge can occur freely under constant bending moment. From the definition of the full plastic moment, the moments in the frame can nowhere exceed M_0; if the component members of a frame have different sizes, it must be understood of course that M_0 refers to the particular member under consideration.

Collapse of a frame is said to occur when a sufficient number of plastic hinges are formed to turn whole or part of the frame into a mechanism of one degree of freedom; in general, the number of hinges exceeds by one the number of redundancies of that part of the frame concerned in the collapse. For example, the simple rectangular portal frame, of constant section throughout, subjected to loads V and H as shown in fig. 2(*a*), may fail in any one of the three basic modes shown in figs. 2(*b*), (*c*) and (*d*). The actual mode is determined by the values of the two loads.

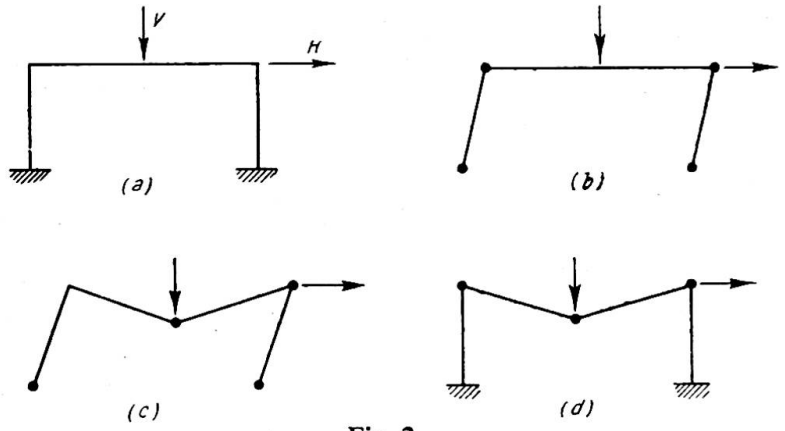

Fig. 2

The first part of this paper deals with methods for the exact determination of the quantities required (location of the hinges, values of collapse loads, etc.); the second part presents methods for determining upper and lower bounds on the loads, it being possible to make these bounds as close as is considered necessary. The third part applies the ideas to space frames, where hinges are formed under the combined action of bending and torsion.

Exact methods

The use of inequalities in the solution of structural problems was first introduced by Neal and Symonds (1950), who used a method due to Dines (1918). The very simple example shown in fig. 3 will be used to illustrate the solution of linear sets of inequalities.

(a) *Collapse analysis under fixed loads*

Suppose in fig. 3 that the two spans of the continuous beam are of length l, and that the fixed loads P_1 and P_2 act at the centres of the spans. The full plastic moment of the beam will be taken as M_0, and it is required to find the minimum value of M_0 in order that collapse shall just occur. (P_1 and P_2 may be taken to incorporate a suitable load factor.)

The general equilibrium state of a frame of n redundancies can be expressed as the sum of one arbitrary equilibrium state and n arbitrary independent residual states.

By a "state" is meant some bending moment distribution, so that a state in equilibrium with the applied loads is *any* bending moment distribution such that equilibrium is attained. A residual state is a bending moment distribution that satisfies equilibrium conditions when no external loads are applied to the frame. Thus, confining attention to any one cross-section in the frame, the bending moment there may be expressed as

$$M^*+M_1'+M_2'+\ldots+M_n' \qquad \ldots\ldots\ldots \quad (1)$$

where M^* is the equilibrium bending moment at the section and M_1', M_2', . . . M_n' are the bending moments, at the section considered, corresponding to n arbitrary residual states. Suppose that the full plastic moment at the section (as yet undetermined) is M_0. Then

$$-M_0 \leqslant M^*+M_1'+M_2'+\ldots+M_n' \leqslant M_0 \qquad \ldots\ldots \quad (2)$$

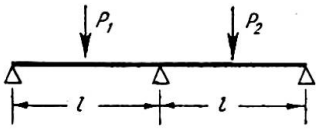

Fig. 3

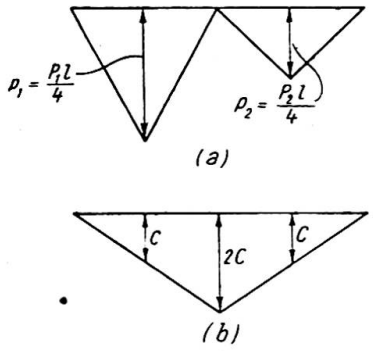

Fig. 4

Since the continuous beam system under consideration has one redundancy, the plastic behaviour can be represented as the sum of an equilibrium state and one residual state, which may be taken as the two bending moment distributions in fig. 4. The continued inequality (2) may be written for the three critical sections:

$$\left.\begin{array}{r} \text{Under the load } P_1,\ -M_0 \leqslant p_1+c \leqslant M_0 \\ \text{At the central support},\ -M_0 \leqslant\ \ 2c \leqslant M_0 \\ \text{Under the load } P_2,\ -M_0 \leqslant p_2+c \leqslant M_0 \end{array}\right\} \qquad \ldots\ldots \quad (3)$$

The set (3) may be rewritten as simple inequalities:

$$\left.\begin{array}{rl} c+p_1+ & M_0 \geqslant 0 \\ c\ \ \ \ +\tfrac{1}{2} & M_0 \geqslant 0 \\ c+p_2+ & M_0 \geqslant 0 \\ -c-p_1+ & M_0 \geqslant 0 \\ -c\ \ \ \ +\tfrac{1}{2} & M_0 \geqslant 0 \\ -c-p_2+ & M_0 \geqslant 0 \end{array}\right\} \qquad \ldots\ldots\ldots \quad (4)$$

If now every inequality in set (4) which has a coefficient of $+1$ for c is added to every inequality which has a coefficient -1 for c, c will be eliminated, and Dines has shown that the resultant set of inequalities (nine in number in this example) gives necessary and sufficient conditions for the existence of a value of c in order that the original set should be satisfied. This is exactly what is required for the present purposes; the actual value of c is of no interest so long as it is known that a c exists such that at each critical section of the frame the bending moment is less than the full plastic value.

In eliminating c from the set (4), it is found that a large number of the resulting inequalities are redundant, and if it is assumed that $P_1 \geqslant P_2$, the single inequality

$$-p_1+\tfrac{3}{2}M_0 \geqslant 0 \qquad \ldots\ldots\ldots \quad (5)$$

is found to be critical. As long as this inequality is satisfied, all the moments in the beam will be less than M_0. For collapse just to occur, the equality sign should be taken in (5), giving $M_0=\frac{2}{3}p_1$. Now inequality (5) was derived by adding the second and fourth of set (4); substituting this value of M_0 into these two inequalities gives

$$\left.\begin{aligned} c+\tfrac{1}{3}p_1 &\geqslant 0 \\ -c-\tfrac{1}{3}p_1 &\geqslant 0 \end{aligned}\right\} \qquad \ldots\ldots\ldots \quad (6)$$

i.e.

$$-\tfrac{1}{3}p_1 \geqslant c \geqslant -\tfrac{1}{3}p_1 \qquad \ldots\ldots\ldots \quad (7)$$

that is, a unique value of c has been derived. Using this value of c, the bending moment distribution shown in fig. 5 has been derived from the analysis; it will be seen that hinges ($M_0=\frac{2}{3}p_1$) are formed under the load P_1, and at the central support, forming a mechanism of one degree of freedom for small (really, infinitesimal) displacements.

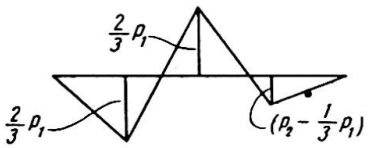

Fig. 5

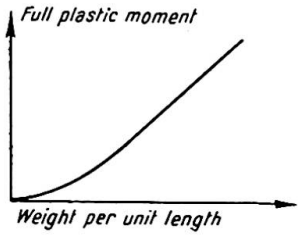

Fig. 6

The type of result obtained in this problem will in general be derived for any more complicated example. For more residual states defined by c_1, c_2, . . . c_n, each parameter c is eliminated successively from the inequalities, and the final inequality, if just satisfied, will generate a unique set of residual states completely defining the collapse configuration.

The method given above may be applied to the analysis of frames collapsing under variable loads; however, this problem will be treated with reference to the slightly more complex condition of minimum weight design.

(b) *Minimum weight design under fixed loads*

The parameters used in order to determine the minimum weight of a structure will be the values of the full plastic moments. If a plot is made for typical structural sections of full plastic moment against weight per unit length, and the points joined by a smooth curve, a non-linear relationship of the type shown in fig. 6 will be obtained. (Owing to the methods used in this paper, the actual relationship is immaterial, but it is of interest to note that a curve given in a British Welding Research Association report (1947) for British structural sections can be approximated by $w=2{\cdot}7M^{0{\cdot}6}$, where w is the weight in lb./ft. of a beam of full plastic moment M tons ft.) In order to develop suitable methods for design, it will be assumed that a continuous range of sections is available so that a section can be used with any specified full plastic moment.

The assumption is made that the moment–weight curve can be replaced in the region which is significant for any particular problem by a straight line. For a frame built up of N members, each of constant section, the total material consumption will be given by the proportionality

$$W \approx \sum_{i=1}^{N} M_i l_i \qquad \ldots\ldots\ldots\ldots \quad (8)$$

where M_i is the full plastic moment of the ith member of the frame, and l_i is its length.

Considering again the two-span beam shown in fig. 3, suppose that the left-hand span has a full plastic moment M_1, that of the right-hand span being M_2. Since the two spans are of equal length, proportionality (8) may be replaced by the weight parameter

$$X = M_1 + M_2 \qquad \ldots\ldots\ldots\ldots \quad (9)$$

The problem of minimum weight design for this problem is then reduced to choosing values of M_1 and M_2 such that X is made a minimum. The work starts in the same manner as for the collapse analysis given above; set (3) is replaced by

$$\left.\begin{aligned} -M_1 &\leqslant p_1 + c \leqslant M_1 \\ -M_1 &\leqslant 2c \leqslant M_1 \\ -M_2 &\leqslant 2c \leqslant M_2 \\ -M_2 &\leqslant p_2 + c \leqslant M_2 \end{aligned}\right\} \qquad \ldots\ldots\ldots\ldots \quad (10)$$

The two continued inequalities are necessary for the central support since it is not known *a priori* whether $M_1 \gtrless M_2$.

Of the sixteen possible inequalities obtained by the elimination of c from set (3), only five are found to be non-redundant if it be assumed that $P_1 \geqslant P_2$. These are

$$\left.\begin{aligned} -p_1 \qquad\quad + \tfrac{3}{2}M_1 \qquad\quad &\geqslant 0 \\ -p_1 \qquad\quad + M_1 + \tfrac{1}{2}M_2 &\geqslant 0 \\ -p_1 + p_2 + M_1 + M_2 &\geqslant 0 \\ -p_2 + \tfrac{1}{2}M_1 + M_2 &\geqslant 0 \\ -p_2 \qquad\quad + \tfrac{3}{2}M_2 &\geqslant 0 \end{aligned}\right\} \qquad \ldots\ldots\ldots\ldots \quad (11)$$

The material consumption parameter X will now be introduced into set (10) by the replacement of M_1 by $(X - M_2)$ from equation (9). Upon slight rearrangement,

$$\left.\begin{aligned} -M_2 + X \quad -\tfrac{2}{3}p_1 &\geqslant 0 \\ -M_2 + 2X - 2p_1 &\geqslant 0 \\ M_2 + X \quad -2p_2 &\geqslant 0 \\ M_2 \qquad -\tfrac{2}{3}p_2 &\geqslant 0 \end{aligned}\right\} \qquad \ldots\ldots\ldots\ldots \quad (12)$$

together with

$$X \geqslant (p_1 - p_2) \qquad \ldots\ldots\ldots\ldots \quad (13)$$

Now for the problem of determining the minimum value of X, the value of M_2 is not required, and Dines' method may be employed again on set (12) to eliminate M_2. On performing this operation, inequality (13) becomes redundant, and the only significant inequality resulting is

$$X \geqslant p_1 + \tfrac{1}{3}p_2 \qquad \ldots\ldots\ldots\ldots \quad (14)$$

It should be repeated that this single inequality is a necessary and completely sufficient condition that values of M_1, M_2 and c can be found to satisfy the original set (10). Since it is required that X should be as small as possible, the equality sign will be taken in (14), so that

$$X = p_1 + \tfrac{1}{3}p_2 \qquad \ldots\ldots\ldots\ldots \quad (15)$$

Substitution of this value of X back into the previous sets gives the unique values

$$\left.\begin{aligned} M_1 &= p_1 - \tfrac{1}{3}p_2 \\ M_2 &= \tfrac{2}{3}p_2 \\ 2c &= -\tfrac{2}{3}p_2 = -M_2 \end{aligned}\right\} \quad \ldots\ldots\ldots \quad (16)$$

The bending moment distribution resulting from the analysis is shown in fig. 7, plastic hinges being formed at all three of the critical points.

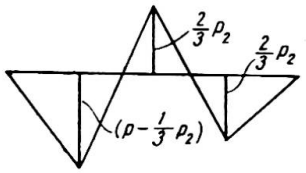

Fig. 7

The method given above for minimum weight design against collapse under fixed loads has been applied by the Author (1950a, 1950b) to the solution of a rectangular portal frame (cf. fig. 2), and also to derive a design method for continuous beams of any number of spans under either concentrated or distributed loads.

(c) *Minimum weight design against collapse under variable loads*

Consider the same beam in fig. 3, but with the loads varying arbitrarily between the limits

$$\left.\begin{aligned} -Q_1 \leqslant P_1 \leqslant Q_1 \\ -Q_2 \leqslant P_2 \leqslant Q_2 \\ Q_1 \geqslant Q_2 \end{aligned}\right\} \quad \ldots\ldots\ldots \quad (17)$$

The work proceeds as before up to the derivation of set (11). Now, in this set, the worst values of p_1 and p_2 (i.e. $\pm q_1$, $\pm q_2$) must be inserted in each inequality, giving

$$\left.\begin{aligned} -q_1 \quad\quad +\tfrac{3}{2}M_1 \quad\quad\quad &\geqslant 0 \\ -q_1 \quad\quad + M_1 + \tfrac{1}{2}M_2 &\geqslant 0 \\ -q_1 - q_2 + M_1 + M_2 &\geqslant 0 \\ -q_2 + \tfrac{1}{2}M_1 + M_2 &\geqslant 0 \\ -q_2 \quad\quad\quad +\tfrac{3}{2}M_2 &\geqslant 0 \end{aligned}\right\} \quad \ldots\ldots\ldots \quad (18)$$

Operating on set (18) as before to find the minimum value of X, it is found that

$$\left.\begin{aligned} M_1 + M_2 = X &= q_1 + q_2 \\ (q_1 + \tfrac{1}{3}q_2) &\geqslant M_1 \geqslant \tfrac{2}{3}q_1 \\ 2q_2 &\geqslant M_2 \geqslant \tfrac{2}{3}q_2 \\ (\tfrac{1}{3}q_1 + q_2) &\geqslant M_2 \end{aligned}\right\} \quad \ldots\ldots\ldots \quad (19)$$

As a specific example, suppose $q_1 = q_2 = q$. Then

$$\left.\begin{aligned} M_1 + M_2 &= 2q \\ \tfrac{4}{3}q &\geqslant M_1 \geqslant \tfrac{2}{3}q \\ \tfrac{4}{3}q &\geqslant M_2 \geqslant \tfrac{2}{3}q \end{aligned}\right\} \quad \ldots\ldots\ldots \quad (20)$$

and any values of M_1 and M_2 satisfying (20) will give a constant material consumption. (It is perhaps of interest to note that for $X = \Sigma(M)^n l$, where $n < 1$, the minimum material consumption is given by $M_1 = 2M_2 = \frac{4}{3}q$ (or *vice versa*), the worst case occurring for $M_1 = M_2 = q$. An asymmetrical solution is obtained for what appears to be a completely symmetrical problem. For $n = 0{\cdot}6$, the symmetrical solution gives an increase of less than 2% in material consumption compared with the asymmetrical solution.)

Inexact methods

The theorems concerning the existence of upper and lower bounds on the collapse load of a structure were first proved rigorously by Greenberg and Prager (1950). It

is assumed that the loads on a structure are all specified in terms of one load, so that when the collapse load is mentioned, this implies the whole system of loads.

An upper bound on the collapse load

Suppose that enough hinges are inserted into a redundant structure in order to turn it into a mechanism of one degree of freedom. Hill (1948) has shown that the stress system is constant during collapse of an ideally plastic body, so that for the frame with one degree of freedom, the equation of virtual work may be written, equating the work done in the hinges to the work done by the external load during a small displacement in the equilibrium state. The work done in a hinge is equal to the full plastic moment multiplied by the absolute value of the change in angle at that hinge (i.e. plastic rotation) and the work done by the load simply the load multiplied by its displacement. There will, of course, be elastic displacements obtaining in the frame, but these do not appear in the equations provided it is assumed that they are small so that the overall geometry of the frame is not disturbed.

For any arrangement of hinges in the frame producing a mechanism of one degree of freedom, the load given by the virtual work equation is either greater than or equal to the true collapse load.

A lower bound on the collapse load

If a state can be found for the structure which nowhere violates the yield condition, and which is an equilibrium state for a given value of the load, then that value is either less than or equal to the value of the true collapse load.

In practice, Greenberg and Prager found it useful to derive a lower bound from the mechanism giving the upper bound. The example will make the ideas clear.

Suppose the values of the loads in fig. 3 are

$$P_1=2P_2=2P \quad . \quad . \quad . \quad . \quad . \quad . \quad . \quad . \quad . \quad (21)$$

and that as a first trial the mechanism in fig. 8 is assumed for failure. The rotation at the central hinge is θ, and at the hinge under the load P, 2θ. Hence, by virtual work,

$$P \cdot \frac{l}{2}\theta = M_0(2\theta)+M_0(\theta) \quad . \quad . \quad . \quad . \quad . \quad . \quad . \quad . \quad (22)$$

i.e.

$$p=\tfrac{3}{2}M_0 \quad . \quad . \quad . \quad . \quad . \quad . \quad . \quad . \quad . \quad . \quad (23)$$

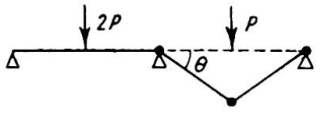

Fig. 8

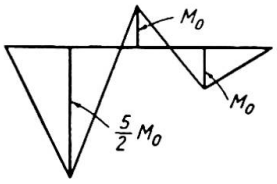

Fig. 9

(It is taken that the beam has the same full plastic moment M_0 in both spans.) By the upper bound theorem, the true value of the collapse load (p_c) is less than $\frac{3}{2}M_0$. The bending moment distribution corresponding to the assumed mechanism and this value of p given in equation (23) is shown in fig. 9, from which it will be seen that the yield condition is exceeded under the load $2P$ in the ratio 5/2. Suppose now that the loads are reduced in the ratio 2/5. Then if the values in fig. 9 are multiplied by 2/5,

an equilibrium bending moment distribution is obtained which nowhere violates the yield condition. Hence the load of $\frac{3}{5}M_0$ is a lower bound on the collapse load, i.e.

$$\tfrac{3}{5}M_0 \leqslant p_c \leqslant \tfrac{3}{2}M_0 \quad . \quad . \quad . \quad . \quad . \quad . \quad . \quad . \quad (24)$$

It can be shown that removing one of the assumed hinges to the point of maximum moment will improve the bounds on the collapse load; in this example, shifting the hinge from under the load P to under the load $2P$, while retaining the central hinge, immediately gives the correct solution $p_c=\frac{3}{4}M_0$. There is, however, no means at present of choosing which hinge to remove, and in any case the bounds cannot be narrowed indefinitely; either they are separated by a finite amount, which may be quite large for even a relatively redundant frame, or the exact solution will be obtained. Accordingly, Nachbar and the Author (1950) have developed more general methods for obtaining both upper and lower bounds which may be made as close to the true collapse value as is considered necessary.

A general method for the upper bound

Suppose yield hinges are inserted into the frame at any suspected critical sections. In general a frame of N degrees of freedom will result, specified in terms of N deflection parameters. If the equation of virtual work is written, then the corresponding value of the load is an upper bound on the true collapse load. In fact, the virtual work equation is inapplicable, since the system is not an equilibrium system, but it may be shown that the value of the load resulting from this equation is in fact a true upper bound, providing that the mechanism is such that the work done by the loads is positive.

For the general mechanism in fig. 10,

$$2P \cdot \frac{l}{2}\theta_1 + P \cdot \frac{l}{2}\theta_2 = M_0(|2\theta_1| + |\theta_1+\theta_2| + |2\theta_2|)$$

i.e.

$$p = M_0\left(\frac{|2\theta_1| + |\theta_1+\theta_2| + |2\theta_2|}{4\theta_1+2\theta_2}\right) \quad . \quad . \quad . \quad . \quad (25)$$

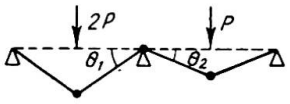

Fig. 10

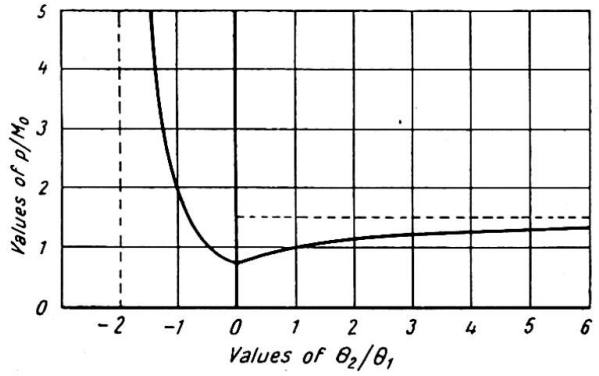

Fig. 11

In equation (25), values of θ_1 and θ_2 must be chosen to give the minimum value of p; since p is always an upper bound on p_c, the minimum value will be equal to p_c. A plot of equation (25) is given in fig. 11, from which it will be seen that $p_c=\frac{3}{4}M_0$ corresponds to $\theta_2=0$. The minimum is not a stationary value, since equation (25) is a ratio of two linear expressions. Nachbar has shown that equations of this type containing absolute values can be reduced by rational successive steps, and the method has been applied to mechanisms with a large number of parameters necessary for their specification.

A general method for the lower bound

Suppose the members of a redundant structure are cut in such a way that a number of separate redundant or statically determinate structures are formed. If the collapse loads are calculated for each of these resulting structures, then the lowest value of these loads is less than the collapse load of the structure as a whole. The proof of this theorem follows immediately from the special lower bound theorem above. An immediate corollary is that if a cut portion of the structure carries no load, then that portion can be ignored in the derivation of the lower bound. In order to make the theorem of practical use, an additional lemma is needed. The collapse load of a structure is unaffected by any initial system of residual stresses (moments, shear forces). That is, at a cut, equal and opposite longitudinal forces, shear forces, and moments may be introduced in an attempt to raise the lower bound.

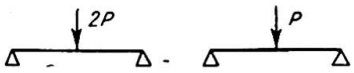

Fig. 12

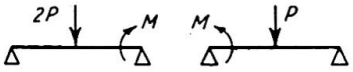

Fig. 13

Suppose the beam in the previous example is cut at the central support; then the two separate beams shown in fig. 12 will be obtained. The collapse loads of the right- and left-hand halves are respectively $p=M_0$ and $p=\frac{1}{2}M_0$, i.e.

$$p_c \geqslant \tfrac{1}{2}M_0 \quad . \quad . \quad . \quad . \quad . \quad . \quad . \quad . \quad . \quad . \quad (26)$$

Now if a central moment is introduced (fig. 13), it is easy to show that the collapse loads are respectively

$$p=\frac{M+2M_0}{2} \quad \text{and} \quad p=\frac{M+2M_0}{4} \quad . \quad . \quad . \quad . \quad . \quad (27)$$

The maximum value which M can take is, of course, M_0, and hence from (27)

$$p_c \geqslant \tfrac{3}{4}M_0 \quad . \quad . \quad . \quad . \quad . \quad . \quad . \quad . \quad . \quad . \quad (28)$$

and the problem has been completed. For other more complicated examples (a two-storey, two-bay portal frame has been solved under both concentrated and distributed loads), it is found that shear and longitudinal forces as well as bending moments must be introduced at the cuts.

SPACE FRAMES

The type of space frame considered has members which lie all in the same plane, all loads acting perpendicularly to this plane. Thus bending moments whose axes lie perpendicular to the plane and shear forces in the plane are zero. Any member of the frame is then acted upon by shear forces parallel to the applied loads and by two moments whose axes lie in the plane, that is, a bending moment (M) and a torque (T). For ideal plasticity, hinges will be formed in exactly the same way as for plane frames; the breakdown criterion will be some such expression as

$$g(M, T)=g(M_0, 0)=\text{const.} \quad . \quad . \quad . \quad . \quad . \quad . \quad . \quad . \quad (29)$$

where M_0 is the full plastic moment in pure bending, as before. At any one hinge, the maximum work principle of Hill (1948) shows that the moment and torque will be constant during collapse, and that the rate at which work is done at a hinge will be a maximum. If β and θ are the incremental changes in angle in bending and twisting

respectively during a displacement in the equilibrium collapse configuration, then the rate at which work is done is

$$M\beta+T\theta \quad . \quad . \quad . \quad . \quad . \quad . \quad . \quad . \quad . \quad . \quad (30)$$

For a maximum,

$$\beta \,.\, \delta M+\theta \,.\, \delta T=0 \quad . \quad . \quad . \quad . \quad . \quad . \quad . \quad . \quad . \quad (31)$$

Now the breakdown criterion, equation (29), gives

$$\frac{\partial g}{\partial M} \,.\, \delta M+\frac{\partial g}{\partial T} \,.\, \delta T=0 \quad . \quad . \quad . \quad . \quad . \quad . \quad . \quad . \quad . \quad (32)$$

that is,

$$\frac{\beta}{\theta}=\frac{\dfrac{\partial g}{\partial M}}{\dfrac{\partial g}{\partial T}} \quad . \quad . \quad . \quad . \quad . \quad . \quad . \quad . \quad . \quad . \quad (33)$$

This flow relationship may be solved simultaneously with the breakdown criterion to give the moment and torque acting at a hinge during any collapse displacement.

The author (1951) has shown that for a box section, equation (29) becomes

$$M^2+\tfrac{3}{4}T^2=M_0^2 \quad . \quad . \quad . \quad . \quad . \quad . \quad . \quad . \quad . \quad (34)$$

For the present purposes, the circular breakdown criterion

$$M^2+T^2=M_0^2 \quad . \quad . \quad . \quad . \quad . \quad . \quad . \quad . \quad . \quad (35)$$

will be used for the sake of simplicity. The restriction in no way affects the generality of the methods proposed for the solution of space frames.

Equation (33) becomes

$$\frac{\beta}{\theta}=\frac{M}{T} \quad . \quad . \quad . \quad . \quad . \quad . \quad . \quad . \quad . \quad . \quad (36)$$

which, taken with equation (35), gives

$$\left.\begin{aligned} M&=\frac{\beta}{\sqrt{\beta^2+\theta^2}}M_0 \\ T&=\frac{\theta}{\sqrt{\beta^2+\theta^2}}M_0 \end{aligned}\right\} \quad . \quad . \quad . \quad . \quad . \quad . \quad . \quad . \quad (37)$$

together with the expression for the work done at the hinge (expression (30))

$$\text{Plastic work}=M_0\sqrt{\beta^2+\theta^2} \quad . \quad . \quad . \quad . \quad . \quad . \quad . \quad (38)$$

Owing to the non-linearity of the breakdown criterion, it is not possible to set up exact systems of linear inequalities to be solved by the Dines' method. However, approximations may be made to the breakdown criterion itself; for example, equation (35) could be replaced by the circumscribed octagon

$$\left.\begin{aligned} M&=\pm M_0 \\ T&=\pm M_0 \\ M\pm T&=\pm\sqrt{2}M_0 \end{aligned}\right\} \quad . \quad . \quad . \quad . \quad . \quad . \quad . \quad . \quad (39)$$

and the moment M and torque T at any section constrained to lie within this yield domain.

As will be shown, simple problems are best solved by a direct method; and the systems of linear inequalities corresponding to equations (39) become too complicated

for practical use in the solution of highly redundant structures. For the latter, the determination of bounds on the collapse load seems to give the quickest results.

Direct solution

As an example of the direct method, consider the symmetrical two-leg right-angle bent shown in fig. 14. The ends A and D are *encastré* against both torque and moment, and the load P acts at the midpoint B of the leg AC. Suppose failure occurs by the formation of symmetrical hinges at A and D, so that the point C moves vertically downward for a small displacement. It is easy to see that $\beta_A=\beta_D=\theta_A=\theta_D=\theta$, say, so that, from equation (38), the work done in the two hinges is

$$2M_0\sqrt{2}\theta^2 \quad . \quad . \quad . \quad . \quad . \quad . \quad . \quad . \quad . \quad . \quad (40)$$

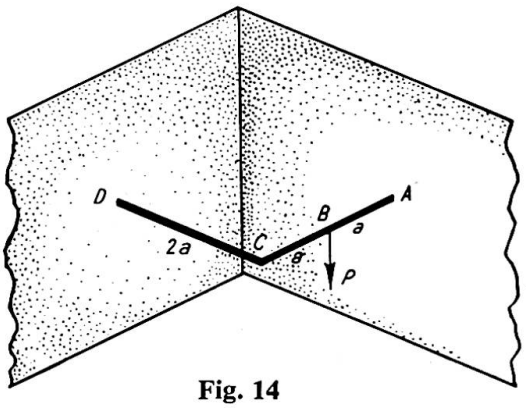

Fig. 14

while the work done by the load P is

$$Pa\theta \quad . \quad . \quad . \quad . \quad . \quad . \quad . \quad . \quad . \quad . \quad (41)$$

Equating these two expressions, and using the upper bound theorem given above,

$$P_c \leqslant P=2\frac{\sqrt{2}M_0}{a} \quad . \quad . \quad . \quad . \quad . \quad . \quad . \quad . \quad (42)$$

The frame is, of course, statically determinate in this collapse configuration, and, by using equations (37) to determine the conditions at the hinges, the forces and moments shown in fig. 15 are obtained. The yield criterion is exceeded by the greatest amount at B, where the moment and torque are $\sqrt{2}M_0$ and $\frac{1}{\sqrt{2}}M_0$ respectively, i.e.

$$M_B^2+T_B^2=\tfrac{5}{2}M_0^2 \quad . \quad . \quad . \quad . \quad . \quad . \quad . \quad . \quad (43)$$

Hence if the load is reduced by a factor $\sqrt{2/5}$, a lower bound will be obtained,

$$\frac{4}{\sqrt{5}}\frac{M_0}{a} \leqslant P_c \leqslant \frac{4}{\sqrt{2}}\frac{M_0}{a} \quad . \quad . \quad . \quad . \quad . \quad . \quad . \quad (44)$$

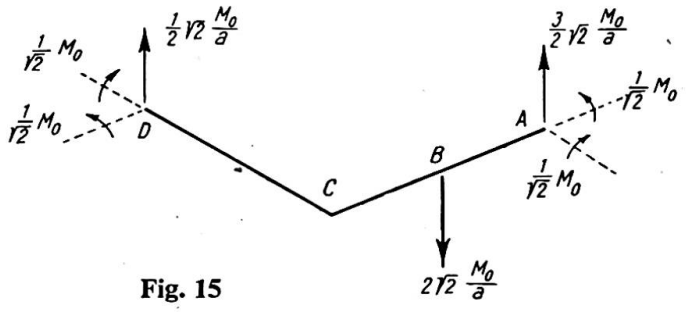

Fig. 15

In order to improve these bounds, a hinge must be inserted at B; but collapse actually occurs with hinges at all three points A, B and D. At first sight this would appear to be a mechanism of three independent degrees of freedom. In fact, owing to the simultaneity of the breakdown and flow criterions (equations (35) and (36)), each hinge as a whole has only one degree of freedom; since a continuity condition is required at each hinge, a space frame of the type considered here may collapse with any number of hinges formed in its members, and an extra hinge may be inserted without actually increasing the number of degrees of freedom.

The general method for the exact solution of a structure with R redundancies may be tabulated as follows:

(1) Construct a mechanism with N hinges.
(2) Specify the mechanism in terms of an arbitrary displacement (one degree of freedom) and $[2N-(R+1)]$ deflection parameters α_j.
(3) $(2N-R)$ equilibrium equations may be formulated in terms of the moments (M_i) and torques (T_i) at the hinges and the applied load.
(4) M_i and T_i at each hinge may be calculated in terms of the α_j from the breakdown and flow criteria.
(5) The load may be eliminated from the $(2N-R)$ equilibrium equations, leaving a set of $(2N-\{R+1\})$ simultaneous equations for the determination of the α_j.
(6) Having determined the α_j, the moments and torques at each hinge may be calculated, and hence the value of the load. This value is an upper bound on the collapse load.
(7) If the yield criterion is violated at any point in the structure, a lower bound may be determined.
(8) If hinges are moved or added to the points where the yield criterion is violated, the whole process can be repeated.

Following these rules, and inserting hinges at A, B and D, the final exact solution is found to be

$$P_c=\frac{8}{\sqrt{10}}\frac{M_0}{a}=2{\cdot}53\frac{M_0}{a} \qquad \ldots\ldots\ldots \quad (45)$$

which as a check lies between the previous limits (44).

Bounds on the collapse load

In the method outlined above, it has been tacitly assumed that the theorems on upper and lower bounds may be extended from plane to space frames; this is in fact the case, and indeed Drucker, Greenberg and Prager (1950) have shown that the special theorems may be applied to the problem of the continuum. The general theorem of an upper bound determined from a non-equilibrium mechanism is also valid for space frames, and this gives the quickest method for the solution of such problems.

The advantage of the kinematic method of determining an upper bound on the collapse load is that no reference is made to equilibrium conditions. Suppose, for

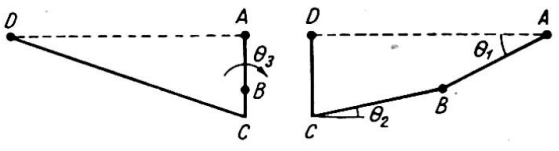

Fig. 16

example, the mechanism in fig. 16 (horizontal projection of frame in fig. 14) is specified by assigning arbitrary deflections to the joints B and C, with hinges occurring at A, B and D. Then an upper bound may be determined simply by equating the work done in the hinges to the work done by the load. By trial of various mechanisms, this bound may be lowered. Alternatively, if, after a trial, the frame is examined statically, it will be found that it is impossible to satisfy equilibrium conditions, the total load at B being either lower or in excess of the value of P determined from the work equation. This implies that an extra (positive or negative) force is required at B in order to produce the originally assumed collapse configuration. The significance of this force is best appreciated by an example.

In fig. 16, take $\delta_B=\delta_C=2a$, say, since the mechanism may be specified in terms of one unknown degree of freedom. The following table gives the conditions at the hinges.

TABLE I

Hinge	β	θ	$\sqrt{\theta^2+\beta^2}$	Moment ($\times M_0$)	Torque ($\times M_0$)
A . . .	2	0·5*	2·062	0·97	0·24
B . . .	2	0·5*	2·062	0·97	0·24
D . . .	1	0	1·000	1·00	0

The asterisked values were chosen to make the torques equal at A and B, as they should be; this is an unnecessary restriction, and improves only slightly the value of the upper bound, and any values of the twist totalling 1·0 could have been used. The work equation gives

$$P\,.\,2a=5{\cdot}124M_0$$

i.e.
$$P_c\leqslant P=2{\cdot}56\frac{M_0}{a} \quad . \quad . \quad . \quad . \quad . \quad . \quad . \quad . \quad . \quad (46)$$

The statical analysis of the frame is shown in fig. 17. The number in a circle at the joint B gives the actual load required to maintain equilibrium, and it appears that a load of $2{\cdot}91M_0/a$ is required as against the calculated value $2{\cdot}56M_0/a$. Since the equilibrium load is greater than it should be, it is indicated that the assumed deflection of the point B was too large; if this deflection is reduced slightly, a better bound should result. Similarly, a negative load is required at C; the deflection should be increased.

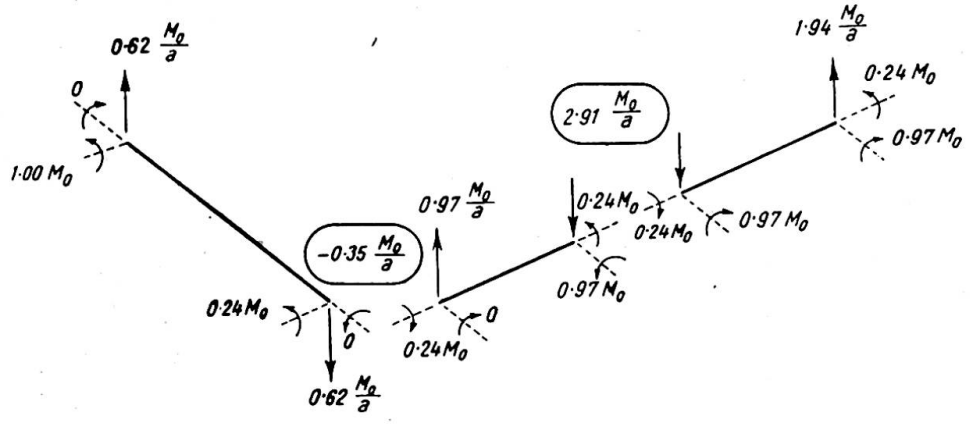

Fig. 17

In working more complicated examples, it is found that the process of adjusting deflections at neighbouring joints bears a marked resemblance to a relaxation process, and that a reduction in the out-of-balance forces at one joint induces increased errors at the ones adjacent. However, the technique is soon mastered, and the Author (1950c) solved, with very little labour, a rectangular grid formed by a set of parallel beams intersecting at right angles another set of 9 beams, loaded transversely at each of the 81 joints, and requiring 108 hinges in the collapse mechanism.

When it is suspected that the upper bound is fairly good, small adjustments in the statical analysis will produce an equilibrium system. For example, in fig. 17, if the torque in CD is increased from 0 to $0{\cdot}35M_0$, the other values remaining unchanged, an equilibrium system results which, however, violates the yield condition at the hinge D in the ratio 1·06. Hence, using the value in equation (46)

$$2{\cdot}41\frac{M_0}{a} \leqslant P_c \leqslant 2{\cdot}56\frac{M_0}{a} \qquad \ldots\ldots\ldots \quad (47)$$

The general procedure for the solution of space frames may be tabulated as follows:

(1) Insert yield hinges at a large number of points in the frame, producing a mechanism of many degrees of freedom. The hinges should be placed at all the sections at which it is suspected actual hinges might occur in the collapse.

(2) Assign arbitrary (reasonable) deflections to the joints of the grid, and determine the corresponding changes in angle at each hinge. Equating the work dissipated in the hinges to the work done by the external loads gives a value of the load which is in excess of the true collapse load.

(3) Calculate the out-of-balance forces at each joint that are necessary to produce the assumed deflections. If the out-of-balance force acts in the same direction as the actual load at a joint, the deflection of that joint was estimated as too large, and *vice versa*.

(4) Adjust the deflections, and repeat the whole process.

(5) At any stage, if the out-of-balance forces are small, and it is suspected that the upper bound is a good estimate of the collapse load, a statical analysis may be made. Small adjustments are made in the values of the various shear forces and moments in order to produce an equilibrium system, from which a lower bound may be determined.

The Author wishes to thank Professors Prager and Drucker of Brown University for their criticism and encouragement of the work reported in this paper.

References

British Welding Research Association. 1947. Report FE1/2.

Dines, L. L. 1918. *Ann. Math.*, **20**, 191.

Drucker, D. C., Greenberg, H. J., and Prager, W. 1950. Technical Report A18-3 from the Graduate Division of Applied Mathematics, Brown University, to the Office of Naval Research, U.S.

Greenberg, H. J., and Prager, W. 1950. To be published in *Proc. A.S.C.E.*

Heyman, J. 1950a. Technical Report A11–45 from the Graduate Division of Applied Mathematics, Brown University, to the Office of Naval Research, U.S.

1950b. *Quart. J. Appl. Math.*, **8**, No. 4, January 1951.

1950c. Technical Report A11–52 from the Graduate Division of Applied Mathematics, Brown University, to the Office of Naval Research, U.S. To be published in *J. Appl. Mech.*

1951. *J. Appl. Mech.*, **18**, No. 2, June 1951.

HILL, R. 1948. *Quart. J. Mech. and Appl. Math.*, **1**.

HORNE, M. R. 1950. Unpublished.

NACHBAR, W., and HEYMAN, J. 1950. Technical Report A11–54 from the Graduate Division of Applied Mathematics, Brown University, to the Office of Naval Research, U.S. To be published in *J. Appl. Mech.*

NEAL, B. G. 1950a. *Phil. Trans. Roy. Soc. A.*, **846**, 197–242.

NEAL, B. G., and SYMONDS, P. S. 1950. *J. Inst. Civ. Engrs.*, **35**, 20.

Summary

The preparation of this paper forms part of a general investigation into the behaviour of rigid frame structures being carried out at the Cambridge Engineering Laboratory under the direction of Professor J. F. Baker. The paper deals with the mathematical analysis and design of both plane and space frames, and the ideas are presented with reference to very simple examples in order to illustrate the techniques developed. The first part considers methods for the exact determination of conditions at collapse of rigid ideally plastic plane structures. In the second part it is shown that inexact methods lead to upper and lower bounds on the collapse loads, and that these bounds may be made as close as is considered necessary. The various theorems are applied in the third part to the solution of space frames.

Résumé

Le présent mémoire rentre dans le cadre d'une investigation générale portant sur le comportement d'ouvrages en cadres rigides, investigation actuellement en cours au Cambridge Engineering Laboratory, sous la direction du Professeur J. F. Baker. L'auteur traite de l'analyse mathématique et du calcul des cadres, tant en plan que dans l'espace, et son exposé est accompagné d'exemples très simples, qui illustrent les procédés adoptés.

La première partie se rapporte aux méthodes de détermination exacte des conditions qui se manifestent au rupture des ouvrages plans rigides idéalement plastiques. Dans la deuxième partie, l'auteur montre que des méthodes non rigoureuses permettent de fixer des limites supérieures et inférieures aux charges sous lesquelles les ouvrages cèdent; ces limites peuvent d'ailleurs recevoir des valeurs aussi étroites qu'il est jugé nécessaire. Les différents théorèmes sont appliqués, dans la troisième partie, au calcul de cadres à trois dimensions.

Zusammenfassung

Die Arbeiten zum vorliegenden Aufsatz stellen einen Teil der umfassenden Untersuchungen über das Verhalten steifer Rahmenkonstruktionen dar, die am Cambridge Engineering Laboratory unter der Leitung von Professor J. F. Baker durchgeführt werden. Der Verfasser behandelt die mathematische Untersuchung und Bemessung ebener und auch räumlicher Rahmen und entwickelt seine Ueberlegungen an Hand sehr einfacher Beispiele, an denen er die gewählten Verfahren darlegt. Der erste Teil behandelt Methoden zur genauen Bestimmung der Bruch-Verhältnisse steifer, ideal-plastischer ebener Tragwerke. Im zweiten Teil wird gezeigt, dass durch Näherungsmethoden eine obere und untere Grenze der Bruchlast ermittelt werden kann und dass diese Grenzwerte so nahe zusammengebracht werden können, wie es für notwendig erachtet wird. Die verschiedenen Theorien werden im dritten Teil zur Berechnung räumlicher Rahmenwerke angewandt.

Leere Seite
Blank page
Page vide

AI 3

Determination of the shape of fixed-ended beams for maximum economy according to the plastic theory

Détermination de la forme à donner aux poutres encastrées d'après la théorie de la plasticité en vue du maximum d'économie

Bestimmung der wirtschaftlichsten Querschnittsform eingespannter Balken nach der Plastizitätstheorie

M. R. HORNE, M.A., Ph.D., A.M.I.C.E.
Cambridge University

1. Introduction

In the design of structures according to the plastic theory, the members are so proportioned that collapse would not occur at a load less than the working load multiplied by a "load factor." The plastic theory provides a means of estimating the collapse loads of ductile structures by considering their behaviour beyond the elastic limit. It has been shown[1] that, in the absence of instability, these collapse loads may be calculated simply by reference to the conditions of equilibrium, without considering the equations of flexure. Hence the design process is essentially reduced to the selection of members with plastic moments of resistance sufficient to withstand the bending moments imposed by the "factored loads"—that is, by the working loads multiplied by the load factor.

The direct nature of the design of structures by the plastic theory facilitates the relative proportioning of the members such that the total weight is an absolute minimum. A method of proportioning simple structures composed of prismatic members for minimum weight has already been presented.[2] Further economy of material can, however, be achieved by using members of varying cross-section, and may be sufficient to compensate for the increased cost of fabrication. It is thus worth while investigating the maximum saving in material theoretically attainable by this means. No consideration will be given to the increased cost of manufacture of such members compared with those of uniform section, since this must depend primarily on the quantities required; for this reason, it is impossible to arrive at any conclusions regarding possible overall economies.

[1] For references see end of paper.

The relationship to be assumed between weight per unit length and full plastic moment of resistance is discussed in 2 below; 3 contains a discussion of a member of continuously varying section fixed at the ends and supporting a uniformly distributed load; while the case of a similarly loaded member in which the cross-section is only to be varied by one or two discrete intervals is discussed in 4.

The term "fixed at the ends" is not here intended to imply complete flexural rigidity at the supports, but rather that the members to which the beam under consideration is attached are together capable of resisting the full plastic moment of the end sections of that beam.

2. The relationship between full plastic moment and weight per unit length

The full plastic moment of a member (denoted by M_p) is the moment of resistance when the whole section is undergoing plastic deformation. If f_y is the yield stress, at which pure plastic deformation can occur, then for a beam of rectangular cross-section, of width b and depth $2d$ (see fig. 1),

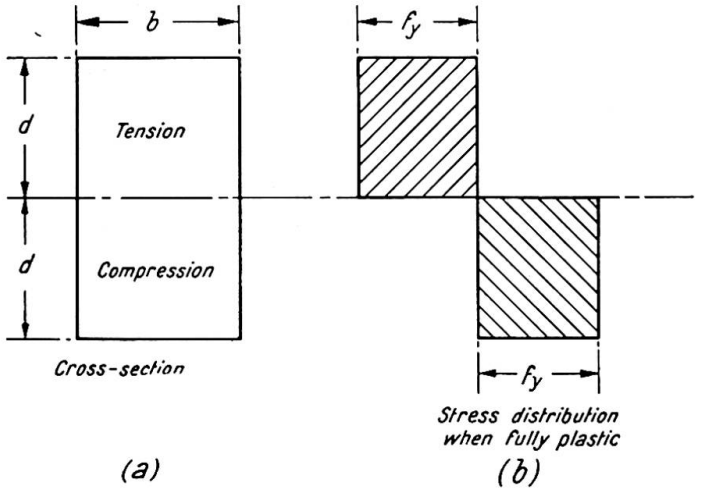

Fig. 1. Fully plastic stress distribution for a rectangular beam

$$M_p = bd^2 f_y \quad . . . . . (1)$$

Let the weight per unit length of the beam be w, and let the density of the material be ρ. Then

$$w = 2bd\rho \quad . . . . . (2)$$

If b is constant and d varies, then

$$w \propto M_p^{\frac{1}{2}} \quad . . . . . (3)$$

If d is constant and b varies,

$$w \propto M_p \quad . . . . . (4)$$

while if b and d both vary such that b/d remains constant

$$w \propto M_p^{\frac{3}{2}} \quad . . . . . (5)$$

Hence, however the section is varied,

$$w = kM_p^n \quad . . . . . (6)$$

where k is a constant and $\frac{1}{2} < n < 1$.

Arguments similar to the above may be applied to sections other than rectangular, and thus equation (6) gives a general relationship between M_p and w. This formula

isfactory in that it takes no account of the effect of shear forces. hear forces have little effect on the value of the full plastic moment,[3] esisting shear forces will prevent the section of a beam being allowed the applied bending moment at collapse is zero. Hence it will in ned that

$$w=w_0+kM_p^n \quad . \quad . \quad . \quad . \quad . \quad . \quad . \quad . \quad . \quad (7)$$

constant.

ENDED BEAM OF CONTINUOUSLY VARYING SECTION

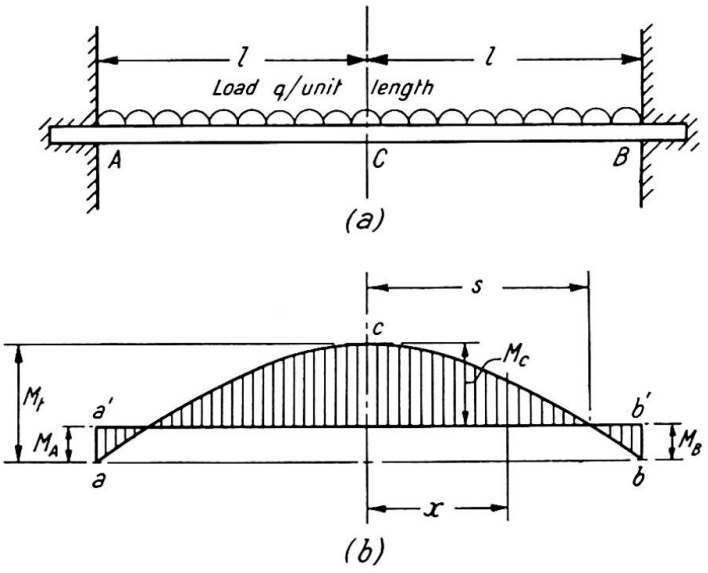

Fig. 2. Bending moment distribution for a beam of continuously varying section (uniformly distributed load)

The beam AB (see fig. 2(*a*)), of length $2l$, is fixed at the ends and carries a uniformly distributed load at collapse of q per unit length. Let the hogging bending moments at the ends (M_A and M_B) be assumed equal at collapse, and let M_C denote the sagging bending moment at the centre. Let M_t be the central bending moment which would be induced in a similar simply supported beam. The bending moment distribution at collapse in the fixed-ended beam may be obtained by superimposing on a parabolic bending moment diagram acb of height M_t (fig. 2(*b*)) the bending moment distribution aa′b′a due to the terminal moments M_A and M , giving the resultant shaded area. Let s denote the distance of the points of contraflexure from the centre of length of the beam.

Then

$$\left.\begin{aligned} M_t &= \frac{ql^2}{2} \\ M_A=M_B &= \frac{l^2-s^2}{l^2}M_t \\ M_C &= \frac{s^2}{l^2}M_t \end{aligned}\right\} \quad . \quad . \quad . \quad . \quad . \quad . \quad . \quad . \quad (8)$$

If x denotes the distance of any section from the centre of length of
then the minimum full plastic moment at that section becomes

when $0<x<s$, $M_p=\frac{s^2-x^2}{l^2}M_t$

when $s<x<l$, $M_p=\frac{x^2-s^2}{l^2}M_t$ . . . . . .

Hence if W denotes the weight of the beam,

$$W=2w_0l+2k\frac{M_t^n}{l^{2n}}\left[\int_o^s(s^2-x^2)^n dx+\int_s^l(x^2-s^2)^n dx\right] \quad . .$$

The most economical design will be obtained with that value of s for which W
minimum, i.e. putting $dW/ds=0$, when

$$\int_o^s(s^2-x^2)^{n-1}dx=\int_s^l(x^2-s^2)^{n-1}dx \quad . . . . . (11)$$

If M_p' and W' denote the full plastic moment and weight respectively of the least prismatic beam sufficient to carry the load, then

$$M_p'=\frac{M_t}{2} \quad . . . . . (12)$$

$$W'=2w_0l+2k\left(\frac{M_t}{2}\right)^n l \quad . . . . . (13)$$

When $n=0{\cdot}5$, the most economical value of s is given by

$$\frac{s}{l}=\operatorname{sech}\frac{\pi}{2}=0{\cdot}3986$$

The corresponding minimum weight is

$$W=2w_0l+0{\cdot}9172kM_t^{\frac{1}{2}}l$$

while $$W'=2w_0l+1{\cdot}4142kM_t^{\frac{1}{2}}l$$

The percentage saving of material depends on the ratio of w_0 to $kM_t^{\frac{1}{2}}$. If the requirements of resistance to shear are ignored ($w_0=0$), an economy of up to 35·1% of the weight of the uniform beam can be achieved. When the effect of shear is allowed for, the percentage economy will become less.

When $n=1{\cdot}0$, the economical value of s is $s/l=0{\cdot}5$,

whence $$W=2w_0l+0{\cdot}5kM_tl$$

while $$W'=2w_0l+kM_tl$$

In this case therefore a maximum economy (ignoring shear) of 50% is possible.

When $\frac{1}{2}<n<1$, it may be shown from equation (11) that the most economical value of s is given approximately by the formula

$$\frac{l}{s}=2+1{\cdot}2467\left(\frac{3}{2}\right)^{1-n}\left(\frac{1-n}{1+n}\right) \quad . . . . . (14)$$

Values of s/l for various values of n are given in Table I.

TABLE I

n	s/l
1·0	0·5000
0·9	0·4835
0·8	0·4651
0·7	0·4447
0·6	0·4226
0·5	0·3986

Points of contraflexure for beam of continuously varying section carrying a uniform load (see fig. 2)

Although for any given value of n the maximum economy is only achieved for some definite value of s, the loss in economy is negligible if $s/l=0{\cdot}45$. This is demonstrated in fig. 3, which shows the percentage economies achieved (assuming $w_0=0$) with various values of s/l for $n=0{\cdot}5$ and $n=1{\cdot}0$.

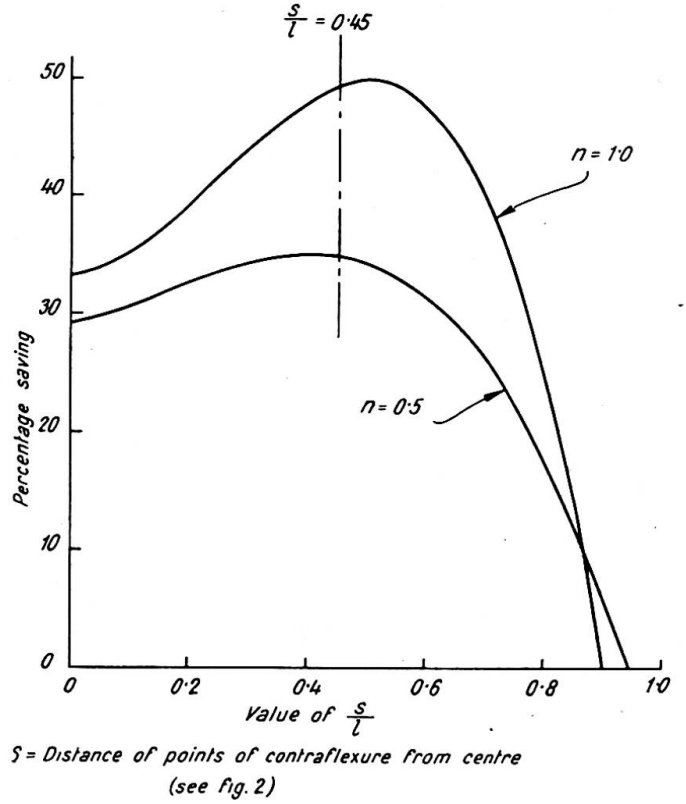

Fig. 3. Economies achieved by continuously varying the section of a fixed-ended beam (uniformly distributed load)

4. FIXED-ENDED BEAM WITH DISCRETE VARIATIONS IN SECTION

Due to the practical difficulties of varying the section of a beam continuously as envisaged above, it is worth while investigating the economies which can be achieved when the full plastic moment is increased by discrete amounts (a) at the centre only, (b) at the ends only and (c) at both centre and ends.

Since the full plastic moment of resistance is nowhere reduced to zero, there will in general be no need to allow for the effects of shear on the relationship between w and M_p (equation (7)). In the following analysis it is therefore assumed that $w_0=0$.

(a) *Section increased over a central length only*

Let the beam previously considered have a uniform value of M_p denoted by M_1, except over a central length $2a$, where it is reinforced so that $M_p=M_2$ where $M_2>M_1$ (see fig. 4(*a*)). The bending moments at collapse are shown by the shaded area in

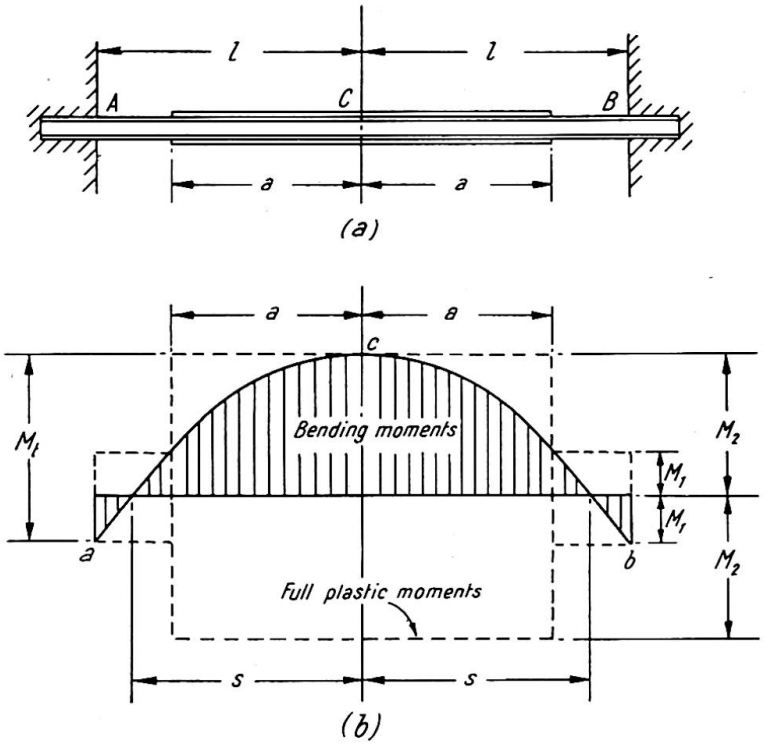

Fig. 4. Bending moment distribution for a beam reinforced at centre only (uniformly distributed load)

fig. 4(*b*), while the moments of resistance M_1 and M_2 are indicated by dotted lines, which must completely enclose the bending moment diagram. Hence

$$M_1=M_A=M_B=\frac{l^2-s^2}{l^2}M_t \quad . \quad . \quad . \quad . \quad . \quad . \quad . \quad . \quad (15)$$

$$M_2=M_C=\frac{s^2}{l^2}M_t \quad . \quad . \quad . \quad . \quad . \quad . \quad . \quad . \quad . \quad . \quad . \quad (16)$$

The value of a is obtained by noting that where the beam changes section, the sagging moment is equal to M_1, and hence

$$M_1=\frac{s^2-a^2}{l^2}M_t \quad . \quad . \quad . \quad . \quad . \quad . \quad . \quad . \quad (17)$$

It follows from equations (15) and (16) that

$$M_1+M_2=M_t \quad . \quad . \quad . \quad . \quad . \quad . \quad . \quad . \quad . \quad (18)$$

while from equations (15) and (17), putting $M_1/M_t=r$,

$$\frac{a}{l}=\sqrt{1-2r} \quad . \quad . \quad . \quad . \quad . \quad . \quad . \quad . \quad . \quad (19)$$

The total weight W of the beam is given by

$$W=2kM_1{}^n(l-a)+2kM_2{}^n a \quad . \quad . \quad . \quad . \quad . \quad . \quad . \quad (20)$$

It may be shown from equations (18), (19) and (20) that

$$W=2kM_t{}^n l[r^n(1-\sqrt{1-2r})+(1-r)^n\sqrt{1-2r}] \quad . \; . \; . \quad (21)$$

When W has its minimum value,

$$\left(\frac{r}{1-r}\right)^{1-n}=\frac{n\sqrt{1-2r}+(2nr-n+r)}{1-(2nr-n+r)} \quad . \; . \; . \; . \; . \quad (22)$$

TABLE II

n	$r=M_1/M_t$	a/l
1·0	0·4444	0·3333
0·9	0·4432	0·3371
0·8	0·4418	0·3412
0·7	0·4403	0·3456
0·6	0·4388	0·3500
0·5	0·4370	0·3550

Plastic moment ratio and proportion of beam to be reinforced for beam reinforced at centre only (see fig. 4)

The most economical values of r and a/l are given in Table II for values of n between 0·5 and 1·0. It may be noted that r represents the ratio of M_1, the full plastic moment of the unreinforced part of the beam, to M_t, the full plastic moment of the uniform simply supported beam which would just carry the same load. Hence r will be termed the "plastic moment ratio." It will be seen that r and a/l (the proportion of the beam to be reinforced) are almost constant, r varying from 0·4444 to 0·4370 and a/l from 0·3333 to 0·3550. As a working rule therefore the beam should be reinforced for about one-third of its length, the reinforced section having a full plastic moment some 25% or 30% greater than the unreinforced section.

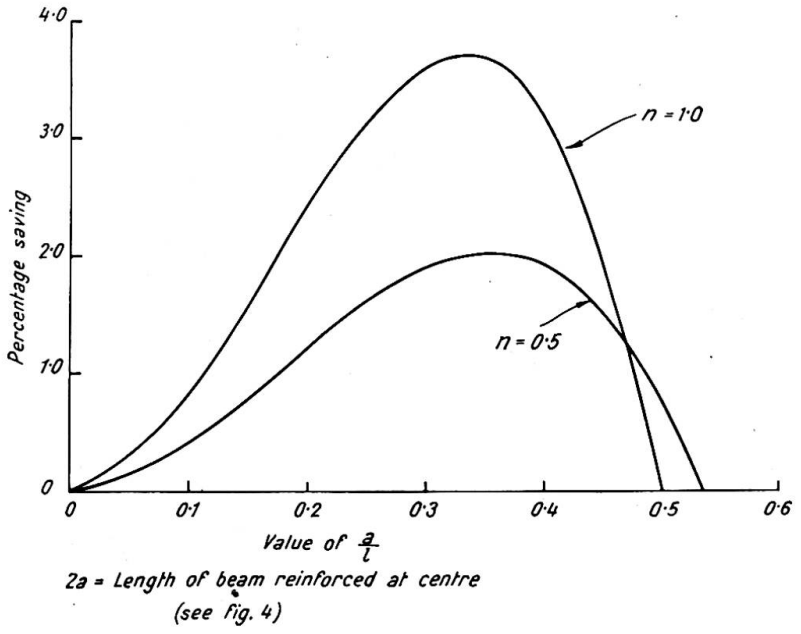

Fig. 5. Economies achieved by reinforcing the centre of a fixed-ended beam (uniformly distributed load)

The variation of the percentage saving (as compared with a beam of uniform section throughout) with a/l for $n=0{\cdot}5$ and $n=1{\cdot}0$ is shown in fig. 5. It will be observed that if more than about half of the beam is reinforced, there is no saving in material. When $n=0{\cdot}5$, the maximum saving possible is $2{\cdot}03\,\%$ as compared with a saving of $35{\cdot}1\,\%$ when the section is varied continuously in an ideal manner. When $n=1{\cdot}0$, the corresponding figures are $3{\cdot}70\,\%$ and $50{\cdot}0\,\%$ respectively. It is therefore apparent that no great advantage accrues by increasing the section only at the centre.

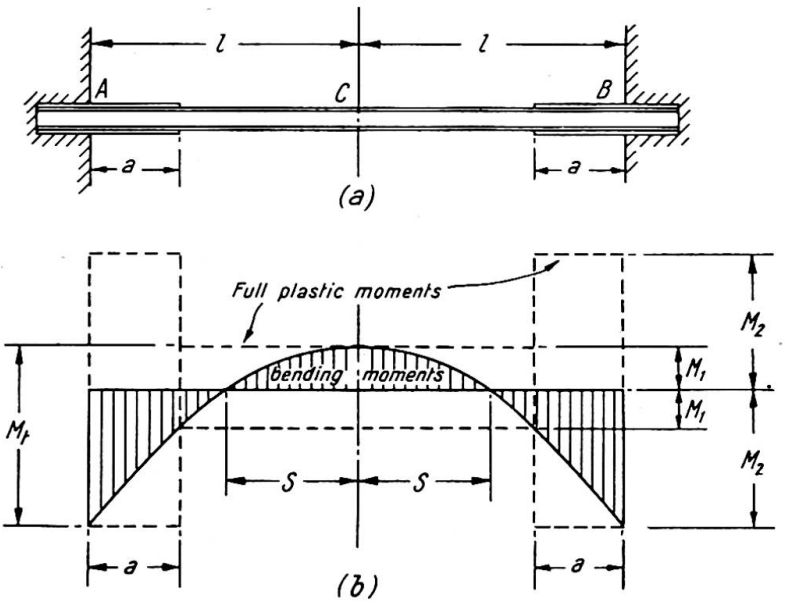

Fig. 6. Bending moment distribution for a beam reinforced at ends only (uniformly distributed load)

(b) *Section increased at ends only*

A beam of uniform plastic moment of resistance M_1 is reinforced for a distance a from either end so that its plastic moment of resistance becomes M_2 (see fig. 6(*a*)). The bending moment distribution at collapse is shown by the shaded area in fig. 6(*b*), while the moments of resistance are superimposed as dotted lines. If full plastic moments are just sufficient to withstand the applied moments, then

$$M_1=M_C=\frac{s^2}{l^2}M_t \quad . \quad . \quad . \quad . \quad . \quad . \quad . \quad . \quad . \quad . \quad . \quad (23)$$

$$M_2=M_A=M_B=\frac{l^2-s^2}{l^2}M_t \quad . \quad . \quad . \quad . \quad . \quad . \quad . \quad . \quad . \quad (24)$$

Since where the beam changes section the hogging moment has the value M_1,

$$M_1=\frac{(l-a)^2-s^2}{l^2}M_t \quad . \quad . \quad . \quad . \quad . \quad . \quad . \quad . \quad . \quad . \quad (25)$$

From equations (23) and (24),

$$M_1+M_2=M_t \quad . \quad . \quad . \quad . \quad . \quad . \quad . \quad . \quad . \quad . \quad . \quad . \quad . \quad (26)$$

while from equations (23) and (25), if $M_1/M_t=r$,

$$\frac{a}{l}=1-\sqrt{2r} \quad . \quad . \quad . \quad . \quad . \quad . \quad . \quad . \quad . \quad . \quad (27)$$

The total weight W of the beam is given by

$$W=2kM_1{}^n(l-a)+2kM_2{}^n a \quad . \quad . \quad . \quad . \quad . \quad . \quad (28)$$

which, by virtue of equations (26) and (27) becomes

$$W=2kM_t{}^n l[r^n\sqrt{2r}+(1-r)^n(1-\sqrt{2r})] \quad . \quad . \quad . \quad . \quad (29)$$

At minimum W,

$$\left(\frac{r}{1-r}\right)^{1-n}=\frac{(2n+1)r}{(1-2nr-r+n\sqrt{2r})} \quad . \quad . \quad . \quad . \quad . \quad . \quad . \quad . \quad . \quad (30)$$

TABLE III

n	$r=M_1/M_t$	a/l
1·0	0·2946	0·2324
0·9	0·2866	0·2429
0·8	0·2777	0·2548
0·7	0·2680	0·2679
0·6	0·2571	0·2829
0·5	0·2449	0·3001

Plastic moment ratio and proportion of beam to be reinforced for beam reinforced at ends only (see fig. 6)

The most economical values of r and a/l are given in Table III for values of n from 0·5 to 1·0. The value of $r(=M_1/(M_1+M_2))$ varies from 0·2946 to 0·2449, and hence the reinforced section has a full plastic moment from 140% to 208% greater than the unreinforced section. The value of a/l varies from 0·2324 to 0·3001. A satisfactory working rule would therefore be to reinforce an eighth of the length of the beam at either end.

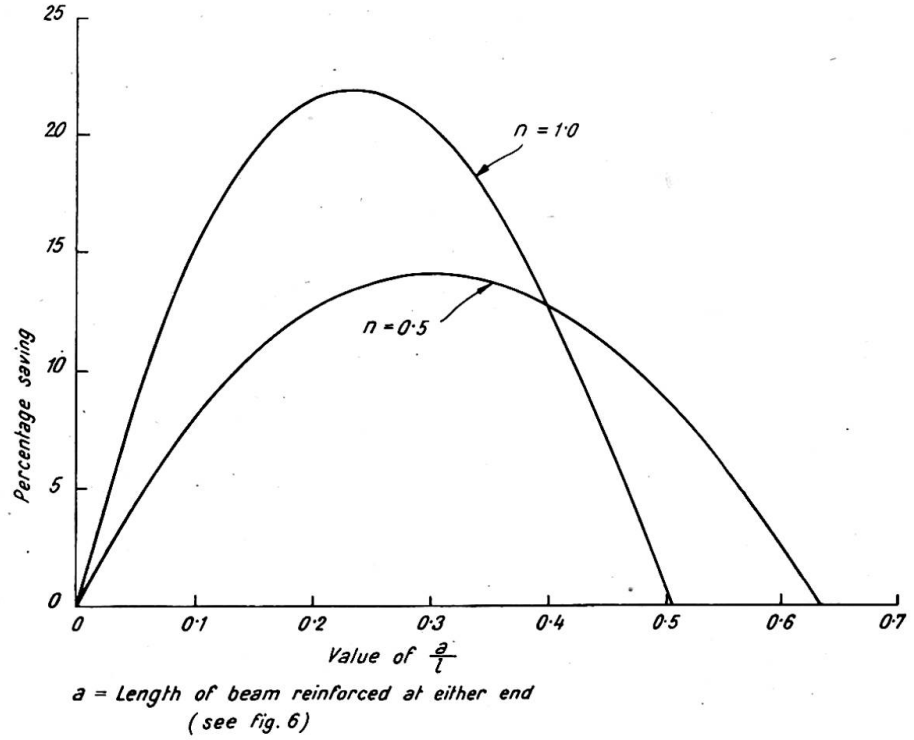

Fig. 7. Economies achieved by reinforcing the ends of a fixed-ended beam (uniformly distributed load)

The variation of the percentage saving (compared with a uniform beam) as a/l is altered is shown in fig. 7 for $n=0{\cdot}5$ and $n=1{\cdot}0$. It will be seen that by taking $a/l=0{\cdot}25$ there is very little loss in economy in either case. When $n=0{\cdot}5$ the maximum saving possible is 14·1 % and for $n=1{\cdot}0$ it is 22·0 %. These figures compare with the ideally attainable economies of 35·1 % and 50·0 % respectively.

The economy practically attainable by reinforcing the ends alone is therefore quite appreciable. It should be noted, however, that the surrounding members must provide a total moment of resistance equal to the full plastic moment of the reinforced part of the beam, and this may sometimes be a serious disadvantage.

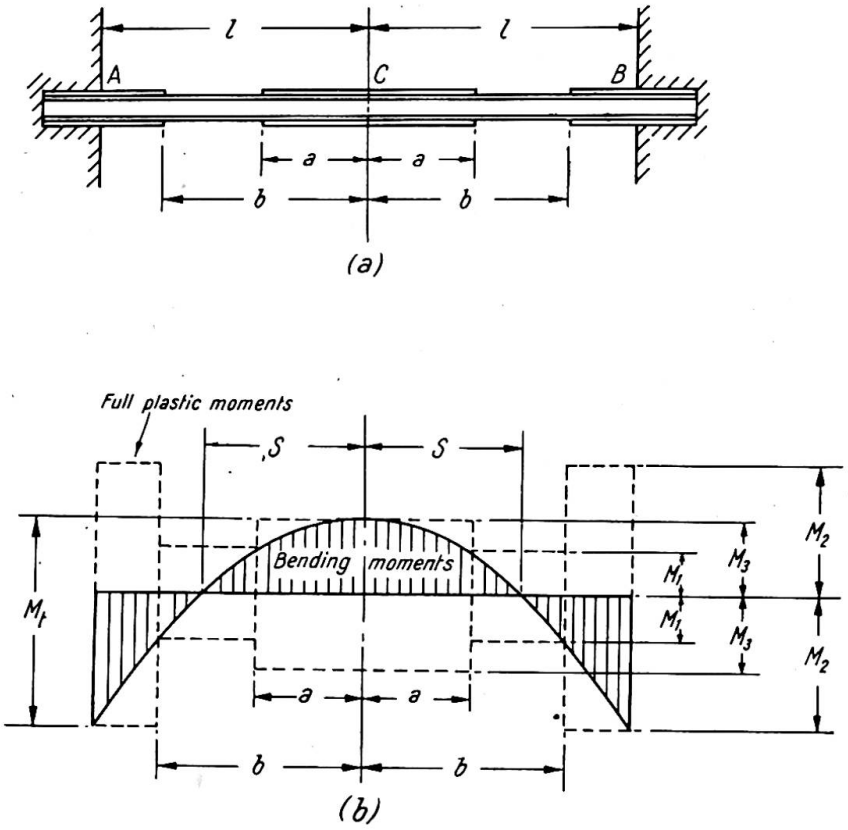

Fig. 8. Bending moment distribution for a beam reinforced at both centre and ends (uniformly distributed load)

(c) *Section increased at both centre and ends*

The advantage obtained by reinforcing both centre and ends may be estimated by considering the beam shown in fig. 8(*a*). This is reinforced for a distance a either side of the centre and at each end for a distance $(l-b)$. The bending moment diagram, shown shaded in fig. 8(*b*), is completely enclosed by the graph of the full plastic moments (shown dotted). The unreinforced section has a moment of resistance M_1, the ends a moment of resistance M_2 and the centre a moment of resistance M_3.

Hence

$$M_3-M_1=\frac{a^2}{l^2}M_t \quad . \quad . \quad . \quad . \quad . \quad . \quad . \quad . \quad . \quad . \quad (31)$$

$$M_3+M_1=\frac{b^2}{l^2}M_t \quad . \quad . \quad . \quad . \quad . \quad . \quad . \quad . \quad . \quad . \quad (32)$$

$$M_2+M_3=M_t \quad . \quad . \quad . \quad . \quad . \quad . \quad . \quad . \quad . \quad . \quad . \quad (33)$$

Solving for M_1, M_2 and M_3,

$$M_1=\frac{b^2-a^2}{2l^2}M_t \quad . \quad . \quad . \quad . \quad . \quad . \quad . \quad . \quad . \quad . \quad (34)$$

$$M_2=\frac{2l^2-a^2-b^2}{2l^2}M_t \quad . \quad . \quad . \quad . \quad . \quad . \quad . \quad . \quad . \quad (35)$$

$$M_3=\frac{a^2+b^2}{2l^2}M_t \quad . \quad . \quad . \quad . \quad . \quad . \quad . \quad . \quad . \quad . \quad (36)$$

The total mass of the beam thus becomes

$$W=2^{1-n}k\frac{M_t^n}{l^{2n}}[a(a^2+b^2)^n+(b-a)(b^2-a^2)^n+(l-b)(2l^2-a^2-b^2)^n] \quad . \quad (37)$$

When W has its minimum value, $\partial W/\partial a=0$ and $\partial W/\partial b=0$.

When $n=1{\cdot}0$ the above conditions give $3a^2-al=0$ and $3b^2-bl-l^2=0$,

whence
$$\frac{a}{l}=\tfrac{1}{3}=0{\cdot}3333$$

$$\frac{b}{l}=\frac{1+\sqrt{13}}{6}=0{\cdot}7676$$

The moment of resistance is 171·8% greater than that of the unreinforced beam at the ends, and 46·5% greater at the centre. The saving is 25·7%, compared with 22·0% with end reinforcement only and 3·7% with central reinforcement only.

When $n=0{\cdot}5$, it is found that

$$\frac{ab}{\sqrt{a^2+b^2}}+\frac{(b-a)(a+2b)}{\sqrt{b^2-a^2}}-\frac{2l^2+lb-a^2-2b^2}{\sqrt{2l^2-a^2-b^2}}=0$$

$$\frac{2a^2+b^2}{\sqrt{a^2+b^2}}-\frac{(b-a)(2a+b)}{\sqrt{b^2-a^2}}-\frac{a(l-b)}{\sqrt{2l^2-a^2-b^2}}=0$$

These equations give $a/l=0{\cdot}3185$ and $b/l=0{\cdot}7074$. The moments of resistance at the ends and centre are respectively 250·5% and 50·9% greater than that of the unreinforced beam. The saving is 16·1%, compared with 14·1% with end reinforcement only and 2·0% with central reinforcement only.

Hence the percentage saving with both central and end reinforcement is very little greater than the saving with end reinforcement only.

5. Conclusions

It has been shown that the adoption of beams of varying cross-section can lead to considerable economies in total material consumption when the basis of design is the ultimate load which the beam will carry as calculated by the simple plastic theory. The best shape for the beams has been calculated for the case of a fixed-ended beam carrying a uniformly distributed load, the minimum cross-sections occurring at about one-fifth the length of the beam from the centre. The maximum theoretical economies are of the order 35–50%.

Since the construction of a beam of continuously varying cross-section may have considerable practical disadvantages, an investigation has been made into the effect of reinforcing either the centre or the ends of the beam, or both centre and ends simultaneously. It has been shown that there is only a negligible advantage in reinforcing the centre, but that reinforcing the ends does lead to appreciable

economies. The economy achieved by reinforcing both centre and ends is virtually no greater than that achieved by reinforcing the ends alone.

REFERENCES

(1) HORNE, M. R. "Fundamental Propositions in the Plastic Theory of Structures," *J. Inst. Civ. Engrs.*, **34**, 174, 1950.

(2) HEYMAN, J. "Plastic Design of Beams and Plane Frames for Minimum Material Consumption," *Quart. J. Appl. Math.*, **8**, 373, 1951.

(3) HORNE, M. R. "The Plastic Theory of Bending of Mild Steel Beams, with Particular Reference to the Effect of Shear Forces," *Proc. Roy. Soc. A.*, Series A, **207**, 216, 1951.

Summary

The simple plastic theory gives a direct means of determining the form of a fixed-ended beam of varying cross-section such that the total weight of material shall be an absolute minimum. The paper shows how this form may be deduced for a uniformly distributed load, both when the cross-section of the beam can be varied continuously, and when the size of the beam can only be adjusted in discrete intervals. The maximum theoretically attainable economies of material are discussed.

Résumé

La théorie simple de la plasticité fournit un moyen direct pour déterminer la forme à donner à une poutre encastrée à ses extrémités et présentant une section non uniforme, pour que le poids total de métal employé constitue un minimum absolu. L'auteur montre comment l'on peut déterminer une telle forme dans le cas d'une charge uniformément répartie, aussi bien lorsque la section de la poutre peut varier d'une manière continue que lorsque ses dimensions effectives ne peuvent être choisies que dans des intervalles déterminés. Il discute l'économie maximum de métal que l'on peut réaliser du point de vue théorique.

Zusammenfassung

Die einfache Plastizitätstheorie erlaubt uns die direkte Bestimmung derjenigen Form eines eingespannten Balkens mit veränderlichem Querschnitt, bei der das Gesamtgewicht des Materials ein absolutes Minimum sein soll. Der Aufsatz zeigt die Ermittlung dieser Form bei gleichmässig verteilter Belastung, einerseits, wenn der Querschnitt des Balkens stetig veränderlich ausgeführt werden kann und andererseits, wenn seine Abmessungen nur in bestimmten Abstufungen verändert werden können. Die höchste theoretisch mögliche Ausnützung des Materials wird untersucht.

AI 3

Sur la plastification de flexion des poutres à âme pleine en acier doux

(Récents essais français—Examen critique des essais antérieurs—Questions restant à résoudre)

Plastification of bending plate-web girders in mild steel

(Recent French tests—Critical study of previous tests—Problems still to be solved)

Plastifizierung der Vollwand-Biegeträger aus Flusstahl

(Neue französische Versuche—Kritische Betrachtung der früheren Versuche—Noch zu lösende Aufgaben)

A. LAZARD

Ingénieur en Chef des Ponts et Chaussées

Chef des Divisions Centrales des Ouvrages d'Art et des Études d'Aménagements de la S.N.C.F.

Introduction

Les recherches sur la plastification de flexion des poutres à âme pleine en acier doux de construction doivent conduire à une économie de métal et à une économie d'argent. Cela s'obtiendra par relèvement des contraintes maxima autorisées par les règlements officiels, basés presque tous sur l'ancienne conception de l'élasticité, en sollicitant soit certaines dérogations, soit des modifications permanentes à ces règlements. Il n'y a espoir d'aboutir que si le dossier présenté aux Organismes responsables des Grandes Administrations est basé sur des faits indiscutables, résultats d'expériences nombreuses et probantes, et si les limites d'utilisation des dérogations sollicitées ou des nouvelles prescriptions proposées sont bien précisées.

Or à la suite d'importantes expériences de flexion effectuées sur poutrelles Grey de 1 mètre de hauteur (c'est-à-dire sur les plus grands laminés du monde) qui nous a permis d'entrevoir quantité de phénomènes de plastification peu ou mal connus, il nous est apparu, en procédant à un examen critique général des théories et des expériences existantes, que les généralisations étaient souvent hâtives, qu'il existait un nombre considérable de questions non posées ou restées sans réponse, que, malgré des tentatives isolées dans ce sens, les limites d'utilisation des nouvelles méthodes n'étaient pas suffisamment précisées, et, qu'en définitive, il fallait procéder à un nouvel examen du problème en opérant avec beaucoup d'ordre.

Pour notre part nous avons mis en train, avec la collaboration de la Chambre Syndicale des Constructeurs Métalliques Français, des séries d'expériences dans le domaine fort vaste, quoique très restrictif, des

laminés I ou H
bruts*
de longueur dépassant 6 fois la hauteur
sollicités à la flexion
statiquement
et isostatiquement
jusqu'à ruine.

Le chapitre I de la présente communication est consacré à une description rapide des expériences déjà réalisées et au développement des conclusions auxquelles on est conduit, en insistant sur les points qui appellent des expériences de contrôle par d'autres chercheurs.

Compte tenu de ces conclusions, les autres essais connus de nous† sont examinés et discutés au chapitre II, en suivant la classification qui a paru la plus adéquate. Chaque fois nous nous sommes basés sur la description détaillée des circonstances expérimentales: malheureusement les détails font souvent défaut.

Les conclusions d'ensemble sont développées au chapitre III. On insiste sur les lacunes des recherches actuelles. On propose d'établir un programme général des expériences à reprendre ou restant à faire, dont on souhaite un partage entre les membres de l'Association.

Chapitre I—Les récents essais français sur la plastification en flexion statique et isostatique de laminés I ou H bruts

On décrira quatre séries d'essais qui tous ont été poussés jusqu'à la ruine.

1*ère Série: Poutrelles H de* 1 *mètre de hauteur*

Ces essais, exécutés pour le compte de la S.N.C.F. en 1948–49, ont été décrits en détail par nous, dans le Xème Volume des Mémoires de l'A.I.P.C., et ont fait l'objet d'un léger complément théorique dans *Travaux*, numéro de mai 1950. Ils sont schématisés figs. 1 et 2.

Ils ont clairement mis en évidence les faits suivants:

(*a*) Les premiers signes de plastification sont apparus bien avant que les contraintes à la Navier (quotient du Moment M par le module de résistance de la section I/v ou W), aient atteint la limite élastique conventionnelle du métal (à $2\,‰$) déterminée sur une éprouvette prélevée dans une semelle d'un about. L'apparition de la plastification dépend essentiellement des appareils de mesure utilisés pour la déceler et du critère choisi pour la définir. Elle semble débuter dans la semelle tendue.

Il apparaît que la notion de "Moment Elastique" (ou produit de la limite élastique par le module de résistance), souvent utilisée par les théoriciens, ne correspond à

* C'est-à-dire sans trous. Nous mettons en route, à l'époque à laquelle nous rédigeons la présente communication—juin 1951—une nouvelle série, avec trous cette fois. Nous espérons pouvoir en rendre compte à l'époque du Congrès.

† Il ne nous a pas toujours été possible de nous procurer tous les articles originaux. Compte tenu du nombre limité de pages dont nous pouvions disposer dans la présente communication, nous ne donnons qu'un aperçu des expériences. Un texte détaillé paraîtra dans *Travaux*, numéros de novembre et décembre 1951.

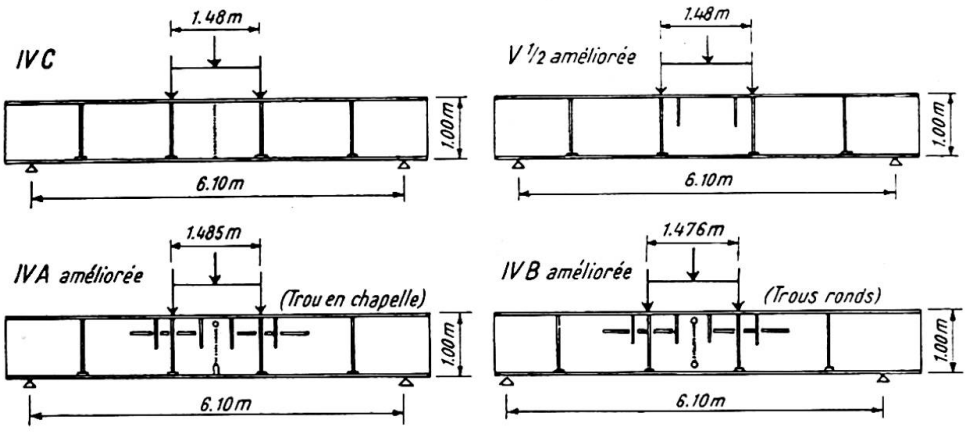

Fig. 1

Fig. 2

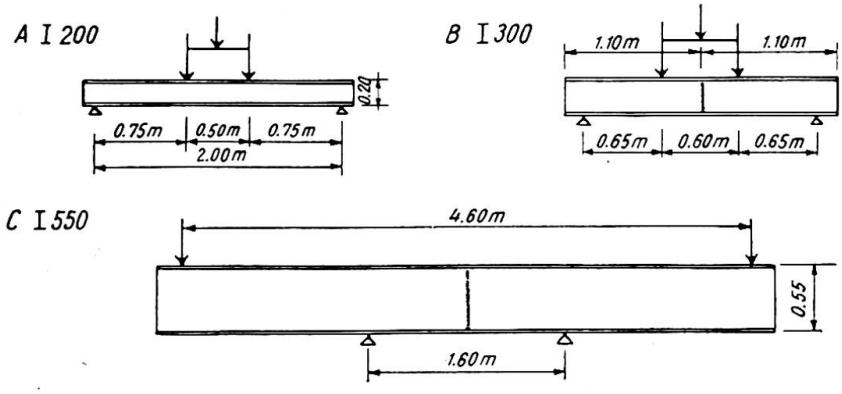

Fig. 3

aucun phénomène physique réel.* Pour cette valeur la poutrelle est déjà partiellement plastifiée. Cela paraît être sous la dépendance des contraintes préalables, enfermées dans la poutre par les traitements: chimique, physique, mécanique, subis antérieurement (et que le prélèvement de l'éprouvette libère partiellement).

(*b*) La plastification est un phénomène essentiellement discontinu. Elle se produit en des points très variables et diversement localisés. Ces points se mettent brusquement à fluer, la limite d'écoulement ayant été localement atteinte; les points voisins

* En réalité c'est la limite du domaine de proportionnalité de la poutrelle qu'on a déterminé. Il faudrait donc la comparer à la limite de proportionnalité du métal. A supposer que cette limite ait un sens pour le métal *in situ* (état contraint) et soit une constante en tous les points.

modifient leur progression de déformation, dans des proportions fort variables, allant d'un simple ralentissement à une régression.*

Les charges augmentant, la plastification se propage graduellement, par à coups, en intéressant des zones de plus en plus considérables. Il ne se passe rien de spécial dans les zones tendues; au contraire dans les zones comprimées on finit par parvenir à des flambements locaux *âme ou semelle* qui entraînent la ruine de la poutrelle.

(*c*) L'hypothèse de Bernoulli sur la conservation des sections planes (ou sur la proportionnalité des déformations aux distances de la fibre neutre) devient de plus en plus inexacte, au fur et à mesure que la plastification progresse.

(*d*) Dans les zones tendues apparaissent des lignes de glissement, dans les zones comprimées des rides de glissement, selon la terminologie du professeur Baes (voir fig. 2).† Lignes et rides n'apparaissent que dans des zones fortement plastifiées. Leur progression permet d'évaluer grossièrement, et probablement avec un certain retard, la progression de la plastification.

(*e*) On est amené à en déduire l'existence de contraintes de compression agissant sur les facettes longitudinales.

Dans l'âme c'est une conséquence de l'effet de courbure de la poutre. Dans les semelles on voit mal à quoi cela correspond.

(*f*) Les dispositions ayant été prises pour empêcher l'apparition de tous les phénomènes d'instabilité élastiques (déversement, flambements élastiques locaux) et dans une certaine mesure les flambements plastiques locaux la ruine des poutrelles est intervenue par plastification quasi totale. La "contrainte à la Navier" lors de la ruine plastique a certainement dépassé 30 kg./mm.^{2}

2ème Série: IPN de 200 *et* 300 *et HPN de* 550

Ces essais, exécutés pour le compte de la Chambre Syndicale des Constructeurs Métalliques en septembre–octobre 1949, ont été décrits, en détails par M. Dawance‡ lors d'une conférence faite à Paris le 13 décembre 1949, suivie d'une intéressante discussion (voir fig. 3).

Les prélèvements d'éprouvettes ont montré que les limites élastiques dans les âmes sont plus élevées que celles des semelles. C'est là d'ailleurs un phénomène tout à fait général.

Les essais ont sensiblement confirmé les conclusions de nos propres essais.

3ème Série: Mâts encastrés en poutrelles HN de 180 *et* 260

Ces essais ont été exécutés en 1950, sur des chantiers de la S.N.C.F., à l'occasion de recherches sur les poteaux supports de caténaires des futures électrifications.

Les essais de Marolles (5 septembre 1950) où des poutrelles HN de 180 étaient profondément encastrées dans un important massif de béton sont représentés à la fig. 4.

3 poutrelles ont été essayées avec efforts dans le plan de l'âme seule (fig. 4(*b*)). Toutes trois ont été ruinées pour une contrainte à la Navier de 35,2 kg./mm.^{2} calculée à la base de l'encastrement.

* Cette régression (à laquelle nous avons donné le nom de "bec d'oiseau" quand elle apparaît similairement dans le béton tendu au moment de la fissuration) a été également observé par M. Soete, professeur à Gand, dans des essais de traction sur éprouvettes soudées. Elle semble correspondre aux phénomènes observés, en rayons X, par les Allemands. Toutefois Schleicher (par exemple Bauingenieur, juillet 1950) prétend qu'on mesure par ce procédé les contraintes vraies.

† Ces phénomènes ont déjà été notés, mais avec beaucoup de prudence, par le prof. Kayser. Congrès de Berlin, Rapport final, 1938, p. 557, et *Stahlbau*, 26.2.1937.

‡ *Annales de l'Institut du Bâtiment et Travaux Publics*, mai 1950. Construction Métallique No. 6: "Nouvelles recherches expérimentales sur la plasticité des éléments de construction métallique."

Nous avons pu suivre avec précision le phénomène de ruine plastique sur l'une d'elles. Malgré les précautions prises l'effort n'était pas rigoureusement exercé dans le plan de l'âme et la poutrelle avait un aspect légèrement vrillé. Brusquement, au moment où l'effort de traction dans le câble atteignait 1 300 kg. (mesuré au dynamomètre), correspondant à un moment à l'encastrement de 14 940 kgm. et une contrainte à la Navier de 35,15 kg./mm.^{2}, nous avons vu sur une des ailes de la semelle tendue se propager vers le bas, et à partir d'une hauteur d'environ 60 cm. au-dessus du sol, comme une sorte de vibration de plastification; le vrillage a disparu et la poutrelle est alors venue, sans résistance, à la demande du câble. Compte tenu de la rapide décroissance du moment en fonction de la hauteur, la contrainte à la Navier, dans la zone d'où est parti l'ébranlement plastique de ruine, atteignait environ 32 kg./mm.^{2}

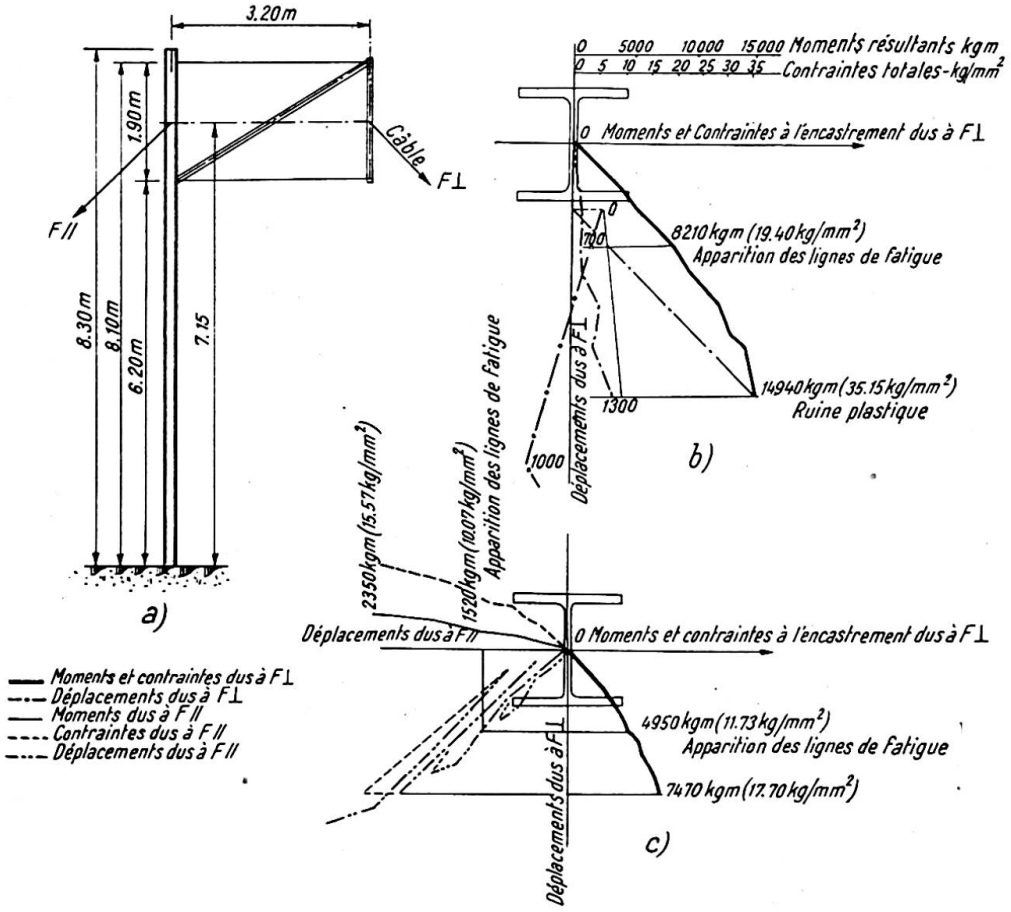

Fig. 4

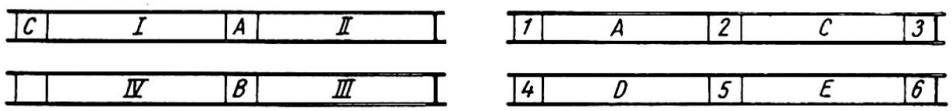

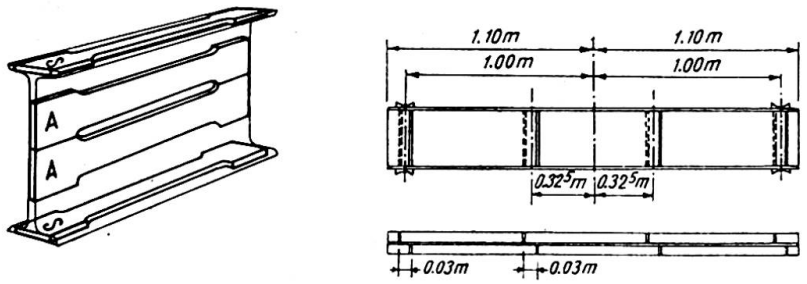

Fig. 5

Dès qu'on arrêtait l'enroulement du câble sur le treuil, les poutrelles cessaient de se déformer. Nous avons alors déchargé complètement (les poutrelles gardant une déformation importante) puis rechargé. A partir de cette déformation résiduelle, les poutrelles se sont comportées sensiblement comme des poutrelles neuves et élastiques tant que la charge n'a pas atteint une valeur très peu inférieure à celle ayant provoqué la ruine plastique; la poutrelle s'est remise alors à se déformer exagérément au simple appel du câble.

Ces essais complémentaires ont donc montré clairement (contrairement à une opinion répandue) qu'une poutrelle peut avoir été amenée à la plastification totale et être réutilisée dans certaines limites à partir de la déformation permanente acquise. Il n'y a ruine définitive que si la sollicitation est maintenue en permanence: si la sollicitation cesse la poutrelle peut être récupérée dans une certaine mesure.*

Une autre poutrelle a été essayée à la flexion déviée (fig. 4(*c*)). La ruine plastique est intervenue pour une valeur des efforts correspondant à une contrainte à la Navier à l'encastrement de l'aile de la membrure la plus comprimée égale à 33,3 kg./mm.^{2}

D'autres essais ont eu lieu à Vigneux avec des HN de 260 enfoncées de 3 m. dans un massif de béton de 55 cm. de diamètre et de 3 m. de profondeur.

Ils ont manifesté des phénomènes d'instabilité élastique qui sont susceptibles de se produire chaque fois qu'on ne prend pas les précautions nécessaires pour les rendre impossibles.

4ème Série: IPN de 200*: Sollicitations cycliques*

Ces essais ont été exécutés, conjointement par la S.N.C.F. et la Chambre Syndicale des Constructeurs Métalliques en 1950 et 1951, par M. Dawance et son équipe de collaborateurs habituels.

Les tronçons de 2,20 m. des poutrelles IPN 200 ont été extraits dans des barres de 7 m. provenant des parcs de la S.N.C.F. Les éprouvettes ont été prélevées dans des sections d'essai repérées en bout de chaque tronçon: deux dans les âmes, une dans chaque semelle (voir fig. 5). Le tableau suivant donne les limites élastiques conventionnelles (en kg./mm.^{2}) des sections d'essai.

Poutrelles des:	1ère sous-série			2ème sous-série			3ème sous-série		
Sections d'essais:	A	C	B	1	2	3	4	5	6
Semelles hautes	24,7	29	28,3	26,9	26,1	26,7	26,6	26,9	27,7
Semelles basses	27	28,3	28,3	26,6	25,4	24,9	26	25,9	24,2
Âmes hautes	29,2	33,8	29,6	26,8	27,9	27,8	28	28,2	29
Âmes basses	30	34,8	32,0	27,8	28,4	29,9	30,2	29,4	28,8

On notera *une très notable dispersion des résultats le long d'une même fibre du métal* ainsi que des valeurs plus élevées dans les âmes que dans les semelles.

Ces essais ont eu pour but de rechercher l'influence de la répétition de cycles de sollicitations sur les phénomènes de plastification et notamment de déterminer la valeur des cycles à partir desquels les déformations permanentes ne se stabiliseraient plus.

On craignait, en particulier, que la ruine plastique intervint, dans ces conditions,

* Dix ans plus tôt nous avions reçu l'ordre de mettre à la ferraille la charpente d'un pont détruit par faits de guerre, dont nous avions proposé la réutilisation partielle. C'est la raison qui nous a poussé à procéder à cette contre épreuve.

bien avant celle qui aurait été observée en suivant le processus des trois premières séries d'essais.

Première sous-série: Sollicitations ondulées—Cycles* 4 *à* $+n$ *kg./mm.*^{2} (*fig.* 6) (*Poutres I et II, III*)—*essais des* 17 *et* 23 *mai, du* 21 *juin et du* 7 *juillet* 1950

Les contraintes à la Navier variaient, dans chaque cycle, entre 4 et $+n$ kg./mm.^{2} La valeur supérieure n du cycle n'était augmentée que lorsque la stabilisation des flèches était obtenue. Deux poutrelles (I et II de la fig. 5) ont été essayées dans ces conditions.

On a pu tirer les conclusions suivantes:

1° *La répétition de cycles de sollicitations ondulées ne modifie pas la valeur du moment entraînant la ruine plastique.* La ruine plastique correspond pour une poutrelle sollicitée statiquement, dans des conditions de flexion déterminées, à un phénomène bien caractérisé qui est indépendant du processus d'application des charges.

2° On peut "accommoder élastiquement" une poutrelle, une fois la déformation permanente acquise. On peut, ce faisant, dépasser, en contrainte à la Navier, la limite élastique conventionnelle.

Nous en avons conçu la possibilité d'utiliser en flexion des poutrelles brutes bien au delà des limites actuellement tolérées par les règlements, *en procédant à une prédéformation volontaire des poutrelles*, sous une contrainte légèrement supérieure aux contraintes maxima d'utilisation.

Mais avant de mettre en application un tel procédé qui peut, naturellement, être conjugué avec un enrobement par du béton de la semelle tendue et déformée, en vue de précontraindre ce béton lorsqu'on retire les charges (les déformations sont, en particulier, très réduites et ne limitent plus l'utilisation des hautes contraintes), *il faut s'assurer que l'accommodation élastique, ainsi acquise, se conserve dans le temps.*

Des essais sont nécessaires pour le vérifier.

Deuxième sous-série: Sollicitations alternées—Cycles 10 *kg./mm.*^{2} *à* $+n$ *kg./mm.*^{2} (*fig.* 7(*a*)), 20 *kg./mm.*^{2} *à* $+n$ *kg./mm.*^{2} (*fig.* 7(*b*))

Les résultats confirment sensiblement les conclusions de la première sous-série; la ruine n'a pas été avancée par les sollicitations alternées et elle est intervenue pratiquement pour les mêmes valeurs de la contrainte à la Navier que dans les essais sans répétitions cycliques.

Troisième sous-série: Sollicitations oscillantes—Cycles entre plus et moins n kg./mm.^{2} (*fig.* 8)

L'essai a montré:

(*a*) que la stabilisation était assez rapidement acquise;†

* Nous adoptons ici la Terminologie que met au point actuellement une sous-commission de l'A.F.N.O.R., présidée par M. Prot:

Une sollicitation périodique est ondulée lorsque les forces varient entre deux limites de même signe.

Une sollicitation périodique est alternée lorsque les forces varient entre deux limites ayant des signes opposés.

Une sollicitation périodique est oscillante lorsque les forces varient entre deux limites ayant des signes opposés et une même valeur absolue.

Une sollicitation périodique est répétée lorsque les forces varient entre zéro et une limite.

† Toutefois le nombre de répétitions (20) n'a peut-être pas toujours été suffisant. La flèche pouvait paraître stabilisée puis brusquement, par exemple à la quinzième répétition, s'accroître à nouveau.

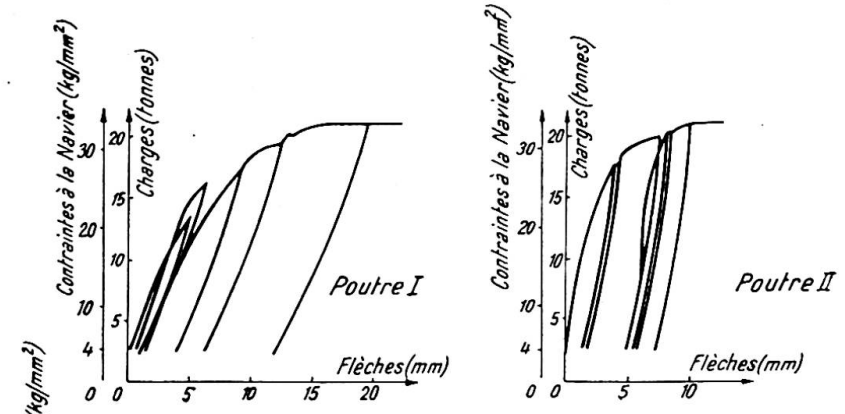

Fig. 6

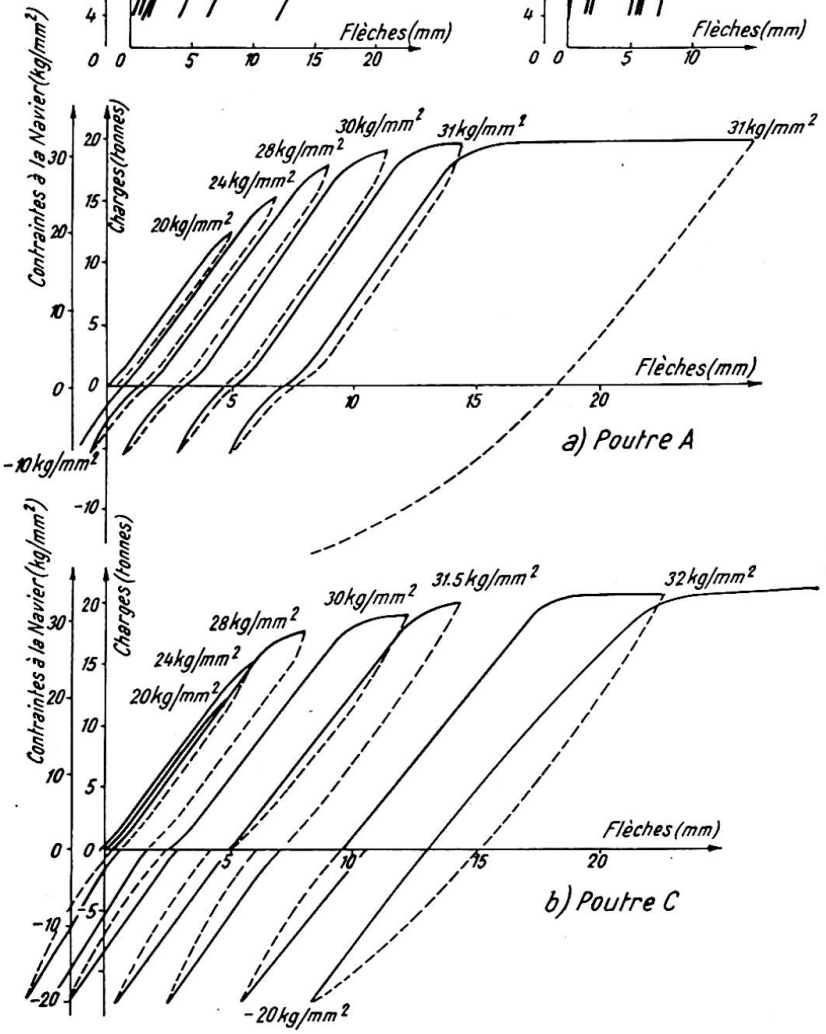

Fig. 7

(*b*) que les cycles d'hystérésis devenaient de plus en plus marqués, la diagonale s'inclinant de plus en plus sur l'horizontale;

(*c*) que l'effet Bauschinger jouait à plein, c'est-à-dire que les déchargements étaient à peu près linéaires, mais que les rechargements (dans un sens ou dans l'autre) montraient au contraire une courbure prononcée;

(*d*) qu'enfin la ruine est intervenue sensiblement pour la même contrainte à la Navier que dans les essais précédents.

Quatrième sous-série: Poutrelles A et D—Essais des 9 *et* 11 *mai* 1951 (*fig.* 9)

Nous nous sommes posé la question suivante: reste-t-il quelques traces, décelables, d'une plastification plus ou moins totale d'une poutrelle? Il est bien certain, en effet,

que lorsqu'une poutrelle est livrée par les forges elle a subi, au cours de son élaboration tant chimique que thermique que mécanique, d'innombrables plastifications. Or le contrôle consiste à mesurer les caractéristiques mécaniques d'une éprouvette prélevée dans le métal; si elles sont satisfaisantes on utilise la poutrelle dans les limites réglementaires. Comment distinguera-t-on une poutrelle "vierge" d'une poutrelle plus ou moins "outrageusement plastifiée" qui, après redressement, aura été remise sur parc.

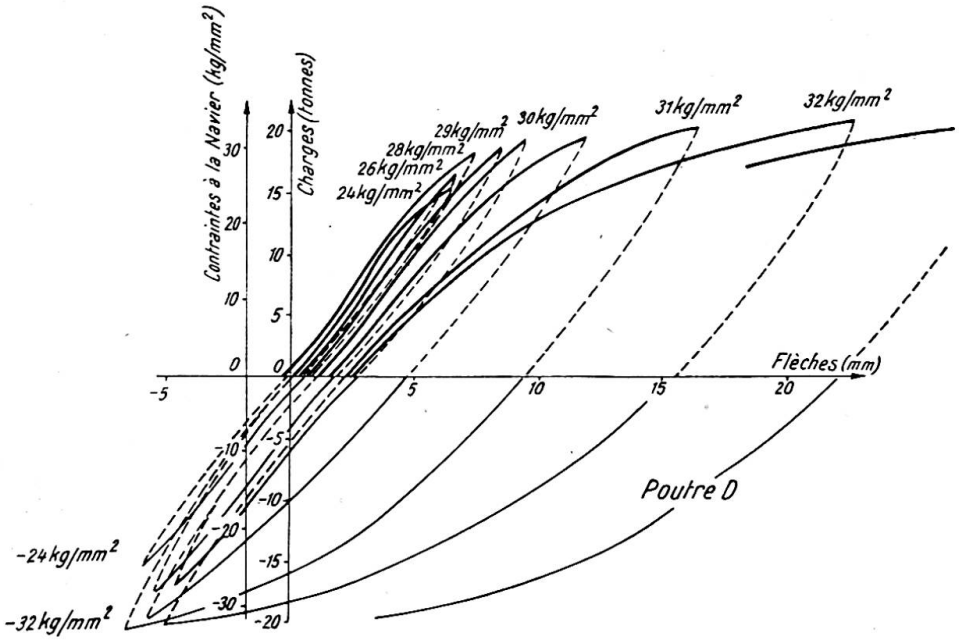

Fig. 8

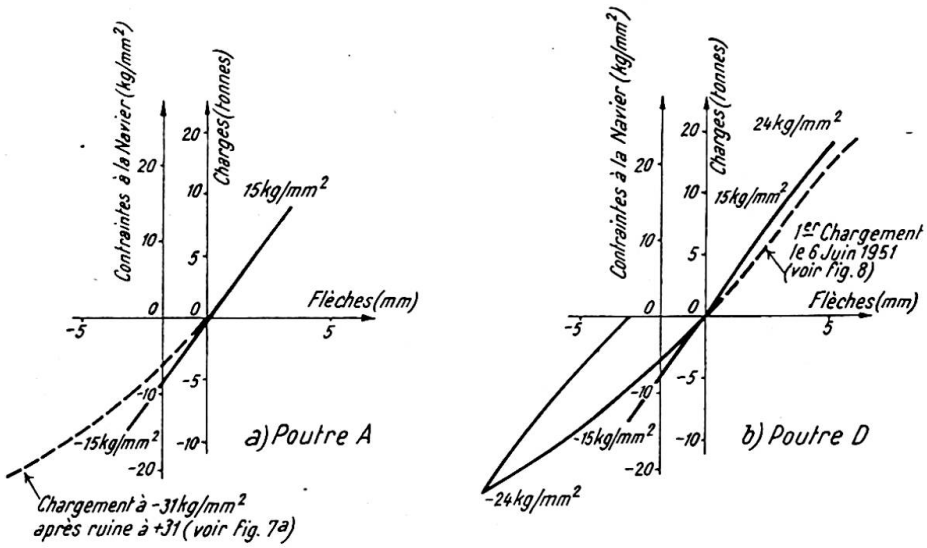

Fig. 9

A cet effet nous avons demandé qu'on soumette à nouveau à des essais de flexion, jusqu'à des contraintes de 15 kg./mm.², la poutrelle A de la 2ème sous-série et la poutrelle D de la 3ème sous-série qui toutes deux avaient été plastifiées jusqu'à la ruine dans des cycles Bauschinger (contraintes positives et négatives).

Selon le sens dans lequel l'effort serait appliqué on pouvait penser que ces poutrelles se comporteraient élastiquement ou manifesteraient la courbure caractérisque de l'effet Bauschinger, sous réserve que le temps n'ait pas modifié les propriétées acquises.

Les essais ont eu lieu le 9 mai 1951. Les poutrelles étaient au repos depuis 2 mois ½ pour A et 1 mois 2 jours pour D. Ils sont schématisés par les fig. 9(*a*) pour des essais sous + ou −15 kg./mm.² et fig. 9(*b*) pour des essais sous + ou −24 kg./mm.²

Il semble qu'on puisse conclure de ces deux essais (qui méritent d'être renouvelés):

1° qu'*après un repos de plusieurs semaines* des poutrelles* même sévèrement plastifiées (et tordues) *ont récupéré leurs qualités élastiques* (fig. 9(*a*)): les phénomènes de plastification ne se manifestent à nouveau que sous des sollicitations importantes voisines de la limite élastique (fig. 9(*b*)).

2° il n'existe pas de moyen de déterminer les plastifications antérieures†: au vrai cela devient sans intérêt à cause du 1° ci-dessus.

Tous ces essais nous conduisent à conclure comme suit:

Conclusions du chapitre I

(1) A la précision des essais et compte tenu de l'extrême dispersion des caractéristiques mécaniques du métal on peut dire que le moment produisant la ruine plastique d'une poutrelle brute sollicitée statiquement et isostatiquement est une donnée physique indépendante du processus de chargement (chargement continu, chargement par paliers avec déchargements, sollicitations cycliques: ondulées, répétées, alternées ou oscillantes).

(2) Si l'on supprime l'application des charges dès que se produit la ruine, la poutrelle est encore réutilisable élastiquement dans un domaine fort étendu qui paraît dépasser largement le domaine des contraintes réglementaires généralement admises. Le temps semble jouer, à ce sujet, un rôle très important, et encore mal défini.

(3) Le moment de ruine plastique est plus élevé, de plusieurs pour cent, que celui qui est déterminé par l'hypothèse du matériau idéalement plastique, la limite élastique étant déterminée sur une éprouvette de traction prélevée dans une semelle.

(4) Les contraintes préalables ne jouent aucun rôle dans la valeur du moment de ruine, car leur moment est nul (système en équilibre). Par contre elles interviennent certainement dans le déclanchement local des premières déformations plastiques. A ce sujet la considération du "moment élastique" est pratiquement dénuée de sens.

(5) Il semble qu'on puisse utiliser les poutrelles brutes à des contraintes très élevées, si l'on prend bien soin d'éviter les phénomènes de déversement et de flambement locaux des zones comprimées (âme et semelle). Les dispositions à prendre doivent varier d'ailleurs avec le profil des laminés; ces phénomènes perturbateurs sont d'autant plus à craindre que le laminé est plus haut ou plus grêle.

(6) La prédéformation volontaire en vue d'obtenir l'accommodation élastique, permet le relèvement des contraintes.

La question n'est, toutefois, pas encore complètement résolue.

Chapitre II—Autres essais sur la plastification en flexion des poutres à âme pleine

Nous distinguerons les essais statiques et de fatigue; dans chaque sous-chapitre les essais isostatiques et hyperstatiques: d'où quatre paragraphes.

On traitera d'abord des laminés bruts, puis percés, ensuite des poutres composées et enfin des poutres dissymétriques. On décrira d'abord les essais où le moment fléchissant joue le rôle principal, ensuite ceux où intervient l'effort tranchant, enfin

* Il pourrait être intéressant de préciser ce délai.

† Il serait intéressant de vérifier si l'approvisionnement des laminés sur parcs améliore leurs qualités élastiques.

on s'attachera aux phénomènes d'instabilité. On insistera sur le processus de chargement.

Ces considérations ont amené à prévoir systématiquement dix sections dans chacun des quatre paragraphes envisagés, avec pour les systèmes hyperstatiques une subdivision supplémentaire des sections en quatre sous-sections, afin de bien mettre en évidence les conditions d'appui. De nombreuses réponses "Néant" font mieux ressortir les lacunes des recherches actuelles, ainsi qu'il ressort du tableau schématique ci-joint.

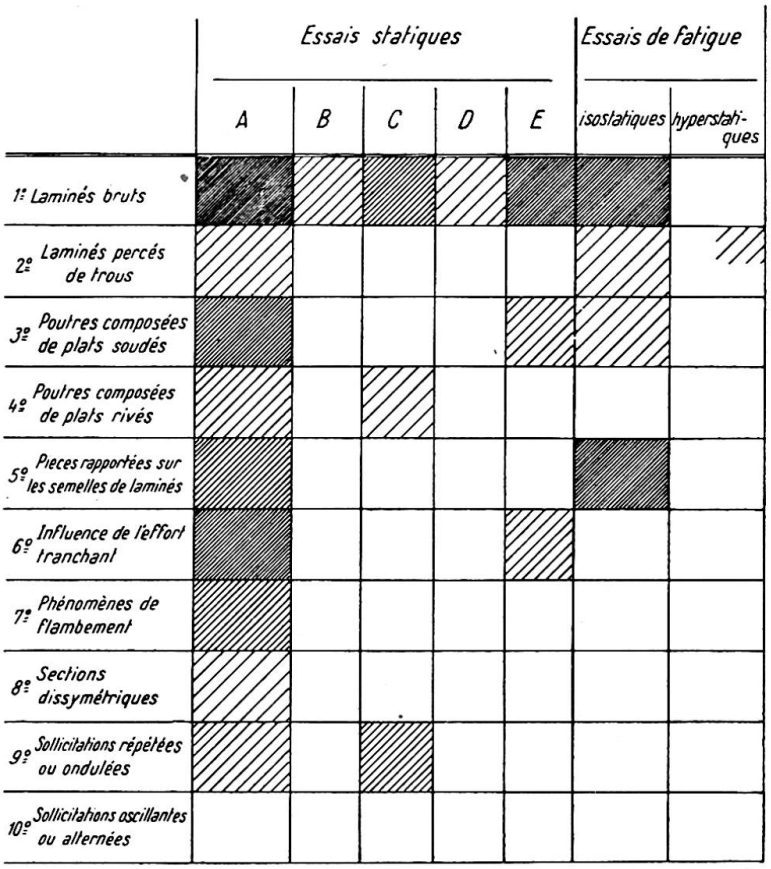

Tableau Schématique

Suivant Dutheil* nous distinguerons *l'adaptation dans la section* en comparant le moment de plastification vrai au moment calculé d'après la théorie élémentaire du matériau idéalement plastique que nous désignerons comme moment plastique théorique, de *l'adaptation entre sections* dans les systèmes hyperstatiques, en comparant les résultats à la théorie de l'égalisation des moments.

La quasi totalité des essais ont porté sur des laminés ou des poutres de petites dimensions. La prudence s'imposera quand on voudra généraliser aux poutres de grandes dimensions.

* *Annales de l'Institut Technique du Bâtiment et des Travaux Publics*—Théories et Méthodes de Calcul No. 2, janvier 1948: "L'exploitation du phénomène d'adaptation dans les ossatures en acier doux"; et *Ossature Métallique*, 3, 1949, p. 143.

SOUS-CHAPITRE I—ESSAIS STATIQUES

PARAGRAPHE 1: ESSAIS ISOSTATIQUES

1ère Section: Laminés bruts

On a étudié divers essais de Maier-Leibnitz; d'autres de Stüssi et Kollbrunner, Kazinczy, Hendry, Wilson, et Graf (aciers mi-durs) qui n'ont pas été tous poussés jusqu'à la ruine, chargements croissants ou par paliers et déchargements. A l'exception de l'essai de Wilson où la contrainte à la Navier a à peine dépassé la limite élastique, les autres montrent, comme nous l'avons trouvé au chapitre 1er, que le moment de ruine *dépasse nettement le moment plastique théorique*: un essai de Kollbrunner donne un dépassement de 32%.

2ème Section: Laminés percés de trous

On cite deux essais de la Chambre Syndicale des Constructeurs Métalliques Français où la section médiane était affaiblie par deux trous dans chaque semelle. Dans l'un les trous étaient *forés*; il y eut ruine plastique et peu de différence avec un laminé sans trou. Dans l'autre les trous étaient *poinçonnés sans alésage*. Il y eut cette fois *rupture, brutale*, dans la semelle tendue à partir d'un trou, avec cassure brillante; l'essai est donc plus défavorable.

Les contraintes à la Navier, calculées en section brute et en section nette sont données dans le tableau ci-après en kg./mm.^{2} où elles sont comparées aux limites de rupture R de l'acier des semelles tendues.

Trous	Section	1er I (très doux)	2ème I (assez dur)	Ruine
forés	brute nette	28,8 ou 0,90R 41,2 ou 1,29R	35,8 ou 0,90R 51,2 ou 1,28R	Plastique
poinçonnés sans alésage	brute nette	28,0 ou 0,84R 40,0 ou 1,20R	31,5 ou 0,79R 45 ou 1,12R	Rupture brutale

3ème Section: Poutres composées de plats soudés

On a étudié: un essai de Kayser où la poutre a péri par voilement de l'âme et pour une contrainte à la Navier supérieure à la limite de rupture de l'acier des semelles (mais l'acier de l'âme était beaucoup plus dur); des essais de Hendry et des essais remarquables de Patton et Gorbunow sous chargements répétés cycliquement, avec ou non introduction de contraintes préalables.

Ces essais montrent que ces poutres se comportent aussi bien, sinon mieux, que des laminés bruts de même section et de même acier. Les contraintes préalables sont sans influence sur la valeur de ruine.

4ème Section: Poutres composées de plats rivés

On a noté un essai peu concluant de Kazinczy et un essai de la Chambre Syndicale des Constructeurs Métalliques Français sur deux poutres où les trous étaient *poinçonnés sans alésage* et où il y a eu *rupture, brutale*, de la semelle tendue à partir d'un trou de rivet.

Les contraintes à la Navier, en kg./mm.^{2}, calculées en section brute et en section nette, sont données dans le tableau ci-après et comparées aux limites de rupture R de l'acier des semelles tendues.

Section	1ère poutre	2ème poutre	Ruine
brute nette	28,8 ou 0,61R 39,2 ou 0,83R	30,8 ou 0,67R 42,0 ou 0,91R	Rupture brutale

Ces résultats paraissent inférieurs à ceux de poutres soudées ou d'I bruts.

5ème Section: Pièces rapportées sur des semelles de laminés

On cite quelques essais comparatifs de Bryla et Chmieloviec et un ensemble très remarquable d'essais de Wilson qui semblent marquer *l'influence défavorable de semelles additionnelles partielles* soudées et au contraire la supériorité des semelles additionnelles soudées de toute la longueur du profilé, les semelles rivées s'inscrivant entre les deux.

6ème Section: Influence de l'effort tranchant ou d'une petite portée ($L<6h$)

On cite deux essais de Kayser où la ruine est intervenue par *voilement de l'âme* sans que puisse intervenir une semelle additionnelle soudée, deux essais d'Albers sur poutre de 1,86 m. de haut où la ruine est également intervenue par *voilement de l'âme* malgré un délardage très important des semelles tendues, qui ont ainsi supporté des contraintes à la Navier considérables, un essai de Wilson et une série d'essais très intéressants d'Hendry à la suite desquels cet auteur a essayé de fixer des règles pratiques pour savoir quand faire intervenir l'effort tranchant; malheureusement il s'agissait de très petits laminés. Son étude pourrait servir utilement de base à des essais systématiques.

7ème Section: Phénomènes de flambement

On cite des essais systématiques, un peu spéciaux, d'Hendry, sur des cadres en forme de L à deux branches égales. L'auteur donne, dans la limite de ses essais, des règles pratiques intéressantes.

8ème Section: Sections dissymétriques

Patton et Gorbunow ont montré que la théorie habituelle de l'adaptation dans la section s'appliquait parfaitement aux sections dissymétriques en essayant des profilés en Π composés de plats soudés ou des profils en caissons avec appendices longitudinaux soudés. Sollicitations ondulées.

La ruine, plastique, intervient pour des contraintes à la Navier dépassant largement la limite élastique (1,81 et 1,54 fois).

Cependant Patton et Gorbunow, en vue d'éviter l'apparition de déformations élastiques trop importantes ou de déformations permanentes, prescrivent de vérifier que la contrainte à la Navier ne dépasse pas la limite élastique.

On pourrait sans doute aller plus loin, grâce à l'accommodation en utilisant la prédéformation.

Il semble qu'il y ait le plus grand intérêt, contrairement aux idées héritées des leçons de Navier, à utiliser en flexion des pièces dissymétriques. En théorie, à quantité de matière donnée, il serait préférable d'utiliser des pièces rectangulaires car les centres de gravité des sections comprimées et tendues sont alors les plus éloignées possible (bras de levier maximum); mais, pratiquement, compte tenu des phénomènes d'instabilité en compression, il faut s'orienter vers des sections dissymétriques en forme de T ou Π.

D'autant plus qu'à l'avenir la Construction Métallique va devoir utiliser largement les tôles minces et abandonner de nombreux laminés symétriques.

En particulier on pourrait renforcer commodément des ouvrages par des *appendices soudés* s'écartant le plus rapidement possible de la fibre neutre.

Il est *regrettable que ces expériences n'aient pas connu le retentissement qu'elles méritaient* et qu'elles n'aient pas été systématiquement poursuivies.

9ème Section: Sollicitation ondulées ou répétées

On a déjà mentionné, à diverses reprises, les essais de Patton et Gorbunow.

10ème Section: Sollicitations alternées ou oscillantes. Néant.

PARAGRAPHE 2: ESSAIS HYPERSTATIQUES

C'est ici qu'il a paru nécessaire de subdiviser chaque section en quatre sous-sections pour tenir compte des conditions spéciales d'hyperstaticité et étudier si la plastification débutait sous les points d'application des charges ou sur les appuis et comment se faisait l'égalisation des moments que postule la théorie élémentaire.

11ème Section: Laminés bruts

1ère sous-section—Poutres continues sur quatre appuis

L'analyse d'un essai bien connu de Maier-Leibnitz nous a conduit aux conclusions suivantes (voir fig. 10):

Dans une 1ère phase les phénomènes sont purement élastiques (jusqu'à $10T$; contrainte à la Navier en travée, 26,2 kg./mm.^{2}).

Une 2ème phase—de transition—de $10T$ à $11{,}2T$ correspond au début de la plastification de la section médiane (contrainte croissant de 26,2 à 29 kg./mm.^{2}). Elle est caractérisée par la formation d'un jarret permanent sous la charge.

Une 3ème phase—de $11{,}2T$ à $17T$, qui correspond à l'accroissement linéaire du moment sur appuis, est marquée par la tendance, conforme à l'hypothèse classique, vers l'égalisation des moments en travée et sur appui. Cette égalisation se produirait pour la valeur du moment plastique *vrai.*

Mais cette égalisation ne peut se produire. Elle est entravée par l'apparition (à partir de $17T$) des phénomènes de plastification dans la section sur appui: contrainte à la Navier sur appui 23,3 kg./mm.^{2} pour une limite élastique des semelles voisine de 24–25 kg./mm.^{2} Cette plastification de la section sur appui, avec jarret, se poursuit difficilement; la section médiane est alors obligée de se plastifier à nouveau avec entrée dans le domaine de raffermissement de l'acier.* C'est la 4ème phase, qui s'achève par la ruine de la poutre à $20{,}7T$, caractérisée par l'apparition de nouveaux jarrets dans la travée médiane et même dans les travées extrêmes.

On note par rapport aux essais isostatiques les trois différences essentielles suivantes:

(*a*) il se forme *un jarret sous la charge* dès le début de la plastification de la section médiane;

(*b*) les sections sur appuis *éprouvent de la difficulté à se plastifier* complètement† il se forme également un jarret;

* C'est le seul cas, à notre connaissance, où le raffermissement ait été indubitablement observé.

† Il est probable que la surplastification de la section médiane, avec raffermissement, est plus facile que la plastification des sections sur appui. Il n'est pas exclu que le contraire se produise dans d'autres conditions d'essai.

(*c*) la section médiane est contrainte d'entrer *dans le domaine de raffermissement.**

L'essai, bien connu lui-aussi, de Stüssi et Kollbrunner, confirme cette analyse. Nous pensons toutefois que la charge de ruine est supérieure à celle que propose Stüssi à cause du dépassement de fait du moment plastique théorique dans la section.

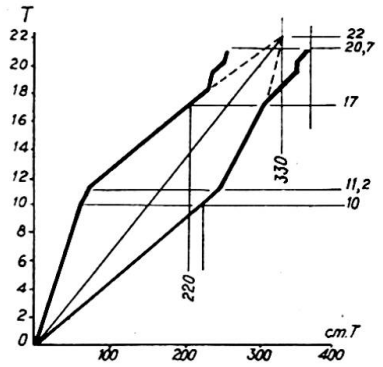

Fig. 10

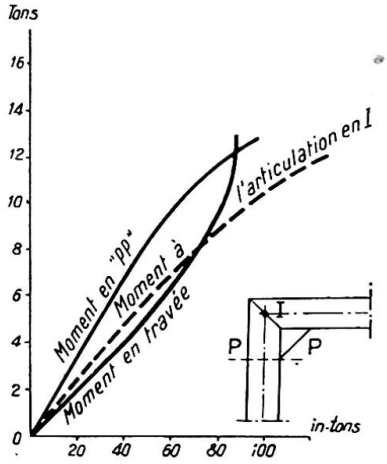

Fig. 11 (Portique A2)

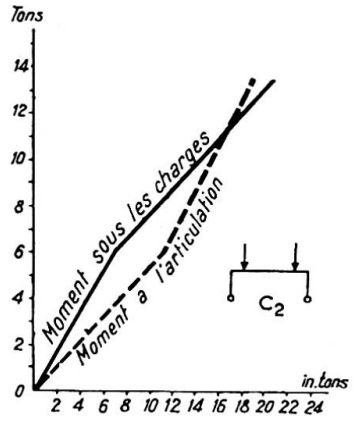

Fig. 12

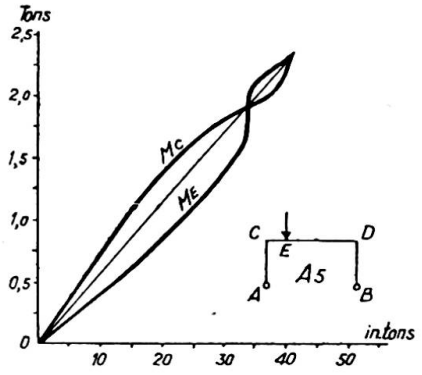

Fig. 13

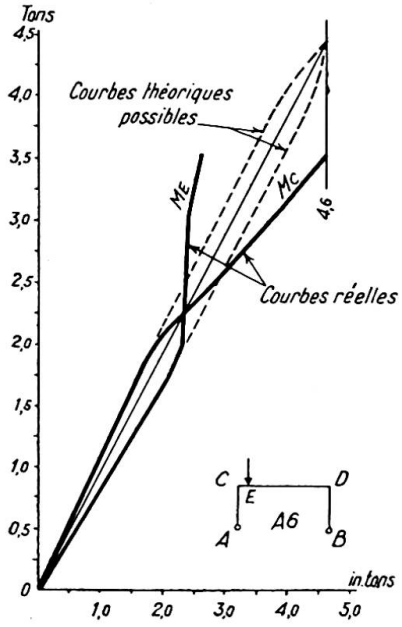

Fig. 14

* Il est probable que la surplastification de la section médiane, avec raffermissement, est plus facile que la plastification des sections sur appui. Il n'est pas exclu que le contraire se produise dans d'autres conditions d'essai.

2ème sous-section—Poutres continues sur trois appuis

On cite des essais de Maier-Leibnitz, Hartmann et Patton et Gorbunow qui systématiquement montrent un dépassement de la charge calculée (à cause, semble-t-il, d'une mauvaise estimation du moment plastique vrai dans la section) et la non influence sur la ruine d'une quelconque dénivellation d'appui. Par contre la succession des plastifications a rarement suivi la théorie élémentaire.

3ème sous-section—Poutres encastrées

On ne cite qu'un essai de Maier-Leibnitz pour lequel on peut répéter sensiblement ce qui a été dit à la 1ère sous-section quoique l'égalisation ait failli ici être parfaite.

4ème sous-section—Portiques

La question semble avoir particulièrement attiré les Britanniques. On cite plusieurs séries d'essais d'Hendry. Dans l'un—voir fig. 11—on trouve *une égalisation des moments avant la ruine* pour laquelle le moment du genou dépassait notablement le moment sous la charge.

Conclusions pour la 11ème section

Il semble qu'on peut conclure comme suit:

A condition de compter avec les moments de plastification *vrais*, la théorie de l'égalisation des moments est vérifiée dans les portiques (hyperstaticité interne); elle ne l'est pas entièrement dans les poutres continues (hyperstaticité extérieure): dans ce cas il se forme des jarrets dès le début de la plastification d'une section.

12ème Section: Laminés percés de trous. Néant.

13ème Section: Poutres composées de plats soudés

On cite une série d'essais de portiques dus à Hendry pour lesquels la ruine est intervenue au moment de l'égalisation des moments pour la valeur du moment plastique *vrai.*

14ème Section: Poutres composées de plats rivés

On ne peut citer qu'un essai de Kazinczy avec poutre continue sur trois appuis mais pour lequel on manque par trop d'éléments de détails.

15ème Section: Pièces rapportées sur les semelles des laminés. Néant.

16ème Section: Influence de l'effort tranchant

On cite plusieurs séries d'essais de portiques, dus à Hendry, dont quelques résultats sont représentés aux figs. 12, 13 et 14. Elles montrent:

fig. 12, des variations linéaires des diagrammes: charges-moments;
fig. 13, un huit fermé, c'est-à-dire ruine par égalisation des moments après une égalisation préalable;
fig. 14, un cas où la charge étant très près du genou, le moment sous la charge n'a pas pu se développer complètement et où la ruine est intervenue quand le moment du genou a atteint la valeur du moment plastique vrai dans la section.

17ème et 18ème Sections: Phénomènes de flambement et sections dissymétriques. Néant.

19ème et 20ème Sections: Sollicitations cycliques

On aborde un point *capital* concernant l'adaptation de plasticité dans les poutres hyperstatiques *quand les charges sont variables ou mobiles*: Il s'agit du problème du "cumul des déformations plastiques" analogue à celui que nous avons traité dans le chapitre 1er avec les essais de la 4ème série.

Un examen serré de la proposition théorique bien connue de Hans Bleich nous a conduit aux conclusions suivantes:

La méthode de H. Bleich tend à améliorer le procédé de l'égalisation des moments élastiques; en fait cela ne doit être possible que dans certaines conditions qu'il reste à préciser. Il faut distinguer au moins deux cas:

1° La disposition des travées et des charges est telle que l'intervention des contraintes résiduelles les plus favorables modifie peu l'égalisation des moments selon la méthode habituelle: autrement dit les moments aux points les plus chargés, calculés en élasticité, sont très voisins.

Dans ces conditions il est probable qu'on atteindra assez aisément un état voisin de l'égalisation des moments plastiques vrais, cela dépendra d'une part, comme on l'a vu dans les essais des 11ème et 13ème sections, des répartitions de travées et d'autre part de l'étendue du domaine dans lequel les moments ondulent.

2° Au contraire les moments aux points les plus chargés sont assez différents pour que les contraintes résiduelles de H. Bleich modifient assez sensiblement l'égalisation habituelle. Dans ce cas, on peut concevoir que le point le plus chargé se plastifiera entièrement avant que n'intervienne la plastification de soulagement d'un point moins chargé, sauf pour les sections à grand coefficient de forme (marge de plastification élevée). Autrement dit l'égalisation envisagée ne se produira probablement pas pour des sections telles que I ou H et il y aura sans doute ruine par divergence des déformations pour des valeurs des charges plus faibles que celles calculées. Au contraire pour des sections à grand coefficient de forme on tendra vraisemblablement vers l'égalisation des moments plastiques vrais et les valeurs calculées seront sans doute dépassées. *De nombreux paramètres sont susceptibles d'intervenir et, a priori, la question n'est pas simple à résoudre.*

Le 1° est sensiblement confirmé par un essai de Klöppel où la valeur de Bleich a été dépassée d'au moins 35%; le 2° par des essais de la Chambre Syndicale des Constructeurs Métalliques Français destinés à vérifier une théorie corrective due à Dutheil.

Le tableau, ci-après, donne en fonction des valeurs des limites élastiques de l'acier des profilés:

colonne 2: les valeurs du moment élastique, en cm. T;

colonnes 3, 4, 5: les valeurs théoriques, en T, des charges pour lesquelles le moment sur appui égalerait: le moment élastique, le moment critique de Dutheil,* le moment plastique théorique;

colonnes 6, 7, 8: les valeurs théoriques, en T, des charges donnant l'égalisation, dans le cas de charge le plus défavorable, des moments sur appuis et sous la charge fixe avec: le moment élastique, le moment de Dutheil, le moment plastique théorique;

colonnes 9, 10: les valeurs théoriques, en T, des charges donnant l'égalisation des valeurs extrêmes des moments sur appui et sous la charge fixe avec: le moment élastique (méthode de H. Bleich), le moment critique de Dutheil (méthode Bleich corrigée par Dutheil);

* Le moment critique de Dutheil est le moment élastique majoré d'un coefficient de forme égal à 1,20; 1,425; 1,10 et 1,10 respectivement.

colonne 11: les valeurs expérimentales, en T, de la charge marquant la fin du domaine de proportionnalité.

colonnes 12, 13: les valeurs expérimentales, en T, des charges pour lesquelles la divergence semble s'être produite; d'après l'estimation du Laboratoire et d'après la nôtre.

1	2	3	4	5	6	7	8	9	10	11	12	13
■ recuit .	249,1	10,7	12,9	16,1	15,5	18,6	23,3	12,2	14,6	11	18	17
◆ recuit .	173,7	7,5	10,7	15,0	10,8	15,4	21,6	8,6	12,1	12,5	17	15
H . .	238,0	10,2	11,3	11,9	14,8	16,3	17,2	11,7	21,8	9	11,5	10
H recuit .	227,7	9,8	10,8	11,4	14,2	15,6	16,5	11,2	12,3	9,5	11,0	10

On voit qu'au point de vue des premières plastifications les prévisions de la colonne 3 ne sont pas (sauf pour le losange) trop éloignées de la réalité, par excès pour les H comme souvent déjà vu.

Au point de vue de la ruine par divergence on voit nettement apparaître les deux groupes que la discussion laissait prévoir:

(*a*) Pour les H, les charges sont très voisines de celles pour lesquelles le moment sur appuis égale le moment élastique ou le moment critique de Dutheil (cols. 3 ou 4) et légèrement *inférieures* au calcul de Bleich (col. 9).

(*b*) Pour le carré et le losange, au contraire, les charges sont voisines de celles pour lesquelles le moment sur appui est égal au moment plastique théorique (col. 5) et *très supérieures* aux calculs de Bleich ou de Dutheil (cols. 9 ou 10): cela tient évidemment à l'énorme réserve de plastification.

En conclusion, pour les cas de la pratique, tels que I et H, on voit qu'ici le calcul de Bleich est probablement trop optimiste, alors que dans l'exemple de Klöppel il était excessivement pessimiste.

La question est donc bien aussi compliquée que notre raisonnement permettait de l'envisager: *il faut tenir compte de la forme des sections*, de la *répartition des travées*, de la *position des charges et des rapports entre les valeurs des différentes charges.*

Il est souhaitable que de nombreuses expériences soient systématiquement entreprises.

Sous-chapitre II—Essais de fatigue

On ne trouve que des essais de Graf et de Wilson plus un essai de la Chambre Syndicale des Constructeurs Métalliques Français sur un assemblage par soudure bout à bout.

A part les essais isostatiques sur laminés bruts où l'auteur allemand n'a obtenu qu'une ruine plastique tandis que l'auteur américain obtenait des ruptures, les autres essais sont complémentaires et laissent beaucoup de lacunes. Les expériences les plus complètes sont celles de Wilson sur des semelles additionnelles soudées sur des laminés: il nous semble que l'on peut en tirer confirmation de la supériorité de semelles additionnelles de toute la longueur du laminé soudées par cordons continus d'une part, et de l'infériorité de plaquettes ou de semelles partielles soudées ainsi que de soudures sur des zones tendues, d'autre part.

Pour le reste les limites d'endurance, par exemple à 2 millions de répétitions, présentent une telle dispersion des valeurs qu'il est difficile, en l'état actuel, de tirer de conclusions nettes. Tout ce qu'on peut affirmer c'est que, dès qu'il y a une entaille

quelconque, la ruine survient par *rupture* et pour des valeurs des contraintes à la Navier *nettement inférieures* à la limite élastique de l'acier utilisé. On ne peut plus dès lors envisager, à proprement parler, de théorie de l'adaptation en flexion basée sur la plastification.

CHAPITRE III—CONCLUSIONS

On traitera d'abord des points qui paraissent acquis, ensuite de ceux qui prêtent encore à discussion ou n'ont pas été suffisamment traités.

1ÈRE PARTIE—POINTS ACQUIS

Si l'on met à part les essais de fatigue sur poutres présentant des entailles (le mot étant pris ici au sens le plus large) pour lesquelles l'adaptation de plastification ne semble pas jouer au sens où l'on entend généralement ces termes, les essais français et etrangers analysés aux chapitres II et III permettent de tirer les conclusions suivantes, en distinguant par nature de poutres:

1° *Laminés bruts*

(*a*) La plastification commence pour des valeurs des contraintes à la Navier inférieures à la limite élastique. Ceci n'empêche pas le laminé de se comporter élastiquement une fois la déformation permanente acquise et stabilisée; dans les poutres continues cette déformation se manifeste par des jarrets sous les charges ou sur les appuis.

(*b*) Si les précautions sont prises pour éviter les flambements locaux des semelles et des âmes comprimées et s'il n'existe pas de fortes charges concentrées à proximité d'appuis, la ruine intervient par plastification totale. Le moment atteint dans la section la plus exposée, ou moment plastique vrai, dépasse de plusieurs pour cent (10 à 20 en moyenne) le moment calculé d'après la théorie élémentaire du matériau idéalement plastique.

(*c*) Dans les systèmes hyperstatiques les moments sous les points les plus chargés et sur les appuis ou les genoux ont bien tendance à s'égaliser, la valeur commune étant celle du moment plastique vrai. Cette égalisation peut être atteinte dans les portiques; elle l'est rarement d'une manière parfaite dans les poutres continues: il y a là des circonstances défavorables dues probablement aux appuis. Enfin dans les cas de sollicitations conduisant au cumul des rotations plastiques, il n'est pas exclu que, dans certaines circonstances encore mal connues, la ruine survienne, par divergence des déformations, pour des valeurs relativement faibles.

(*d*) En définitive il semble qu'au regard des questions de sécurité les contraintes maxima réglementaires pourraient être fixées à des valeurs élevées dépendant:

de la dispersion des valeurs des limites élastiques conventionnelles (et non des limites de rupture) en différents points des laminés,
de la forme des sections,
éventuellement de la taille des laminés,
de l'isostaticité ou de l'hyperstaticité du système (poutres continues ou portiques),
dans certains cas de la nature des sollicitations (par exemple possibilité du cumul des rotations plastiques dans les systèmes hyperstatiques).

Des dispositions constructives appropriées, variables avec la taille des laminés, telles que raidisseurs dans les zones comprimées, devraient alors être prises pour éviter des flambements locaux des semelles et des âmes comprimées.

2° *Poutres composées de tronçons de laminés bruts assemblés par soudure bout à bout*

Si les soudures sont convenables et le mode de soudage approprié, il semble que de telles poutres peuvent être utilisées exactement comme des laminés bruts.

Celà est bien net dans les systèmes isostatiques. Les essais manquent dans les systèmes hyperstatiques; il semble toutefois que les conclusions peuvent être étendues dans ce cas à condition de ne pas disposer les soudures sur les appuis. Telle est, du moins, la tendance française: elle ne semble pas être générale à l'etranger.

3° *Poutres, à profil constant, composées de plats assemblés par soudures longitudinales continues*

Compte tenu du nombre limité d'essais probants il semble que les conclusions du 1° (laminés bruts) peuvent être également adoptées, tout au moins dans les systèmes isostatiques.

Toutefois ici le moment plastique vrai dans la section est sensiblement égal au moment calculé d'après la théorie du matériau idéalement plastique.

4° *Laminés percés de trous, poutres chaudronnées (rivées), laminés complétés par des semelles additionnelles rivées*

Il n'existe pas d'essais hyperstatiques. En isostatique la question n'est pas encore suffisamment éclaircie pour permettre des conclusions nettes. Sauf les cas bien précisés où les trous étaient poinçonnés sans alésage et où la ruine a été provoquée par une rupture brutale, il semble que l'adaptation de plastification joue; mais les domaines d'utilisation restent à préciser.

5° *Poutres composées de plats soudés et laminés complétés par des semelles additionnelles soudées*

La question est loin d'être éclaircie.

Il semble bien que le seul cas net soit celui où, en isostatique, ces semelles ont la longueur totale du laminé: la plastification est alors intégrale. Au contraire les semelles de longueur partielle semblent être nettement défavorables: celà dépend de plusieurs facteurs qui sont mal précisés.

2ème Partie—Questions restant à résoudre

En plus des points de la 1ère partie encore mal précisés on aura remarqué que de nombreux points restent à étudier, tels que:

l'influence de l'effort tranchant,
les phénomènes de flambement,*
l'influence du temps sur certaines accommodations élastiques,
le cumul des déformations plastiques dans les poutres continues.

De nombreux essais n'ont même pas été tentés. La plastification des sections dissymétriques n'a été réalisée qu'une seule fois. Il n'y a pas d'essais avec semelle partielle soudée sur un seul côté, soit tendu, soit comprimé. Il n'y a jamais eu d'essais de fatigue commencés par une plastification lente: ces essais seraient pourtant de première utilité pour essayer de résoudre le conflit qui oppose les écoles opposées affirmant ou niant l'existence des phénomènes de fatigue dans les ponts et dans les charpentes métalliques, sans que les arguments avancés de part et d'autre soient réellement convaincants.

* A cet égard les nouvelles recherches théoriques et expérimentales de Stüssi sur le flambement des plaques seront sans doute du plus grand secours.

Enfin l'essai le plus intéressant à réaliser, malgré son évidente difficulté, celui de poutres continues sous charges roulantes: ici intervient au minimum les phénomènes hyperstatiques, le cumul des déformations plastiques, l'influence de l'effort tranchant.

En conclusion il apparaît qu'il reste de nombreux essais systématiques à entreprendre. La tâche dépasse les possibilités d'un seul organisme ou d'un seul pays. C'est pourquoi nous souhaiterions qu'à l'issue de la discussion du Thème AI3 de ce Congrès, une sous-commission établisse un vaste programme de recherches (basé ou non sur la classification adoptée dans le cours du présent mémoire) et le répartisse entre les Membres de notre Association. Rendez-vous serait pris dans quatre ans, au prochain Congrès, pour tirer les conclusions.

Nous insistons sur la nécessité de détailler minutieusement les circonstances de chaque expérience.

BIBLIOGRAPHIE

ALBERS. *Stahlbau*, 9.6.1939.
BAKER, J. F. *J. Inst. Civ. Engrs.*, **31**, No. 3, 1948–49.
The Structural Engineer, **27**, No. 10, 1949.
BLEICH, F. *Ossature Métallique*, février 1934.
BLEICH, H. *Bauingenieur*, 1932, p. 161.
BRYLA et CHMIELOWIEC. Congrès de Berlin, Rapport final, 1938, pp. 561 et 766.
DAWANCE. *Annales de l'I.T.B.T.P.* (Institut Technique du Bâtiment et des Travaux Publics), Construction Métallique No. 6, mai 1950.
DUTHEIL. *Annales de l'I.T.B.T.P.*, Théories et Méthodes de Calcul No. 2, janvier 1948.
Ossature Métallique, 1949, No. 3, p. 143.
GRAF. *Stahlbau*, 26.10.1934, 24.4.1936 et 15.1.1937.
Bauingenieur, 16.9.1938 et 5.2.1942.
HARTMANN. *Schweizerische Bauzeitung*, 18.2.1933.
HENDRY. *The Structural Engineer*, octobre et décembre 1950.
KAYSER. *Stahlbau*, 26.2.1937.
KAZINCZY. Congrès de Berlin, Rapport final, 1938, p. 56.
KLÖPPEL. Congrès de Berlin, Rapport final, 1938, p. 77.
LAZARD, A. *Mémoires de l'A.I.P.C.*, **X**, p. 101.
Travaux, mai 1950; novembre et décembre 1951.
LEVI, R. Congrès de Berlin, Publication préliminaire, 1936, p. 81.
MAIER-LEIBNITZ. *Bautechnik*, 1928, cahiers 1 et 2 (pp. 11 et 27).
Stahlbau, 25.9.1936.
Congrès de Berlin, Publication préliminaire, p. 101.
Congrès de Berlin, Rapport final, p. 70.
PATTON et GORBUNOW. *Stahlbau*, 3.1.1936.
SCHREINER. *Stahlbau*, 30.9.1938.
STÜSSI et KOLLBRUNNER. *Bautechnik*, 17.5.1935.
Congrès de Berlin, Publication préliminaire, 1936, p. 121.
Congrès de Berlin, Rapport final, 1938, p. 74.
WILSON. Bulletin 377 de la Station Expérimentale de l'Illinois, 22.1.1948.

Résumé

Se basant sur les derniers essais français sur des laminés bruts I et H de différentes tailles sollicités isostatiquement jusqu'à la ruine dans des conditions très diverses, et étudiant la dispersion des aciers, les contraintes préalables, la non-conservation des sections planes, l'importance des volumes plastifiés, l'existence de compressions transversales, le flambement des zones comprimées, l'article conclut que, pour des laminés bruts sollicités isostatiquement:

la ruine plastique survient, si les précautions nécessaires sont prises contre le flambement, pour une valeur supérieure à celle qu'on peut calculer en admettant la plastification totale d'un acier idéalement plastique;

le laminé s'accommode élastiquement après un nombre très faible de répétitions des sollicitations. Il est possible d'en déduire un procédé systématique de prédéformation en vue de travailler sous contraintes élevées. A ce sujet le temps semble jouer un rôle important mais encore mal défini.

Elevant le débat à toutes les poutres à âme pleine en acier doux et passant en revue les essais antérieurs généralement exécutés sur petits échantillons, l'article cherche à distinguer les points définitivement acquis de ceux qui prêtent à discussion ou n'ont pas encore été suffisamment traités. Parmi ces derniers on relève plus particulièrement:

l'effet de l'effort tranchant,
l'effet des surcharges roulantes sur poutres continues,
les études sur profils dissymétriques.

En conclusion l'article propose qu'une sous-commission du Congrès dresse un programme des essais restant à réaliser et les répartisse entre les divers membres de l'Association Internationale.

Summary

Based on the latest French tests with plain rolled I and H joists of various sizes, isostatically loaded up to failure under very different conditions, and by studying the dispersion of the steel, the residual stresses, the non-conservation of plane sections, the size of the plastified volumes, the existence of transverse compressions and the buckling of the compressed zones, the author of the paper comes to the conclusion that, for plain rolled joists isostatically loaded:

if the required precautions against buckling are taken, plastic failure happens for a load which is higher than that which can be calculated by supposing the total plastification of an ideally plastic steel;

the rolled joist adapts itself flexibly after very few repetitions of the loads. It is possible from this fact to deduce a method of systematic prestraining in order to work under high stresses. Time seems here to play a part which is important but has not yet been clearly defined.

By extending the discussion to all plate-web girders in mild steel and by surveying previous tests which generally were made on joists of small cross-section, this paper tries to distinguish the points which are definitively established from those which are still disputable or have not yet been sufficiently treated.

Among the latter, particular emphasis is put on:

the effect of shearing-stress,
the effect of rolling loads on continuous girders,
the studies on unsymmetrical sections.

It is finally proposed that a sub-committee of the Congress should assume the task of establishing a programme for the tests which are still to be made and allotting these to different members of the International Association.

Zusammenfassung

Der Aufsatz stützt sich auf die neuesten französischen Versuche an unbearbeiteten normalen und Breitflansch-I-Walzträgern unterschiedlicher Grösse, die bei statisch

bestimmter Anordnung unter sehr verschiedenen Bedingungen bis zum Versagen beansprucht wurden und untersucht die Streuungen in der Stahl-Qualität, die inneren Spannungen, das Nicht-Ebenbleiben der Querschnitte, das Ausmass der plastifizierten Querschnittsteile, das Auftreten von Quer-Kontraktionen und das Ausknicken der Druckzonen. Für statisch beanspruchte und statisch bestimmt gelagerte unbearbeitete Walzträger kommt der Verfasser zu den nachstehenden Schlussfolgerungen:

Wenn die notwendigen Vorkehrungen gegen Ausknicken getroffen sind, tritt das plastische Versagen für einen Wert ein, der höher ist als derjenige, den man unter der Voraussetzung totaler Plastifizierung eines ideal-plastischen Stahles errechnen kann.

Der Träger erfährt nach einer sehr geringen Zahl wiederholter Beanspruchungen eine elastische Anpassung. Daraus kann ein systematisches Vorverformungs-Verfahren zwecks Zulassung höherer Nutzspannungen abgeleitet werden. In diesem Zusammenhang scheint der Faktor Zeit eine wichtige, aber noch ungenau definierte Rolle zu spielen.

Durch Erweiterung der Diskussion auf sämtliche Vollwandträger aus Flusstahl und an Hand eines Überblicks über die früheren, hauptsächlich an kleinen Probeträgern durchgeführten Versuche wird versucht, die endgültig gelösten Fragen von denjenigen zu trennen, die noch umstritten oder ungenügend untersucht sind. Unter den letzteren werden insbesondere erwähnt:

der Einfluss der Querkraft,
der Einfluss der beweglichen Lasten auf durchlaufende Träger,
die Untersuchung unsymmetrischer Profile.

Als Schlussfolgerung schlägt der Verfasser vor, dass ein Unter-Ausschuss des Kongresses ein Programm der noch durchzuführenden Versuche aufstellen und diese unter verschiedene Mitglieder der Internationalen Vereinigung verteilen soll.

Leere Seite
Blank page
Page vide

AI 3

Experimental investigations into the behaviour of continuous and fixed-ended beams

Recherches expérimentales sur le comportement des poutres continues ou encastrées à leur extrémités

Experimentelle Untersuchungen über das Verhalten durchlaufender und eingespannter Balken

M. R. HORNE, M.A., Ph.D., A.M.I.C.E.
Cambridge University

1. Introduction

The behaviour beyond the elastic limit of mild-steel beams subjected to pure bending moments or bending moments combined with shear forces has been studied by Ewing (1903), Robertson and Cook (1913) and many others. The various theories suggested and the experimental evidence relating to them have been reviewed by Roderick and Phillipps (1949). It appears that, when considering annealed beams, the most satisfactory theory is that in which it is assumed that initially plane sections remain plane during bending, the longitudinal stress being related to the longitudinal strain as in a tension or compression test (see Roderick, 1948). Good correlation between bending and tension tests may be obtained if due regard is paid to the upper yield stress and to the rate of straining in the plastic range. The influence of shear forces has been investigated experimentally by Baker and Roderick (1940) and Hendry (1950) and theoretically by Horne (1951). It has been shown that, for practical purposes, shear forces have negligible effect on the behaviour of a beam. The stress distributions are also modified in the vicinity of concentrated loads, and this has been investigated experimentally by Roderick and Phillipps (1949) and theoretically by Heyman (unpublished). The simple plastic theory has also been found to apply approximately to rolled steel sections (Maier-Leibnitz, 1936), although correlation between bending and tension tests is here more difficult due to the variation in properties of the steel over any cross-section.

The simple plastic theory leads to important deductions regarding the behaviour of continuous and fixed-ended beams and rigid-jointed unbraced structures such as building frames. Due to the considerable pure plastic deformation which mild steel

can undergo (of the order of 1 % strain, or ten times the strain at the commencement of yield), the curvature of the longitudinal centre line of an initially straight beam increases rapidly with practically no increase of bending moment as the section becomes fully plastic. The bending moment then approaches the "full plastic" value (see Roderick, 1948), and although at extremely high curvatures the beam may develop a higher moment of resistance due to strain hardening, the full plastic moment may be regarded as the highest moment to which the beam may be subjected and still retain its usefulness. When beams are continuous over a number of supports or *encastré* (i.e. fixed in position and direction at their ends), the high curvature which occurs in the vicinity of fully plastic sections enables the applied loads to be increased until the full plastic moment is reached at a sufficient number of sections for a "mechanism" to be formed, these sections being regarded as "hinges" with constant moments of resistance. Similar considerations apply to rigid-jointed unbraced frames as long as axial forces are small enough to have negligible effect on the bending moments in the members in which they occur. The application of such results to the calculation of collapse loads has been considered extensively by Bleich (1932), Baker (1949), Neal and Symonds (1950), Horne (1950) and others.

The above theoretical developments have been achieved by making certain extensions of the simple plastic theory as established by tests on simply supported members. The "plastic hinge" concept is only an approximation to the truth, corresponding as it does to infinite curvature at the assumed fully plastic sections. It is thus essential that these theoretical deductions should be tested experimentally. In the case of continuous beams, the simple plastic theory indicates that the order in which the spans are loaded, or the sinking of one support relative to the others, should have no effect on the value of the collapse load. In beams partially fixed against rotation at the ends, the degree of end restraint should similarly have no effect on the collapse loads as long as the moment of resistance of the end supports is at least equal to the full plastic moment of resistance of the beam. Moreover, the fact that full plasticity has been produced at some section or sections of a beam for one set of loads should not reduce the carrying capacity of that beam for any subsequent set.

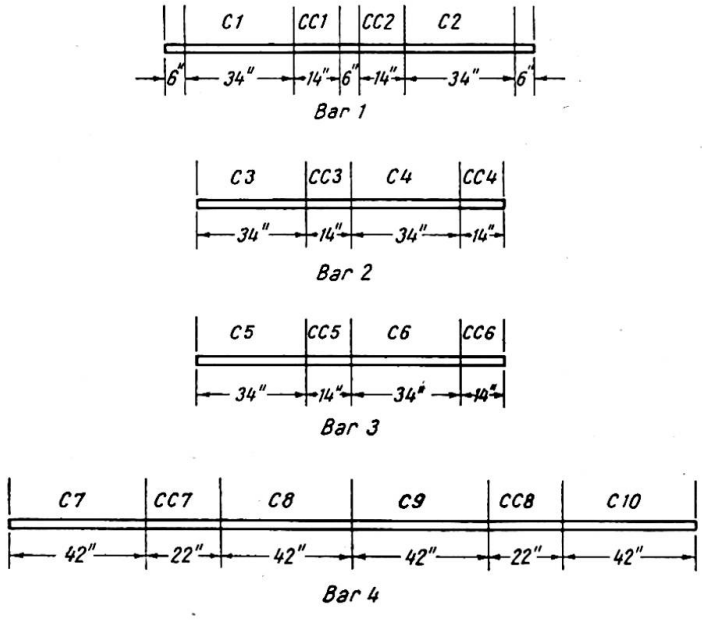

Fig. 1. Division of bars for continuous beam tests

While certain investigations on continuous beams have already been made by Maier-Leibnitz (1936) and Volterra (1943), no attempt to check these deductions systematically has yet been reported. It was for this reason that the investigations here described were undertaken.

2. Tests on continuous beams

(a) *Preparation of beams*

The beams were taken from 1-in. square bars of rolled mild steel in the "as received" condition, the bars being cut according to the scheme shown in fig. 1. All

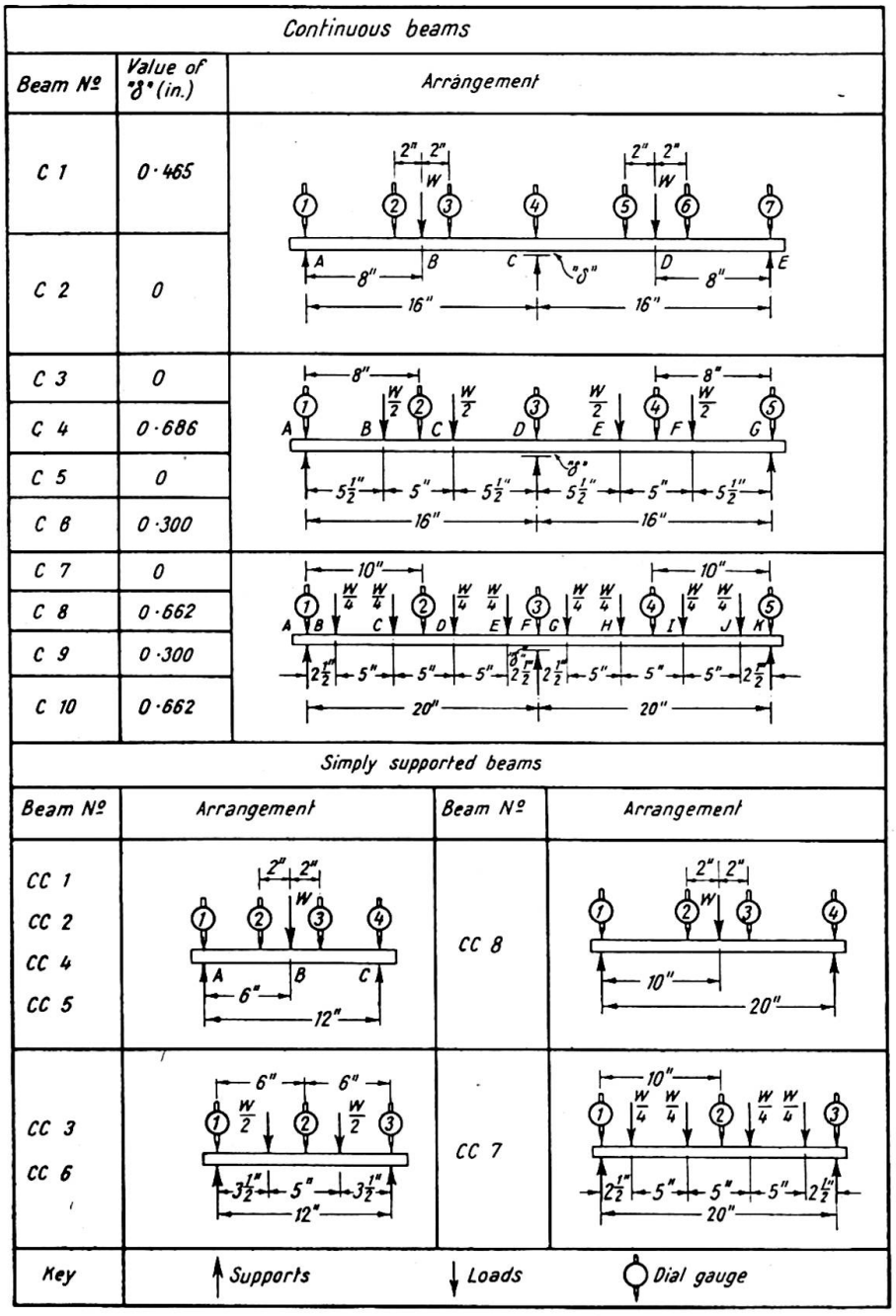

Fig. 2. Summary of continuous beam tests
(In beam CC8, for 2″ read 2½″)

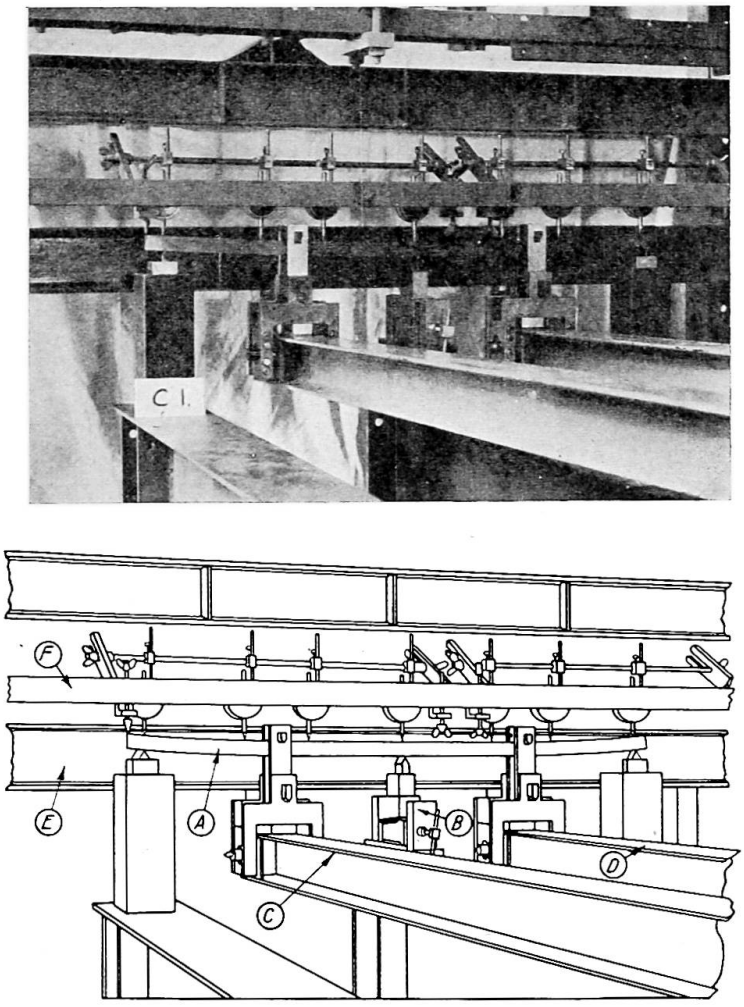

Fig. 3. Arrangement for testing continuous beams

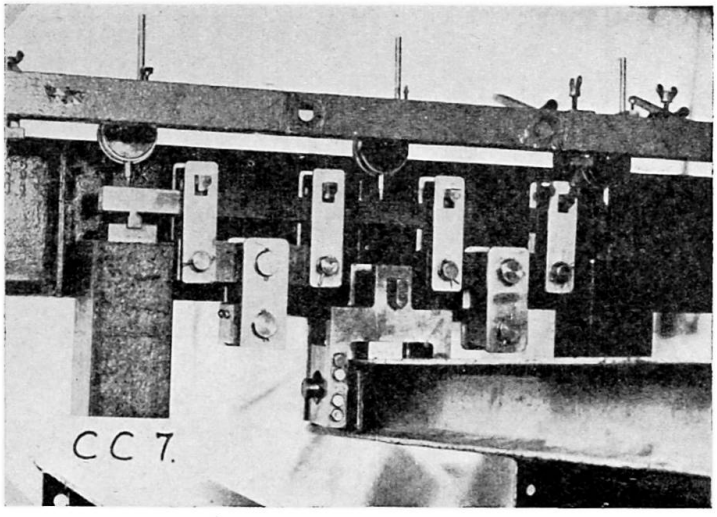

Fig. 4. Arrangement for testing simply supported beams

the beams were roughly planed to the required dimensions ($\frac{7}{8}$ in. square) and finished by surface grinding, thus imparting a polished surface which, as described below, enabled Lüders' wedges to be observed during the tests.

(b) *Description of tests*

The tests are summarised in fig. 2, which shows for each beam the positions of the supports, loads and dial gauges used to measure deflections. Some lengths were tested from each bar as continuous beams, while other lengths were tested as simply supported in order to obtain direct measurements of the full plastic moments. In some of the tests on the continuous beams, the central support was set a certain depth below the outer supports, and this is also indicated. Increasing loads were applied simultaneously to both spans of all the continuous beams except beam C5, in which span AD (see fig. 2) was loaded to collapse with only a small load on span DG. For all beams, when collapse had occurred in one span, the load on the other span was further increased until it also collapsed.

The tests were performed in a dead-load testing frame, a full description of which has been given by Baker and Roderick (1942). The arrangement for testing the continuous beam C1 is shown in fig. 3, in which A is the beam supported on knife-edges and B is a block by means of which it is possible to adjust the height of the central knife-edge. The load is applied by the levers C and D whose fulcra react against the member E, while the dial gauges for measuring deflections are supported on an independent frame of which F is a member. The simply supported beam CC7 was tested as shown in fig. 4, which also shows the linkage used to distribute the load from the lever equally to four knife-edges acting on the upper surface of the beam.

During the tests, as long as the beams remained elastic, finite increments of load were added at intervals of approximately two minutes, the dial gauges being read between each increment. After the first signs of creep had been observed, the addition of each load increment was delayed until no dial gauge showed a rate of increase greater than 10^{-4} in. per minute. Loading was continued until collapse occurred, this being characterised by a large increase of deflection for a small increase of load.

(c) *Test results*

The test results for all the beams are summarised in Table I, and are grouped according to the bar from which the beams were cut. The mean dimensions are given in columns 3 and 4. In the case of the simply supported beams, the values of the modulus of elasticity E calculated from the linear portions of the load deflection curves are given in column 5. The values of E quoted for the continuous beams are the mean of the values obtained for the simply supported beams cut from the same bar. Column 6 gives the collapse loads. In the case of the continuous beams, the mean of the values for the two spans is given; in no case did the difference between these values exceed 3·3%. Values of the full plastic moments may be deduced from the collapse loads by means of the simple plastic theory, giving the lower yield stresses quoted in column 7 of Table I. Assuming that each bar is of uniform material, the agreement between these stresses for beams cut from the same bar is a check on the accuracy of the simple plastic theory. The percentage variations of these yield stresses as compared with the average for the bar are given in column 9.

It has been shown by Heyman (to be published) that the assumption made in the simple plastic theory that there is no restraint in directions perpendicular to the longitudinal axis of a beam is invalidated in the vicinity of heavy load concentrations. This tends to increase the full plastic moment except where the maximum moment

TABLE I

	1	2	3	4	5	6	7	8	9	10	11	12
							Analysis by simple plastic theory ignoring the effect of load concentration			Analysis in which allowance is made for the effect of load concentration		
	Bar No.	Beam No.	Mean Width, in.	Mean Depth, in.	Estimated Modulus of Elasticity E, tons/in.^{2}	Load, tons	Lower Yield Stress, tons/in.^{2}	Mean Lower Yield Stress for bar, tons/in.^{2}	Per cent Difference	Lower Yield Stress, tons/in.^{2}	Mean Lower Yield Stress for bar, tons/in.^{2}	Per cent Difference
1	1	C1	0·875	0·876	13,360	1·125	17·83	18·02	−1·1	16·53	16·71	−1·1
2		C2	0·875	0·876	13,360	1·138	18·04		0·1	16·72		0·1
3		CC1	0·876	0·876	13,380	1·000	17·90		−0·7	16·59		−0·7
4		CC2	0·876	0·876	13,340	1·025	18·33		1·7	16·99		1·7
5	2	C3	0·875	0·875	13,120	1·560	19·03	18·34	3·8	17·96	17·48	2·7
6		C4	0·875	0·875	13,120	1·525	18·60		1·4	17·55		0·4
7		CC3	0·875	0·875	13,010	1·680	17·43		−5·0	17·43		−0·3
8		CC4	0·875	0·875	13,220	1·020	18·32		−0·1	16·98		−2·9
9	3	C5	0·875	0·875	12,930	1·225	14·93	14·91	0·1	14·09	14·21	−0·8
10		C6	0·875	0·874	12,930	1·230	15·01		0·7	14·16		−0·4
11		CC5	0·875	0·875	13,270	0·850	15·26		2·3	14·14		−0·5
12		CC6	0·875	0·875	12,590	1·380	14·44		−3·2	14·44		1·6
13	4	C7	0·875	0·876	12,945	1·670	18·13	17·84	1·6	16·46	16·60	−0·8
14		C8	0·876	0·875	12,945	1·670	18·12		1·6	16·45		−0·9
15		C9	0·876	0·876	12,945	1·650	17·92		0·4	16·27		−2·0
16		C10	0·876	0·876	12,945	1·700	18·38		3·0	16·69		0·5
17		CC7	0·875	0·875	13,060	1·150	17·16		−3·8	17·16		3·4
18		CC8	0·875	0·875	12,830	0·580	17·30		−3·0	16·54		−0·4

occurs uniformly over some length of the beam. This explains the lower than average yield stresses obtained for beams CC3, CC6 and CC7 (Table I, column 7). Roderick and Phillipps (1949) found that in their tests a satisfactory empirical allowance could be made for this effect by assuming that collapse was delayed until the full plastic moment had been reached at a section a distance away from the concentrated load equal to half the depth of the beam. The yield stresses for all the beams corresponding to this assumption are shown in column 10 of Table I, and the percentage variations from the mean values for separate bars are given in column 12.

There does not appear, from the figures given in columns 9 and 12 of Table I, to be any distinct advantage in accepting the complications introduced by Roderick and Phillipps. In either case the agreement is as good as could reasonably be expected, taking into account probable variations in yield stress in the bars. Ignoring signs, the mean values of the percentage variations given in columns 9 and 12 are 1·87 and 1·18 respectively. The application of the "t" test for the difference between means gives $t=1{\cdot}646$, corresponding to a probability of 0·12 that the difference between the means is due entirely to random causes. The improvement achieved with the second method of analysis, although discernible, is not therefore outstandingly significant. In their tests on simply supported beams, Roderick and Phillipps (1949) obtained much improved agreement by using this method, but it is to be noted that while these investigators tested carefully heat-treated beams, the tests here described were performed with the steel in the "as received" condition.

In a further attempt to decide between the two methods of analysis, tension tests were carried out on three specimens. Since the mean yield stresses given by the second method (column 11, Table I) are lower than those given by the first (column 8), it should thus be possible to reach some significant conclusion. The first two specimens (CT1 and CT2) were taken one from each end of beam C8, while the third (CT3) was taken from one end of beam C9. The specimens had a gauge length of 2·00 in. and a diameter of 0·282 in., and were tested in the Quinney Autographic Machine (see Quinney, 1938). The upper and lower yield stresses and the rates of strain in the plastic range are given in Table II. Calculations show that, during the

TABLE II

Tension Specimen	Upper Yield Stress, tons/in.^{2}	Lower Yield Stress, tons/in.^{2}	Rate of Strain in Plastic Range/sec. $10^{-6}\times$
CT1	22·48	17·99	18·20
CT2	19·53	17·32	0·767
CT3	22·31	18·16	18·20

beam tests, the mean rate of strain in the extreme fibres of the most highly stressed sections varied between $0{\cdot}7\times10^{-6}$ and $2{\cdot}0\times10^{-6}$ per sec. Hence the appropriate lower yield stress for bar 4 (see fig. 1) would be about 17·40 tons/in.^{2} Since the values obtained by the two methods of analysis were 17·84 and 16·60 tons/in.^{2} (columns 8 and 11 of Table I), the result is again inconclusive.

As an example of the load-deflection curves obtained, those for beams C1 and C2 are presented in figs. 5 and 6 respectively. In the case of beam C2, a theoretical load-deflection curve for dial gauges 3 and 5 has been calculated by means of the simple plastic theory, and is seen to be in good agreement with the observed values.

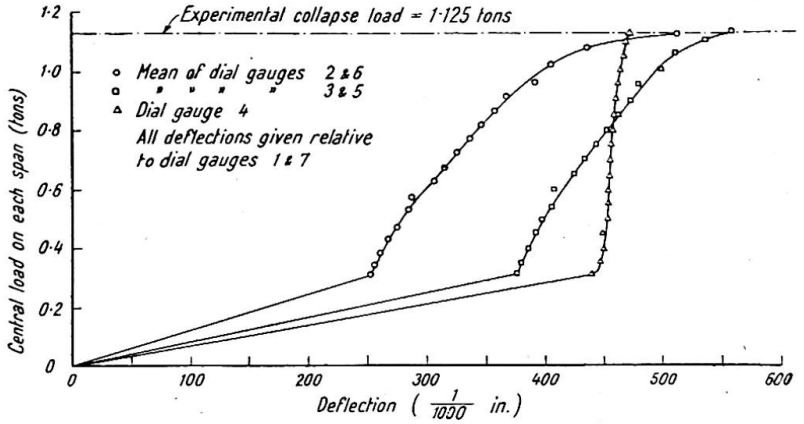

Fig. 5. Load-deflection curves for Beam C1

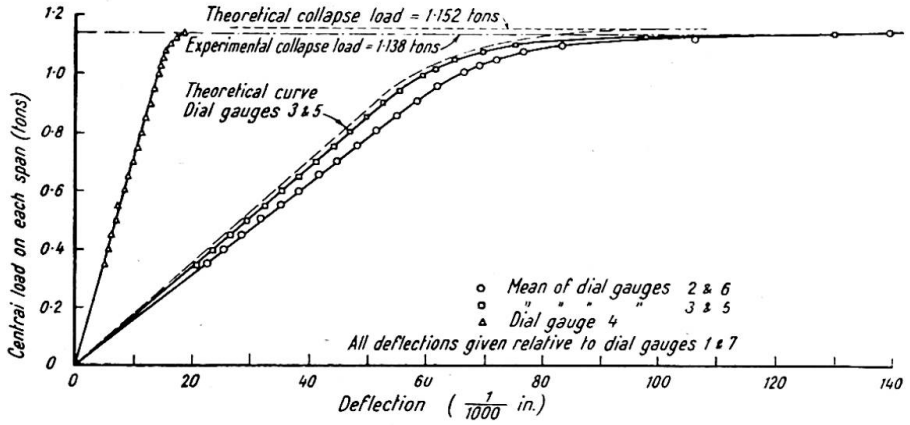

Fig. 6. Load-deflection curves for beam C2

In testing beams C1, C4, C8 and C10, the central support was set at such a distance below the outer supports that yield stress under a sagging bending moment was reached in the extreme fibres of the central section of the beam before contact occurred. As the loads on these beams were further increased, the central bending moment first decreased to zero and then increased until at collapse full plasticity under a hogging bending moment occurred over the central support. Simultaneously the position of the maximum sagging moment moved along the beam, as can be seen most clearly in the cases of beams C4 and C8. Thus in beam C4 (see fig. 2), a certain amount of yield under sagging moment occurred first at C and E, and finally at B and F, where full plastic moments developed at collapse. This may be traced in the appearance of Lüders' wedges on the side face of part of beam C4 after testing (fig. 7), in contrast to the absence of such wedges except at B and D on the face of beam C3, for which the supports were initially level. It will be observed from Table I that the sinking of the support and the occurrence of Lüders' wedges along the beam did not lead to any significant decrease in the carrying capacity of beam C4 as compared with beam C3. Similar remarks apply to beam C8, in which the maximum sagging moment moved first to sections E and G (see fig. 2), then to sections D and H, until finally full plastic moments were reached at collapse at

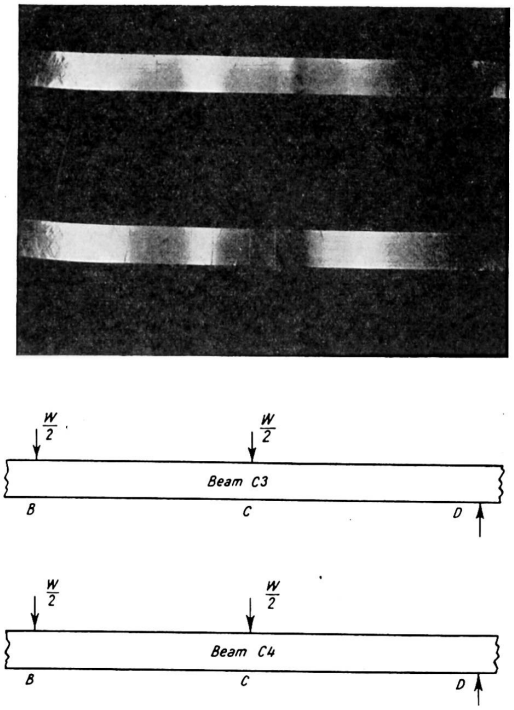

Fig. 7. Comparison of Lüders' wedges on beams C3 and C4

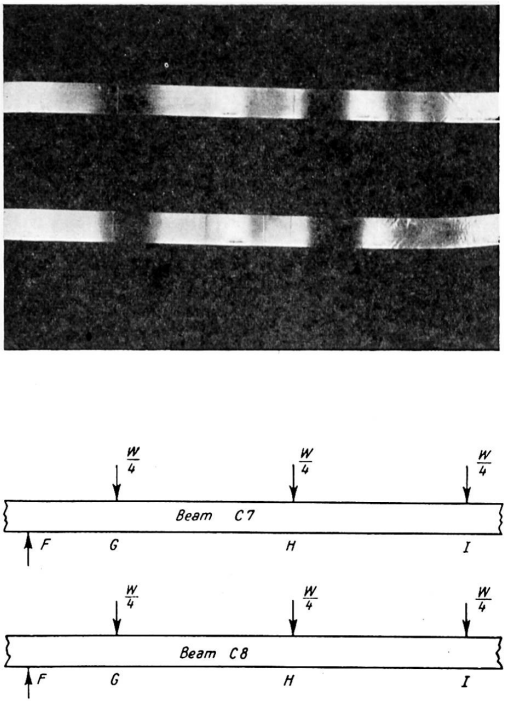

Fig. 8. Comparison of Lüders' wedges on beams C7 and C8

sections C and I. The side faces of parts of beams C7 and C8 after testing are compared in fig. 8. The theoretically deduced values of the moments at various sections of beam C8 at all stages of loading up to the collapse load are shown in fig. 9, and the progressive movement of the positions of the maximum sagging moments is apparent.

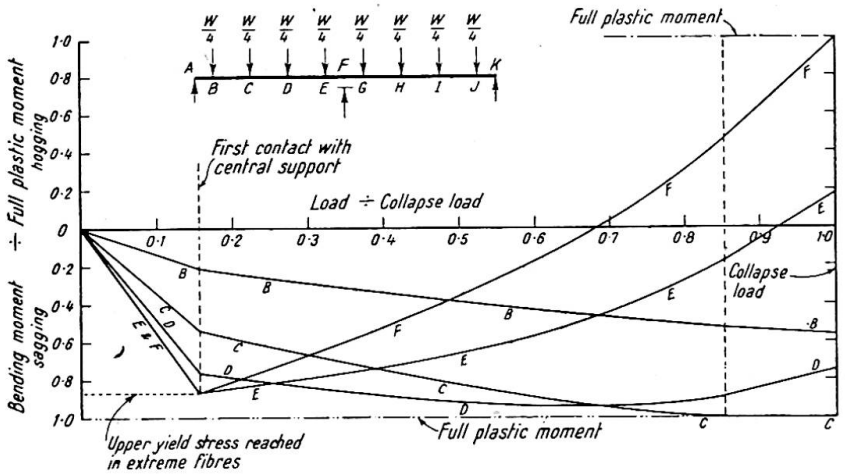

Fig. 9. Theoretical bending moment curves for beam C8

In test C5, the supports were at the same level, and equal loads of 0·50 tons were applied to each span. The load on span DG (fig. 2) was then kept constant while that on span AD was increased until collapse occurred at 1·20 tons. Finally the load on span DG was increased until this part of the beam also failed at a load of 1·25 tons.

3. Tests on fixed-ended beams

(a) *Preparation of beams*

The beams were all prepared from the same black mild-steel plate (dimensions 17 in. × 2 in. × $\frac{1}{4}$ in.) by cutting longitudinally (in the direction of rolling) into strips. The small size of the beams ($\frac{1}{4}$ in. × $\frac{1}{4}$ in. section) made it desirable to anneal at 900° C. and cool in air in order to reduce some of the effects of rolling and work-hardening. The beams were bent about axes perpendicular to the plane of the original plate.

(b) *Description of tests*

The tests are summarised in fig. 10. The beams E1–6 were tested over a span of 6·0 in. between end fittings which provided moments of resistance proportional to the rotations of the end sections of the beam. If a moment M lb. in. at the end of a beam corresponded to a rotation of θ radians, then $\theta = KM$ where K had the values for each beam given in the second column of fig. 10. The simply supported beams EC1 and EC2 had a span of 4·0 in. Fig. 10 shows the positions of the dial gauge used to measure deflections and of the mirror gauges used to measure rotations.

Tests E1, E2 and E3 were conducted to investigate the effect of various degrees of end fixity. Beams E4, E5 and E6 were subjected to loads at several sections (1, 2, 3 in fig. 10) in turn, each load being just sufficient according to the simple theory, to bring about collapse.

The arrangement for testing those beams which had the highest degree of end

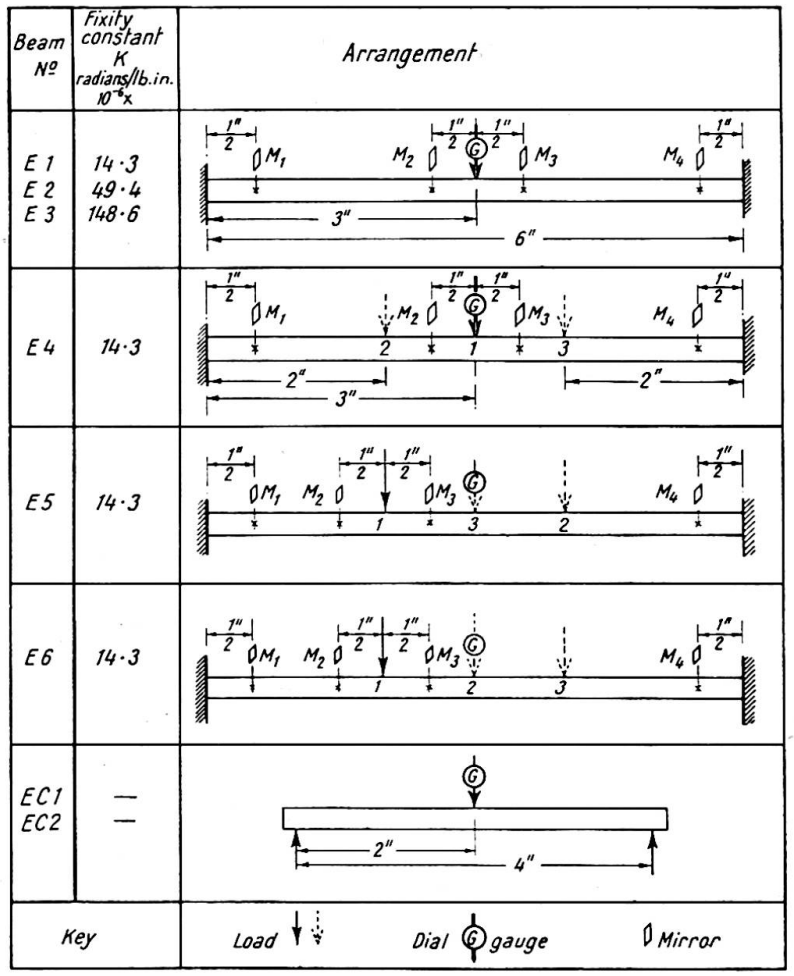

Fig. 10. Summary of tests on fixed-ended beams

fixity (beams E1, E4, E5 and E6) is shown in fig. 11, the load being applied by a chain acting through a yoke. The arrangement for testing beams E2 and E3 is shown in fig. 12, the clamping blocks on the end fittings having been removed for the sake of clarity.

During all the tests, load increments were made at approximately two-minute intervals until creep was first observed. Before each subsequent increment, the rate of creep on the dial gauge was allowed to drop to 10^{-4} in. during any two-minute interval.

(c) *Test results*

Beams E1, E2, E3, EC1 and EC2

The results are summarised in Table III, and columns 1 to 4 require no explanation. The end-fixity constants for the partially fixed-ended beams are given in column 5, from which it is possible to calculate the theoretical ratio of end to central moments for a central point load in the elastic range (column 6). The collapse loads are given in column 7, from which the lower yield stresses may be calculated by means of the simple plastic theory (see Table III, column 7). The percentage differences from the mean are given in column 10.

On the basis of the method suggested by Roderick and Phillipps for allowing for load concentration, these same collapse loads give the yield stresses shown in

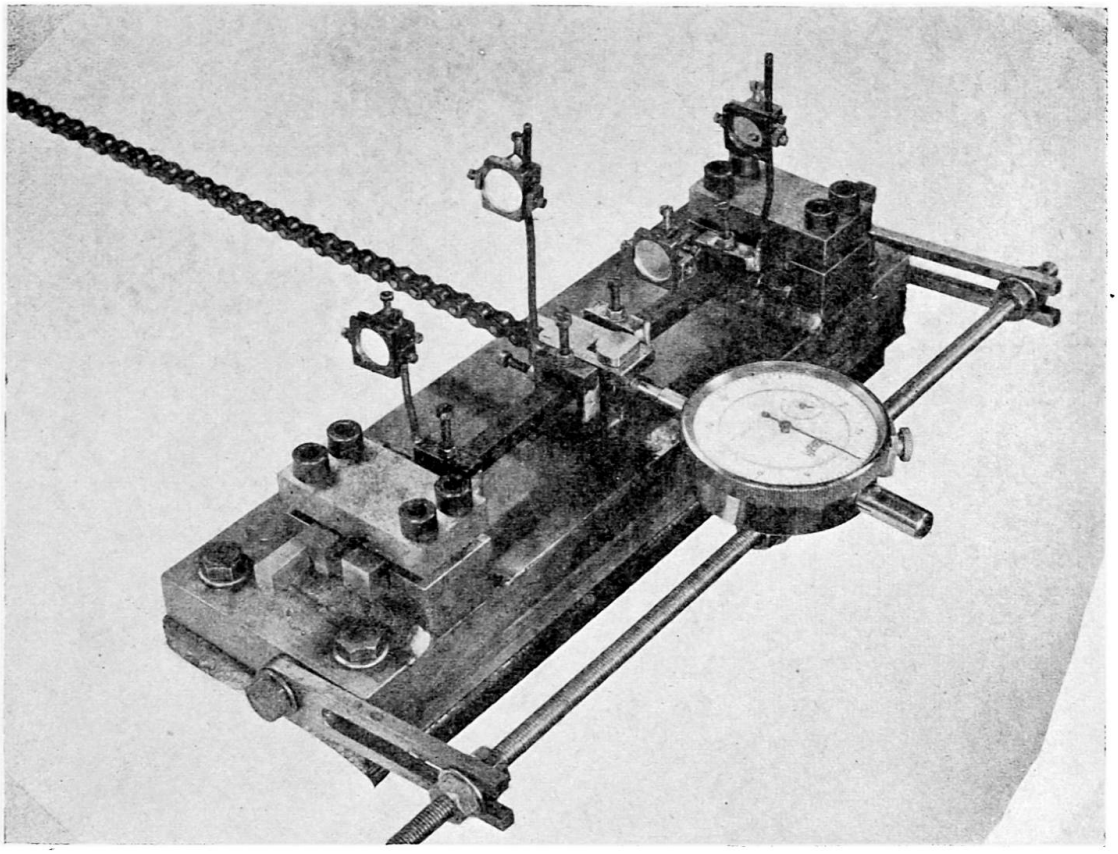

Fig. 11. Arrangement for testing fixed-ended beams

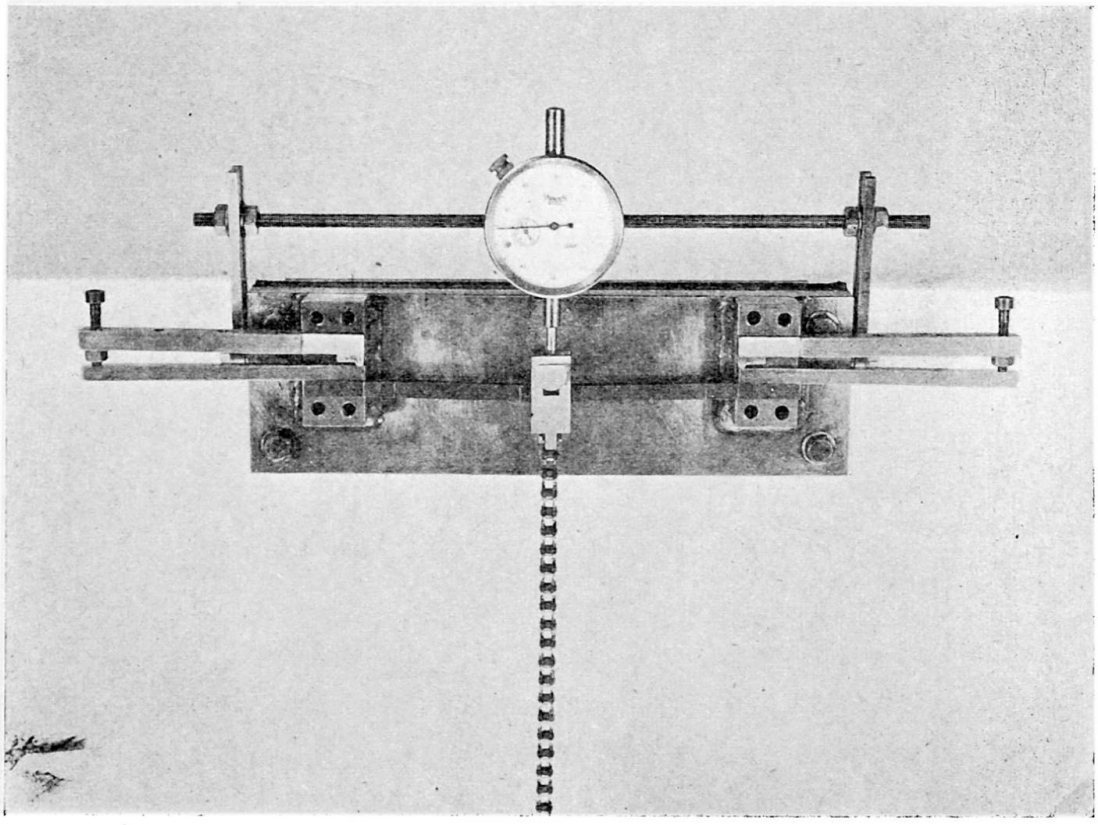

Fig. 12. Method of obtaining reduced end fixity

TABLE III

	1	2	3	4	5	6	7	8	9	10	11	12	13
								Analysis by simple plastic theory ignoring the effect of load concentration			Analysis in which allowance is made for the effect of load concentration		
	Beam No.	Mean Width, in.	Mean Depth, in.	Estimated Modulus of Elasticity E, tons/in.^{2}	End Fixity Constant K, radians/lb. in. $10^{-6}\times$	Ratio of End Moment to Central Moment in Elastic Range	Collapse Load, lb.	Lower Yield Stress, tons/in.^{2}	Mean Lower Yield Stress, tons/in.^{2}	Per cent Difference	Lower Yield Stress, tons/in.^{2}	Mean Lower Yield Stress, tons/in.^{2}	Per cent Difference
1	E1	0·254	0·253	13,440	14·3	0·912	258	21·3		−3·4	20·4		−2·6
2	E2	0·249	0·255	13,440	49·4	0·746	263	21·8		−1·2	20·9		−0·3
3	E3	0·250	0·256	13,440	148·6	0·490	269	22·0	22·1	−0·3	21·1	21·0	0·7
4	EC1	0·246	0·252	13,140	—	—	199	22·8		3·4	21·4		2·2
5	EC2	0·247	0·250	13,730	—	—	194	22·4		1·5	21·0		0

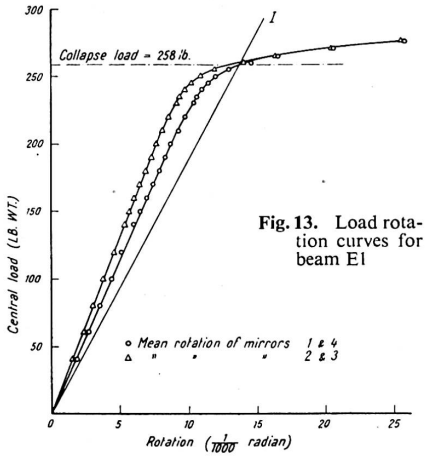

Fig. 13. Load rotation curves for beam E1

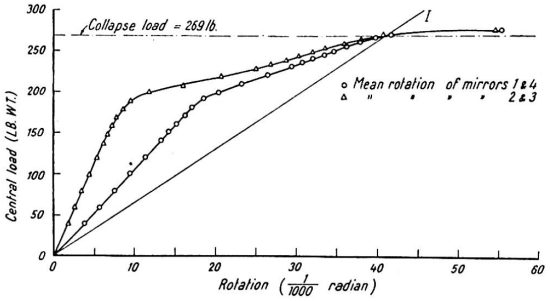

Fig. 14. Load rotation curves for beam E3

column 11, and the percentage differences from the mean are given in column 13. There is a certain improvement in the agreement between the yield stress values as compared with those given in column 8.

Load rotation curves are given for beams E1 and E3 in figs. 13 and 14 respectively. These curves do not indicate such definite collapse loads as obtained for the $\frac{7}{8}$-in. square beams described above. This may be due to strain hardening, and in order to obtain a consistent interpretation of test results, the collapse loads have been determined as follows.

Taking the value for the modulus of elasticity given in column 4 of Table III, and assuming some value for the collapse load, it is possible to calculate by means of the simple plastic theory of bending the rotation at any section of the beam when it is just about to collapse. Then the relationship between the assumed collapse load and the rotation is obtained as a straight line OI (figs. 13 and 14), and the collapse load is taken as the intersection of this line with the experimental load rotation curve. The figure quoted for any beam in column 7 of Table III is the mean of the three values obtained from the central deflection and the two pairs of mirrors (M_1, M_4 and M_2, M_3).

In the case of beam E1, the end moments were in the elastic range almost equal to the central moments (see column 6 of Table III), and the full plastic moment was reached at all three sections at practically the same load. With beam E3, however, the end moments were in the elastic range less than half the central moment, and the load rotation curves (fig. 14) indicate that full plastic moment was reached at the centre at a load of about 200 lb. Thereafter the rotations increased almost linearly with load up to 255 lb., soon after which full plastic moments developed at the ends and collapse occurred.

Beams E4, E5 and E6

The results for beams E4, E5 and E6 are summarised in Tables IV and V. Sufficient load was applied successively to the three loading positions (see fig. 10) to produce full plastic moments at the ends and under the load. Values of the lower yield stress calculated on the basis of the simple plastic theory are given in column 8 of Table IV.

TABLE IV

	1	2	3	4	5	6	7	8
	Beam No.	Mean Width, in.	Mean Depth, in.	Estimated Modulus of Elasticity, E, tons/in.^{2}	End Fixity Constant K, radians/lb. in. 10^{-6} ×	Order of Loading Positions	Maximum Load Actually Applied	
							Load, lb.	Corresponding Lower Yield Stress, tons/in.^{2}
1	E4	0·249	0·255	13,440	14·3	C	260·0	21·5
2						D	292·5	21·5
3						E	292·5	21·5
4	E5	0·248	0·253	13,440	14·3	D	287·5	21·6
5						E	287·5	21·6
6						C	255·6	21·6
7	E6	0·247	0·254	13,440	14·3	D	285·0	21·3
8						C	253·3	21·3
9						E	285·0	21·3

TABLE V

	1	2	3	4	5	6	7	8	9
				1st Load Position		2nd Load Position		3rd Load Position	
	Beam No.	Quantity	Unit	Observed Maximum	Calculated Value at Collapse	Observed Maximum	Calculated Value at Collapse	Observed Maximum	Calculated Value at Collapse
1	E4	Central deflection	in. $\times 10^{-3}$	60·0	45·5	66·1	87·2	89·7	100·0
2		Rotation θ_1	radians $\times 10^{-3}$	18·1	13·6	30·9	46·4	28·7	31·6
3		,, θ_2	,,	18·8	13·6	22·7	39·4	10·1	15·0
4		,, θ_3	,,	17·5	13·6	4·0	15·0	29·7	39·4
5		,, θ_4	,,	18·4	13·6	22·0	22·9	46·5	53·5
6	E5	Central deflection	in. $\times 10^{-3}$	50·1	63·1	71·3	83·7	83·5	86·3
7		Rotation θ_1	radians $\times 10^{-3}$	29·2	39·6	26·8	29·7	32·8	32·5
8		,, θ_2	,,	31·4	39·6	7·5	15·1	11·3	13·7
9		,, θ_3	,,	9·3	15·1	27·1	39·6	12·5	13·7
10		,, θ_4	,,	12·2	15·1	35·6	44·1	33·9	35·2
11	E6	Central deflection	in. $\times 10^{-3}$	50·3	62·1	66·2	65·8	77·9	94·2
12		Rotation θ_1	radians $\times 10^{-3}$	28·1	39·0	27·4	27·6	27·2	31·5
13		,, θ_2	,,	31·4	39·0	14·3	13·5	7·8	14·9
14		,, θ_3	,,	10·0	14·9	11·0	13·5	25·4	39·0
15		,, θ_4	,,	11·7	14·9	20·5	17·8	36·5	49·1

It is possible by means of the simple plastic theory to calculate the theoretical deflections and rotations at collapse for the various positions of the load. These calculated values are compared with those observed in Table V. The rotations θ_1, θ_2, θ_3 and θ_4 refer respectively to mirrors M_1, M_2, M_3 and M_4. Except for the first loading position practically all the observed deflections and rotations are less than the calculated values. Hence the ability of a beam to sustain a given ultimate load is not adversely affected by the attainment of the full plastic moment at various sections due to other critical load distributions. This is true whatever the order in which the loads are applied.

Tension tests

Tension tests were performed on four specimens, of diameter 0·178 in. and gauge length 0·70 in., in a Hounsfield Tensometer. Specimens ET1 and ET2 were cut from the ends of beam E2 after testing, and specimens ET3 and ET4 were cut from the ends of beam E6. The upper and lower yield stresses obtained are given in Table VI.

TABLE VI

Tension Specimen	Upper Yield Stress, tons/in.^{2}	Lower Yield Stress, tons/in.^{2}
ET1	21·68	20·88
ET2	21·57	20·57
ET3	22·70	20·56
ET4	21·08	20·17

The lower yield stresses are in good agreement with each other, and have a mean value of 20·54 tons/in.^{2} Considering beams E1, E2, E3, EC1 and EC2 (see Table III), the method of analysis suggested by Roderick and Phillipps gives a mean yield stress in closer agreement with the yield stress from the tension tests than is obtained when the simple plastic theory is applied.

4. CONCLUSIONS

The general agreement between the values of the lower yield stress calculated from the collapse loads for both the continuous and the fixed-ended beams is satisfactory and shows that the simple plastic theory gives predictions of the collapse loads of such beams with sufficient accuracy for practical purposes. The method of allowing for stress concentration suggested by Roderick and Phillipps (1949) does not lead to any distinct improvement for the continuous beams, but does lead to slightly better agreement for the fixed-ended beams. The tension tests carried out in connexion with the continuous beams did not establish any conclusive results, but with the fixed-ended beams tension tests favoured the method of Roderick and Phillipps.

The tests on the continuous beams confirm that the predictions of the plastic theory are not upset by sinking of supports, even if sinking is sufficient to cause yield in the beam. The plastic theory is equally successful for all the load distributions investigated, and the failure of one span does not decrease the ultimate carrying capacity of an adjacent span.

The tests on the fixed-ended beams show that ultimate carrying capacity is independent of the degree of rigidity of the end connections as long as these are capable of resisting the full plastic moment. The carrying capacity is not adversely affected when full plastic moments are produced at a number of sections by different successive load distributions, and this is true whatever the order in which the loads are applied.

The work described in this paper was carried out at the Engineering Laboratory, Cambridge University, and forms part of a general investigation into the behaviour of rigid-frame structures under the direction of Professor J. F. Baker, Head of the Department of Engineering.

References

BAKER, J. F. *J. Inst. Struct. Engrs.*, **27**, 397, 1949.
BAKER, J. F., and RODERICK, J. W. *Trans. Inst. Welding*, **3**, 83, 1940; **5**, 97, 1942.
BLEICH, H. *Der Bauingenieur*, **19/20**, 261, 1932.
EWING, A. *The Strength of Materials*, Cambridge U.P., 1903.
HENDRY, A. W. *Civil Engineering and Public Works Review*, **45**, 172, 1950.
HEYMAN, J. "The Determination by Relaxation Methods of Elasto-Plastic Stresses in Two Transversely Loaded Beams" (unpublished).
HORNE, M. R. *J. Inst. Civ. Engrs.*, **34**, 174, 1950.
HORNE, M. R. *Proc. Roy. Soc. A*, **207**, 216, 1951.
MAIER-LEIBNITZ, H. Proc. Int. Assn. Bridge Struct. Engng., Berlin, 1936.
NEAL, B. G., and SYMONDS, P. S. *J. Inst. Civ. Engrs.*, **35**, 21, 1950.
QUINNEY, H. *Engineering*, **145**, 309, 1938.
ROBERTSON, A., and COOK, G. *Proc. Roy. Soc. A*, **88**, 462, 1913.
RODERICK, J. W. *Phil. Mag.*, **39**, 529, 1948.
RODERICK, J. W., and PHILLIPPS, I. H. *Research, Engineering Structures Supplement*, **9**, 1949.
VOLTERRA, E. *J. Inst. Civ. Engrs.*, **20**, 349, 1943.

Summary

According to the simple plastic theory, the collapse loads of mild-steel continuous and fixed-ended beams may be calculated by considering merely the requirements of equilibrium in relation to the external loads and the full plastic moments of resistance of the beams. It follows that sinking of supports, order of loading and degree of end fixity should have no influence on such collapse loads. In order to check these deductions, tests were performed on $\frac{7}{8}$-in. square beams continuous over two spans and on $\frac{1}{4}$-in. square single-span beams provided with varying degrees of end fixity. The influence of various types of loading and of varying orders of application of the loads were investigated. Control tests were performed on similar simply supported members, and tension tests carried out at controlled rates of strain on material taken from unyielded sections of the beams.

The results give consistent confirmation of the simple plastic theory, and show conclusively that the collapse loads may be calculated with sufficient accuracy for practical purposes by this means. During the loading of a continuous beam in which one support is initially lower than the others, there is, according to the simple plastic theory, a progressive movement of the sections of maximum sagging moments along the beam. This is demonstrated in the tests by the appearance of Lüders' wedges on the polished surfaces of the $\frac{7}{8}$-in. square beams.

Résumé

Suivant la théorie simple de la plasticité, les charges de rupture des poutres en acier doux, continues ou encastrées à leurs extrémités, peuvent être calculées par simple considération des exigences d'équilibre corrélativement aux charges extérieures et aux pleins moments plastiques de résistance des poutres. Il en résulte que l'affaissement des appuis, l'ordre de mise en charge et le degré de rigidité aux extrémités ne doivent exercer aucune influence sur ces charges de rupture. Pour vérifier ces déductions, des essais ont été effectués sur des poutres carrées de $\frac{7}{8}$ in. (22,2 mm.), continues sur deux portées, ainsi que sur des poutres carrées de $\frac{1}{4}$ in. (6,35 mm.) sur portée simple, avec différents degrés de rigidité aux extrémités. On a étudié l'influence de divers types de charges et de divers ordres de mise en charge. Des essais ont été effectués, à titre de contrôle, sur des éléments simplement posés sur leur appuis; on a également procédé à des essais de traction, sous des taux de tension contrôlés, sur des éprouvettes prélevées sur des sections n'ayant subi aucune déformation.

Les résultats obtenus fournissent une bonne confirmation de la théorie simple de la plasticité et montrent d'une manière concluante que les charges de rupture peuvent être calculées avec une précision suffisante pour les besoins de la pratique, d'après la méthode ci-dessus. Au cours de la mise en charge d'une poutre continue dont un appui est initialement plus bas que les autres, il se produit, suivant la théorie simple de la plasticité, un déplacement progressif des sections présentant les moments maxima d'affaissement, le long de la poutre. Ceci est mis en évidence, au cours des essais, par l'apparition de figures de Luders sur les surfaces polies des poutres carrées de $\frac{7}{8}$ in.

Zusammenfassung

Nach der einfachen Plastizitätstheorie können die Bruchlasten von durchlaufenden und eingespannten Balken aus Flusstahl allein aus der Betrachtung der Gleichgewichtsbedingungen bezüglich der äusseren Lasten und der vollen plastischen Widerstandsmomente der Balken berechnet werden. Es folgt daraus, dass Auflagersenkungen, Lastanordnung und Einspannungsgrad keinen Einfluss auf solche Bruchlasten haben sollten. Zur Ueberprüfung dieser Feststellungen wurden Versuche an über zwei Felder durchlaufenden, $\frac{7}{8}$ in. (22,2 mm.) starken und an einfeldrigen, verschieden stark eingespannten, $\frac{1}{4}$ in. (6,35 mm.) starken Rechteck-Balken durchgeführt. Die Einflüsse verschiedener Arten von Lasten und verschiedener Formen der Last-Aufbringung wurden untersucht. Zur Kontrolle wurden Untersuchungen an entsprechenden einfach gelagerten Balken gemacht und unter kontrollierten Spannungen Zugversuche an Material aus unverformten Trägerteilen ausgeführt.

Die ermittelten Resultate bedeuten eine gute Bestätigung der einfachen Plastizitätstheorie und zeigen überzeugend, dass die Bruchlasten mit für praktische Bedürfnisse genügender Genauigkeit nach dieser Methode berechnet werden können. Während der Belastung eines durchlaufenden Balkens, bei dem ein Auflager von Anfang an tiefer liegt als die anderen, ergibt sich, in Uebereinstimmung mit der einfachen Plastizitätstheorie, entlang dem Balken ein fortlaufendes Fliessen der Zonen grösster Momentenbeanspruchung infolge Einsenkung. Dies zeigt sich im Versuch durch das Auftreten von Fliessfiguren von Lüders auf den polierten Oberflächen der $\frac{7}{8}$ in. Rechteckbalken.

AI 4

Calcul du coefficient de sécurité

Safety factor calculation

Die Berechnung des Sicherheitsbeiwertes

PROF. DR. h.c. E. TORROJA et ING. A. PAEZ
Madrid Madrid

Dans le domaine de la construction, peu de problèmes peuvent présenter autant d'intérêt économique et théorique que celui du juste établissement des coefficients de sécurité. Leur importance justifie par elle-même la nécessité de quelques principes fondamentaux et d'un processus mathématique qui conduisent à l'établissement logique des valeurs de ces coefficients, avec l'approximation suffisante compatible avec les exigences pratiques et avec l'inéluctable variabilité des données du problème.

Il existe, sans aucun doute, une discontinuité accusée dans la rigueur avec laquelle se développe le calcul d'une structure. Après une étude mécanique minutieuse et une déduction détaillée des régimes de contraintes à l'intérieur des divers éléments résistants, on adopte un coefficient de sécurité empirique qui, sans justification préalable, s'applique comme facteur à une étude fonctionnelle scrupuleuse et précise.

L'opportunité de lier les résultats définitifs à des considérations économiques objectives empêche de développer l'étude sur des valeurs et des erreurs moyennes. Elle oblige à calculer la probabilité pour chaque variable d'atteindre une valeur déterminée, c'est-à-dire de produire une certaine réduction des caractéristiques de résistance des matériaux employés, ou une augmentation déterminée des sollicitations prévues, comme dans le cas des surcharges accidentelles. D'autre part, si l'on fait abstraction d'une corrélation explicite entre le coefficient de sécurité et la probabilité d'effondrement, ce coefficient ne peut être déterminé que lorsque cette probabilité a été fixée au préalable, ce qui enlève toute objectivité au résultat puisqu'il est lié à une probabilité qui, suivant ce critérium, est arbitraire.

Il est certain qu'à chaque système de charges qui sollicite un ouvrage correspond toujours une répartition déterminée des contraintes dans chacune des diverses sections des différents éléments qui la composent. Si le taux maximum dans une section est inférieur au taux de rupture du matériau, cette section ne subira de rupture dans aucune de ses fibres.

Le champ d'application de la présente étude est limité au cas le plus fréquent où l'effondrement de l'ouvrage est dû au fait que la contrainte maximum résultante

dépasse la charge limite du matériau. L'effondrement peut se produire quand il intervient simultanément une combinaison malencontreuse de causes en quelque sorte imprévisibles.

Ces causes dérivent de l'ensemble de phénomènes fortuits et ne répondent à d'autre loi qu'à celles du hasard. L'une d'entre elles est la présence d'une surcharge exceptionnelle capable par elle-même, ou bien de détruire l'ouvrage, ou bien de contribuer indirectement à son effondrement.

D'autres causes qui peuvent être à l'origine de la ruine d'un ouvrage parfaitement conçu sont, l'existence d'un défaut grave dans le matériau (vides du béton, bulles ou soufflures de l'acier, etc.) ou dans l'exécution même en chantier (mise en place défectueuse des éléments, mauvaise disposition des armatures ou dosage inadéquat du béton).

D'autre part, le calcul réalisé peut ne pas correspondre à la réalité, soit que l'on ignore les lois qui régularisent le comportement réel de l'ouvrage, soit que la complication qui résulte de leur application soit trop grande et rende impossible leur développement.

En dernier lieu, le processus de calcul lui-même est exposé, comme toute œuvre humaine, à des erreurs ou à des fautes de calcul, d'autant plus susceptibles de surgir et de passer inaperçues que sera plus grande la complication de ce calcul.

En définitive, les différentes variables qui interviennent dans le phénomène peuvent être classées en cinq groupes:

(1) Dépassement des surcharges prévues (variable x),
(2) Défauts dans les bases théoriques du calcul (variable y),
(3) Erreurs numériques dans le calcul (variable z),
(4) Insuffisance de résistance des matériaux (variable u),
(5) Défauts d'exécution (variable t).

Chacune de ces variables aléatoires doit être représentée sous forme de fonction statistique déduite des expériences réalisées.

Dans le but de simplifier dans la mesure du possible les opérations ultérieures, il convient d'affecter à ces variables la forme de coefficients de correction.

S'il était possible de connaître la réalité des faits, on pourrait calculer les erreurs unitaires commises dans les cinq points énumérés. Par exemple, on saurait qu'au cours de la période de service de l'ouvrage, l'effort maximum appliqué à une section déterminée, produit par la présence d'une surcharge maximum S_x, devrait être s_v au lieu de l'effort s_p théoriquement déduit de la surcharge S'_x admise.

L'effort calculé s_p aussi bien que l'effort réel s_v différeront à leur tour de l'effort s_R nécessaire pour rompre une fibre de la section considérée. En général, les trois sollicitations appliquées s_v, s_R et s_p seront inégales, le fait que

$$s_v < s_R \qquad \ldots\ldots\ldots\ldots \quad (1)$$

étant la condition nécessaire pour qu'aucune des fibres ne se rompent pas.

La relation

$$C_v = \frac{s_R}{s_v} \qquad \ldots\ldots\ldots\ldots \quad (2)$$

a été appelée coefficient de sécurité efficace réel et le quotient

$$C = \frac{s_R\, s_r}{s_p} \qquad \ldots\ldots\ldots\ldots \quad (3)$$

coefficient de sécurité efficace prévu, ou simplement coefficient de sécurité efficace. Dans cette expression, s_r représente l'effort maximum qui, appliqué à la section,

pourrait être supporté par celle-ci si les matériaux employés avaient les mêmes caractéristiques et les mêmes propriétés que l'on a supposé dans le calcul et qui, en général, sera différent de leur valeur réelle s_R.

Suivant ces principes, si S_x représente le train réel de charges le plus lourd ou le système de forces maximum appliqué extérieurement à la pièce et S'_x est la surcharge admise dans le projet, l'erreur relative en supposant connue la réalité, serait:

$$\epsilon_x=\frac{S_x-S'_x}{S'_x}$$

positive ou négative selon que le critérium établi est insuffisant ou excessivement conservateur.

En conséquence, pour corriger les résultats théoriques, il serait nécessaire de commencer par appliquer, pour cette seule raison, un coefficient de correction:

$$x=1+\epsilon_x=\frac{S_x}{S'_x} \quad . \quad . \quad . \quad . \quad . \quad . \quad . \quad . \quad . \quad (4)$$

qui, appliqué à la surcharge admise comme probable, donnerait comme produit le système réel des efforts qui agissent sur la pièce ou sur l'ouvrage que l'on considère.

Les divergences naturelles entre le comportement réel de l'ouvrage et son comportement théorique font que, même en partant d'un même système final de forces extérieures S'_x, les efforts s'_y déterminés par le calcul dans une section déterminée de la pièce que l'on étudie diffèrent des s_y que l'on obtiendrait réellement pour la même surcharge S'_x. Pour que le premier s'identifie avec le résultat véritable, il est nécessaire d'appliquer un deuxième coefficient de correction:

$$y=\frac{s_y}{s'_y} \quad . \quad . \quad . \quad . \quad . \quad . \quad . \quad . \quad . \quad . \quad . \quad (5)$$

Enfin, les erreurs numériques sont la cause de nouvelles erreurs qui, pour être éliminées, exigent l'introduction d'un troisième coefficient:

$$z=\frac{s_z}{s'_z} \quad . \quad . \quad . \quad . \quad . \quad . \quad . \quad . \quad . \quad . \quad . \quad (6)$$

Par conséquent si s_p est la sollicitation propre d'une pièce, déterminée par le calcul suivant un certain processus numérique, basé sur certaines surcharges et hypothèses approximatives, la sollicitation que l'on devrait faire intervenir dans ce calcul pour obtenir des résultats en accord avec la réalité est

$$s_v=xyzs_p \quad . \quad . \quad . \quad . \quad . \quad . \quad . \quad . \quad . \quad . \quad . \quad (7)$$

De même, si s_r est la sollicitation de rupture assignée aux matériaux et s_R leur véritable sollicitation limite, on peut écrire:

$$s_R=\frac{s_r}{u \, . \, t} \quad . \quad . \quad . \quad . \quad . \quad . \quad . \quad . \quad . \quad . \quad . \quad (8)$$

où u et t sont les deux facteurs de correction à faire intervenir, le premier pour compenser les divergences entre les caractéristiques mécaniques réelles des matériaux et celles qui ont été adoptées dans le calcul et le second pour tenir compte des anomalies ou défauts introduits sur le chantier. En divisant (8) par (7), on obtient:

$$\frac{s_R}{s_v}=\frac{s_r}{u \, . \, t} \cdot \frac{1}{xyzs_p} \quad . \quad . \quad . \quad . \quad . \quad . \quad . \quad . \quad . \quad (9)$$

Selon les égalités (2) et (3), l'expression (9) se transforme en:

$$C_v=\frac{C}{x\,.\,y\,.\,z\,.\,t\,.\,u} \quad . \quad . \quad . \quad . \quad . \quad . \quad . \quad . \quad . \quad (10)$$

ce qui, écrit de la façon suivante:

$$\frac{C}{C_v}=x\,.\,y\,.\,z\,.\,t\,.\,u=\gamma \quad . \quad . \quad . \quad . \quad . \quad . \quad . \quad . \quad . \quad (11)$$

suggère un concept plus ample et plus rigoureux de la signification de ces facteurs de correction, en ce sens que chacun de ces facteurs représente la relation entre les coefficients de sécurité prévu et le réel, se rapportant à n'importe lequel des cinq concepts de base, lorsque les autres sont satisfaits d'une manière complète et parfaite, c'est-à-dire si les quatre autres coefficients correspondants sont égaux à l'unité.

Quant au produit

$$\gamma=x\,.\,y\,.\,z\,.\,t\,.\,u, \quad . \quad . \quad . \quad . \quad . \quad . \quad . \quad . \quad . \quad (12)$$

sa signification est immédiate, chaque fois qu'il représente la relation entre les coefficients C et C_v à la suite de l'intervention globale de toutes les causes d'erreur.

Etant donné que la condition de permanence ou de non-rupture de l'ouvrage s'exprime par l'inégalité:

$$C_v>1 \quad . \quad . \quad . \quad . \quad . \quad . \quad . \quad . \quad . \quad . \quad . \quad (13)$$

on en déduit que la valeur du coefficient de sécurité adopté doit être:

$$C>\gamma \quad . \quad . \quad . \quad . \quad . \quad . \quad . \quad . \quad . \quad . \quad . \quad (14)$$

On comprend logiquement que les valeurs des cinq facteurs de correction soient essentiellement inconnus. Toutefois, à l'aide d'une statistique adéquate on peut relier à chaque fluctuation de ces facteurs, entre deux limites établies arbitrairement, la probabilité d'occurrence d'un fait semblable.

Ce concept qui interprète les facteurs de correction, non comme un nombre plus ou moins certain, mais comme une fonction de probabilité, pose le problème de l'établissement d'un critérium mathématique à l'aide duquel on puisse développer les opérations qu'il est nécessaire de réaliser avec ces variables aléatoires.

Dans les grandes lignes, si $X(x)$ et $Y(y)$ sont deux fonctions de probabilité, il devient nécessaire d'établir un procédé opératoire à l'aide duquel on puisse obtenir la loi de probabilité d'une nouvelle variable w liée aux variables antérieures par la relation

$$w=f(x,\,y) \quad . \quad . \quad . \quad . \quad . \quad . \quad . \quad . \quad . \quad . \quad (15)$$

ou ce qui revient au même, au moyen de l'équation:

$$y=\phi(x,\,w) \quad . \quad . \quad . \quad . \quad . \quad . \quad . \quad . \quad . \quad . \quad (16)$$

A cet effet, (fig. 1), considérons un système d'axes cartésiens rectangulaires.

En prenant comme origine des coordonnées le point O, on peut représenter, sur le premier quadrant, la fonction

$$y=\phi(x,\,w_1) \quad . \quad . \quad . \quad . \quad . \quad . \quad . \quad . \quad . \quad . \quad (17)$$

qui relie la variable x à la y, au moyen de la fonction ϕ qui doit être uniforme pour les différentes valeurs w_i que la variable w peut prendre.

En supposant que la variable x varie entre une limite inférieure $x=a$ et une limite supérieure $x=A$ et que, de même, la variable y soit comprise entre deux limites $b<y<B$ on peut dessiner sur les quadrants II et III, les fonctions $X(x)$, $Y(y)$ représentatives respectivement, de la probabilité pour x d'atteindre une valeur comprise entre a et x et pour y de prendre une valeur comprise entre b et y.

Etant donné que la probabilité de $x_2 > x > a$ est toujours plus grande que celle de $x_1 > x > a$ quand $x_2 > x_1$ et que

$$dX = X'(x)dx \quad . \quad . \quad . \quad . \quad . \quad . \quad . \quad . \quad . \quad . \quad (18)$$

a toujours et seulement une solution, dans tout l'intervalle compris entre a et A, la fonction $X = X(x)$ est non seulement monotone, mais aussi continue, de même que sa dérivée première dans cet intervalle; on peut en dire autant de la fonction analogue $Y = Y(y)$ dans l'intervalle de b à B.

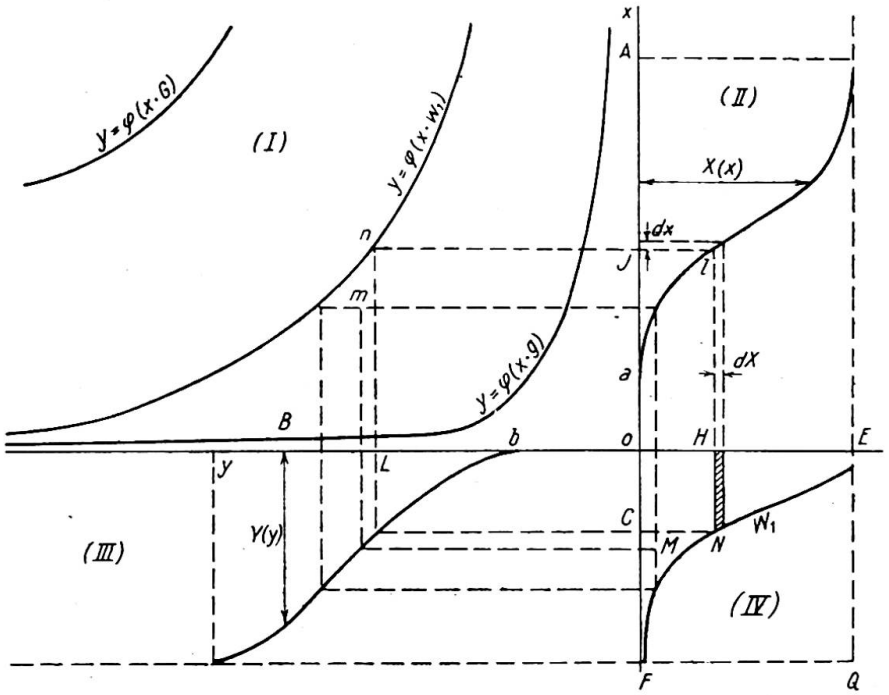

Fig. 1

Selon ce qui a été exposé antérieurement, à tout valeur OJ arbitraire de x, correspondra toujours une seule valeur OH de la fonction $X(x)$.

D'autre part, en vertu de l'hypothèse admise sur l'uniformité de la fonction $y = \phi(x)$, à toute valeur OJ de x correspondra aussi une seule valeur OL de y, telle que

$$y = \phi(x, w_1)$$

et par conséquent, une valeur

$$OC = Y(y)_{y=\phi} = \Phi(x, w_1), \quad . \quad . \quad . \quad . \quad . \quad . \quad . \quad . \quad (19)$$

qui jointe à OH, définit le point N dans le quadrant IV, établissant ainsi une correspondance univoque, entre chacun des points n de la courbe $y = \phi(x, w_1)$ et chacun des points N de la courbe W_1.

En vertu de la propriété commune aux fonctions X et Y d'être monotones dans tout l'intervalle considéré, tout point générique m, du système I, situé entre la courbe $y = \phi(x, w_1)$ et les axes coordonnés, aura toujours un point réciproque M et seulement un, dans le système IV, entre la courbe W_1 et les axes OE et OF.

Puisque le système N a été construit en rapportant aux axes coordonnés OE et OF les probabilités d'occurrence de certains phénomènes, ce système correspondra à un domaine d'égale probabilité; par conséquent, la probabilité pour un point générique M d'être situé dans la zone comprise entre la courbe W_1 et les axes OE et OF sera exprimée par le rapport des aires:

$$\frac{\text{aire } OEW_1FO}{\text{aire } OEQFO}$$

x et y étant des variables qui sont comprises entre les limites extrêmes a et A, b et B, la probabilité de vérification des inégalités:

$$A>x>a \qquad B>y>b \quad . \quad . \quad . \quad . \quad . \quad . \quad . \quad (20)$$

sera, sans aucun doute, la certitude; c'est-à-dire que l'on aura:

$$X(A)=Y(B)=OE=OF=1 \quad . \quad . \quad . \quad . \quad . \quad . \quad . \quad (21)$$

et

$$\text{aire } OEQFO=1 \quad . \quad . \quad . \quad . \quad . \quad . \quad . \quad . \quad . \quad (22)$$

c'est-à-dire que la probabilité pour le point M d'être à l'intérieur du contour OEW_1FO sera la valeur de cette aire qui, selon l'égalité (19), est:

$$\text{aire } OEW_1FO=\int_a^A \Phi(x,z_1)dX \quad . \quad . \quad . \quad . \quad . \quad . \quad (23)$$

Puisque la fonction $y=\phi(x)$ est, par hypothèse, une fonction uniforme pour toutes les valeurs paramétriques que peut adopter w, les valeurs extrêmes g et G de ce paramètre seront obtenues pour deux des quatre combinaisons auxquelles peuvent donner lieu les quatre limites des deux variables aléatoires x et y (a, A, b et B).

Soit, à cet effet, g la valeur extrême que peut atteindre sa valeur minimum a et soit de même G la limite extrême du paramètre w, quand x arrive à sa valeur maximum A.

Dans ces conditions, les fonctions $y=\phi(x, g)$ et $y=\phi(x, G)$ du premier quadrant représenteront les limites des valeurs possibles de w.

Etant donné la correspondance univoque entre les points M du système IV et les points M du premier système, la probabilité pour le point M d'être compris dans la zone limitée par les courbes représentatives des fonctions $\phi(x, w_1)$ et $\phi(x, g)$ et compatible avec les domaines de fluctuation des variables x et y, c'est-à-dire la probabilité pour la variable w d'être limitée par les valeurs g et w, sera la même que celle pour le point M d'être situé entre W_1 et les axes DE et OF.

Par conséquent la probabilité pour la variable w d'être limitée par la valeur g et la valeur particulière w_1, sera:

$$W=W(w_1)=\int_a^A \Phi(x, w_1)dX \quad . \quad . \quad . \quad . \quad . \quad . \quad . \quad (24)$$

De même, pour une valeur arbitraire w de w_1,

$$W=W(w)=\int_a^A \Phi(x, w)dX \quad . \quad . \quad . \quad . \quad . \quad . \quad . \quad (25)$$

Et finalement, en différenciant sous le signe intégral, on aura la probabilité pour la variable w d'être comprise entre une valeur générique w et une valeur $w+dw$ qui sera:

$$dW=dw\int_a^A \frac{\partial\Phi}{\partial w}dX \quad . \quad . \quad . \quad . \quad . \quad . \quad . \quad (26)$$

En dérivant, par rapport à w, la fonction (19) deviendra:

$$\frac{\partial\Phi}{\partial w}=\frac{\partial\phi}{\partial w}\cdot\frac{dY}{d\phi}=\frac{\partial\phi}{\partial w}\left(\frac{dY}{dy}\right)_{y=\phi(x, w)} \quad . \quad . \quad . \quad . \quad . \quad . \quad (27)$$

En reportant cette expression dans l'équation (26), il restera enfin:

$$dW=dw\int_a^A \frac{\partial\phi}{\partial w}\cdot dX\left(\frac{dY}{dy}\right)_{y=\phi(x, w)} \quad . \quad . \quad . \quad . \quad . \quad . \quad (28)$$

Dans le cas particulier auquel se réfère ce rapport, les variables w, x, y sont reliées entre elles par la relation $w=x \,.\, y$; c'est-à-dire que:

$$y=\phi(x, w)=\frac{w}{x} \quad . \quad . \quad . \quad . \quad . \quad . \quad . \quad . \quad . \quad (29)$$

d'où l'on déduit:

$$\frac{\partial \phi}{\partial w}=\frac{1}{x} \quad . \quad . \quad . \quad . \quad . \quad . \quad . \quad . \quad . \quad (30)$$

D'autre part, le caractère fortuit des coefficients de correction x, y, z, t, u oblige à étendre la domaine de fluctuation de ces variables à tout le champ réel positif:

$$0<x<\infty, \qquad 0<y<\infty, \qquad 0<u<\infty$$

conditions qui, tenant compte de l'équation (30), transforment l'égalité (28) en l'expression:

$$dW=\int_0^{\infty} \frac{dX}{x}\left(\frac{dY}{dy}\right)_{y=w:x} \quad . \quad . \quad . \quad . \quad . \quad . \quad . \quad (31)$$

qui, comme (28), exprime la probabilité pour la variable $w=x \,.\, y$ d'être comprise entre w et $w+dw$.

L'opportunité d'opérer avec les fonctions $X(x)$, $Y(y), \ldots$, déduites directement de l'expérimentation, au lieu de considérer les lois gaussiennes similaires, oblige à developper cette méthode selon des procédés graphiques, pour ne pas altérer le caractère véritable des distributions expérimentales par des simplifications additionnelles qui pourraient diminuer leur précision.

Pour cela, il suffit de dessiner à une échelle convenable les fonctions $X(x)$, $Y(y)$ ainsi que le réseau des hyperboles:

$$y=\frac{w_i}{x}$$

représentatives de la condition de lien imposée aux variables $w=x \,.\, y$.

Suivant la méthode indiquée dans la fig. 1, à chaque valeur particulière w_1, correspondra une courbe W_1 dans le quadrant (IV) qui délimitera un contour OEW_1F, dont l'aire

$$\Omega_1=\int_0^{w_1} dw=W(w_1)$$

définit l'ordonnée $W_1=W(w_1)$ correspondant à l'abscisse w_1. En répétant ce processus autant de fois qu'on le juge nécessaire, on peut dessiner, par points, la fonction $W=W(w)$. Une fois trouvée la fonction $W=W(w)$, représentative de la probabilité pour la variable $w=x \,.\, y$ d'être comprise entre une valeur 0 et une autre valeur générique w, on peut déterminer la nouvelle distribution $W'=W'(w')$ de la variable auxiliaire w':

$$w'=w \,.\, z$$

ainsi que les fonctions de probabilité $W''=W''(w'')$ et $\Gamma=\Gamma(\gamma)$ correspondant aux variables:

$$w''=w' \,.\, u$$

$$\gamma=w'' \,.\, t=xyztu$$

Puisque, selon l'équation (14), la probabilité de non-effondrement est conditionnée par l'inégalité $C>\gamma$, on en déduit que la probabilité pour un ouvrage calculé avec un coefficient de sécurité égal à C, de s'effondrer est:

$$\Gamma_h=1-\int_0^{C} d\Gamma=1-\Gamma(C),$$

chaque fois que $\Gamma(o)=0$

L'on ne prétend pas, avec ces méthodes, établir un nouveau théorème mathématique destiné à résoudre d'une façon académique le problème général de la composition des variables de probabilité. L'on essaie seulement d'établir un critérium pratique qui permette d'obtenir, d'une façon suffisamment précise et générale, la loi de distribution du produit:

$$\gamma = x \,.\, y \,.\, z \,.\, t \,.\, u,$$

ou, ce qui est équivalent, la probabilité d'effondrement:

$$\Gamma_h = 1 - \Gamma(C) \quad . \quad . \quad . \quad . \quad . \quad . \quad . \quad . \quad . \quad (32)$$

en fonction du coefficient de sécurité C. On peut facilement comprendre que la fonction Γ_h n'est pas unique, mais qu'elle varie selon les conditions de surveillance en chantier, le type de surcharge qui agit sur la structure, la rigueur qui a présidé au développement des calculs ou le genre de matériaux employés. Bref, elle varie avec les diverses circonstances qui modifient les distributions individuelles correspondant aux cinq variables énumérées.

Dans le but de faciliter aux théoriciens la tâche fastidieuse de determiner la fonction de probabilité qui correspond aux caractéristiques particulières de l'ouvrage en projet, on a calculé, au cours d'expériences que nous décrirons plus loin, les distributions individuelles relatives aux cas de plus fréquente utilisation pratique, ainsi que les 75 différentes fonctions de probabilité Γ_h correspondant aux diverses combinaisons auxquelles donnent lieu les différentes sous-classifications (calculs rigoureux, normaux ou approximatifs, surcharges dans les maisons, les ponts ou les édifices industriels, ouvrages métalliques, ou de béton, très contrôlés, normalement ou peu contrôlés, etc.).

Au moyen d'un jeu d'abaques calculés à cet effet, on peut connaître par leur simple lecture la probabilité d'effondrement relative à un coefficient de sécurité déterminé, dans le cas concret que l'on envisage.

D'autre part, tout ouvrage implique le risque inhérent de son effondrement, origine de dommages déterminés. Si l'on considère n ouvrages identiques en tous points, avec une probabilité $1/n$ d'effondrement et dont les dommages totaux, pour cette cause improbable, seraient égaux à D pour chacun, on peut espérer que, dans un délai équivalent à la période habituelle de service de ces ouvrages, un d'entre eux s'effondrera, et que cette catastrophe donnera lieu à des pertes humaines et matérielles équivalentes à D. Si P est le coût du premier établissement dans l'ensemble des n ouvrages, chacun réalisés, la perte totale sera $P+D$. Etant donné que l'on ignore *a priori* quelle sera l'ouvrage qui s'effondrera, puisque tous ont la même probabilité, on en déduit qu'il correspond à chaque ouvrage des dommages virtuels égaux à $1/n(D+P)$; c'est-à-dire, équivalents au produit de la probabilité d'effondrement $\Gamma_h = 1/n$ par les dommages totaux occasionnés, en y incluant le coût du propre ouvrage détruit.

Dans un critérium de vaste économie nationale, la perte économique virtuellement consécutive à la destruction possible de l'ouvrage est représentée suivant le raisonnement précédent, par l'espérance mathématique de l'effondrement, c'est-à-dire, par la quantité:

$$\frac{1}{n}(D+P) \quad . \quad . \quad . \quad . \quad . \quad . \quad . \quad . \quad . \quad (33)$$

où $1/n$ représente la probabilité d'effondrement, probabilité qui, antérieurement, a été désignée par Γ_h.

En ajoutant à cette partie le coût P du premier établissement, on constate que, dans le sens économique général, le débours total affectué par le propriétaire et les

sinistrés, c'est-à-dire le coût total que suppose pour la collectivité la construction de l'ouvrage précité, est:

$$P+\Gamma_h\times(D+P)=R \quad . \quad . \quad . \quad . \quad . \quad . \quad . \quad . \quad (34)$$

où le deuxième terme du premier membre, c'est-à-dire la quantité $\Gamma_h(D+P)$, a la même signification conceptuelle et quantitative qu'une prime d'assurance de la construction pour couvrir les risques et les pertes de son effondrement improbable.

La solution la plus économique est par conséquent celle où l'expression (34) est minimum. D'une façon plus précise, on peut énoncer le principe précédent en disant que, dans le champ des solutions infinies que l'on peut imaginer en faisant varier seulement le coefficient de sécurité d'un même ouvrage en projet, la solution logique parce que la plus économique, est celle pour laquelle le coût d'ensemble de l'ouvrage en lui-même et de la prime d'assurance des dommages possibles qui peuvent être occasionnés par l'effondrement (en y incluant la reconstruction de l'ouvrage) atteint une valeur minimum.* Une fois établi ce principe économique, le processus opératoire qu'il convient de suivre pour la détermination du coefficient de sécurité résulte immédiatement, comme conséquence logique, de la condition de minimum imposée. A cet effet, on essaiera plusieurs coefficients arbitraires qui, introduits premièrement dans la fonction de probabilité Γ_h et ensuite dans la relation (34), conduiront à une série de résultats numériques représentatifs des frais totaux d'ouvrage assurés, dont la valeur minimum définira la solution la plus économique. Le coefficient de sécurité C, qui correspond à cette solution de valeur minimum, sera le coefficient qu'on devra adopter pour l'ouvrage étudié, la probabilité d'effondrement apparaissant comme une fonction dépendante de C.

Pour le développement et l'application pratique des principes et de la théorie exposée, il est nécessaire d'établir, en se conformant le plus possible à la réalité, les fonctions individuelles de probabilité correspondant aux cinq groupes précités, en partant des données statistiques. Une des difficultés qui se pose ici est celle qui résulte de la forte interférence et de la connexion étroite de certaines variables avec d'autres. Cette dépendance mutuelle fait que les résultats expérimentaux permettent rarement l'établissement direct d'une distribution déterminée. Ils sont très fréquemment troublés par des phénomènes de caractère étrange, soit qu'il soit impossible de les éliminer, soit que les données publiées ne soient pas aussi adéquates que le ferait désirer l'objet fondamental de cette étude.

Une des distributions qui peut être déterminée directement est celle qui se rapporte aux erreurs numériques qui s'infiltrent dans le calcul. En partant d'une révision méticuleuse des opérations intervenant dans le calcul des efforts et des contraintes de 116 éléments différents d'ouvrages industriels, de bâtiments, de ponts et de tribunes, on a pu tracer la loi de probabilité $Z=Z(z)$ de ces erreurs numériques qui, comme conséquence de son caractère fortuit et libre d'erreurs systématiques, affecte une forme nettement gaussienne, avec valeur la plus probable pour $z=1$.

Les lois de probabilité $U(u)$ correspondant aux coefficients de correction u dans les bétons et dans les aciers ont été déterminées à partir des séries étendues d'essais réalisés sur ces matériaux par l'Institut Technique du Bâtiment et des Travaux Publics de Paris pendant la période 1935–1947. De même que dans le cas antérieur, l'expérimentation groupe directement les éléments cherchés, c'est-à-dire la concentration des résultats, autour de la valeur moyenne pour les différentes séries essayées.

Il n'en est pas de même pour la détermination de la loi de probabilité $Y(y)$ représentative des erreurs ou des défauts de précision dans les hypothèses de calcul. Un

* Ce principe a été formulé par le Professeur E. Torroja lors du IIème Congrès International des Ponts et Charpentes, à Liège, en 1948.

calcul parfaitement idéal est celui qui reproduit, avec une fidélité absolue, les déformations et les contraintes qui se manifesteraient rigoureusement dans un ouvrage construit avec des matériaux exactement identiques à ceux que l'on a envisagés dans le calcul comme éléments de départ.

Or, tout ouvrage présente certaines divergences avec les dimensions stipulées et, dans de nombreux cas, d'importants défauts de construction qui altèrent son comportement. Seuls les modèles à échelle réduite ou naturelle construits dans un laboratoire et étroitement surveillés pourraient servir de point de comparaison.

Même ainsi, il est nécessaire d'effectuer quelques corrections. Si l'on mesure des déformations ou des flèches, les résultats peuvent être affectés par le manque de concordance entre les modules d'élasticité et de déformation supposés et ceux que le matériau possède réellement. Si l'on étudie les charges de rupture, leurs écarts propres et leur hétérogénéité peuvent fausser la comparaison avec le calcul.

Pour essayer d'éliminer tous ces phénomènes perturbateurs dans l'étude présente, on a corrigé par les méthodes mathématiques, de la fig. 1, les lois de variabilité des modules indiqués et des résistances antérieurement déterminées, en établissant que la loi $Y(y)$ cherchée doit être une fonction statistique telle que la loi $Y_1(y_1)$, où $y_1 = y \,.\, m$, coïncide avec la fonction de probabilité donnée par l'expérimentation quand la distribution $M(m)$ représente la loi de variation des modules d'élasticité ou des résistances.

Ces fonctions de probabilité $Y_1(y_1)$ ont été déterminées en se basant sur les effets exercés sur des poutres droites, sur des dalles et sur des ponts réalisés par l'Engineering Experiment Station de l'Université d'Illinois, sur les épreuves réalisées sur le Pont de Djedeida, sur les résultats obtenus à l'aide des modèles du Fronton Recoletos de Madrid et sur l'expérimentation effectuée sur des ouvrages déterminés, en Suisse, par le Eidgenössische Material Prüfungs-und Versuchsanstalt für Industrie und Bauwesen de Zürich.

Mais c'est dans la détermination de la distribution $T(t)$ des coefficients de correction pour des défauts introduits pendant la construction de l'ouvrage que se manifeste la plus grande complication. D'un côté, il est nécessaire de décomposer la variable t en deux facteurs, dont l'un t_2 représente les erreurs de piquetage, de mise en place des armatures, de liaisons défectueuses, etc. (c'est-à-dire, qui n'affectent pas la résistance intrinsèque du matériau); l'autre t_3 exprime la possibilité de défaut qui l'affecte, par exemple gâchage ou dosage défectueux du béton.

Pour déterminer le premier de ces facteurs, on a eu recours à l'expérimentation réalisée sur divers ouvrages et sur des ponts suisses, par le Laboratoire Fédéral de ce pays, en éliminant par les méthodes mathématiques de composition de variables antérieurement décrites, les causes d'erreurs dues aux imperfections possibles du calcul développé et aux écarts entre les modules d'élasticité réels et supposés.

Le second facteur a été déterminé en se basant sur les expériences réalisées par A. R. Collins et publiées dans le n° 3 de la Revue *Road Research* et sur les références fournies par M. Billiard, de l'Institut Technique du Bâtiment et des Travaux Publics, sur les résultats des essais effectués sur des ouvrages contrôlés par le Bureau Securitas, dans les années 1947 et 1948.

Ces références permettent de déterminer l'importance statistique des défauts d'exécution dans des chantiers rigoureusement, normalement et faiblement contrôlés, au moyen des combinaisons opportunes entre les lois de distribution partielles.

Enfin, la variabilité des surcharges a été déterminée en se basant sur les données publiées par M. A. Freudenthal* et sur l'examen comparatif des critériums adoptés

Trans. Amer. Soc. Civ. Engrs*, **112, 125, 1947.

dans les instructions des divers pays pour fixer les surcharges estimées maxima.

Lorsque ces données n'ont pas été, même de loin, aussi abondantes qu'on l'aurait désiré, elles ont été malgré tout suffisantes pour prouver qu'en tablant sur elles, la théorie exposée permet d'arriver à des résultats pratiques. Bien que les développements théoriques soient compliqués et laborieux, il a été possible d'établir des tables et des abaques auxiliaires, au moyen desquels et en fonction du prix de l'ouvrage que l'on étudie, calculé avec un coefficient de sécurité quelconque, on peut déduire les prix correspondants aux divers coefficients que l'on essaie. En classant les calculs selon des cadres-types et à l'aide des tables ou abaques précités, l'ensemble des opérations requises dans un cas concret se réduit à des additions et des multiplications qui peuvent être effectuées en peu de minutes.

Comme on devait logiquement l'espérer, les coefficients de sécurité que l'on obtient en appliquant ces procédés à des pièces différentes ou à des groupes fonctionnels d'un même ouvrage sont différents d'un élément à un autre. Leur variation dépend de la plus grande ou de la plus petite importance de la pièce considérée, de l'influence relative de la surcharge comparée avec son poids propre et de l'amplitude des dommages qui pourraient être occasionnés par la rupture possible.

De même, le coefficient de sécurité propre d'un élément déterminé ou d'un ensemble de pièces de caractéristiques égales, varie quand on modifie les conditions primitives supposées en ce qui concerne la surveillance du chantier ou quand on remplace le calcul par un autre calcul plus rigoureux.

Le critérium économique qui sert de base à la détermination de ces coefficients de sécurité et la subordination de ceux-ci au degré de surveillance prévu et à la précision avec laquelle ont été effectués les calculs du projet, permettent de poser objectivement le problème du degré de contrôle auquel doivent être soumis les travaux de bétonnage et de construction, ainsi que l'opportunité d'une étude minutieuse du bâtiment. Une surveillance étroite et un calcul précis supposent des réductions déterminées dans la valeur du coefficient de sécurité et, par conséquent, une économie dans les matériaux employés. Selon que ces économies sont supérieures ou non au surplus que l'une ou l'autre solution exige, il est nécessaire ou anti-économique de recourrir à une plus grande surveillance de l'ouvrage ou à employer un plus grand nombre d'heures à préciser les dimensions des différents éléments.

Enfin, il convient de signaler le fait que les résultats définitifs auxquels on arrive par l'application de cette méthode coïncident avec ceux auxquels l'humanité est parvenue lentement jusqu'à l'époque actuelle, peut-être sans raison apparente.

On pourrait penser que cette coïncidence enlève un intérêt à ce thème, puisque son étude semble servir seulement de justification à des coutumes établies selon un critérium purement subjectif. Néanmoins, cette même conclusion sert à mettre en valeur les résultats; en effet d'une part, elle apporte garantie à la méthode elle-même et d'autre part, elle indique, dans l'ordre, des chiffres que les techniciens utilisent, l'opportunité d'introduire des variations bien définies d'un cas à l'autre, en fonction des différentes variables. Ces modifications n'avaient pu être appréciées et mises en valeur jusqu'à présent et on ne pouvait seulement qu'en avoir une intuition vague, sans possibilité de les libérer de dangereux critériums personnels, ni de les utiliser avec la précision raisonnée que l'économie et la sécurité des ouvrages exigent en même temps.

Il ne convient pas icî et nous ne disposons pas de la place suffisante, d'exposer le développement complet de la théorie, ni les résultats numériques que l'on peut obtenir, puisqu'ils sont différents pour chaque cas concret, avec des variations qui atteignent aisément par exemple $\pm 20\%$ et même plus et aussi parce que les auteurs espèrent pouvoir présenter bientôt un mémoire assez long en anglais.

Ils ne prétendent pas que la présente étude épuise la question ou lui apporte une solution définitive. Ils estiment seulement avoir établi un processus permettant de déterminer le coefficient de sécurité sur des bases objectives et de résoudre ainsi le problème en fournissant des résultats d'intérêt pratique. On peut en déduire des directives susceptibles d'orienter les recherches ultérieures, dans les multiples aspects du problème. Les auteurs attirent enfin l'attention sur l'intérêt qu'il y a à pousser l'étude statistique de tous les facteurs qui interviennent ici, c'est-à-dire de toutes les causes d'erreurs, de défauts ou d'autres, dont la conjonction est susceptible de produire l'effondrement des ouvrages.

Résumé

Le but principal de cette étude est l'établissement d'une méthode de calcul générale qui permette d'arriver à connaître la valeur numérique du coefficient de sécurité dans un cas déterminé. Ce résultat doit être complètement dégagé de toute subjectivité et doit dépendre exclusivement des données concrètes qui caractérisent l'ouvrage projeté.

Le développement du problème a été établi sur des principes mathématiques. Les lois de la probabilité, déterminées sur la base de l'expérimentation existante, sont combinées en vue de la détermination de la probabilité d'effondrement.

La condition de prix minimum de l'ouvrage assuré suppose une nouvelle équation qui, associée à la précédente, permette de déterminer la valeur la plus appropriée du coefficient de sécurité, compatible avec la sécurité nécessaire et exprimée par la probabilité d'effondrement qui est ainsi également définie.

Summary

The main purpose of this investigation is to establish a general method of calculation which, in any particular case, will enable the determination of the numerical value of the factor of safety. The calculated value obtained must be free from arbitrary or subjective factors. It should be entirely derived from the factual circumstances appropriate to the particular work or design.

The problem has been approached mathematically. Laws of probability, based on existing experimental data, have been suitably applied and manipulated to work out the probability of a structural failure.

A further equation can be formulated from the condition that the insured cost of the work shall be a minimum. This condition, in conjunction with accident probability, enables the most appropriate value for the design safety factor to be calculated, compatible with a suitable margin of safety. This safety margin will be expressed by the accident probability, which, by this procedure, will become automatically defined.

Zusammenfassung

Die vorliegende Studie macht sich zur Aufgabe eine allgemeine Berechnungsweise aufzustellen, die zu einer ziffernmässigen Festsetzung des Sicherheitsbeiwertes für einen gegebenen Fall führt. Diese Festsetzung muss in jeder Hinsicht objektiv sein und darf sich nur auf konkrete Angaben stützen, die den Besonderheiten des fraglichen Entwurfes oder Bauvorhabens entsprechen.

Diese Aufgabe wird auf mathematischer Grundlage entwickelt. Die aus vorhandenen Erfahrungen und Versuchen abgeleiteten Gesetze der Wahrscheinlichkeit werden miteinander in Verbindung gebracht und zur Bestimmung der Wahrscheinlichkeit des Versagens eines Bauwerks herangezogen.

Die notwendige Festsetzung eines Mindestgestehungspreises für ein versichertes Bauwerk bedingt eine weitere Gleichung, welche zusammen mit der vorangehenden, die Bestimmung des geeignetsten Sicherheitsbeiwertes im Einklang mit der erforderlichen Sicherheit ermöglicht, der somit gewissermassen automatisch zum Ausdruck kommt.